Universitat Autònoma de Barcelona

Chromatin remodeling in neuroblastoma
BAF complex links epigenetics to metastasis

Carlos G. Jiménez Jiménez

PhD thesis

Chromatin remodeling in neuroblastoma

BAF complex links epigenetics to metastasis

Presented by

Carlos G. Jiménez Jiménez

Submitted to obtain the degree of Doctor of Philosophy (PhD) in

Biochemistry, Molecular Biology and Biomedicine

Performed at the **Neural Tumors laboratory** of the
Group of Translational Research in Child and Adolescent Cancer at
Vall d'Hebron Institute of Research

Supervisor: Miguel F. Segura Ginard

Candidate: Carlos G. Jiménez Jiménez

Thesis affiliated to the PhD program in Biochemistry, Molecular Biology and Biomedicine
Department of Biochemistry and Molecular Biology
Universitat Autònoma de Barcelona

Academic tutor: Dr. Ibane Abasolo Olaortua

2021

Ten decisions shape your life
You'll be aware of five about

Seven ways to go through school
Either you're noticed or left out

Seven ways to get ahead
Seven reasons to drop out

I'll Try Anything Once ('You Oly Live Once' demo)
The Strokes
Heart In A Cage
2006

ACKNOWLEDGEMENTS

Agradecimientos

Agraïments

In many ways
They'll miss the good old days
Someday, someday

Someday
The Strokes
Is This It
2001

Barcelona, Noviembre de 2021

En los momentos más oscuros de esta tesis llegué a asegurar que en vez de agradecimientos escribiría un apartado de reproches. Ahora, al final de todas las cosas, tengo la sensación de que todo lo que he vivido de forma desordenada estos años está cristalizando; de que muchas de las cosas que me han pasado y que he aprendido están adquiriendo sentido; de que lo malo, desde la distancia, se vuelve irrelevante en comparación con lo bueno; y de que, como mínimo, les debo unas palabras de agradecimiento a unas cuantas personas. Quería ser breve, original y diferente, pero creo que esta es una oportunidad que no quiero desaprovechar para decir lo que me siento en la obligación de decir pero nunca digo, porque me cuesta horrores, y para quitarme las cien capas de sarcasmo que me separan del mundo.

Quiero empezar dando las gracias a Miquel. Sé que ha estat una tesi complicada, amb un parell d'hòsties inesperades que em patit per igual, i que en alguns moments foscos no s'entreveia cap sortida. En aquells moments de desesperació tu em deies que llavors no ho podria entendre, però que aquests obstacles m'ajudarien a aprendre i a créixer com a científic molt més que quan les coses surten a la primera. La veritat és que llavors no m'ho creia, pensava que m'ho deies simplement per a tranquil·litzar-me (cosa que no passava). Però amb la perspectiva crec que tenies raó. Vull donar-te les gràcies per no tirar la tovallola amb el projecte quan semblava que s'enfonsava, per aguantar les meves crisis existencials i ajudar-me a sortir del forat. Gràcies per donar-me l'autonomia que he tingut en el desenvolupament de la meva tesi, la qual crec que ha estat un factor crucial per a formar-me com a investigador. També per valorar tant el meu criteri a l'hora de prendre decisions i de dissenyar i portar a terme experiments, per molt arriscats que fossin, i per no posar impediments ni limitacions a l'hora d'explorar idees noves. I sobretot per la confiança que he sentit que has depositat en mi durant aquests anys, la qual crec que m'ha ajudat a no perdre la pròpia autoconfiança. De la teva direcció de la meva tesi m'enduc el teu interès permanent en explorar noves vies, voler anar un pas més enllà, arriscar-te i cercar ajuda i col·laboracions allà on fos necessari; qualitats que admiro molt de tu com a investigador, i que de segur marcaran la forma en la que vull desenvolupar la meva carrera científica. Crec que el que hem aconseguit després d'aquests anys ha valgut la pena, tant els bons resultats, com els no tant bons. Gràcies per tot.

Esta tesis se ha llevado a cabo en el contexto de un grupo de investigación fundado y guiado por los responsables del servicio de Oncología y Hematología Pediátricas del Hospital Vall d'Hebron. Quiero aprovechar para dar las gracias a los que han sido jefes del grupo de Investigación Traslacional en Cáncer de la Infancia y la Adolescencia durante estos años, Josep Sánchez de Toledo y Soledad Gallego, y de forma más reciente Lucas Moreno, así como al resto de clínicos que participan de diferentes formas en los proyectos de investigación, por el interés que demuestran desde la clínica por nuestro trabajo de laboratorio, por hacernos mantener los pies en la tierra y recordarnos el objetivo final de la investigación traslacional, y por apoyar y hacer posible de muchas formas el progreso y la continuidad de nuestros proyectos de investigación. En especial quiero agradecer a Sole su particular interés, apoyo y valoración crítica de nuestros proyectos en las reuniones semanales durante estos años, que creo que han aportado mucho valor y mejorado la dirección de nuestro trabajo.

Llegué al laboratorio de tumores neurales en octubre de 2014, como estudiante de prácticas de grado, cuando sólo tenían dos poyatas y cuatro miembros: Miquel, Aroa, Luz y Laia. No soy para nada la misma persona que empezó ese día, y creo que gran parte lo debo a las personas con las que he coincidido estos años en este grupo.

Aroa, eres un pilar fundamental de este grupo de investigación, y para mí un punto de referencia importantísimo. Gracias por estar dispuesta a prestar ayuda incluso cuando estás desbordada de trabajo y tenemos que buscar un hueco, por ejemplo un domingo, para acabar algo. Y sobre todo gracias por tu actitud comprensiva, asertiva y tranquilizadora, que creo que aporta un ambiente de serenidad y buen rollo al laboratorio que tiene muchísimo valor. Quiero agradecer a también Luz por ayudarme a dar los primeros pasos en este mundillo, por acogerme como estudiante de prácticas cuando no sabía ni coger una pipeta, por integrarme en su proyecto e iniciarme en la formación como investigador. Y, por supuesto, quiero darle las gracias a Laia. Laia, has sido un punto de apoyo clave para mí durante la primera mitad del doctorado, aunque sólo fuese para comentar la jugada o compartir las penas, las alegrías, música o cualquier parida de YouTube. Esos años no habrían sido ni la mitad de soportables ni divertidos sin ti. Creo que ya te lo he dicho alguna vez, pero para mí has sido un ejemplo de superación y dedicación, de cómo sacar frutos de historias que no acaban yendo como uno se espera, y además creo que has dejado un buen legado en el laboratorio que perdurará. Gracias por haber estado allí, y por seguir estando.

También quiero agradecer al resto de miembros que se han ido incorporando con los años al lab de tumores neurales. Ari, per mi ets un exemple de fortalesa i resiliència enfront de les adversitats, una capacitat que personalment considero molt admirable i que a em comformaria amb tenir-ne menys de la meitat de la que tu has demostrat aquests anys. Marc, vull agrair-te haver estat disposat a ajudar en moments clau, incloent l'explotació a la que t'he sotmès amb la revisió i amb els últims experiments; també per la teva minuciositat i perfeccionisme en la feina, per la paciència que has tingut i per haver compartit aquesta etapa tan important en les nostres vides, en paral·lel des del màster fins a aquí. Quiero acordarme también de los estudiantes de prácticas que han pasado temporalmente por el lab (Núria, Jaume, Patri). En especial quiero agradecer a Josep-Lluís, mi primer 'becario', por su trabajazo y contribución clave en un mini-proyecto en el que tenía personalmente puesta mucha ilusión, y que se hubiese quedado en nada sin su contribución; estoy seguro de que podrás desarrollar una buena carrera científica si te empeñas en ello.

Pero si a alguien le debo toneladas de gratitud, es a Roberta. Roby, te admiro mucho. No sólo por tu forma de trabajar y la pasión que tienes por este trabajo aunque las cosas no vayan bien (que creo que tienes, aunque ni tú misma lo veas); también como persona, por tu increíble generosidad y empatía. Obviamente me has ayudado en el lab en lo que necesitase, incluso dejando lo que estuvieses haciendo para echarme una mano en cualquier momento; y me has hecho partícipe de tus proyectos, haciéndome aprender más de lo que me hubiese imaginado. Pero lo que más valoro es el soporte emocional que me has prestado estos años. Me siento muy afortunado de haberte conocido, de haberte tenido a mi lado, mano a mano, en el despacho durante estos años y de haber podido empaparme de tu experiencia y tus consejos; de tener tu compañía en esas tardes, o noches, eternas en las que ya sólo quedamos el celador, tú y yo; y de saber que si tenía un bajón tu estarías dispuesta a dejar a medias lo que estuvieras haciendo e irnos a tomar un café de la alegría y hablar un rato. Me alegro mucho de poder considerarte mi amiga. Gracias por estos años.

Y también quiero agradecer a Ainara. Tengo la sensación de que has estado siempre en el lab. Y creo que eso es algo muy bueno, porque significa que eres ya alguien indispensable, tanto en el plano laboral como en el personal. Tu aparición fue un verdadero soplo de aire fresco en ambos sentidos. Quiero agradecerte el valor humano que aportas al grupo en general, y personalmente a mí. Gracias por preocuparte y tratar de mejorar los malos momentos, y gracias

por hacer mil veces mejores los buenos. Gracias por tu sentido del humor, por las clases de vasco, por los cafés de por la mañana que se alargan y por todos los consejos vitales.

También quiero agradecer a los compañeros del laboratorio de sarcomas, a.k.a. OP, liderados por Pep Roma. Gràcies Pep per la teva disposició i ajuda, sobretot amb els models animals amb els quals haguéssim anat perduts sense la teva experiència. Y también a las (no tan) nuevas incorporaciones: a Gabriel, por la ayuda y los consejos, por tu sentido del humor y por aguantar mis bromas de mal gusto sobre tu nacionalidad; y a Guillem, por aguantar mis bromas de mal gusto sobre el anarco-comunismo, y porque en el fondo siempre serás el joven estudiante de doctorado de primer año, y lo sabes.

Y no me quiero olvidar a una de las veteranas de OP, Irina. Irina, desde que os fuisteis Laia y tú todos sentimos un hueco enorme en el grupo que no se ha vuelto a llenar. Quiero agradecerte todos los buenos momentos que pasamos tanto en el VHIR como fuera, que recordaré siempre. Admiro mucho la forma que tienes de vivir la vida y de demostrar tu afecto a las personas que te importan. Siento que he tenido mucha suerte al conocerte y espero poder contar contigo mucho más tiempo.

Y bueno, por supuesto que tengo que hablar de dos de las personas más importantes que me llevo de estos años. Por una parte, Patri. Somos libra y se nota. No sé quién de los dos ha acabado ganando la batalla moral de cuál es más veterano, pero creo que finalmente podemos declarar un empate técnico. De todas formas, echando la vista atrás, me parece un golpe de suerte haber coincidido contigo desde el principio, haber crecido juntos estos años, y haber podido llegar a conocer a una persona tan increíble como tú. Gracias por todos los buenos recuerdos, anécdotas e historias que ya no se saben si son reales o inventadas, pero que voy a guardar siempre como un tesoro; hasta que nos convirtamos definitivamente en los nuevos cejas y vikinga. Sinceramente, me parece raro agradecerle a una persona el simple hecho de que sea mi amiga, pero es lo que me nace, y creo que esa palabra, con todo lo que conlleva, es la que lo resume mejor lo que hemos vivido estos años.

Y por otro lado, Natalia. Natelga, qué decir. Siento también que ha sido una suerte que hayamos empezado y acabado juntos este viaje a la vez. Conocerte a lo largo de estos años me ha hecho ver lo mucho que tenemos en común y lo mucho que puedo ponerme en tu lugar en muchos aspectos. Sé que eres una persona en la que puedo contar para buscar consejo, y un punto de

referencia de estabilidad emocional que me ha hecho mucho bien en bastantes ocasiones los últimos años. Quizás no dimos la talla que se esperaba de nosotros como líderes naturales; pero por lo menos creamos un logo gracioso para nuestros seminarios. Y aunque no seamos los más populares, creo que ambos hemos crecido en este tiempo, y básicamente ya no somos lo becarios pringados que llegaron con una maleta llena de ilusiones, y somos un poco más espabilados y tenemos las ideas un poco más claras.

Quiero agradeceros a las dos todo el tiempo que hemos pasado tanto en el lab como fuera, y que ha sido un bálsamo en momentos que personalmente han sido muy oscuros para mí. Desde la poca seriedad de nuestras "horas de escritura" en la sala de reuniones a las meriendas de máquina de vending, pasando por los veranos con heladitos en las escaleras de delante, mirando a los pájaros e intentando ver ardillas. Nos lo hemos pasado muy bien, y también lo hemos pasado muy mal, sobretodo esta última etapa. Más de lo que nos esperábamos. No os imagináis lo afortunado que me siento de haber vivido esto con vosotras. Gracias por hacer que vaya a tener buenos recuerdos hasta de estos últimos meses de mierda. Puedo decir que de este doctorado me llevo dos buenas amigas, y eso no es algo para nada habitual en mi vida, creedme.

Volviendo a un plano más profesional, quiero aprovechar para agradecer a todos los colaboradores más allá del grupo de investigación que han aportado algo, tanto a los resultados que se presentan en esta tesis, como a los que no forman parte de ella o no se han acabado incluyendo: Mariona Nadal, Carme Solé y Pablo Latorre, del lab de Francesc Posas y Eulàlia de Nadal (IRB), por su insustituible ayuda y generosidad a la hora de, no sólo enseñarme, si no también hacerse cargo de un punto tan importante para este proyecto como el ATAC-*Seq* (no ha arribat a temps a la tesi, però ja ho tenim gairebé!); a Laura Pascual, del lab de Sandra Peirò (VHIO), también por su ayuda, paciencia y generosidad a la hora de enseñarme todo lo que pudo sobre ChIP-seq; a Laura Devis y David Llobet (Idibell), por su disposición, capacidad y eficacia en los análisis estadísticos en un momento clave como fue la revisión de mi primer *paper*; también quiero incluir en esta lista a Jessica Camacho, del servicio de Anatomía Patológica de Vall d'Hebron, por su compromiso y dedicación en esa misma revisión, que fue crucial. Quiero agradecer también el soporte prestado desde las diferentes *facilities* integradas en la UAT del VHIR durante todos estos años, desde la plataforma de genómica (Pilar y María), pasando por la de microscopia (Marta), hasta la de citometría (Joan, y Norber e Irene en su

momento), cuya contribución, no sólo actuando como mero servicio, si no también asesorando y contribuyendo activamente a la calidad científica de los diseños experimentales, ha sido crucial para los resultados y mi aprendizaje. Gracias a todos.

Quiero hacer una mención a los compañeros del VHIR en general, y en especial a los del edificio Collserola, tanto de los grupos de investigación vecinos y los compañeros de la sala de cultivos (Rosi, María, etc), como de los miembros de coordinación de laboratorios, auxiliares, celadores y demás, por crear un ambiente tan familiar en ese pequeño rincón alejado del resto del campus, al que he acabado cogiendo hasta cariño, aunque se caiga a pedazos.

Y por último quiero agradecer a las personas de mi vida que, sin estar directamente implicadas en este doctorado, han tenido algo que ver en el camino hasta aquí.

Con la distancia, me he dado cuenta de que la motivación que me ha llevado hasta este punto, sin la que ni hubiese empezado esta etapa, tiene su origen en una serie de estímulos que despertaron mi ilusión y curiosidad por la ciencia. En ese sentido, quiero agradecer a los diferentes profesores que han despertado eso en mí a lo largo de mi etapa como estudiante, aunque probablemente no lo vayan a leer nunca: desde Cecilia Sales, mi profesora de biología de secundaria, por despertar mi interés y motivación planteándome retos y no poniéndomelo nada fácil; hasta profesores de la UAB que han sido una fuente de inspiración, que me hicieron descubrir algunas de mis disciplinas favoritas, y que hasta me aconsejaron de forma muy honesta y acertada sobre cómo dirigir mi carrera: Alfredo Ruiz (Genética de poblaciones, Genómica), Gemma Armengol (Genética Humana, Genética del Cáncer), y Susana Campoy (Microbiología molecular, Genómica microbiana). Creo que es de justicia reconocer y valorar los estímulos que han guiado tus elecciones, cuando éstas han resultado correctas. Así que muchas gracias a todos.

Pero de esa etapa en la UAB, sobretodo quiero daros las gracias a los amigos que hice en Barcelona a raíz de la carrera, que se hizo mucho más ligera y agradable con vuestra ayuda, compañía y amistad, la cual sé que guardaré toda la vida: Diego, Víctor, Laia, Marc y Jordi. Y, a través de este último, a Rebeca, Germán y Alba: gracias por hacerme sentir parte de algo especial y de mostrarme formas insospechadas de evasión, porque han sido esenciales en muchos momentos. Habéis sido mi vía de escape y os lo agradeceré siempre.

Quiero agradecer también a mis amigos de Palma de toda la vida, junto a los que literalmente he crecido, y seguiré creciendo: Miguel, Xisca, Ana, Miriam, María, Cris, Raquel, Guillem, Toni, etc. Y a Mar, por estar allí pase lo que pase.

Y a mi familia en general. No os nombraré a todos, porque sois muchos, pero en este punto quiero hacer una mención especial a mi tía Marta, quien fue paciente de cáncer. El impacto de esta enfermedad en tu vida personal hace que lo que escribes en una tesis como ésta adquiera otro significado y otro tono, y que valores la importancia que tiene el trabajo y la investigación que haces, al darle un sentido humano y un objetivo claro. Lamentablemente Marta no podrá leer esto, pero quiero dedicar esta tesis doctoral a su memoria, así como a Nando y a Fer.

Finalmente, sólo me queda dedicarles las últimas palabras a Javi, Lucía, papá y mamá. Por creer en mí más de lo que yo nunca seré capaz. Os quiero.

Carlos

ABSTRACT

Resumen

Resum

Those days taught me everything I know
How to catch a feeling
And when to let it go

Alien days
MGMT
MGMT
2013

Abstract

Epigenetic programming of cells during development is essential for the determination and maintenance of cell lineages and for tissue homeostasis. Embryonal tumors are originated by molecular alterations during developmental steps that result in aberrant transcriptional programs controlled by altered epigenetic landscapes. In the case of neuroblastoma, neural crest progenitors aimed at becoming cells of the sympathetic nervous system aberrantly block their natural differentiation course and initiate a neoplastic process leading to a potentially aggressive and metastatic pediatric oncologic disease. Thus, the study of the epigenetic regulators determining, interpreting or executing these oncogenic gene expression networks is crucial to fully understand these tumors and develop new epigenetic-based therapies.

In this PhD thesis, a systematic and functional analysis of the ATP-dependent mSWI/SNF chromatin remodeling complex in neuroblastoma cells is presented. This chromatin remodeler acts genome-wide translating epigenetic signals into opened chromatin states, allowing the interaction of transcription factors and other regulatory proteins with DNA.

Neuroblastoma cells contain the three main subtypes of mSWI/SNF complexes, but only BAF subcomplex is relevant for proliferation. BAF complex disruption through silencing of the specific and key structural subunits ARID1A and ARID1B promotes a transcriptional reprogramming of neuroblastoma cells affecting cell cycle progression and metastasis-related genes. This assembly disruption exerts a strong cell cycle blockade and a reduction of extracellular matrix adhesion and invasion *in vitro*, and drastically reduces metastasis formation *in vivo*, extending the survival of metastatic neuroblastoma mouse models. Finally, candidate molecules for the pharmacological disruption of BAF complex by inhibition of protein-protein interactions were identified in a druggability analysis and virtual screening of ARID1A structure. One of them seems to exert on-target effects and a strong proliferation inhibition on neuroblastoma cells. These findings represent a promising starting point for the development of a BAF disruption-based first-in-class therapeutic strategy against metastatic high-risk neuroblastoma.

Resumen

La programación epigenética de las células durante el desarrollo embrionario es esencial para la determinación y mantenimiento de los diferentes linajes celulares y la homeóstasis tisular. Los tumores embrionarios se originan a partir de alteraciones moleculares durante etapas del desarrollo que resultan en programas transcripcionales aberrantes controlados por perfiles epigenéticos alterados. En el caso del neuroblastoma, progenitores de la cresta neural destinados a convertirse en células del sistema nervioso simpático bloquean de forma aberrante su curso natural de diferenciación e inician un proceso neoplásico que conduce a una enfermedad oncológica pediátrica potencialmente agresiva y metastásica. Es por ello que el estudio de los reguladores epigenéticos que determinan, interpretan o ejecutan estas redes de expresión génica oncogénicas es crucial para comprender por completo el comportamiento de este tipo de tumores, así como para desarrollar nuevas terapias basadas en la epigenética.

En esta tesis doctoral se presenta un análisis sistemático y funcional del complejo remodelador de la cromatina dependiente de ATP mSWI/SNF en células de neuroblastoma. Este remodelador de la cromatina actúa a nivel genómico traduciendo señales epigenéticas a estados abiertos de la cromatina, facilitando la interacción de factores de transcripción y otras proteínas reguladoras con el ADN.

Las células de neuroblastoma contienen los tres principales subtipos de complejos mSWI/SNF, pero sólo el complejo BAF es relevante para su proliferación. La disrupción del complejo BAF mediante el silenciamiento de las subunidades clave y específicas ARID1A y ARID1B produce una reprogramación transcripcional en estas células que afecta a genes relacionados con la progresión del ciclo celular y con el proceso de metástasis. La interrupción del ensamblado de este complejo produce un fuerte bloqueo del ciclo celular así como una reducción de la adhesión a la matriz extracelular y capacidad de invasión *in vitro*, además de reducir drásticamente la formación de metástasis *in vivo*, extendiendo la supervivencia de modelos murinos de neuroblastoma metastásico. Por último, un análisis de susceptibilidad de unión a fármacos y un posterior cribado virtual de moléculas se llevó a cabo sobre la estructura de ARID1A, identificando moléculas candidatas para la disrupción farmacológica del complejo BAF mediante la inhibición de interacciones proteína-proteína. Uno de estos candidatos parece ejercer efectos sobre la diana molecular de interés y una fuerte inhibición de la proliferación de las células de neuroblastoma. Estos resultados representan un punto de partida prometedor para el desarrollo de una estrategia terapéutica pionera basada en la disrupción del complejo BAF para el tratamiento del neuroblastoma metastásico de alto riesgo.

Resum

La programació epigenètica de les cèl·lules durant el desenvolupament embrionari és essencial per a la determinació i manteniment dels diferents llinatges cel·lulars i la homeòstasi tissular. Els tumors embrionaris s'originen a partir d'alteracions moleculars durant etapes del desenvolupament que resulten en programes transcripcionals aberrants controlats per perfils epigenètics alterats. En el cas del neuroblastoma, progenitors de la cresta neural destinats a convertir-se en cèl·lules del sistema nerviós simpàtic bloquegen de forma aberrant el seu curs natural de diferenciació i inicien un procés neoplàsic que condueix a una malaltia oncològica pediàtrica potencialment agressiva i metastàtica. Per això, l'estudi dels reguladors epigenètics que determinen, interpreten o executen aquestes xarxes d'expressió gènica oncogèniques és crucial per a comprendre per complet el comportament d'aquest tipus de tumors, així com per a desenvolupar noves teràpies basades en l'epigenètica.

En aquesta tesi doctoral es presenta una anàlisi sistemàtic i funcional del complex remodelador de la cromatina depenent d'ATP mSWI/SNF en cèl·lules de neuroblastoma. Aquest remodelador de la cromatina actua a nivell genòmic traduint senyals epigenètiques a estats oberts de la cromatina, facilitant la interacció de factors de transcripció i altres proteïnes reguladores amb l'ADN.

Les cèl·lules de neuroblastoma contenen els tres principals subtipus de complexes mSWI/SNF, però només el complex BAF és rellevant per a la seva proliferació. La disrupció del complex BAF mitjançant el silenciament de les subunitats clau i específiques ARID1A i ARID1B produeix una reprogramació transcripcional en aquestes cèl·lules que afecta a gens relacionats amb la progressió del cicle cel·lular i amb el procés de metàstasi. La interrupció de l'assemblatge d'aquest complex produeix un fort bloqueig del cicle cel·lular així com a una reducció de l'adhesió a la matriu extracel·lular i capacitat d'invasió *in vitro*, a més de reduir dràsticament la formació de metàstasis *in vivo*, estenent la supervivència de models murins de neuroblastoma metastàtic. Per últim, una anàlisi de susceptibilitat d'unió a fàrmacs i un posterior cribratge virtual de molècules es va portar a terme sobre l'estructura d'ARID1A, identificant molècules candidates per a la disrupció farmacològica del complex BAF mitjançant la inhibició d'interaccions proteïna-proteïna. Un d'aquests candidats sembla exercir efectes sobre la diana molecular d'interès i una forta inhibició de la proliferació de les cèl·lules de neuroblastoma. Aquests resultats representen un punt de partida prometedor per al desenvolupament d'una estratègia terapèutica pionera basada en la disrupció del complex BAF per al tractament del neuroblastoma metastàtic d'alt risc.

INDEX

Echando la vista atrás no te odio tanto
Siempre he sido algo dramático

La verdad es que estuvo bien
La verdad es que eres lo mejor que me ha pasado
En estos años

Pero no volverá a ocurrir, no me odio tanto

KLK
Carolina Durante
Carolina Durante
2019

List of figures

List of tables

ABBREVIATIONS

There's no reason, there's no secrets to decode
If you can't save it, leave it dying on the road
Wide open arms can feel so cold
So cold

Siberian Breaks
MGMT
Congratulations
2010

	Abbreviation	Meaning
#	**3'-UTR**	3'-Untranslated Region
	5caC	5-carboxylcytosine
	5fC	5-formylcytosine
	5hmC	5-hydroxymethylcytosine
	5mC	5-methylcitosine
A	**ABC**	Ammonium Bicarbonate
	Ac	Acetylation
	act	Actin gene group (*Drosophila*)
	ACTA1	α-actin 1
	ACTB	β-actin
	ACTG1	γ-actin 1
	ACTL6A/B	Actin Like 6A/B
	ADP	Adnosine diphosphate
	AKT	V-Ak-Thymoma Murine Viral Oncogene-Like Protein
	ALK	Anaplastic Lymphoma Kinase
	ANOVA	Analysis of variance
	ANT-C	Antennapedia Complex
	ARID	AT-Rich Interaction Domain
	ARID1A	AT-Rich Interaction Domain 1A
	ARID1B	AT-Rich Interaction Domain 1B
	ARID2	AT-Rich Interaction Domain 2
	ARM	*Armadillo* sequence repeats
	Arp	Actin-related protein (yeast)
	ARP	Actin-Related Protein
	ArpNα/β	Actin-related proteins family 4 (ACTL6B/A)
	ATAC-Seq	Assay for Transposase-Accessible Chromatin-sequencing
	ATCC	American Type Culture Collection
	ATM	Ataxia Telangiectasia Mutated Kinase
	ATP	Adnosine triphosphate
	ATPase	Adenosine triphosphatase
	ATR	Ataxia Telangiectasia And Rad3-Related Kinase
	ATRT	Atypical Teratoid/Rhabdoid Tumor
	ATRX	Alpha Thalassemia/Mental Retardation Syndrome X-Linked
	AURKB	Aurora Kinase B
	AXL	Anexelekto Receptor Tyrosine Kinase
B	**BAF**	BRG1-/BRM-Associated Factor
	BAH	Bromo-adjacent homology domain
	BAP	*brm* associated proteins (*Drosophila*)
	BCL2	B-Cell CLL/Lymphoma 2 Apoptosis Regulator
	BCL7A/B/C	B-Cell Chronic lymphocytic leukemia/Lymphoma 7 Protein Family Member A/B/C
	BD	Bromodomain
	BDC	BAF Disruptor Candidate
	BET	Bromodomain and extra-terminal
	BFDR	Bayesian False Discovery Rate
	BICRA	BRD4 Interacting Chromatin Remodeling Complex Associated Protein
	BICRAL	BRD4 Interacting Chromatin Remodeling Complex Associated Protein Like
	BiP	Binding-Immunoglobulin Protein
	BMP	Bone Morphogenetic Protein
	BP75	75 KDa Bromodomain Protein
	BPTF	Bromodomain PHD Finger Transcription Factor

B	**BRCA1**	Breast Cancer Type 1 Susceptibility Protein
	BRD2/3/4	Bromodomain-containing protein 2/3/4
	BRD4	Bromodomain Containing 4
	BRD7	Bromodomain Containing 7
	BRD9	Bromodomain Containing 9
	BRDT	Bromodomain Testis Associated
	BRG1	BRM/SWI2-related gene 1
	BRM	Brahma homolog
	brm	*Brahma* (*Drosophila*)
	BSA	Bovine Serum Albumin
	BuMel	Busulphan, Melphalan
	BX-C	Bithorax Complex
C	***C. elegans***	*Caenorhabditis elegans*
	CAMTA1	Calmodulin Binding Transcription Activator 1
	CASP3	Caspase 3
	CBP	CREB (CAMP Responsive Element Binding Protein 1) Binding Protein
	CBR	Core binding regions
	CCND1	Cyclin D1
	CDH11	Cadherin 11
	CDK1/4/6	Cyclin-Dependent Kinase 1/4/6
	CDKN2A	Cyclin Dependent Kinase Inhibitor 2A
	CDS	Coding Sequence
	c-fos / FOS	FBJ Murine Osteosarcoma Viral Oncogene Homolog
	CHD	Chromodomain helicase DNA-binding
	CHEK1	Checkpoint Kinase 1
	ChIP-Seq	Chromatin immunoprecipitation-sequencing
	c-jun / JUN	Jun Activation Domain Binding Protein
	cLogP	Partition Coeficient
	CNS	Central Nervous System
	Co-IP	Co-Immunoprecipitation
	COJEC	Cisplatin, Vincristine, Carboplatin, Etoposide, Cyclophosphamide
	CpG	Cytidine-Guanidine dimers
	CPS1-IT1	Carbamoyl-Phosphate Synthase 1 Intronic Transcript 1
	CREST	Calcium-Responsive Transactivator
	cryo-TEM	cryogenic transmission electronic microscopy
	CTCF	CCCTC-Binding Factor
	C-terminal	Carboxyl-terminus of polypeptide
	CTNNB1	β-catenin
D	***D. melanogaster***	*Drosophila melanogaster* (Fruit fly)
	DAPI	4',6-diamidino-2-phenylindole
	DGCR5	DiGeorge Syndrome Critical Region Gene 5
	DLX6-AS1	Distal-Less Homeobox 6 Antisense RNA 1
	DMEM	Dulbecco's modified Eagle's medium
	DMSO	Dimethyl sulfoxide
	DNA	Deoxyribonucleic acid
	DNMT	DNA-methyltransferase
	DOT1L	DOT1 (Disruptor of telomeric silencing-1) Like Histone Lysine Methyltransferase
	DPF1/2/3	Double PHD Fingers 1/2/3
E	**E2F**	E2F Transcription Factor
	ECL	Enhanced Chemiluminescence
	ECM	Extracellular Matrix
	EDTA	Ethylenediaminetetraacetic acid

E	**EMT**	Epithelial-mesenchymal transition
	ER	Endoplasmic Reticulum
	esBAF	Embryonic stem cell BAF
	ESC	Embryonic Stem Cell
	EZH2	Enhancer Of Zeste Homolog 2
F	**FACS**	Fluorescence-activated Cell Sorting
	FAK	Focal Adhesion Kinase
	FBS	Fetal Bovine Serum
	FC	Fold Change
	FDA	U.S. Food and Drug Administration
	FDR	False Discovery Rate
	FITC	Fluorescein isothiocyanate
	FOSL2	FOS Like Antigen 2
	FOXD3	Forkhead Box D3
	FRET	Fluorescence resonance energy transfer
G	**GATA2/3**	GATA Binding Protein 2/3
	GBAF	GLTSCR1-associated BAF
	GCN5L2	General Control Of Amino Acid Synthesis Protein 5-Like 2
	GLI1	Glioma-Associated Oncogene Homolog 1
	GLTSCR1	Glioma Tumor Suppressor Candidate Region Gene 1 Protein
	GLTSCR1L	Glioma Tumor Suppressor Candidate Region Gene 1 Protein-Like
	GNAT	Glycine-N-Acyltransferase Like 1
	GSEA	Gene Set Enrichment Analysis
H	***H. sapiens***	*Homo sapiens* (Human)
	H1	Histone H1
	H2A	Histone H2A
	H2A.X	H2A.X Variant Histone
	H2A.Z	H2A.Z Variant Histone
	H2B	Histone H2B
	H3	Histone H3
	H3K27	Histone H3 lysine 27
	H3K27ac	Histone H3 acetylated at lysine 27
	H3K27me3	Histone H3 tri-methylated at lysine 27
	H3K4	Histone H3 lysine 4
	H3K4me2	Histone H3 di-methylated at lysine 27
	H3K4me3	Histone H3 tri-methylated at lysine 4
	H3K79	Histone H3 lysine 79
	H3K9	Histone H3 lysine 9
	H4	Histone H4
	HAT	Histone acetyltransferase
	HBD	Histone-binding domain
	HDAC	Histone deacetylase
	HDM	Histone demethylase
	Hir1/2	Histone Regulation 1/2 (yeast)
	HIV	Human Immunodeficiency Virus
	HMG	High-Mobility Group
	HMT	Histone methyltransferase
	HO	HOmothallic switching endonuclease
	HOTAIR	HOX Transcript Antisense RNA
	HP1	Heterochromatin Protein 1
	HRP	Horseradish peroxidase
	HSA	Helicase/SANT-associated domain

H	**hSNF5**	Human SNF5 (SMARCB1)
	HSPA5	Heat Shock Protein Family A (Hsp70) Member 5
	Htl1	High-Temperature Lethal (Yeast)
	HTVS	High-throughput Virtual Screening
I	**IC50**	Half inhibitory concentration
	IDRF	Image-Defined Risk Factors
	IgG	Immunoglobulin G
	IL-7-AS	Interleukin 7 antisense transcript
	IMDM	Iscove's modified Dulbecco's medium
	INGR	International Neuroblastoma Risk Group
	INGRSS	International Neuroblastoma Risk Group Staging System
	INI1	Integrase Interactor 1 Protein (SMARCB1)
	INO80	INOsitol requiring
	INSS	International Neuroblastoma Staging System
	ISWI	Imitation SWItch complex
	ITGA	Integrin α
	ITGB	Integrin β
	IVIS	*In vivo* imaging system
J	**JARID**	Jumonji And AT-Rich Interaction Domain
	JHDM	JmjC (Jumonji C) domain-containing histone demethylation protein
K	**KAT**	Lysine acetyl transferases
	kDa	kiloDalton
	KDM	Lysine demethylase
	KIF1B	Kinesin Family Member 1B
	KPNA2	Karyopherin Subunit α2
	KRAS	Kirsten Rat Sarcoma Viral Oncogene Homolog
L	**LC-MS/MS**	Liquid chromatography-tandem mass spectrometry
	LDS	Lithium dodecyl sulfate
	lincRNA-Cox2	Cyclooxygenase-2-associated long intergenic noncoding RNA
	LMO1	Lin11, Isl-1 and Mec-3 (LIM) Domain Only 1
	lncRNA	Long non-coding RNA
	lncBRM	BRM-associated lncRNA
	lncFZD6	Frizzled Class Receptor 6-associated lncRNA
	lncTCF7	T-Cell-Factor-7-associated lncRNA
	lncZic2	Zinc Finger Protein Of The Cerebellum 2- associated lncRNA
	LOH	Loss of Heterozygosity
	LOXL2	Lysyl Oxidase Like 2
	LSD	Lysine-Specific Demethylase
M	***M. musculus***	*Mus musculus* (Mouse)
	MALAT1	Metastasis Associated Lung Adenocarcinoma Transcript 1
	MAP kinase	Mitogen-Activated Protein Kinase
	marcoH2A	Macro H2A Histone
	MBD	Methyl-CpG-binding domain
	MBT domain	Malignant Brain Tumor domain
	MCM3/4	Minichromosome Maintenance Complex Component 3/4
	MDR1	Multidrug Resistance Mutation 1
	Me	Methylation
	MeCP2	Methyl CpG binding protein 2
	MEIS2	Myeloid Ecotropic Viral Integration Site 1 Homolog 2
	MES	2-[N-morpholino]ethanesulfonic acid
	MHRT	Myosin Heavy Chain Associated RNA Transcript
	miRNA	Micro RNA

M	**MITF**	Melanocyte Inducing Transcription Factor
	MLL	Myeloid/lymphoid or mixed-lineage leukemia histone methyltransferase
	MNase-Seq	Micrococcal nuclease digestion-sequencing
	mor	*moira (Drosophila)*
	MPNST	Malignant peripheral nerve sheath tumour
	MRLN	Myoregulin
	mRNA	Messenger RNA
	MRT	Malignant rhabdoid tumor
	MSigDB	Molecular Signature Database
	mSWI/SNF	Mammalian SWItch/Sucrose Non-Fermentable complex
	mTOR	Mechanistic Target Of Rapamycin Kinase
	MVIH	Microvascular invasion in HCC-associated lncRNA
	MW	Molecular Weight
	MYC	Avian Myelocytomatosis Viral Oncogene Homolog
	MYCN	Neuroblastoma MYC
	MYST	MOZ, Ybf2/Sas3, Sas2, and Tip60 histone acetyltransferases
N	**nBAF**	Neuron BAF
	NBAT-1	Neuroblastoma-Associated Transcript 1
	ncBAF	Non-canonical BAF
	NCBRS	Nicolaides–Baraitser syndrome
	ncRNA	Non-coding RNA
	NDR	Nucleosome-depleted regions
	NEAT1	Nuclear Paraspeckle Assembly Transcript 1
	NES	Normalized Enrichment Score
	npBAF	Neural progenitor BAF
	N-terminal	Amino-terminus of polypeptide
	NuRD	Nucleosome remodeling and deacetylation complex
O	**OB-cadherin**	Osteoblast-cadherin
	OCT4	Octamer-binding transcription factor 4
P	**p16Ink4a**	Protein p16, Inhibits Kinase CDK4
	PARP	Poly(ADP-Ribose) Polymerase
	PAT1	Protein Associated with Topoisomerase II
	PBAF	Polybromo-Associated BAF
	PBAP	*polybromo*-associated *brahma*-associated protein
	PBRM1	Polybromo 1
	PBS	Phosphate-Buffered Saline
	PCBP2	Poly(RC) Binding Protein 2
	PDB	Protein Data Bank
	PD-L1	Programmed Cell Death 1 Ligand 1
	PHD finger	Plant Homeodomain finger
	PHF10	PHD Finger Protein 10
	PHOX2B	Paired Like Homeobox 2B
	PI3K	Phosphoinositide 3-kinase
	PIK3CA	Phosphatidylinositol-4,5-Bisphosphate 3-Kinase Catalytic Subunit Alpha
	PIPES	Piperazine-N,N'-bis(2-ethanesulfonic acid)
	PKMT	Protein Lysine methyltransferase
	POLA2	DNA Polymerase α2, Accessory Subunit
	POLE	DNA Polymerase ε, Catalytic Subunit
	p-Rb	Phosphorylated-Retinoblastoma protein
	PRC	Polycomb Repressing Complex
	PRMT	Protein Arginine methyltransferase
	PROTAC	Proteolysis targeting chimera

P	**PSA**	Polar Surface Area
	PTEN	Phosphatase And Tensin Homolog
	PTM	Post-Translational Modification
	PVDF	Polyvinylidene fluoride
R	**RA**	Retinoic Acid
	Rb	Retinoblastoma protein
	RIP	RNA-immunoprecipitation
	RIPA buffer	Radioimmunoprecipitation assay buffer
	RNA	Ribonucleic acid
	RNAi	RNA interference
	RNA-Seq	RNA sequencing
	RPL10A	Ribosomal Protein L10a
	Rsc	Remodeling the Structure of Chromatin (Yeast)
	Rtt102	Regulator of Ty1 Transposition (Yeast)
	Runx1	Runt-Related Transcription Factor 1
S	***S. cerevisiae***	*Saccharomyces cerevisiae* (Yeast)
	SAGA	Spt-Ada-Gcn5 Acetyltransferase complex
	SAHA	Suberoylanilide hydroxamic acid
	SAINT	Significance Analysis of INTeractome
	SANT	Swi3, Ada2, N-CoRand and TFIIIB domain
	SatIII	Satellite III ncRNA
	SCCOHT	Small cell carcinoma of the ovary, hypercalcemic type
	SChLAP1	SWI/SNF Complex Antagonist Associated With Prostate Cancer 1
	SCID	Severe combined immunodeficiency mutation
	SDS	Sodium dodecyl sulfate
	SEM	Standard Error of the Mean
	Sfh1	Snf Five Homolog (Yeast)
	shARID1A	shRNA against ARID1A
	shARID1A/B	Combination of shRNAs against ARID1A and ARID1B
	shARID1B	shRNA against ARID1B
	shBRG1	shRNA against BRG1
	SHL2	Super helical location 2 (nucleosome)
	shRNA	Short hairpin RNA
	shSMARCC1	shRNA against SMARCC1
	shSMARCC2	shRNA against SMARCC2
	shSMC1	shRNA against SMARCC1
	shSMC2	shRNA against SMARCC2
	siARID1A	siRNA against ARID1A
	siARID1B	siRNA against ARID1B
	SIN	Switch Independent
	SIOPEN	International Society of Pediatric Oncology European Neuroblastoma
	siRNA	Small interfering RNA
	SMARCA	SWI/SNF Related, Matrix Associated, Actin Dependent Regulator Of Chromatin, Subfamily A
	SMARCB1	SWI/SNF Related, Matrix Associated, Actin Dependent Regulator Of Chromatin, Subfamily B, Member 1
	SMARCC	SWI/SNF Related, Matrix Associated, Actin Dependent Regulator Of Chromatin, Subfamily C
	SMARCD	SWI/SNF Related, Matrix Associated, Actin Dependent Regulator Of Chromatin, Subfamily D
	SMARCE1	SWI/SNF Related, Matrix Associated, Actin Dependent Regulator Of Chromatin, Subfamily E, Member 1
	SnAc	Snf2 ATP coupling domain
	SNAI1/2/3	Snail-1 (Snail), Snail-2 (Slug), Snail-3 (Smuc) genes
	sncRNA	Small non-codign RNA
	SNF	Sucrose Non-Fermentable genes
	SNF5	Sucrose Non-Fermentable 5

S	**SNHG1**	Small Nucleolar RNA Host Gene 1
	snr1	Snf5-related 1 (*Drosophila*)
	SOX2/9	SRY-Box Transcription Factor 2/9
	SP	Standard Precision
	SRC	Steroid Receptor Coactivator
	SS18	Synovial Sarcoma Translocation, Chromosome 18
	SS18L1	SS18-Like Protein 1
	SSX	Sarcoma, Synovial, X-Chromosome
	SSXT	Synovial Sarcoma, Translocated To X Chromosome
	STAT3	Signal Transducer And Activator Of Transcription 3
	Sth1	SNF Two Homolog (Yeast)
	SUC2	SUCrose
	SWI	Switch genes
	SWI/SNF	SWItch/Sucrose Non-Fermentable complex
	SWINGN	SWI/SNF Interacting GAS6 enhancer Noncoding RNA
	Swp	Swi/Snf protein (yeast)
	SWR	Swi2/Snf2-Related
	SYT	Synovial Sarcoma, Translocated
T	**TAD**	Topologically associated domain
	Taf14	ATA binding protein-Associated Factor (Yeast)
	TBS-T	Tris-buffered saline, 0.1% Tween 20
	TERT	Telomerase Reverse Transcriptase
	TET	Ten-Eleven Translocase
	TGFβ	Transforming Growth Factor β
	TP53	Tumor Protein P53
	TRAILR	TNF-Related Apoptosis Inducing Ligand-Receptor
	TUG1	Taurine-upregulated gene 1
	TWIST1	Twist Family BHLH Transcription Factor 1
U	**UCA1**	Urothelial Cancer Associated 1
	UV	Ultraviolet
V	**VS**	Virtual Screening
W	**WEE1**	WEE1 G2 Checkpoint Kinase
	Wnt	Wingless-Type MMTV Integration Site Family
X	**XIST**	X Inactive Specific Transcript
Y	**YAP**	Yes-Associated Protein
	γ-H2A.X	H2A.X Variant Histone phosphorylated at Serine 139

1. **INTRODUCTION**

The deeper I get, the less that I know
That's the way it goes
The less that I know, the deeper I'll go

Brooklyn Bridge to Chorus
The Strokes
The New Abnormal
2020

1.1. **Epigenetics and cancer**

The tissue specialization characteristic of higher multicellular eukaryotes is one of the most relevant evolutionary steps in life history. The distribution of tasks between different cell types made possible the generation of highly specialized organs and systems, exemplified in the development of biological systems of such relevance in humans as the immune or the nervous systems. This level of complexity is achieved from the divergence during embryonic development of different committed cell lineages with specific properties, starting from a group of few identical cells[1]. This differentiation between cell lineages and posterior commitment is regulated by an intricate network of signaling pathways and molecular mechanisms that integrate external and internal inputs into a specific output leading to cell lineage determination[2]. Today, it is widely accepted that these differences are the result of specific gene expression programs: tissue specialization requires both the activation of concrete genes required for the specialized roles, but also the strict silencing of genes unnecessary, undesired or even antagonistic for these functions[3,4]. Different levels of gene expression regulation can take part, from transcriptional activation or repression, to post-transcriptional and translational control. This cell lineage-dependent gene expression programming is not only required for the differentiation of the tissues at determined developmental times, but also needs to be temporally regulated, since different steps of the embryonic development have different gene expression requirements for a specific lineage. Moreover, the need of lineage commitment for tissue specialization demands the maintenance of these expression programs through every round of cell division that is produced during the complete formation of the organism. It is in this specific point in which transcriptional expression control through epigenetic mechanisms takes an important role[5].

Epigenetics refers to those biological traits stably heritable that result from modifications of the chromatin without alterations in the DNA sequence[6]. This heritability is due to the intrinsic capacity of epigenetic traits to remain through meiosis, resulting in intergenerational epigenetic heritability, as well as through mitosis, resulting in the maintenance of epigenetic traits in cell lineages within an individual organism[5]. These epigenetic traits are the response to certain external or internal stimuli and consist in different chemical modifications of the chromosomes, known as epigenetic signals, which condition at different genomic loci the condensation states of the chromatin, which is the nuclear substance formed by the complex of DNA and its

associated structural and regulatory proteins[6]. These chromatin states have been classified into the opened and transcriptionally active euchromatin, and the closed and transcriptionally repressed heterochromatin[7]. Chromatin structural conformations produce transcriptional changes of determined genes, which need the active function of a specific maintenance machinery for its heritability through meiosis and mitosis. The chromatin modifications that trigger these processes, or epigenetic signals, can be summarized in three main levels: DNA methylation, histone modifications and non-coding RNA regulation (Figure 1).

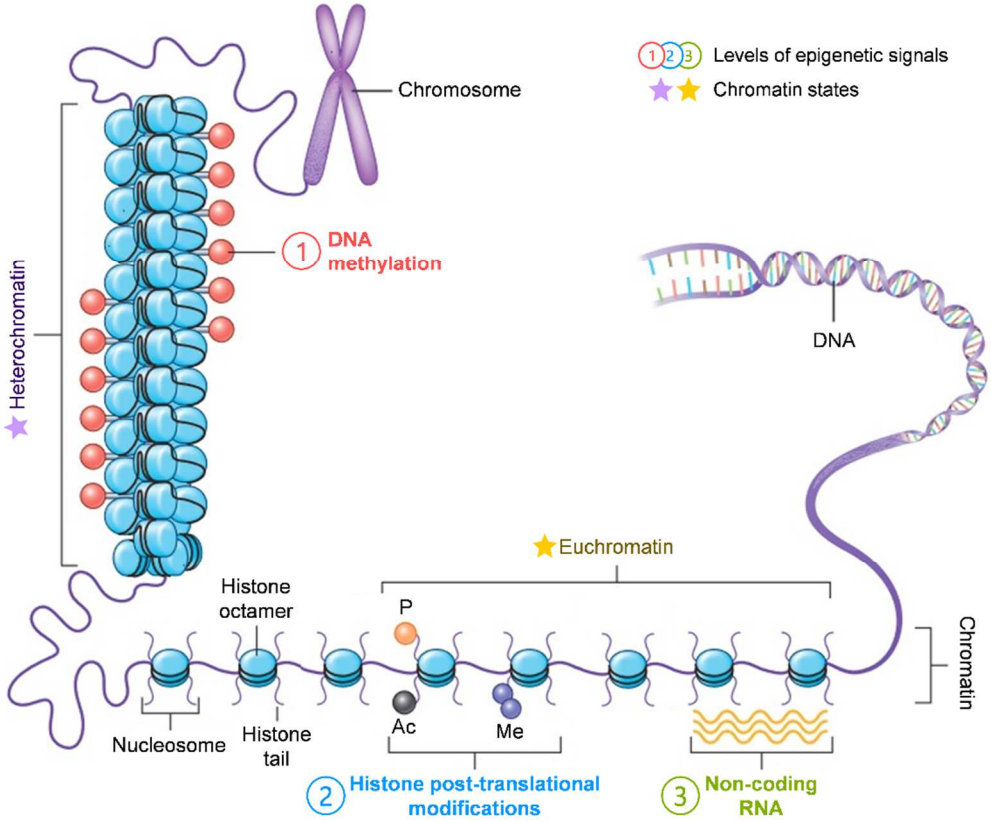

Figure 1: The three layers of epigenetic regulation, adapted from Ahuja *et al.* (2016)[8]. Chromatin states, classified in silent closed heterochromatin and active opened euchromatin, are determined by three major levels of epigenetic signals: DNA methylation (1); histone post-trancriptional modifications (2), such as methylation (Me), acetylation (Ac) or phophosrylation (P); and non-coding RNA (3).

1.1.1. DNA methylation

The methylation of the cytosines of the DNA at their carbon 5 (5-methylcitosine, 5mC), proved in 1948[9], occurs in both prokaryotic and eukaryotic cells. While in the first ones the function of this chemical modification is the identification of the own DNA and the defense from external DNA from bacteriophages and other bacteria[10], the functionality of this change in eukaryotic cells is one of the fundaments of epigenetics. Although the presence of a methyl group in the cytosine does not alter the reading of DNA protein-coding sequences by means of the genetic code, nor the corresponding amino acid sequence of the encoded peptides, it has an impact on eukaryotic genome stability and gene expression[11]. This latter effect makes DNA methylation an important epigenetic signal.

The main epigenetic function of DNA methylation is the silencing of genes by its deposition at promoters. Cytosine methylation occurs in eukaryotic genomes at cytidine-guanidine dimers of the DNA, called CpG. Clusters of multiple CpG, or CpG islands, are found in or nearby the promoters of multiple genes. Hyper-methylation of these promoter CpG islands was initially found in epigenetically silenced genes[11], promoting a stable and long-term transcriptional repression of the downstream gene heritable throughout generations, whereas cytosine methylation of the gene body did not affect the transcriptional expression of the gene[12,13]. Conversely, hypo-methylated CpG islands in promoters were correlated with active gene expression[11]. The link between methylation and transcriptional control was later found to be the chromatin condensation state: hyper-methylated regions promote higher condensation states of the chromatin (heterochromatin), leading to a reduced accessibility of transcriptional machinery and gene silencing[14]. These findings founded the bases of molecular epigenetics.

Today it is known that DNA methylation promotes the highest level of mitosis and meiosis-transmittable epigenetic silencing. It triggers a cascade of molecular processes leading to high levels of chromatin condensation that protect the specific genomic sites from transcription. The greater exponent of this process is the inactivation of one of the X chromosomes for gene dosage-compensation in mammalian females, in which DNA-methylation plays a key triggering role[15]. Besides methylation, different chemical DNA modifications not altering the reading pattern have been discovered, including 5-hydroxymethylcytosine (5hmC), 5-formylcytosine (5fC) and 5-carboxylcytosine (5caC), the function of which, however, remains less studied and still uncertain[16].

1.1.2. Histone modifications and variants

Histones are low molecular weight and highly basic proteins that tightly interact with DNA through electrostatic interactions. Five histone families are found in higher eukaryotes: core histones H2A, H2B, H3 and H4; and linker histones H1. The core histones associate in octamers, formed by two H2A-H2B dimers and one H3-H4 tetramer, which act as spools around which DNA wraps[17,18]. The complex of DNA and histone octamer is called nucleosome, the chromatin compaction unit with which eukaryotes are able to fit huge genomes up to the order of giga base pairs[19] into small nuclei with an average diameter of 10 µm[20]. H1 histones do not form part of nucleosomes, but rather serve as linkers between them, increasing the compaction state of the chromatin[18]. Since the 1970s, histone association to DNA has been observed to exert transcriptional repressive effects, through an increase in the chromatin compaction and condensation state[21], putting this family of proteins on the focus of epigenetic investigations.

Histone residues can be covalently modified, by the addition of different chemical groups. These histone post-translational modifications, or histone marks, act as signals for the remodeling of the chromatin into either opened or closed states and, therefore, are important epigenetic signals. The two first discovered and most studied and characterized histone marks are acetylation and methylation. Reversible acetylation and methylation of histones were first suggested in 1964 to be associated with transcriptional activation and repression, respectively[22]. Acetylation of histone residues at promoters has been widely associated to active transcriptional activity through the increase of chromatin accessibility[23,24]. On the other side, methylation of histones has been shown to exert either repressive or activating effects, depending on the residue affected[25,26]. For example, while acetylation of histone H3 at the lysine 27 (H3K27ac) is a general activating mark, its mutually exclusive tri-methylated counterpart (H3K27me3) impedes the acetylation and acts as a general repressive mark[27,28]. On the contrary, tri-methylation of histone H3 at lysine 4 (H3K4me3) is strongly associated with transcriptional activation[29]. In fact, domains of overlapping activating H3K4 and repressing H3K27 methylations, called bivalent chromatin, are found regulating several genes during embryonal development, being essential for the precise in time activation of genes at early developmental steps[30].

These modifications can be found in different parts of histone polypeptides, but a hot-spot of histone modifications are the N-terminal tails of core histones, which protrude from the

nucleosome body and serve as scaffold for the deposition and detection of these epigenetic signals[31]. The signaling through histone marks is crucial for the chromatin compaction state and accessibility at gene promoters, and the combination of multiple histone marks determines the resulting spatiotemporal expression pattern of a certain gene, through what has been called the 'histone code'[31–33]. Moreover, specific combinations of histone marks define important distal *cis* regulatory elements such as enhancers[34].

Multiple additional histone marks have been identified and characterized since the discovery of histone acetylation and methylation, such as histone ubiquitination, related to processes of gene repression, among others[35], histone phosphorylation, related to chromatin condensation during mitosis[36]; or the recently discovered histone crotonylation, of yet uncertain functions, but somewhat related to gene activation[37]. Other less studied modifications of uncertain or ambiguous functions are sumoylation, ADP ribosylation, propionylation or butyrylation[38].

Moreover, for each histone family, numerous subtypes encoded by different genes are found, some of which with functional differences upon chromatin organization that can condition the transcriptional expression of certain genes. These functionally relevant histone variants are positioned by histone chaperones into specific genomic sites, and their presence is maintained through mitosis, making them to be considered as epigenetic signals. For example, histone variant marcoH2A is found in heterochromatin and related to chromatin condensation, while H2A.X variant phosphorylated at serine 139 (γ-H2A.X) is an important signal for the recruitment of the DNA repair machinery[39,40].

1.1.3. Non-coding RNA

Only between a 1-2% of the human genome contains information for the synthesis of proteins. In recent years it has become clear that the remaining non-coding part of the genome has more functions beyond the mere structural role. An unexpected part of it (~80%) was determined in 2012 to have biochemical functions, related to a transcriptional or a chromatin-associated event[41]. Transcripts generated in the non-coding genome do not produce a functional polypeptide, but many of them have functionality by themselves. These are called non-coding RNAs (ncRNA), and are classified according to their length into *small* ncRNA (sncRNA), shorter than 200 nucleotides, or *long* ncRNA (lncRNA), of 200 nucleotides or longer[42].

Among the intrinsic functionalities attributed to ncRNAs, which includes the participation in protein synthesis, mRNA splicing and mRNA post-transcriptional regulation, participation in chromatin structure have been repeatedly reported[42,43]. For example, some of them participate in the initiation of transcriptional silencing processes that affect broad genomic regions. Such is the role of XIST lncRNA in X-inactivation, the transcription of which is one of the triggering events in this relevant dosage-compensation regulatory process in female mammals[44]. Also, multiple studies have observed that regulatory proteins can be recruited to specific genomic loci by interaction with nascent lncRNAs, which act as epigenetic signals by altering chromatin structure through the genomic targeting of epigenetic regulators at specific sites[45]. These findings, among others, are the reason why many authors have proposed ncRNA as a third level of epigenetic regulation.

1.1.4. Epigenetics of cancer

Epigenetics is determinant in the maintenance of lineage identity of the multiple cell types that constitute the different tissues of an organism, which makes the correct epigenetic programming of cells crucial for the maintenance of tissue homeostasis[5]. Indeed, epigenetic aberrations can promote a non-programmed loss of cell specialization and identity, disrupting equilibrium between cell types of a tissue and favoring the initiation and progression of diseases such as cancer. Cancer is a wide group of diseases characterized by the loss of tissue homeostasis by the aberrant proliferation of a specific cell type that accumulates both genetic and epigenetic errors that confers adaptive advantage through a clonal selection process. The emergence of this abnormal cell population generates a loss of tissue structuring, called neoplasia, which impedes the regular performance of the tissue physiological functions[46,47]. This new population can also protrude from the limits of the original tissue, invading other tissues and organs, and is even able to use the circulatory system for the invasion of distant organs, in a process known as metastasis. In all these steps, epigenetic aberrations can promote the capacities of cancer cells to adapt, proliferate and survive[48].

The first association of epigenetics and cancer was observed at the DNA methylation level, during the 1960s, when different patterns of methylation were found between the DNA of tumors and their corresponding healthy tissues[49,50]. For example, while an aberrant decrease of

intergenic and gene-body DNA methylation has been associated to the initiation of cancer, or tumorigenesis, by increasing genome instability[51–53], a general increase of the methylation of promoters has been recurrently observed in genes that negatively regulate the proliferation capacities of cells, among other oncogenic properties, which are called tumor suppressor genes[54]. Promoter hyper-methylation of relevant tumor suppressor genes, such as the relevant cell cycle progression inhibitors *RB* and *CDKN2A*, has been reported as an inactivating mechanism with the same oncogenic potential as loss-of-function mutations[55]. Indeed, changes in promoter methylation have been associated with changes in expression of large sets of cancer-related genes and in very early steps of the tumorigenic process, such as in pre-malignant lesions (i.e. non-invasive hyper-proliferative cell populations)[8]. Nevertheless, DNA hypo-methylation at promoter CpG islands leading to aberrant gene activation has been also observed in multiple cancer scenarios, including stomach, kidney, colon, pancreas, liver, uterus, lung and cervix cancers, on which specific hypo-methylation of pro-survival and proliferation genes, such as those encoding important cell cycle regulators like cyclin D2 or drug resistance enzymes like MDR1, are crucial as well for tumor initiation and progression (reviewed in [55]). Therefore, a general 'promoter hyper-methylation oncogenic driving' would be too simplistic to explain the intricate contribution of epigenetic regulation through DNA methylation to tumor initiation and progression. Tumor- and gene-specific events of both promoter hyper- and hypo-methylation need to be assumed as relevant for the oncogenic process through adaptive advantage selection.

On the other side, histone mark aberrations have also been reported in tumors and important oncogenic function regarding their biosynthesis as well as their reading and interpretation by downstream chromatin readers and remodelers have been determined to be relevant events in tumor initiation and progression (reviewed in [56,57]). Multiple driving mutations are found in different types of tumors in genes encoding the enzymes responsible for the synthesis and erasing of histone acetylation or methylation, the preeminently studied histone marks. The miswriting of these chromatin modifications is related to wide expression changes in large sets of genes, having pleiotropic effects in cancer biology. For example, histone lysine acetyl transferases are usually found involved in genomic translocations resulting in fusion proteins in hematologic cancers, or overexpressed in certain solid tumors[38]; moreover, the gain of function mutations of the catalytic subunit of the *Polycomb* repressing complex 2 (PRC2) EZH2, a histone methyltransferase, in B-cell lymphomas causes a genome-wide oncogenic increase of

H3K27me3 levels[56]. Besides aberrant positioning or erasing, histone mark misinterpretation by defects on the proteins responsible for their recognition (chromatin *readers*) and/or implementation (chromatin *remodelers*) are also involved in the promotion of tumorigenic traits by aberrant gene activation or repression[56].

Current research is focusing in the appearance of aberrant oncogenic super-enhancers, distal *cis* regulatory elements that promote a potent activation of the expression of genes, or sets of genes, defined by the specific enrichment of certain activation histone marks, which reflects the importance of these epigenetic signals in the transcriptional reprogramming of cancer cells[58,59]. Recent advances have revealed additional interesting oncogenic events involving histone marks, such as the misuse or excess of the metabolite precursors of histone modifications, relevant for epigenetic signaling; the recurrence of mutations on histones that alter the histone mark landscape; or the connection of histone modifications and the oncogenic alterations in high-order organization of chromatin architecture (reviewed in [57]). The epigenetic regulation trough the already mentioned 'chromatin-decorating' non-coding RNAs has also been related to different oncogenic processes in various types of cancer, acting these transcripts either as oncogenic or tumor suppressive RNAs[60,61].

In addition to the implication of aberrant epigenetic signaling in cancer, multiple mutations in genes encoding different epigenetic regulators are found as driving events of many tumor types[62], being this family of genes one of the most recurrently mutated in adult cancers, and the most mutated in pediatric cancer[63]. These high numbers highlight the need for investigation on cancer epigenetics for the understanding of tumor biology and the development of new therapies.

1.1.5. Epigenetic regulators as cancer therapeutic targets

Owing to the importance of epigenetic deregulation in neoplasms, epigenetic therapies have been lately proposed as a new therapeutic alternative[8,38]. These consist in the pharmacological targeting of epigenetic regulators of the different levels, as a strategy to revert oncogenic traits gained through epigenetic alterations in cancer. Epigenetic control of gene expression is a multi-level network in which multiple players take part. Any epigenetic event responds to internal or external triggering stimuli, which have been named *'epigenator'*, such as the

activation of developmental pathways or hormone-mediated signaling[6]. This first stimulus induces the chemical changes upon chromatin known as *epigenetic signals,* already explained. The regulators implicated in these modifications are known as *epigenetic writers* and *erases* and are mainly proteins with the enzymatic capacity of positioning or eliminating the epigenetic signals from DNA or histones. These signals do not exert chromatin structural effects by themselves, but rather act as flags for their recognition by specific proteins, known as *epigenetic readers*, which bind to the epigenetic signals and recruit the proteins responsible for actively generating the pertinent chromatin changes. This last group of proteins have been named *remodelers*, but also *epigenetic maintainers*, because on its function relies the responsibility of maintaining chromatin states throughout time[6,8] (Figure 2).

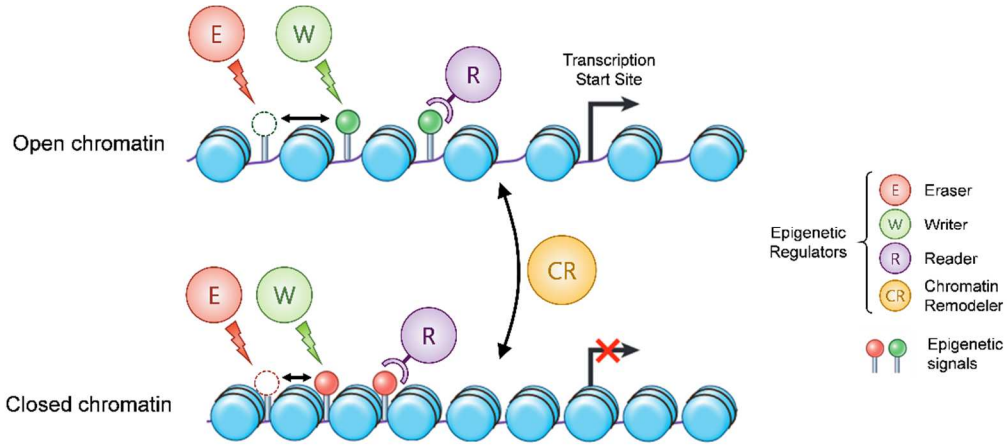

Figure 2: The four groups of epigenetic regulators, adapted from Ahuja *et al.* (2016)[8]. While epigenetic writers (W) and erasers (E) balance the levels of the different epigenetic signals, readers (R) recognize them and trigger the signaling process that ends in changes of the chromatin state through the action of chromatin remodelers (CR).

Epigenetic writers and erasers

The enzymes responsible for the generation of the main epigenetic signals, namely DNA methylation and histone acetylation and methylation, are DNA-methyltransferases (DNMT), histone acetyltransferases (HAT) and histone methyltransferases (HMT), respectively. On the contrary, the specific erasers of these modifications are histone deacetylases (HDAC) and histone demethylases (HDM), together with the Ten-Eleven Translocase (TET) family of proteins, which mediate the active erasing of DNA methylation through multiple steps of oxidation[38,64]. These are large groups of proteins, from the 18 HDACs to the more than 60 HMTs identified in

the human genome, that have been classified in subfamilies according to homology and functional similarities, such as the histone residue of preference modification, or the cellular compartment where they exert their functions (Table 1). These enzymes have been widely implicated in oncogenic processes, and some of them are proposed as therapeutic targets for the treatment of certain cancers.

For example, DNMTs have been widely studied as cancer therapeutic targets for the reversion of aberrant DNA methylation patterns. While DNMT1 is required for the maintenance of methylation after DNA replication, DNMT3A/B are implicated in the *de novo* methylation of promoters, which is related to the silencing of several tumor suppressor genes in different scenarios[65,66]. Inhibition of these proteins by cytidine analogues was one of the first epigenetic therapy strategies. The most tested inhibitors of this class are 5-azacytidine and its more potent modification 5-aza-2'-deoxycytidine (also known as decitabine)[67], which are able to reactivate silenced genes under hyper-methylated CpG islands, being a therapeutic strategy for a certain group of tumors[68]. Indeed, although with problems of toxicity, low doses of DNMT inhibitors have been proved to exert efficient anti-cancer effects in different clinical trials, receiving the FDA approval for the treatment of hematologic malignancies such as myelodysplastic syndrome[69]. In the case of the recently discovered DNA methylation eraser TET proteins, multiple and varied functions have been found for several tumor types, both oncogenic and tumor suppressive[64], but there is still a lack of inhibitors for the targeted inhibition of these family of proteins.

Table 1: Epigenetic writers, erasers and readers families and subfamilies of the main epigenetic signals. Based on [8,70].

Epigenetic signal	*Writers*		*Erasers*		*Readers*
DNA methylation	**DNMT**:	DNMT1 DNMT3A/B	**TET**:	TET1 TET2 TET3	MBD MeCP2
Histone acetylation	**HAT**:	GNAT p300/CBP MYST SRC	**HDAC**:	Class 1 Class 2a Class 2b Class 3 Class 4	Bromodomain PHD finger
Histone methylation	**HMT**:	PKMT PRMT	**HDM**:	LSD JHDM	Chromodomain Tudor-domain MBT domain PHD finger

HDACs are, together with DNMTs, the epigenetic regulators most studied in cancer and for which several therapeutic strategies have been already developed. HDAC are a big group of proteins classified in 5 classes according to homology criteria (Table 1). Their implication in cancer is similar to that of DNMTs, since HDAC-mediated reduction of histone acetylation generates closed chromatin domains and transcriptional silencing of genes, in many cases concomitant with DNA hyper-methylation, and HDAC inhibition therapies reactivate aberrantly silenced genes[71]. Multiple HDAC inhibitors have been developed: from the first reported class 1/2 inhibitor valproic acid, to the most studied and potent pan-HDAC inhibitor vorinostat (or SAHA) which have been already approved for the clinical management of cutaneous T-cell lymphoma. Other more specific inhibitors, such as romidepsin or tucidinostat class I HDAC inhibitors, have also been approved for the treatment of lymphomas (reviewed in [72]). Many other HDAC inhibitors are under clinical trial testing[8]. Moreover, clinical trials evaluating the effects of combining DNMT and HDAC inhibitors have shown efficacy in aggressive tumors such as lung cancer[73].

On the other side, HATs, also known as lysine acetyl transferases (KATs) were the first histone modifiers discovered. Two types of lysine acetyltransferases are defined: type-A, corresponding to the majority of known HATs from GNAT, MYST and CBP/p300 families, which are nuclear and modify histones already assembled into nucleosomes; and the less numerous type-B, such as HAT1, which are cytoplasmic and modify free histones before assembly into nucleosomes[74]. Involvement of some HATs on genomic rearrangements generating fusion proteins have been widely reported[38]. The fusion of a HAT domain with transcription factors leads to a transcriptional hyper-activation of certain genes which drives tumor progression in certain leukemias. However, development of HAT inhibitors is much less advanced. Some naturally occurring low specific molecules such as curcumin were determined to exert HAT inhibition activity[75]. Nevertheless, small molecules are being designed for the inhibition of certain HATs, such as A-485, against p300/CBP, with anti-tumor effects in leukemias and prostate cancer, and PU139 and PU141 HAT inhibitors, which reduced tumor growth of neuroblastoma[76].

Histone methyltransferases are the group of epigenetic writers with more known members, with more than 60 genes encoding this kind of enzymes identified in the human genome[77], and are divided in lysine methyltransferases (PKMTs) and arginine methyltransferases (PRMTs). PKMTs include cancer-relevant HMTs such as the H3K79 methyltransferase DOT1L, known to have

oncogenic roles in certain leukemias[78]; the H3K27 methyltransferase EZH2, catalytic subunit of the developmental epigenetic regulator PRC2, mutations on which, as mentioned before, are widely implicated in certain cancers[56]; and the H3K4 methyltransferase MLL, frequently implicated in genomic rearrangements in myeloid and lymphoblastic leukemia. MLL fusion proteins promote a gain of function of the methyltransferase activity, increasing the levels of the activation mark H3K4me2, favoring the expression of stemness genes[79]. Multiple inhibitors against this class of epigenetic writers have been developed, being those against EZH2 the ones with more clinical projection nowadays (reviewed in [76]).

Finally, HDMs are also being studied as cancer therapeutic targets[80]. There are two main families of this kind of epigenetic erasers: LSD (or KDM1) family, which demethylate mono- o bi-methylated lysine 4 of histone H3 (H3K4), a transcriptional activation mark[81]; and the JHDM family, which demethylate both transcriptional activation or repression-related tri-methylated lysines[80] and, some of them, methylated arginines[82]. LSD1 activity on H3K4 methylation state has been observed to be essential for the viability of several cancer types[80]. A big number of LSD1 candidate inhibitors have been intensively studied, and up to 7 of them have reached clinical trials for hematologic malignancies and some solid tumors[83]. Different inhibitors still in early development stages have also been designed against a subgroup of the JHDM-family KDM5 demethylases, also known as JARID[84,85], which also demethylate H3K4 and promote oncogenic traits and drug resistance in different malignancies[86].

Epigenetic readers

The specific recognition of epigenetic signals for the translation into functional chromatin changes is carried out by certain protein domains with highly conserved and specific binding affinities (Table 1). DNA methylation is recognized by different specific binding proteins, concretely four different methyl-CpG-binding domain (MBD)-containing proteins (MBD1/2/4 and MeCP2), which recruit further machinery for heterochromatin formation[87]. In the case of histone methylation, these functions rely on chromodomain, *Tudor*-domain, MBT domain and PHD finger-containing proteins[88], which are present in specific proteins, or carried in epigenetic writers, erasers or remodelers. One important chromodomain-containing protein is HP1, a crucial regulator for the formation of high levels of heterochromatin, in which the chromodomain binding affinity for repressive histone methylation mark at H3K9 is essential for its chromatin condensation functions[89]. PHD fingers, on the contrary, are versatile epigenetic

readers that can also bind to activation methylation histone marks, such as the binding to tri-methylated H3K4 by BPTF transcriptional activator[90], and inhibitors against this kind of domains are starting to be discovered[91,92]. The versatility of PHD fingers reaches the point in which they are also able to recognize acetylated marks, as in the case of the transcriptional activator DPF3[93].

Nevertheless, the most studied epigenetic readers, and most implicated in cancer, are by far the lysine-acetylated histone binding bromodomains. Up to 46 different genes encoding bromodomain-containing proteins are found in the human genome, including relevant transcriptional regulators such as the histone acetyltransferase GCN5L2, the transcriptional activators of the bromodomain and extra-terminal (BET) protein family (BRD2, BRD3, BRD4, and BRDT), and subunits of the SWI/SNF chromatin remodeler such as SMARCA2, SMARCA4 or BRD7[94]. The implication of bromodomain-containing proteins in cancer has been extensively reviewed and many tumors show dependencies on some of these proteins[95]. Bromodomains have been a model for structure-based design of protein-protein interaction inhibitors, and consequently multiple inhibitors have been generated during the last ten years, since the development of the first BRD2/3/4 inhibitor, JQ1, in 2010[96]. Together with JQ1, up to 20 different BET and other bromodomain-containing protein inhibitors have been shown to have preclinical anti-cancer effects, and at least 4 BET inhibitors, including JQ1, and one inhibitor of the p300/CBP bromodomain have reached the clinical trials against prostate cancer and different types of leukemia[95].

Chromatin remodelers

The terminal consequence of epigenetic signaling through *writing*, *erasing* and *reading* are structural changes in chromatin, for the achievement and maintenance of which the active function of specific regulators, named remodelers, is necessary. Some chromatin modifying proteins have been classified as chromatin remodelers, such as the histone chaperones able to interchange histone variants that promote structural changes in chromatin condensation[39], or multi-protein complexes that integrate and synchronize the activity of multiple epigenetic *writers* and *erasers* such as the *Polycomb* repressing complexes[97]. However, the most canonical group of molecular complexes exerting mechanical functions that promote structural changes in chromatin in response to epigenetic signals are the ATP-dependent chromatin remodelers.

In eukaryotes, four families of ATP-dependent chromatin remodelers have been defined: ISWI, CHD, INO80 and SWI/SNF complexes. Each one has specific remodeling functions (Figure 3), although all of them exert their activities through DNA translocation and repositioning of nucleosomes (reviewed in [98]). On the one hand, ISWI and CHD complexes are directly implicated in the assembly of new nucleosomes as well as in their regular spacing throughout the chromatin, repressing chromatin accessibility and transcriptional expression[99,100]. Some CHD complexes, however, have been implicated in the generation of open regions of chromatin accessibility and nucleosome editing, that is to say, the interchange of different histone variants in already assembled nucleosomes[101,102]. INO80 complexes are highly specialized in these nucleosome editing functions, inducing the incorporation of H2A.Z and H2A.X variants, for example[103]. Finally, SWI/SNF ATP-dependent chromatin remodelers have opposite effects to those of ISWI complexes: they disorder nucleosome patterns by sliding and ejection of histone octamers, increasing chromatin accessibility at promoters and other regulatory elements, and facilitating the access of the transcriptional machinery and other regulatory proteins.

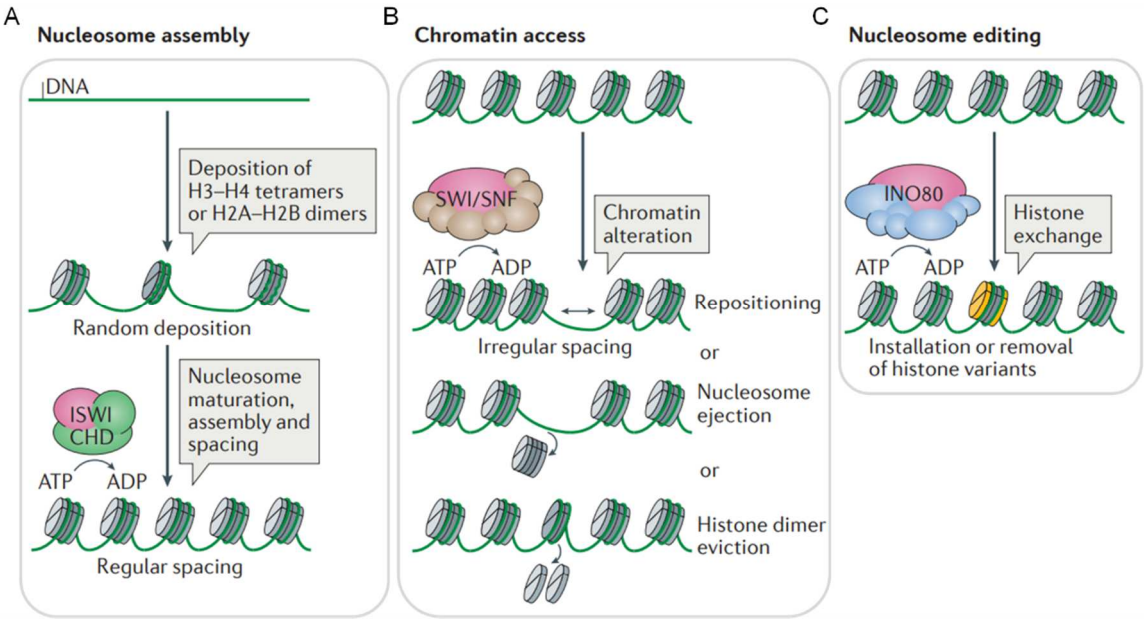

Figure 3: The three functions of eukaryotic ATP-dependent chromatin remodelers, extracted from Clapier *et al.* (2017)[98]. ISWI and CHD remodeler generally have respressive effects on gene expression, by mediating the assembly of histone octamers and the spatial deposition of nucleosomes (**A**), whereas SWI/SNF complex has opposite effects: it disrupts the regular histone octamers spacing by generating nueclosome-depleted regions (**B**). INO80 remodelers are more specialized in nucleosome editing by exchange of histone variants (**C**).

1.2. **The SWI/SNF chromatin remodeling complex**

Among the different ATP-dependent chromatin remodelers found in eukaryotic cells, the Switch/Sucrose Non-Fermenting (SWI/SNF) complex is the most studied one, with increasing amounts of scientific literature being produced yearly for the last two decades (Figure 4A). The reasons behind the broad interest on the study of this molecular machine are, presumably, the great importance found of this chromatin remodeler in controlling gene programs during development of multicellular organisms[104–106] and, most importantly, the discovery during the last twenty years of numerous molecular alterations of its structure and function associated with human disease, and especially its involvement in an illness of such scientific interest and social relevance as cancer is[107–110]. Concretely, almost half of the SWI/SNF chromatin remodeling complex published literature is related to cancer, approximately twice the percentage of cancer-related publications involving the other three main groups of eukaryotic chromatin remodelers (Figure 4B). The increasing interest made this chromatin remodeler focus the efforts of many research lines, generating a large amount of knowledge about SWI/SNF's structure, molecular functions and role in health and disease.

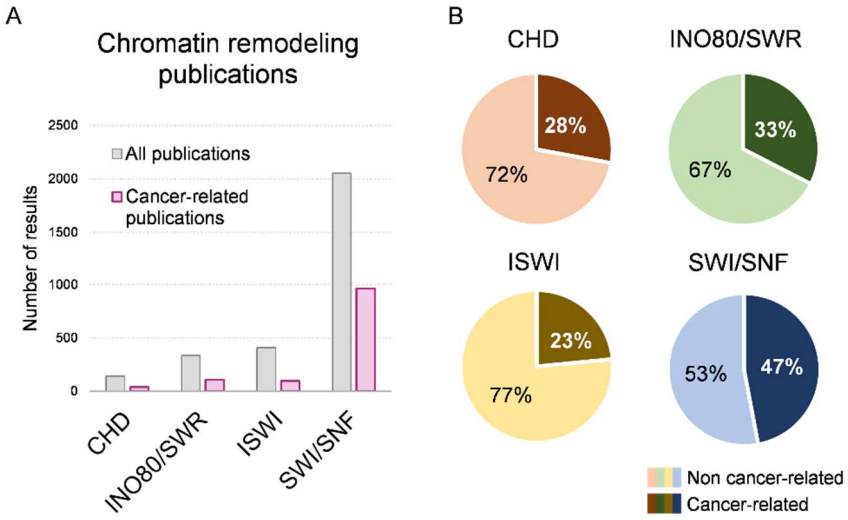

Figure 4. Impact of eukaryotic chromatin remodelers on the scientific literature. **A**. Number of scientific publications found in MEDLINE database for each chromatin remodeler group. Number of results is shown for searches in PubMed using the following query: *'name of the chromatin remodeler' AND chromatin (remodeling OR remodeler)*. For cancer-related publications, *AND cancer* was added to the query. **B**. Percentage of cancer related and non-related publications for each group of chromatin remodelers. Source: PubMed (pubmed.ncbi.nlm.nih.gov), consulted on August 25th, 2021, at 9:37h (UTC +01:00).

1.2.1. The yeast SWI/SNF complex

The group of genes encoding the subunits of the SWI/SNF complex were first discovered in yeast (*Saccharomyces cerevisiae*) during the 1980s in two independent and parallel research lines focused on the discovery of regulators of gene expression. On the one hand, a group of genes named *SWI* (*SWI1*, *SWI2* and *SWI3*) were found to be involved in the mating type switch of *S. cerevisiae* by regulating the expression of *HO* gene, which is essential for this process[111,112]. Subsequent studies showed the capacity of this family of proteins to control the expression of several groups of genes through transcriptional regulation[113–115]. In parallel, another group of proteins was found to be necessary in yeast for the catabolism of sucrose by controlling the expression of *SUC2* gene, which encodes the invertase enzyme. These genes were named as 'Sucrose Non-Fermenting' or *SNF* genes (*SNF2*, *SNF5* and *SNF6*)[116,117] and were found to be responsible as well for the expression regulation of different groups of genes beyond sucrose metabolism[118–121]. These findings led to the conception of *SWI* and *SNF* genes as generic regulators of gene expression at the transcriptional level. Later studies determined by sequencing that *SNF2* and *SWI2* were the same gene[122,123] and identified overlapping functions on gene transcriptional control by the two groups of genes[114,124], establishing the first links between both families of transcriptional regulators. Eventually, the proteins encoded by *SWI* and *SNF* genes were found to physically interact, together with at least four additional proteins, forming a high molecular weight multi-subunit SWI/SNF complex, named after both gene families, able to assist in the expression control of multiple gene sets[125–127].

The first evidences pointing to a link between *SWI* and *SNF* genes and chromatin remodeling came from the study of suppressing mutations in yeast. Mutations in a group of genes, called *SIN* after 'Swicth Independent', were found to suppress the effects of *SWI* mutations on the transcription of target genes[113,128]. Intriguingly, these genes included chromatin-related proteins such as *SIN1*[129], and even histone coding genes such as *SIN2*, which encodes for histone H3[130,131]. On the other side, similar suppressing mutations were found for *SNF* genes[132,133] and hemizygous loss of histones H2A and H2B suppressed the effects of mutations in these genes[134]. This antagonistic relationship between SWI/SNF genes and chromatin structural components pointed towards the transcriptional activation by SWI/SNF complex through alleviation of the constraints of chromatin condensation[131,135–137]. Posterior evidence fully demonstrated the specific and conserved molecular function through which SWI/SNF is able to perform the

regulation of gene expression at the transcriptional level. The *SWI2/SNF2* subunit, which contains sequence motives found in DNA-dependent ATPases[138], is the catalytic subunit of the complex[125,126,139] and provides it with the ability of using ATP as energetic resource for changing the compaction state of the chromatin, creating nucleosome-depleted regions (NDR) and facilitating the access to DNA[126,134,140,141]. This gain of accessibility is produced by the sliding of nucleosomes and their eviction from DNA[142–145]. Through this mechanism the SWI/SNF complex acts as a transcriptional coactivator that facilitates the access of transcription factors to genetic regulatory elements in an ATP-dependent manner, controlling this way the expression of target genes at a genome-wide range[146].

Detailed study and characterization has determined the composition and stoichiometry of the yeast SWI/SNF complex, showing high levels of structural complexity: it is formed by up to 12 different subunits, including the originally discovered five *SWI* and *SNF* gene products together with 7 additional subunits. These additional subunits include the structural and essential subunit Swp73[147], the two actin-related proteins Arp7 and Arp9, relevant for regulation of the catalytic activity[148,149], and Rtt102, identified later by mass spectrometry proteomic approaches[150,151] and also found to be a regulator of the ATPase activity of the complex[152]. The rest of the accessory subunits, which have been determined to be less functionally necessary, are the transcription factor Taf14/Swp29[153] and the subunits of uncertain role Snf11[154] and Swp82[155]. Moreover, stoichiometry and structural analysis have shown that the majority of the subunits are present individually in the complex, but some of them bound in multiple copies. This is the case of Swi3 protein, found in dimers inside the complex[156,157].

Moreover, the finding of a *SWI2/SNF2* paralogue, named *STH1*, with ATPase activity[138,158] together with the posterior identification of multiple paralogues of SWI/SNF subunits revealed the existence of another ATP-dependent chromatin remodeling complex in yeast, named RSC complex (after *Remodeling the Structure of Chromatin*)[158], also exerting the same effects on chromatin remodeling and genome-wide transcriptional control[159,160]. It is a bigger 16-subunit complex whose catalytic activity is located at Sth1 protein[161]. It is formed by the subunits Arp7, Arp9 and Rtt102, which are shared with SWI/SNF complex[162,163], together with the four highly similar paralogues of SWI/SNF subunits Sth1 (Snf2/Swi2 paralogue), Rsc6 (Swp73 paralogue), Rsc8 (Swi3 paralogue) and Sfh1 (Snf5 paralogue), and up to 10 RSC-dedicated subunits[158,164,165]. Although the four homologous subunits found were complex-specific and each variant was

only present in one out of the two complexes, the fact that the core of proteins conserved between both remodelers consisted in those proteins of most functional relevance for chromatin remodeling[165,166], in addition to the quasi-identical molecular functions[167,168], led to the classification of SWI/SNF and RSC as siblings of the same chromatin remodeling family, named SWI/SNF chromatin remodeling complexes.

1.2.2. Evolutionary conservation of SWI/SNF: from lower to higher eukaryotes

Since its discovery in yeast, multiple SWI/SNF counterparts have continuously been discovered by identification of orthologous proteins in a wide range of different eukaryotic organisms, from plants (*Arabidopsis thaliana*)[169,170] to metazoans, both protostomes, such as *Caenorhabditis elegans*[171] and *Drosophila melanogaster* (fruit fly)[172], and deuterostomes of increasing complexity, including *Danio rerio* (zebrafish)[173], *Gallus gallus domesticus* (chicken)[174,175], *Mus musculus* (mouse)[176], up to *Homo sapiens* (human)[177]. This level of conservation, which is wider than that of other epigenetic regulatory mechanisms such as Polycomb repressing complexes, condensation by histone H1 or DNA methylation[107], illustrates the functional relevance of this chromatin remodeler in eukaryotic organisms.

Drosophila melanogaster was the second organism in which SWI/SNF homologues were discovered, by the identification of *Brahma* (*brm*) gene. This gene was first found by its interplay with the *Polycomb* gene family, an important group of developmental regulators known to control the expression of homeotic genes. Homeotic genes form the *Antennapedia* (ANT-C) and *Bithorax* (BX-C) complexes, transcription factors that control de identity of the different segments of *D. melanogaster*[178,179], and its specific spatio-temporal expression is regulated by two main groups of genes: *Polycomb* repressors[180,181], and their antagonistic activating counterparts *Trithorax* genes[182]. *brm* was identified as one of the Trithorax family of activators due to its suppressive effects on *Polycomb* mutations and the homeotic-like phenotypic effects of its mutations[183,184], what suggested its implication in the active regulation of homeotic gene expression. Indeed, *brm* was determined to be an orthologue of yeast *SWI2/SNF2*[172,184], and also found to exert the same ATPase-dependent functions[185]. Posterior purification of the *brm* associated complex identified several *brm* associated proteins (BAP) that included *Trithorax* genes *moira* (*mor*) and *osa*, but also previously unknown subunits, resulting many of them to be orthologous of some of the yeast SWI/SNF subunits[171,186–192] (listed in Table 2). This

Drosophila BAP complex was observed to be less genetically heterogeneous than yeast SWI/SNF, since the majority of the subunits were codified by single genes and no paralogues were found[186]. However, an alternative complex was found, characterized by the presence of BAP170 instead of *osa* and the additional subunit *polybromo*. Due to the similarities of the latter with Rsc1/2 and Rsc4, this *polybromo*-associated *brahma*-associated protein (PBAP) complex was determined to be the *Drosophila* counterpart of the RSC complex[193]. These BAP and PBAP complexes, as expected, showed the same transcriptional regulatory functions at the level of chromatin remodeling as in yeast at a genome-wide level[193–196], although the dissimilarities of structural composition suggested functional differences between both species[186]. In fact, the expression of this complex was found to be sensibly higher in *D. melanogaster* tissues than in *S. cervisiae*, and BAP complex was essential for the viability of *D. melanogaster* embryos, unlike in yeast[197].

Eventually, a human homologue of yeast *SWI2/SNF2* and *Drosophila brm* with ATPase activity was found and named *brahma*-related gene 1 (*BRG1*), or *SMARCA4*[177], together with a close paralogue with high rates of sequence similarity, human *brahma* (*BRM*) or *SMARCA2*[198]. Human SWI/SNF complex was later purified, characterized and named BAF after *BRG1-associated factor*[199,200]. Due to the high levels of similarity of human and mouse SWI/SNF complexes, both were grouped together as mammalian SWI/SNF (mSWI/SNF) complexes[176,200]. Two different complexes, first named SWI/SNF-A and B, were also discovered in human cells[200], which later became known as BAF and PBAF (*Polybromo-associated BAF*) complexes, respectively[201]. PBAF was found to be the human counterpart of yeast RSC and *Drosophila* PBAP complexes, since it contained specific and committed subunits orthologous of its lower eukaryotic counterparts: *PBRM1* (*Rsc1/2*, *Rsc4* and *polybromo* orthologue) and *ARID2* (*Rsc9* and *bap170* orthologue)[193,201–205]. An important finding from the evolutionary study of this remodeler is the humongous genetic, structural and functional variability observed in human SWI/SNF in comparison with *Drosophila* complexes. As shown in Table 2 and Figure 5, when complexes of the three species are compared, 9 subunits are lost from yeast to *Drosophila*, and 5 new subunits appear in mammals. These mammalian subunits are codified by a total of 10 genes, as 3 of them have multiple interchangeable paralogues. Indeed, this is the main source of variability of mammalian complexes, giving place to an exponential increase of possible subunit combinations when compared to that of *Drosophila*, which only present two strict variants of the complex.

The simplicity of BAP and PBAP complexes in comparison with the functional heterogeneity of mSWI/SNF complexes is thought to be a reflection of the increasing tissue and organ specialization. For example, multiple paralogue exchanges during mammalian development have been reported to be essential for the correct formation of the nervous system: for correct differentiation of proliferative neural progenitors to non-proliferating differentiated neurons, specific changes in paralogue composition need to be produced, including substitution of DPF2 by DPF1/3, ACTL6A by ACTL6B, and SS18 by CREST (SS18L1)[206–209].

Table 2: Evolutionary conserved and non-conserved SWI/SNF subunits among three eukaryotic organisms.

	S. cerevisiae		*D. melanogaster*		*H. sapiens*	
	SWI/SNF	RSC	BAP	PBAP	BAF	PBAF
ATPase	***Swi2-Snf2***	***Sth1***	***brm***		***SMARCA2 / 4***	
Histone binding	***Snf5***	***Sfh1***	***snr1***		***SMARCB1***	
Structural	***Swi3***	***Rsc8***	***mor***		***SMARCC1 / 2***	
	Swp73	***Rsc6***	***bap60***		***SMARCD1 / 2 / 3***	
			bap111		***SMARCE1***	
ATPase accessory	***Arp7***		***act***		***ACTB***	
	Arp9		***bap55***		***ACTL6A / B***	
					BCL7A / B / C	
ARID-containing	***Swi1***		***osa***		***ARID1A / B***	
		Rsc9		***bap170***		***ARID2***
PBAF-like specific		***Rsc4***		***polybromo***		***PBRM1***
		Rsc1 / 2				
		Rsc3 / 30				
		Rsc58				
		Rsc7				
		Rsc14				
		Htl1				
						BRD7
						PHF10
BAF-like specific	*Taf14*					
	Swp82					
	Snf11					
	Snf6					
					DPF1 / 2 / 3	
					SS18 / SS18L1	
Other	*Rtt102*					

Orthologous between and paralogues within species are represented in the same row. Interchangeable paralogues are separated by "/". Subunits without orthologous counterparts are marked in grey.

The study of these molecular machines in multiple organisms has revealed its functional relevance, reflected in the high levels of conservation among eukaryotes, but also the differences between them have revealed interesting insights into its evolutionary sense. Changes in subunit composition and complexity have been proposed to be a reflection of the molecular consequences of the evolutionary leap from uni- to multicellularity, two life forms with different needs of gene expression[107]. While organisms such as *S. cerevisiae* tend to maintain expressed the majority of their genes in the same cell and only need differential expression of genes in response of external stimuli, multicellular organisms are able to develop differentiated and specialized tissues by setting specific transcriptional programs for each cell type that are generated and maintained by epigenetic mechanisms, of which chromatin remodelers, and especially the SWI/SNF complex, are active effectors. The evolution in composition and variants of the SWI/SNF complex observed from yeast to low and high complexity multicellular life forms might be the evolutionary answer for the needs of higher multicellular eukaryotes for tissue specialization and complexity.

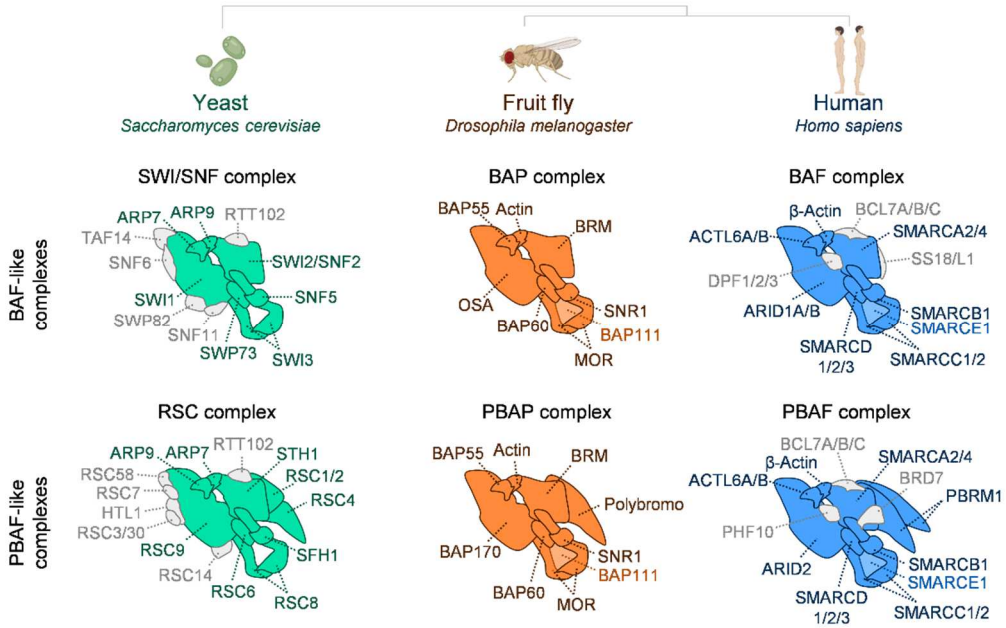

Figure 5: Evolutionary conservation of mSWI/SNF complexes, represented by the subunit composition of yeast, fruit fly and human complexes. Conserved subunits across species are shown colored, non-conserved in grey.

1.2.3. The mammalian SWI/SNF complex: composition, subtypes and assembly

The mSWI/SNF complexes are 1 to 1.5 megadalton (MDa) multiprotein macro-complexes formed by a variable number of subunits, ranging from 10 to 13 polypeptides per individual complex. However, the proteins forming part of the different forms of mSWI/SNF are encoded by a total of 29 different genes. As mentioned before, this immense genetic complexity in mammalians is mainly based on the presence of multiple mutually-exclusive exchangeable paralogues, adding up to 10 different homology families[198,210–214] (Table 3). The mSWI/SNF complex has a modular structure: it is composed by structural and functional modules with clear physical delimitation and co-stability[215], and certain level of functional independence[216]. The two main constitutive modules are the core –or base– and the ATPase –or catalytic– modules, which form part of all complex variants and are fundamental for its proper assembly, structural integrity and remodeling activity. Besides these two structural modules, additional facultative subunits are optionally included, with both structural and functional relevance, and determine the existence of different 'subcomplex' variants.

The core module

The core, or base, structural module is formed by five of the most conserved subunits: two dimerized units of the SMARCC1/2 paralogue family, which can be homo- or heterodimers; and one unit of each of the following: SMARCD1/2/3, SMARCB1 and SMARCE1[210,215,217,218]. The core module contains well conserved and tight interactions among its members and acts as a structural scaffold, being essential for the assembly of the whole complex and ensuring the correct interaction between and with the rest of the subunits[215,219,220]. In fact, two of the core subunits, SMARCC1/2 and SMARCD1/2/3, are essential for the structural integrity of the whole complex and, consequently, for its activity[215,216,221].

Besides structural integrity, relevant properties necessary for the chromatin remodeling activities of the complex are present in this module. SMARCD1 has been observed to establish important interactions with different proteins external to the complex, including several transcription factors and nuclear receptors, suggesting its importance for the targeting of the complex to specific genomic sites[222–226].

Table 3: Genes encoding human mSWI/SNF subunits, grouped by structural module and paralogue family.

Module	*Paralogue Family*	*Official Gene Symbol*	*Also known as*
Core		*SMARCB1*	hSNF5, INI1, BAF47
	SMARCC	*SMARCC1*	BAF155
		SMARCC2	BAF170
	SMARCD	*SMARCD1*	BAF60A
		SMARCD2	BAF60B
		SMARCD3	BAF60C
		SMARCE1	BAF57
ATPase	SMARCA	*SMARCA2*	BRM, BAF190B
		SMARCA4	BRG1, BAF190A
	BCL7	*BCL7A*	
		BCL7B	
		BCL7C	
	Actin-like	*ACTB*	β-Actin
		ACTL6A	BAF53A, ArpNβ
		ACTL6B	BAF53B, ArpNα
BAF-specific	ARID1	*ARID1A*	BAF250A
		ARID1B	BAF250B
	DPF	*DPF1*	BAF45B
		DPF2	BAF45D
		DPF3	BAF45C
	SS18	*SS18**	SYT, SSXT
		*SS18L1**	CREST
PBAF-specific		*ARID2*	BAF200
		PHF10	BAF45A
		*PBRM1**	Polybromo 1, BAF180
	BRD	*BRD7*	BP75
ncBAF-specific		*BRD9*	
	BICRA	*BICRA*	GLTSCR1
		BICRAL	GLTSCR1L

*SS18/L1 and PBRM1 are BAF and PBAF-specific subunit, respectively, but they have been reported to structural and functionally be part of the ATPase module, each of its respective complex. SS18/L1 is also present in ncBAF[214,215].

SMARCB1, also known as INI1 or human SNF5 (hSNF5)[227], is not necessary for structural integrity of the complex[155,228] but is relevant for the remodeling activity, since it is responsible for the tight binding of the complex to the nucleosome acidic patch[229]. SMARCE1 is also not necessary for structural integrity[215], but has DNA-binding properties contained in its high-mobility group (HMG) domain, an activity observed to be relevant for the correct remodeling activity of the complex[191,230,231].

The ATPase module

The other constitutive part of the complex is the ATPase module, which carries the catalytic activity necessary for active chromatin remodeling. This module has been observed to display a marked independence in a structural sense, since the integrity of its subunits and interactions are maintained when separated from the rest of the complex[215], but also in a functional sense, since it preserves chromatin remodeling capacities at some extent when isolated[216]. The main and most essential subunit of this catalytic module is the ATPase subunit that, as explained before, in humans corresponds to the pair of mutually-exclusive homologues SMARCA4/BRG1 and SMARCA2/BRM[177,198]. Thus, ATPase module is composed by one unit of the SMARCA2/4 paralogue family together with three constitutive ATPase accessory subunits with relevant functions in the regulation of the catalytic activity. These three accessory subunits are one out of the two paralogous actin-related proteins (ARP) ACTL6A/B, one unit of β-actin (ACTB) and one out of the three BCL7 paralogues[232] (see Table 3).

The presence of globular actin and ARPs in the nucleus and its role in chromatin remodeling has been reported for quite a long time[233,234]. One unit of β-actin and one of the ACTL6 ARP paralogue family are assembled into the ATPase module of SWI/SNF complex forming dimers, and interacting with SMARCA2/4 catalytic subunit[235–237]. The main function of these group of accessory subunits is to assist the ATPase subunit in its catalytic functions. On the one hand, β-actin has full ATPase capacity by itself, and this property has been shown to potentiate the catalytic activity of the complex[238]. On the other hand, ARPs are actin homologues with regulatory functions and ATP-binding properties, which have been proved promote the stabilization of the ATPase module[237] and to be key modulators of the catalytic activity of SMARCA2/4, thereby modulating the intensity of chromatin remodeling[238–241].

Moreover, besides their role in catalytic modulation, ACTL6A/B have been shown to display other significant functions, such as binding to histones[237] and different transcription factors[242–244], suggesting a potential genomic occupancy targeting role of these subunits. Conversely, BCL7A/B/C are recently identified subunits[232,245] with yet uncertain role, but known to interact through its N-terminal domain with the complex[246] and to form part of the ATPase module in all mSWI/SNF complex variants.

The core and ATPase constitutive modules are necessary for the assembly and function of the mSWI/SNF complex, but not sufficient. Additional non-ubiquitous facultative subunits need to be incorporated in the forming complex, for both to complete the structural assembly by bridging core and ATPase module[215] and to confer specific properties to the different complex subtypes formed by different facultative subunits, mostly related to different genomic occupancies[247,248]. As far as is known today, mammalian cells contain three main mSWI/SNF complex subtypes or variants: BAF (or canonical BAF), PBAF and non-canonical BAF (ncBAF) complexes (Figure 6). These three complexes are cellular-coexistent, meaning that can be found expressed and assembled simultaneously in the same cell[200,248], and are defined by different compositions of facultative subunits. Therefore, different complex subtypes share all –or almost all– the constitutive subunits explained before, and differ in the subtype-specific facultative subunits that contain. These specific subunits include structurally relevant proteins, but also DNA and histone-modification binding proteins, which are thought to provide them of specialized targeting functions.

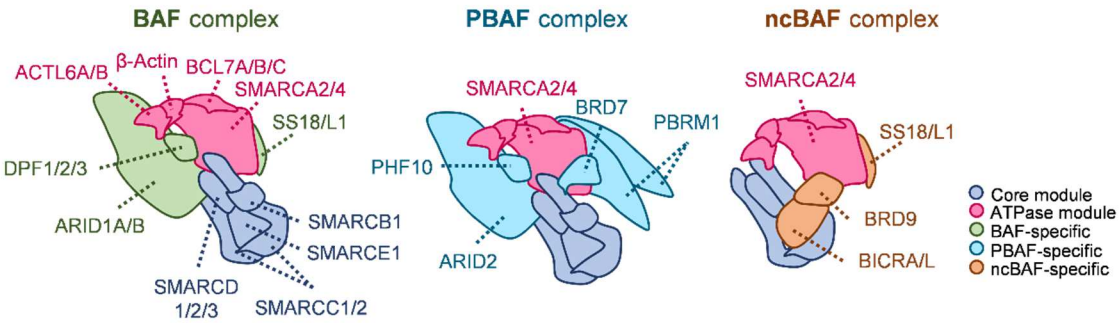

Figure 6: Known same cell-coexistent human mSWI/SNF complex variants: BRG1-associated factor 'BAF' complex (green), Polybromo-associated BAF 'PBAF' complex (blue) and non-canonical BAF 'ncBAF' complex. Subtype-specific and shared subunits are shown, indicated whether pertaining to core or ATPase modules. Graphical representation based on the design from Mashtatalir *et al.* (2018)[215].

BAF complex

The canonical BAF complex contains three specific proteins that belong each one to three different paralogue families: ARID1A/B, DPF1/2/3 and SS18/SS18L1 (see Table 3). ARID1 proteins are a pair of mutually exclusive highly similar paralogues, ARID1A and ARID1B, which happen to be the subunits with higher molecular weight found in any SWI/SNF complex[213,249–253]. These subunits contain AT-rich interaction domains (ARID), characterized by conferring non-sequence specific DNA-binding properties to their containing proteins. In fact, ARID1 proteins have been reported to confer this kind of DNA-binding capacity to the complex[249,254–256], and this feature is nowadays believed to contribute to the nucleosome binding capacities of the complex[98]. However, this family of subunits has been recently proved to be one of the most relevant structural pieces of BAF complex, on the base of its direct interactions with other subunits and its tridimensional positional relevance. On the one hand, ARID1 proteins accumulate the majority of intra-complex protein-protein interactions, assessed by means of cross-linking mass spectrometry in two independent and consistent studies. These interactions involve several constitutive subunits of both core (SMARCC, SMARCD, SMARCE1) and ATPase (SMARCA, ACTL6A) modules, and are specially concentrated in its C-terminal fragment, where specific interaction domains have been identified, known as core binding regions (CBR), coincident with the previously described *armadillo* (ARM) sequence repeats[215,257,258]. On the other side, tridimensional structure of the complex revealed the high levels of organization and conservation of the surface residues in these interfaces, suggesting that ARID1 proteins act as stabilizers of the complex, bridging the two constitutive modules[258,259].

Therefore, ARID1 proteins are believed to be key structural bridges crucial for the specific assembly progression of BAF complex and the proper interaction of the core and ATPase constitutive modules in this complex subtype. Indeed, ARID1 assembly is necessary for the subsequent incorporation of the DPF subunit, another BAF-specific facultative member. DPF1/2/3 subunits are another interchangeable paralogue family specific of the BAF complex[206,211,260]. These proteins contain each one a double plant homeodomain (PHD) finger, which are evolutionary conserved epigenetic reader domains. Concretely, they have been shown to be versatile readers of histone tail modifications[261]. Indeed, members of the DPF family have been demonstrated to bind to different histone marks related to active gene expression at promoters and enhancers, including acetylation of histones H3 and H4[262,263], mono-

methylation of lysine 4 of histone H3[264] and the recently discovered histone mark crotonylation[265,266]. These features suggest that DPF subunit exerts genomic occupancy targeting through histone mark reading, and could be a key factor in the functional differentiation between different mSWI/SNF subtypes.

Finally, the third BAF-specific subunit is SS18[267], or its paralogue SS18L1, also known as CREST[212,245]. Although not constitutive, it has been proved to associate directly with SMARCA catalytic subunit[268] and form structural part of the ATPase module[215]. Its molecular function is still unclear, although, as mentioned before, an exchange of paralogues from SS18 to CREST is essential for proper neuron maturation[207,208], and recurrent chromosomal aberrations involving these subunits are found in the rare synovial sarcoma resulting in the fusion protein SS18-SSX, which produces aberrant BAF complexes by defective assembly of SMARCB1[269,270].

PBAF complex

The discovery of a human mSWI/SNF rapidly revealed the existence of two different variants of the complex, with different molecular weights and subunit compositions[200]. As mentioned before, these alternative complexes were named SWI/SNF-A and SWI/SNF-B, corresponding the first one to the canonical BAF described first. SWI/SNF-B, on the other hand, resulted to be a divergent form characterized by the absence of ARID1 subunits[250] and the presence of the specific subunit PBRM1 (orthologous of *Drosophila* Polybromo)[201], being renamed to Polybromo-associated BAF (PBAF) complex. The compositional divergences between BAF and PBAF complexes have been related to functional differences regarding their genomic occupancy and selectivity of gene transcriptional control[247,271–273], but non-transcriptional related PBAF activities have also been described, which diverge from BAF functions and are mostly related to DNA repair[274–276]. Detailed analysis of PBAF subunit composition have shown that this complex subtype differs from canonical BAF complexes in the substitution of ARID1 subunits by ARID2[250,277], and of DPF1/2/3 paralogues by PHF10[206]; together with the presence of PBRM1[201] and BRD7[278] specific subunits. Additionally, this complex does not contain the ATPase module subunits SS18 and SS18L1[245]. Initial studies reported that PBAF only presented SMARCA4/BRG1 catalytic subunit, in contrast with BAF complex, in which both paralogues, SMARCA2/BRM and SMARCA4/BRG1, could alternatively be found[200,201]. However, recent evidence with deepest and refined detection techniques have identified both catalytic paralogues assembled in the PBAF complex[215].

ARID2 is high-molecular weight ARID-containing protein[279] that replaces ARID1A/B in the PBAF complex[250,277]. Indeed, although ARID1 and ARID2 are separated by a marked sequence dissimilarity, its presence in PBAF complex has been shown to exert the same structural relevance as its BAF counterparts: the incorporation of ARID2 onto the core module during the assembly process has been proved to be determinant for the further incorporation of the rest PBAF-specific subunits and ATPase module, and therefore for the specific and terminal assembly of the PBAF complex[215,277]. Moreover, and again in an analogous way to its BAF counterparts, DNA-binding properties have been attributed to this subunit through its ARID domain[279].

The incorporation of ARID2 facilitates the assembly of the rest of PBAF-specific subunits. BRD7 is a bromodomain-containing protein[280] that, as such, is able to specifically bind to certain histone acetylation marks[281,282], acting as an epigenetic reader. Previous studies reported its physical interaction with other bromodomain-containing proteins[283,284] and with different transcriptional regulators[285,286], suggesting its role on gene expression regulation. BRD7 was eventually identified as a PBAF-specific member[278] and its role inside the complex is thought to be related to specific genomic targeting through the acetyl-histone affinity of its bromodomain, although other functions have been reported, such as specific binding to external proteins like BRCA1[287]. PHF10 subunit, on the other side, is a remote paralogue of the DPF family of proteins found in canonical BAF complexes, and it is their substitute in the PBAF complex[206,245]. This protein, as well as their BAF counterparts, contains two PHD fingers, with histone binding properties. However, two different isoforms of PHF10 have been detected, conserving or losing these domains[288], respectively, with functional differences on the activity and targeting of the PBAF complex[289], increasing the complexity and heterogeneity of human mSWI/SNF complexes.

Finally, the assembly of the PBAF complex is completed with the incorporation of PBRM1. This subunit, although a PBAF-specific subunit not present in other complex variant, has been determined by structural means to belong to the ATPase module, and to be present in PBAF complexes in multiple copies, most probably by multimerization[215]. PBRM1 is a large protein containing a total of six bromodomains in tandem, and an additional evolutionary conserved bromo-adjacent homology (BAH) domain[201,290]. The molecular functions of the last one are not completely known, but it is widely accepted that it mediates protein-protein interactions[291,292] and has been observed to be essential for the assembly of the PBRM1 orthologue RSC1/2/4 to

the RSC complex, yeast counterpart of human PBAF[202]. On the other side, the six tandem bromodomains promote a high affinity of PBRM1 for histone acetylation that has been dissected in detail[293], reflecting a more than plausible genomic targeting of the complex through epigenetic reading. In fact, PBRM1 is relevant for the activation of several PBAF-controlled genes, but its presence in the complex is structurally accessory and not relevant for the integrity and assembly of the rest of the PBAF-specific subunits[277].

ncBAF complex

The third known variant of mSWI/SNF complexes was recently identified in human cells, expanding the previously known functional complexity of these chromatin remodelers. Deep mass spectrometry studies revealed the presence in different human cell lines of a smaller 0.87 MDa complex subtype divergent from BAF and PBAF complexes in subunit composition. Concretely, this new complex contained the exchangeable paralogues GLTSCR1/GLTSCR1 (or BICRA/BICRAL, respectively), together with BRD9 subunit, which were only found present in this complex, and not in BAF nor PBAF complexes. This complex has been named non-canonical BAF (ncBAF), or GBAF, after 'GLTSCR1-associated BAF'[214,248]. Interestingly, apart from these three ncBAF-specific subunits, this complex differs from the two classical ones in the absence of SMARCB1 and SMARCE1 core module subunits. Moreover, it only contains the paralogues SMARCC1 and SMARCD1, from SMARCC and SMARCD families, respectively. Interestingly, it does contains the SS18/CREST ATPase module subunits, shared with BAF complex but absent in PBAF[214,215]. Although it lacks of subunits such as SMARCB1, so far considered to be functionally relevant, this complex has been shown to exert chromatin remodeling functions and to have genome-wide occupancy on promoters and other regulatory regions where it controls the expression of specific sets of genes[294,295]. Interestingly, ncBAF complex coexist with BAF and PBAF complexes in the same cells, but have differential, although overlapping, genomic occupancies and functions[248,296,297].

GLTSCR1 or *BICRA*, and it homologue *GLTSCR1L* or *BICRAL*, are genes of uncertain molecular role first identified by the recurrent loss of the chromosome 19q arm, where *BICRA* is encoded, in glioma[298]. To this day, the only advance in the knowledge of its functions has been its identification as essential and specific member of the ncBAF complex, and the fact that some studies have detected interactions of uncertain significance with BRD4, a member of the BET family of bromodomain-containing proteins[214,299]. On the other side, BRD9 is a bromodomain-

containing protein homologous of the PBAF-specific subunit BRD7. Indeed, both BRD7 and BRD9 belong to the family IV of bromodomain-containing proteins[300]. BRD9 was initially thought to be part of the canonical BAF complex[232,245] until the discovery of ncBAF. The presence of a bromodomain in its sequence denotes its probable role of genomic-targeting of ncBAF complex through acetyl-histone binding. In fact, BRD9 seems to be necessary for the correct targeting to specific genomic sites, and consequently for the correct performance of the ncBAF complex[301].

The mSWI/SNF assembly tree

In a 2018 study, Mashtalir and colleagues[215], among other relevant insights into the composition and structure of the three human mSWI/SNF complexes, dissected in detail the ordered in time incorporation of individual subunits onto the modules of the different complexes, resulting in the fully assembly of BAF, PBAF and ncBAF subtypes. This study highlighted the importance of the assembly process, not only for the proper structural integrity of the fully assembled complexes, but also for the determination of the complex subtype, and drew the network of divergent assembly pathways, or 'assembly tree', that mSWI/SNF subunits sequentially follow for the composition of these macromolecular structures (Figure 7).

The formation of the three complex subtypes starts from a shared root in the assembly of the core module. The dimerization of SMARCC1/2 and the posterior incorporation of one SMARD1/2/3 subunit marks the formation of an initial BAF core, which is crucial for the structural integrity of the whole complex[216,221,302]. At this point, the first divergence point occurs: the incorporation of the two remaining core subunits SMARCB1 and SMARCE1 defines the pathway to BAF and PBAF assembly, while ncBAF assembly pathway diverges with SMARCB1/SMARCE1-free initial BAF cores. These smaller cores bind to ncBAF specific-subunits BICRA/BICRAL and BRD9, and fully assemble by joining to an independently assembled BAF-like ATPase module. In the case of BAF and PBAF common pathways, SMARCB1 and SMARCE1 are incorporated into the initial BAF core, forming a canonical BAF core. The second point of divergence comes after, when the incorporation of whether ARID1A/B or ARID2 determines the way towards BAF or PBAF assembly, respectively. On the one hand, the incorporation of ARID1A/B allows the sequential assembly of the BAF-specific DPF1/2/3 and the BAF-specific ATPase module. On the other hand, ARID2 incorporation leads to the sequential assembly of PBAF-specific BRD7 and PHF10 subunits, and the later incorporation of PBAF-specific ATPase module, containing PBRM1.

The assembly of the ATPase module, whether BAF/ncBAF- or PBAF-specific, is produced independently from the rest of the complex, and consists in the binding of accessory proteins to SMARCA2/4 catalytic subunits. Finally, the assembly process of the three tree ramifications ends with the incorporation of each subtype-specific core module with its respective ATPase module. This parallel assembly process explains the stability and functional independence previously attributed to the ATPase module[216].

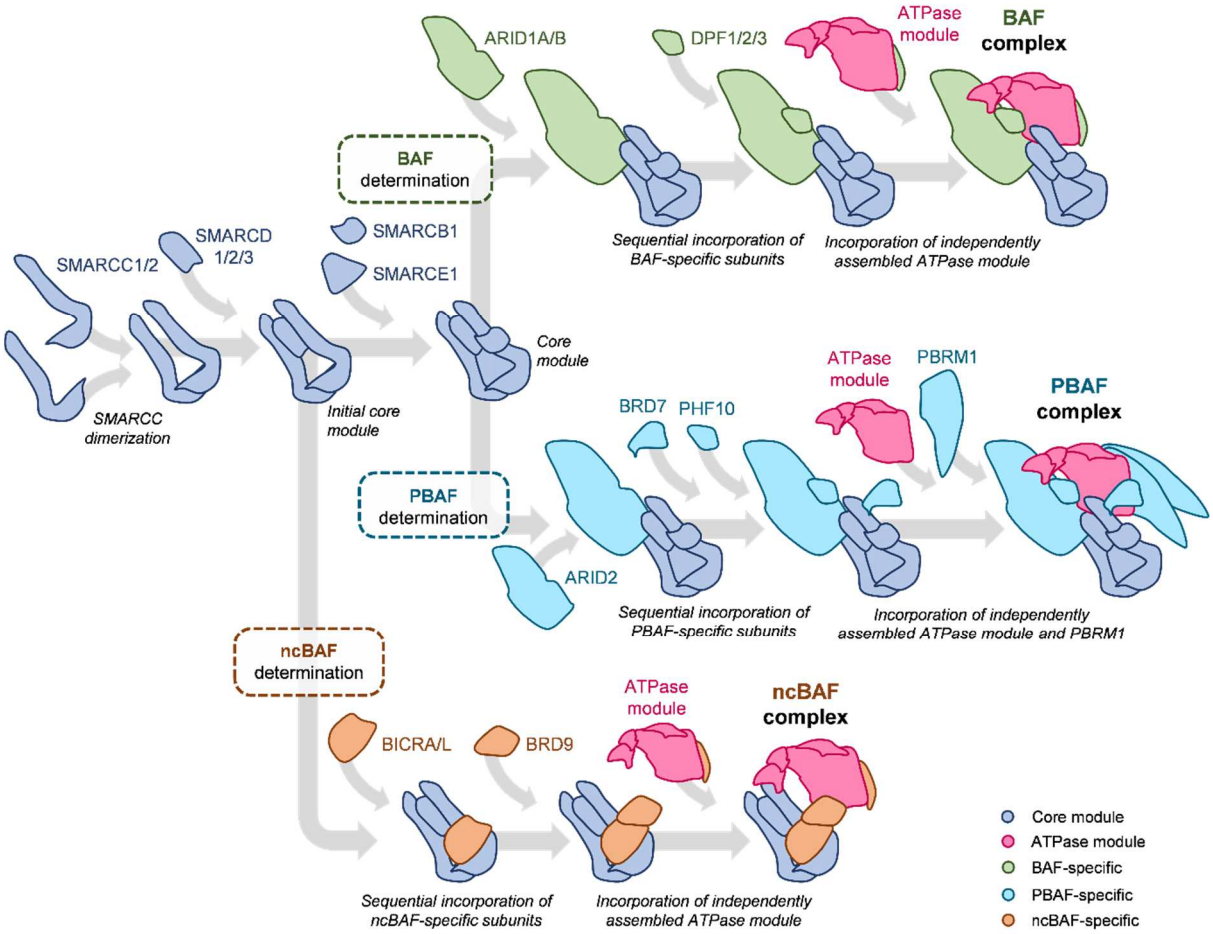

Figure 7: The mSWI/SNF assembly tree. Ordered incorporation of subunits as well as subtype divergence steps are indicated with grey arrows. Color code, detailed in the legend, represents the structural and subtype-specific modules to which subunit belong. Adapted from Mashtalir *et al.* (2018)[215].

1.2.4. Remodeling mechanism and molecular structure

Meticulous molecular analyses have demonstrated that the remodeling activity of these complexes promotes accessibility to DNA by generating NDRs at specific genomic sites where direct interactions between DNA and regulatory proteins must be produced, such as transcription start sites, distal regulatory regions or DNA repair events. Different models have been proposed over the last 25 years for the molecular mechanical process driven by the SWI/SNF complex that generates accessibility regions, and the two most accepted nowadays are those which argue that SWI/SNF complexes promote the sliding or the ejection of nucleosomes, respectively. These two *sliding* and *ejection* proposed mechanisms are not mutually exclusive, they differ on the degree of nucleosome unfolding provided by the remodeler, and are currently accepted as the two main effects of SWI/SNF complexes on nucleosomes[98,100,303].

Shortly after its discovery, SWI/SNF complexes where clearly seen to interact with chromatin by binding to nucleosomes with high affinity, but also to DNA in a non-sequence specific manner[254,255,304]. A series of studies determined that SWI/SNF reduced the binding of nucleosomal DNA to histones, rather than disrupting the histone octamer[305,306]. *In vitro* experiments with artificial nucleosome arrays demonstrated that the activity of the complex promotes a stable and reversible ATP-dependent conformational change of the nucleosomes to an altered state of lower electrophoretic mobility, which contains a longer DNA fragment[167,307–309]. These altered nucleosomes increased DNA exposition to the action of nucleases and transcription factors[140,141,308]. SWI/SNF complexes were observed to promote nucleosome free regions by displacing the histone octamers along the DNA strands but physical barriers blocked this translocation, meaning that nucleosomes were mobilized in *cis*, without full nucleosome unfolding[142,143]. These findings shaped the hypothesis that SWI/SNF remodelers reduce DNA-histone interactions, creating a loop that propagates around the nucleosome and loosens it just enough to promote its sliding, exposing DNA to transcription factors and other regulatory factors.

However, alternative *in vitro* studies showed a reduction in nucleosome number and transference of nucleosome between different DNA molecules after SWI/SNF activity[145,168,310], indicating mobilization of nucleosomes in *trans*, necessarily implying the full unfolding of the nucleosome and ejection of the histone octamer. This, together with increasing evidence of

nucleosome ejection at transcriptional start sites necessary for transcription initiation[311,312] tipped the scale towards the models in which nucleosomes are fully unfolded by SWI/SNF remodelers through complete disruption of DNA-histone interactions.

These two proposed activities of SWI/SNF complexes on nucleosomes are not incompatible, and current knowledge on their molecular structure and function support both models. Today it is known that the catalytic activity subunit of the complex, BRG1/BRM in humans, acts as a DNA translocase[313]. Its catalytic domain was first classified as helicase because its similarity with proteins with the ability of separating DNA strands[138]. However, nor BRG1/BRM neither their yeast orthologue SWI2/SNF2 show helicase activity[308,314]. In fact, helicases and ATP-dependent remodelers belong to a bigger protein family of DNA-dependent ATPases that have in common the capacity of DNA translocation, meaning that bind to DNA and use ATP in order to move along the DNA backbone[315]. The identification of the catalytic subunit of the complex as DNA translocase eased the understanding of its molecular functions, and the reconciliation of sliding and ejection models. The nucleosome-bound SWI/SNF complex binds to the ribose-phosphate backbone of one of the strands of nucleosomal DNA and consumes ATP in order to translocate DNA in a 3′ to 5′ direction[313,316,317]. The proposed mechanism of translocation is explained by the *mitten* model, which consist in a cyclic process involving interaction with DNA at two physical points that alternate in time steps of binding, movement and unbinding[318–320]. This DNA translocation is combined with a tight fixation of the complex to the nucleosomes through SWI/SNF-histone interactions[229,321,322]. The combination of these two concrete molecular properties generates a disruption of DNA-histone interactions that is transmitted as a wave throughout nucleosomal DNA[316,323].

Although initial inquiries on molecular structure by means of low resolution electronic microscopy were made during the 2000s[156,324], the advances on high-resolution cryogenic electronic microscopy (cryo-TEM) analyses have accelerated the recent determination of the atomic-resolution molecular structure of the SWI/SNF complex (Figure 8A). The structure of both human and yeast nucleosome-bound SWI/SNF complexes determined by multiple and consistent studies reinforced the already explained model of nucleosome-fixated DNA-translocation activity[157,258,259,325]. The SWI/SNF complexes show a modular structure with two main domains: a ‘body’ or base module, formed by the core structural subunits; and a ‘head’ or catalytic domain, formed by the ATPase BRG1/BRM and the associated proteins. These two

modules are connected by a 'bridge' formed by a long α-helix of the HSA domain of BRG1/BRM subunit. The complex has a characteristic shape in 'C' that allows it to surround the nucleosome, forming a 'sandwich' with two points of interaction with histones: one in the catalytic module, at the SnAc domain of BRG1/BRM, and other in the base module, at SMARCB1/hSNF5 subunit, which binds to the acidic patch of the histone core[258,259,326]. The catalytic subunit interacts with nucleosomal DNA and promotes its translocation at a specific intra-nucleosome point, SHL2, two DNA turns away from the nucleosome dyad, the central axis of the nucleosome[327,328]. (Figure 8B).

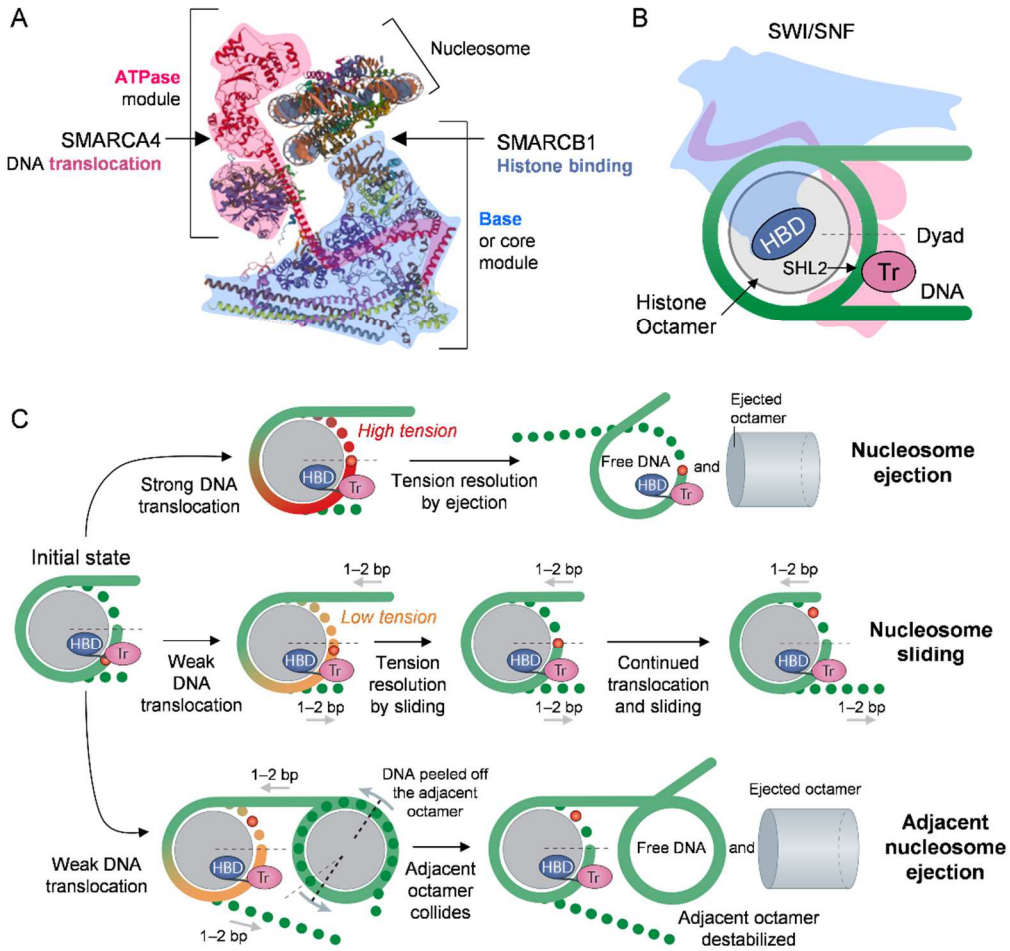

Figure 8: mSWI/SNF molecular structure and chromatin remodeling mechanism. **A**. Molecular structure of nucleosome-bound BAF complex (PDB: 6TLJ) showing structural modules and key molecular functions. **B**. Scheme of the SWI/SNF-nucleosome interaction and the involved domains: histone-binding domain (HBD) and DNA translocase (Tr). **C**. Models for the molecular mechanism of chromatin remodeling by SWI/SNF complexes. Adapted from Clapier *et al.* (2017)[98].

The relevant information provided by this data have settled and unified the molecular mechanism model of SWI/SNF remodelers[98,100,303]. The translocation of nucleosomal DNA, resulting in a debilitation of histones-DNA binding that propagates along the nucleosome, generates a tension. The consensus today is that different circumstances make up a balance of forces that determines whether this tension is resolved by nucleosome sliding or ejection (Figure 8C). This factors include the intensity of the ATPase activity, which can be modulated by its associated subunits (ACTB, ACTL6A). Low or moderated catalytic activity would allow the homogeneous propagation of DNA-histone breaks and translocation of DNA along the histone octamer, promoting the sliding of nucleosome. An increased catalytic activity, however, would generate a higher tension that cannot be alleviated fast enough by incorporation of DNA into the nucleosome, resolving this tension by nucleosome disassembly[98,241]. Another factor determining the resolution of the remodeling activity is the topological constrains of chromatin at the specific site[329]. In fact, topoisomerases assist and modulate the activity of the SWI/SNF complex[143]. Moreover, some evidences point towards a hybrid scenario in which SWI/SNF complex would slide the target nucleosome, making it collide with the neighboring one, which would be the one to be ejected[144,330] (Figure 8C)..

Whether nucleosome are fully or partially unfolded, what is consensually accepted nowadays is that the mechanic force produced from ATP-hydrolysis by the SWI/SNF complex is used for the translocation of nucleosomal DNA, generating localized regions of DNA accessibility, by nucleosome sliding or ejection, that allow the action of transcriptional regulators, among other factors.

1.2.5. Genome-wide functions of the mSWI/SNF complexes

The chromatin remodeling functions of the mSWI/SNF complex have been widely shown not to be only restricted to localized and sporadic chromatin remodeling events, but rather be a global chromatin remodeling agent that acts as a whole genome regulator. As explained before, the main effect of the remodeling activity of these complexes in the chromatin is the active regulation of gene expression by generating the necessary accessibility to transcriptional regulators and essential machinery. Early studies in yeast already demonstrated the conserved function of controlling large amounts of genes at the transcriptional level under this mechanism[146,159,160]. This was also widely proved for human cells, in which different mSWI/SNF

genomic occupancies were reflected in different controlled transcriptional networks, depending on the cell or tissue type analyzed, reinforcing the idea of mSWI/SNF as relevant players in cell identity[273,331,332]. Occupancy studies of these complexes have revealed during the past twenty years the elevated number of genomic loci where binding of mSWI/SNF complexes is detected, ranging from 20,000 to 40,000 peaks in chromatin immunoprecipitation-sequencing (ChIP-Seq) assays. These binding sites are mainly located in *cis* upstream regulatory regions of genes, namely in promoters and enhancers[302,333,334]. The use of new state-of-the-art technologies able to assess the chromatin condensation state at a genome-wide level such as micrococcal nuclease-sequencing (MNase-Seq)[335,336] or the assay for transposase-accessible chromatin-sequencing (ATAC-Seq)[337] has proved that the presence in these binding sites promotes the increase in chromatin accessibility, further corroborating the postulated role of the mSWI/SNF chromatin remodeling complexes[209,229,338–340].

The biological consequences of this tissue-dependent genome-wide targeted chromatin remodeling-based transcriptional control is reflected in the fact that many developmental steps, from early to later stages, of different tissues and organs have been proved to depend on the activity of this remodeling complex[341]. The proper function of mSWI/SNF complexes is essential, for example, for the maintenance of pluripotency of embryonic stem cells (ESCs)[218] and for the correct embryonic development of different structures such as heart[342], immune system organs[343], muscle[344], bone[273] and nervous system[206]. The study of mSWI/SNF complexes in embryonic development has led to the identification and characterization of tissue-specific complex variants, with concrete combinations of subunits and responsible for the maintenance of transcriptional programs relevant for pluripotency or lineage identity determination at different stages of development (Figure 9).

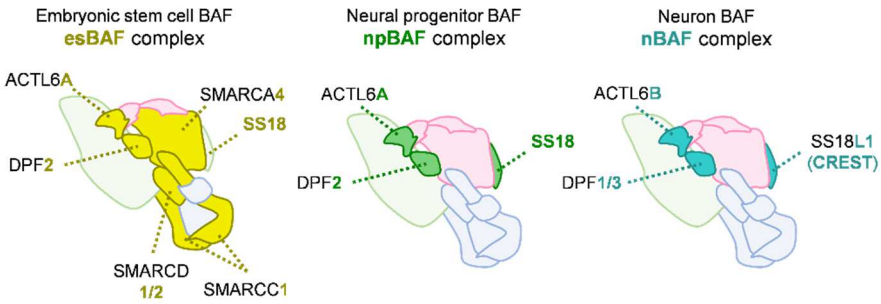

Figure 9: Subunit composition of the tissue-specific developmental variants of mSWI/SNF complexes. esBAF, npBAF or nBAF defining paralogues are indicated with different colors for each subtype. Based on Hohmann *et al.* (2014)[345].

On the one hand, a specific variant of BAF complex named *embryonic stem cell* BAF (esBAF) contains a unique BAF subunits combination, restricting the presence of members of each paralogue family[218] (Figure 9). The specific subunit composition of this complex is required for the self-renewal and pluripotency capacities of ESCs[218,346], and it exerts these functions by priming the chromatin for the access of critical pluripotency transcriptional regulators such as OCT4[218,302] or STAT3[347,348]. On the other hand, two specific variants of the BAF complex were specifically identified in the nervous system, *neural progenitor* BAF (npBAF) and *neuron* BAF (nBAF)[206–208]. These two have concrete subunit compositions (Figure 9) and are responsible for the correct activation of specific transcriptional networks at concrete developmental stages. Moreover, the switch from npBAF to nBAF by the exchange of paralogous subunits is crucial for the terminal differentiation of neurons[206] and has been proved to be a pan-neuronal essential process in different neurological structures such as neural crest development[349,350] or brain cortex[209].

Differences in genomic occupancy and transcriptional network control have not only been attributed to the action of the complex in different tissues and cell types, but also to the different same cell-coexistent mSWI/SNF complex subtypes previously explained: BAF, PBAF and ncBAF. In fact, since the discovery of SWI/SNF and RSC complexes in yeast, dissimilar functions between both of them were observed related to their relevance for cell viability[161], but also to divergent, although at some extent overlapping, genomic occupancies between the two types of complex[159,160]. Differential functions have been also reported between the counterparts of these two complexes in *Drosophila* (BAP and PBAP)[193] and humans (BAF and PBAF)[247,278,351].

When talking about transcriptional control, differences between BAF and PBAF complexes remain still unclear and ambiguous, although recent research has shed light on these differences. BAF complex has been recently seen to mediate chromatin remodeling at distal *cis* regulatory sites (enhancers), in addition to proximal sites (promoters), whereas PBAF complex activity seemed to be restricted to promoters[228,352,353]. These differences have obvious functional implications, suggesting a role of BAF complexes in the transcriptional regulation and potentiation of distant genes or groups of genes under the control of enhancers[354], instead of a more precise single gene activation control at the promoter level, which might be attributed to PBAF. These occupancy differences could be explained by the differential presence of histone marks in promoters and enhancers[34]. For example, mono-methylation of histone H3 at lysine 4

has been shown to define enhancer in contraposition to promoters[355]. The compositional differences of epigenetic *readers* between BAF and PBAF could change their affinity for these marks and, consequently, for the type of *cis* regulatory region to bind.

Whatever the reason, the differential affinity for distinct genomic loci generates differences in function in a tissue or cell type-dependent manner. For instance, the two complexes were observed to modulate different sets of genes in ESCs, with some level of overlapping, and even antagonistic functions upon the same gene were described[278]. In addition, BAF, but not PBAF, mediates transcriptional activation through certain nuclear hormone receptors in breast cancer cells, while both of them facilitate retinoic acid (RA) receptor-mediated transcription[351]. Differentiated tasks of these two complexes were also found in their contribution to transcriptional control of the integrated human immunodeficiency virus (HIV), on which different occupancies have been attributed to BAF and PBAF[356]. While BAF exerts repressive effects on transcription of HIV, promoting virus latency, PBAF is recruited and necessary for transcriptional expression upon reactivation[272]. These are just few examples of how the different compositions and chromatin affinities of BAF and PBAF complexes determine specialized and divergent functions between the two of them.

The same could apply to the ncBAF complex. Although its existence has been known only for few years, different studies have already revealed differences in genomic occupancy in comparison with the other mSWI/SNF complexes. Comparison between genomic occupancies of ncBAF and esBAF in ESCs showed a clear differential binding affinity, with a higher presence of the non-canonical complexes in promoters enriched in tri-methylation of histone H3 at lysine 4, while esBAF showed a tendency of occupying enhancers, which are enriched in the mono-methylation of the same residue, as explained before. Interestingly, ncBAF-specific binding sites were also located at the boundaries of topologically associated domains (TAD)[248]. TADs are chromatin loops that delimit big regions of the genome under the same transcriptional control through tridimensional physical interactions between distant genomic loci[357]. A recurrent TAD boundary regulator is the DNA-binding protein CTCF[358,359], and ncBAF was observed to co-localize with CTCF and to bind to CTCF motifs[248,296]. This specific binding has functional consequences. For example, ncBAF maintains a transcriptional program essential for an earlier naive pluripotency state of ESCs, in comparison with esBAF, whose activity is required in later states of primed pluripotency[248]. Furthermore, the specific distribution of ncBAF at CTCF sites

generates a therapeutically exploitable synthetic lethality in SS18-SSX fusion positive synovial sarcoma and SMARCB1-lost malignant rhabdoid tumors[296,297]. Additional functions in early stages of embryonic development[360] and the progression of certain neoplasms[294,295] have already been attributed exclusively to ncBAF-controlled transcriptional networks.

Despite being firstly identified and characterized as transcriptional coactivators, several studies have revealed transcriptional repressive functions of SWI/SNF complexes in different scenarios[361]. In yeast, multiple examples have been shown of genes transcriptionally upregulated after the inhibition of the complex[362–364]. However, in many of these reports no direct evidence of a necessary activity of the complex at the promoter of the supposedly repressed genes is reported, although occupancy at promoters of repressed genes has been proved in some cases[365]. An interesting scenario in yeast is the repression of two histone genes, *Hir1* and *Hir2*, in which the complex binds to the promoter of these genes and plays a role in its repression[159]. However, contradictory evidence on this genomic locus reported an activating activity of the complex in this promoter, but in the context of a cell cycle dependent activation of these genes: SWI/SNF is recruited by transcriptional repressors bound to these promoters for the transient activation and synthesis of histones during phase S[366]. Moreover, multiple repressive functions have been reported for the mSWI/SNF complex, such as the inhibition of *c-fos* gene[367] or of multiple genes in ESCs[346]. Inhibition of transcription in regions neighboring events of DNA repair have been proved for PBAF complex[274,276].

However, regarding regular transcriptional control, again a unified explanation of the repressive mechanism of the complex remains elusive. Some reports associate the repression of certain genes with an increase in chromatin accessibility, what is in concordance with the known molecular mechanism of the complex, and would support the theory of the transcriptional repressor access[368,369], some of them even demonstrating the recruitment of repressors such as HDACs[370,371], E2F6[372], Runx1[373] and others[374–377]. Nevertheless, and surprisingly, other studies report chromatin condensation by mSWI/SNF complex[272,378,379] and it has been proposed that it is the chromatin remodeling activity by itself that can promote the loss of accessibility at these promoters, by nucleosome repositioning[146]. Interesting theories propose that the repression is produced by displaced nucleosomes accumulated by the regular nucleosome sliding of the complex[380]. Indeed, this regular nucleosome sliding activity is able to detach previously bound transcription factors from chromatin, what would explain repressive functions of chromatin

remodeling by SWI/SNF[381]. Some authors have proposed that the upregulation of genes is an indirect effect of SWI/SNF inhibition, and for instance might be the result of different transcriptional regulators, such as PRC or other transcriptional repressors, occupying the newly generated free genomic sites, releasing the expression of genes previously repressed by them[382]. In summary, the ambiguous data related to these inhibitory functions hampers a clear explanation about the repression mechanism by SWI/SNF remodeling complexes.

Non transcriptional-related chromatin remodeling activities have been also described for the mSWI/SNF complex[108], all of them related to molecular processes in which chromatin must be unfolded making DNA accessible for direct interactions with regulatory proteins. A well-studied case is DNA repair: mSWI/SNF complexes have been determined to be essential for the proper completion of different processes of DNA repair, including homology repair and non-homologous end joining[383]. BAF and PBAF have been observed to bind to specific DNA repair signaling histone marks, such as phosphorylated histone H2A.X (γ-H2A.X), through the interaction between acetylated histone H3 and BRG1 bromodomain[384]. This recruitment facilitates the access and activity of the DNA repair machinery[275,276,385,386]. In addition, as mentioned before, PBAF complex is responsible for the essential transcriptional repression of genes neighboring DNA repair events[274,276]. In fact, PBAF occupancy at centromeres and different chromosomal structural DNA sequences has revealed the importance of this complex subtype for genomic stability[201,275,387]. For example, during mitosis, it is relevant for sister chromatid cohesion, avoiding the generation of aneuploidies and other chromosomal aberrations[275]; or during the DNA replication process, it is essential for the post-replication DNA repair and the progression of the replication fork[388]. An important PBAF subunit widely related to these processes is PBRM1[389,390] and it has also been proposed as a therapeutically exploitable synthetic lethality for combination with DNA repair inhibitors in cancer[390].

Finally, mSWI/SNF complexes also interact with CTCF and other structural elements that regulate the tridimensional architecture of chromatin[333], and incipient research has attributed this specific structural role to ncBAF[248,296], implying relevant functions on this field yet to discover.

1.2.6. Mechanisms of mSWI/SNF genomic targeting

Despite regulating many sets of genes in different tissues, mSWI/SNF complexes do not show random positioning along the genome, and some targeting factors must be directing which genomic loci to bind to and which genes to transcriptionally control. How mSWI/SNF complexes are targeted to specific genomic sites is still an open question. Some suppositions arise from the protein domains of mSWI/SNF subunits. Whereas core and ATPase module are essential for raw chromatin remodeling *in vitro*, the presence and relevance of the accessory subunits *in vivo* must be at least partially explained by their role in genomic targeting. These accessory subunits are mostly the facultative subcomplex-specific ones, so they can easily be implicated in the functional differences between subcomplexes, which are primarily of genomic occupancy. Research has shed light on this topic over the last decades, and the main non-incompatible models for mSWI/SNF genomic targeting can be summarized in the action of three different recruitment agents: transcription factors, histone marks and non-coding RNAs (Figure 10).

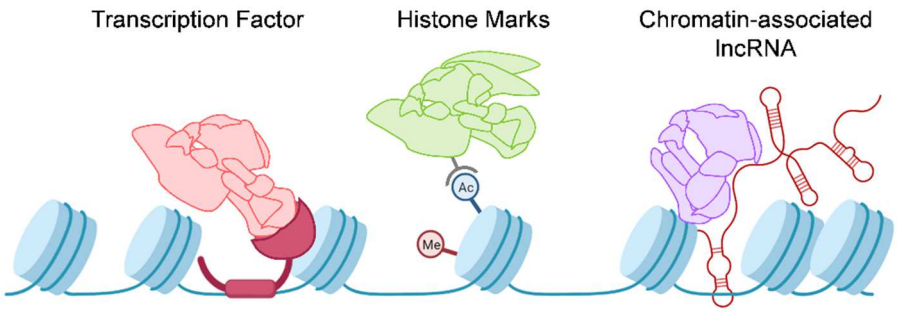

Figure 10: Three proposed factors for mSWI/SNF genomic targeting. Recruitment of SWI/SNF complexes to specific genomic loci has been reported to be produced whether by specific protein-protein interactions with transcription factors (red complex in the figure), affinity to histone marks attributed to epigenetic reader domains of different subunits (green) or interaction with chromatin-decorating lncRNAs (purple).

Transcription factor-directed genomic targeting

When talking about the interaction between SWI/SNF complexes and transcription factors, an important confounding factor is the order in time of events or, in other words, the cause-consequence chain followed by both transcription factors and remodeling complexes. Right after the discovery of the complex, recruitment by transcription factors was the first model to

be proposed, by the clear and functionally relevant protein-protein interactions established between the complex and nuclear receptors of different lipophilic agents, such as estrogen, RA or glucocorticoids[198,391,392]. These and later studies have suggested that the affinity of the transcription factors for specific DNA sequences recruits and targets the SWI/SNF complex to specific genomic loci[224,243,392], marking an order of cause-consequence of transcription factor binding causing the chromatin remodeling. In this model, chromatin accessibility would not be necessary for the recognition and binding of the specific DNA regulatory elements by their respective nuclear receptor, but rather for the later incorporation of the transcriptional machinery[221,393–395].

However, alternative evidence has also shown that the cause-consequence chain might be inverted in other scenarios, and precisely the DNA accessibility produced by SWI/SNF chromatin remodeling would be the initial step for the later interaction of specific transcription factors to its target DNA elements. An important example of this is the interplay between esBAF and the STAT3 transcription factor observed in ESCs: esBAF is essential for the proper chromatin conditioning necessary for the STAT3 interaction with its target promoters, and the specific expression of pluripotency genes[302,348]. A similar need for previous chromatin remodeling by SWI/SNF was reported for the transcriptional program controlled by TGFβ[396]. This suggests that the remodeling of the chromatin, in some cases, occurs previously and is necessary for the posterior binding and action of specific transcription factors.

Multiple studies have reported genomic co-localization and functional co-dependency between mSWI/SNF complexes and transcription factors[397], and even preferential specificities of the different subtypes for different transcription factors[248], but the sequential order of events has not been determined in all cases. Some authors have already proposed that these differences in the cause-consequence interplay between SWI/SNF remodelers and transcription factors are highly specific and depend on the binding and interaction dynamics between both players[221], so the coexistence of both directions of targeting is more than likely. However, in the case of the transcription factor access by prior chromatin remodeling, the targeting of the SWI/SNF complex to the specific genomic site remains unsolved, implying the necessity of a different targeting agent.

Histone mark-directed genomic targeting

The affinity of mSWI/SNF complexes for histone post-translational modifications (PTM) is denoted by the large proportion of its components containing histone PTM-binding domains, turning these complexes into a sort of histone mark sensors (Figure 11). Four types of these domains are found in the different complexes: the bromodomains of SMARCA2/4, PBRM1, BRD7 and BRD9 subunits; the PHD fingers of the DPF paralogue family members and PHF10; the histone tail-binding SANT domain[398] of SMARCC family subunits; and the histone methylation-binding chromodomains present also in this latter paralogue family, which however were recently shown to be non-functional[399].

Bromodomains are the most studied and characterized histone-binding domains of the mSWI/SNF complexes. These domains have been widely proved to interact specifically with different histone acetylation marks in different specificities rates, depending on the amino acid sequence of the domain[281]. Today, the interactions between mSWI/SNF bromodomains and acetylated histone tails are well described and are being widely studied as models for molecular structure-driven drug design[94]. The SMARCA2/4 (BRM/BRG1) catalytic subunit, present in all complex subtypes, has one of the most well investigated bromodomains[400,401]. Indeed, these protein motifs were named after *SMARCA2/4 Drosophila* orthologue *brahma* (*brahma*-domains), in which they were discovered[172]. Its acetylated histone binding properties have been shown to be essential for the specific binding and targeting of the complex to acetylated histones H3 and H4[326,402–404].

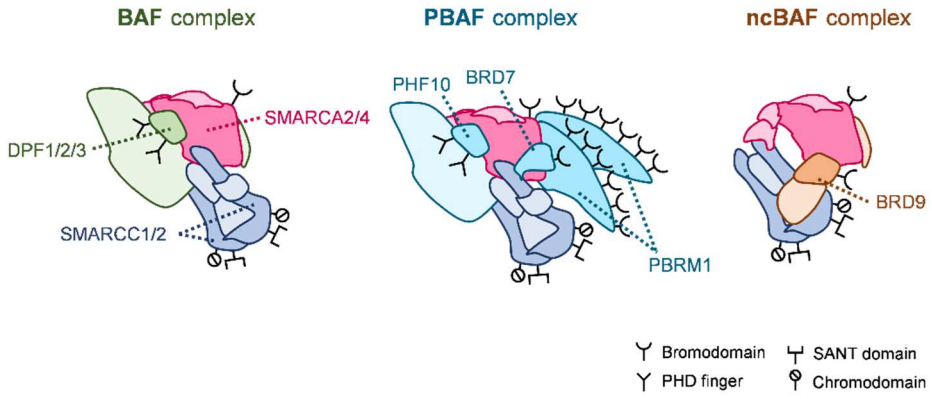

Figure 11: Histone binding domains contained in mSWI/SNF subunits. Based on Pulice and Kadoch (2016)[405].

Moreover, the presence of bromodomains is especially notable in PBAF complexes, in which, besides the ATPase contained bromodomain, the bromodomain containing protein BRD7 and the six-bromodomain containing PBRM1 are specifically incorporated (Figure 11). These bromodomains are also relevant for specific binding to chromatin through acetylated-histone recognition[285,406,407]. This high number of bromodomains increases the specificity and binding regulation of PBAF complex to histones[408] and could be an explanation for the observed preferences of PBAF complexes for promoters than for enhancers, in comparison to BAF complexes. Finally, ncBAF also present a bromodomain-containing protein besides BRM/BRG1, BRD9, from the same protein family as BRD7[214]. Several examples have shown the specific recruitment of mSWI/SNF complexes at regulatory regions through the signaling of acetylated histones generated by histone acetyltransferase complexes like SAGA[402,404,409–412], and this specific targeting has been attributed to the different bromodomains contained in the composing subunits of the complex[326,403]. In summary, acetylation states of the chromatin have been repeatedly found to direct the genomic targeting of mSWI/SNF complexes through bromodomains[413]. However, single and specific acetylation of histones are reported to not be sufficient for full targeting of complexes to genomic loci, since single marks have low to moderate affinity for chromatin remodelers, suggesting that this targeting is the result of a combinatorial crosstalk of different histone marks and other agents[98].

PHD fingers, another less specific and of uncertain role histone binding domains[261], are present in BAF and PBAF components, suggesting additional targeting of the complex through these subunits. Different transcriptional activation-related histone marks affinities have been observed for PHD finger including methylation, acetylation and crotonylation[262–266,414]. Some of these studies have implicated DPF proteins as relevant for the targeting of BAF complexes to enhancers through interactions with mono-methylated histone H3 at lysine 4[264]. However, the implication and relevance of histone-mark binding through these domains, together with the SMARCC-contained chromodomains, has not been yet well studied and remains unclear.

In a very recent 2021 study by Mashtalir and colleagues[415], a systematic analysis of mSWI/SNF complexes affinity and remodeling activity using a library of histone marks and variants corroborated much of the above mentioned theorizations. This study has not only confirmed and dissected the specificity of the three mSWI/SNF complexes for different histone marks, but also the impact that these marks have on the remodeling activity have on the complex,

independently of the binding. Additionally, numerous new mSWI/SNF complex/histone mark interactions were discovered: ubiquitination in the acidic patch of H2A/H2B reduces activity by loss of binding of SMARCB1 in BAF and PBAF complexes; modifications in DNA-histone interfaces increase the remodeling activity; also, histone H3 tail acetylation increase binding and activity of the three complexes. Interestingly, they showed that the effect of histone mark combinations is based on hierarchical dominance interplays among these epigenetic signals, being mSWI/SNF complexes integrators of multiple signaling inputs from the chromatin.

This study has also demonstrated the high histone mark binding specificity of the three complexes, even with antagonistic effects. Many histone marks were found to restrict BAF activity, without necessarily reducing the binding, in a more restrictive way than PBAF and ncBAF activities. This inhibitory effect of certain histone marks increase the specific genome-wide targeting and activity of BAF complex and are in concordance with some predictions postulated long before, that genomic targeting of the complex not only should direct mSWI/SNF to desired sites, but also 'untarget' or inhibit its activity in undesired genomic loci[416]. Tri-methylation of histone H3 at lysine 3 in combination with acetylation of histone H4 tail inhibits the effect of BAF and has no impact on PBAF and ncBAF. Since these two marks preferentially co-localize at promoters, these differential affinities might be explaining the preferential occupancy of BAF complexes at enhancers. In addition, a strong and specific affinity of ncBAF for acetylation of histone H4 tails was observed, opposed to the inhibitory effects of these marks for BAF and PBAF, and this difference was directly attributed to the presence of BRD9 and the absence of SMARCB1 in ncBAF complexes. This, together with the fact that the ATPase module alone was found to exert the most promiscuous unspecific nucleosome remodeling independently of histone marks, corroborates the relevance of core module subunits, such as DPF, on the genomic targeting of the complex, as speculated before.

In summary, histone marks have been long studied as putative directors of the genomic occupancy of the different mSWI/SNF complexes, and last minute research have forcefully validated the relevance of these epigenetic signals in the specific targeting of the different chromatin remodelers. This interplay adds an additional layer of regulation for the correct performance of mSWI/SNF genome-wide functions and, considering histone modifications as epigenetic signals heritable through mitosis[417], it highlights the relevance of the mSWI/SNF complexes as effectors of tissue-specific and stable-in-time epigenetic landscapes.

Long non-coding RNA-directed genomic targeting

The latest studied level of genomic targeting of mSWI/SNF complexes is a consequence of the identification during the last decade of multiple physical interactions of this chromatin remodeler with different long non-coding RNAs (lncRNAs). These are RNA molecules of 200 nucleotides or longer, transcribed from genomic regions without open reading frames, what makes them non-coding for proteins. The increasing study of these transcripts has revealed the many functions of these RNA molecules by themselves, being involved in the regulation of processes related to gene expression both at the post-transcriptional level, through mRNAs stability regulation, microRNA (miRNA)-sponging or translational modulation, among others, and at the transcriptional level, by recruiting transcription factors, altering chromatin architecture or, remarkably, modulating the remodeling of chromatin by recruiting or conditioning the activity of chromatin remodelers at specific sites[42,43].

Of note, several lncRNAs have been shown to physically interact with the mSWI/SNF complex and modulate its functions in different ways[45,418]. As shown in Table 4, up to 24 different lncRNAs have been shown to bind to different subunits of the complex, conditioning its genomic occupancy and remodeling activity. In fact, 11 are thought to recruit the complex to specific genomic sites, and 4 of them, on the contrary, to physically displace it from chromatin. Interestingly, the subunit most involved in lncRNA interaction is the ATPase SMARCA4/BRG1. This protein contains a high mobility group-like AT-hook motif in its sequence[419], which has a putative RNA binding role[420], suggesting a possible specialized role of this subunit in this kind of interactions. Interestingly, some of these genomic targeting lncRNA, such as lncFZD6 or lncTCF7, are thought to recruit the mSWI/SNF complex to the genomic site where they are being transcribed, indicating a possible targeting mechanism by signaling through nascent lncRNAs[421,422]. On the other hand, other lncRNAs, such as lncZic2 or IL-7-AS, would be implicated in the genomic targeting to multiple non-related loci[423,424]. Additionally, some of them are related to the modulation of the remodeling activity rather than genomic targeting. That is the case of MHRT, the first lncRNA found to interact with mSWI/SNF, which binds to the catalytic site of SMARCA4/BRG1 and inhibits its functions[425]; or lncBRM, which inhibits the formation of SMARCA2/BRM-containing complexes, favoring the formation of SMARCA4/BRG1 ones[426]. Structural roles of these interactions have also been described, as the recruitment of SWI/SNF by NEAT1 or SatIII lncRNAs for the formation of different nuclear bodies[427].

Table 4: mSWI/SNF-interacting lncRNAs, sorted by their functional effect on the complex.

lncRNA	*Effects on mSWI/SNF complex*	*Interacting subunit*	*Reference*
DGCR5	Genomic targeting	ARID1A	428
DLX6-AS1	Genomic targeting Activity inhibition	SMARCA4/BRG1	429
IL-7-AS	Genomic targeting	SMARCA4/BRG1	424
LINC00163	Genomic targeting	ARID1A	430
lincRNA-Cox2*	Genomic targeting	*Not reported*	431
lncFZD6	Genomic targeting	SMARCA4/BRG1	422
lncTCF7	Genomic targeting	SMARCA4/BRG1	421
lncZic2	Genomic targeting	SMARCA4/BRG1	423
MANTIS	Genomic targeting Activity potentiation	SMARCA4/BRG1	432
MRLN	Genomic targeting	SMARCA4/BRG1 through MyoD	433
SWINGN	Genomic targeting	SMARCB1	434
CPS1-IT1	Genomic displacement	SMARCA4/BRG1	435
SChLAP1	Genomic displacement	SMARCB1	436
UCA1	Genomic displacement	SMARCA4/BRG1	437
Xist	Genomic displacement	BRG1	438
MALAT1	Activity inhibition	SMARCA4/BRG1	439
MHRT	Activity inhibition	SMARCA4/BRG1	425
uc.291	Activity modulator	ACTL6A	440
lncBRM	Activity modulator	SMARCA2/BRM	426
NEAT1	Formation of nuclear bodies	SMARCA4/BRG1	427
Sat III	Formation of nuclear bodies	SMARCA4/BRG1	427
TUG1	Protein stabilization	SMARCA4/BRG1	441
MVIH	Uncertain role	ARID1A	442
HOTAIR	Uncertain role	ARID1A	443

* lincRNA-Cox2 was studied in mouse, a human counterpart has not been discovered.

Nevertheless, discrepancies and ambiguous results have been observed regarding this level of genomic targeting of the complex. For example, the mSWI/SNF genomic displacing functions of the lncRNA SChLAP1[436] were later refuted by an independent study[444]. High technical variability of protein-RNA interaction detection approaches might be behind this and other discrepancies. These techniques are based in different methods of crosslinking –either chemical or physical– followed by immunoprecipitation (RNA-immunoprecipitation, or RIP), and differences in the parameters of this multistep process can deeply change the results, leading to artifactual results by loss of whether sensibility or specificity. Different studies refined these technical methodologies with rigorous controls and used it for global identification of RNA interactions of the complex by RIP-sequencing[434,444,445]. These have identified a general binding of mSWI/SNF complexes to nascent primary transcripts of active genes, the function of which

remains unclear but opens encouraging research lines. Moreover, site-directed recruitment through specialized lncRNAs have been demonstrated with these approaches, as in the case of SWINGN[434], reinforcing the idea of lncRNAs as previously unknown interactors of the complex that add a layer of complexity to the genomic targeting of mSWI/SNF complexes.

In summary, the myriad of combinatorial histone marks, transcription factors and lncRNAs existing in the different cell types may be directing the activity of SWI/SNF complexes, not only by targeting its genomic occupancy but also by modulating its activity on the target sites, allowing the maintenance of tissue-specific transcriptional programs by promoting DNA accessibility at specific sets of promoters and enhancers through chromatin remodeling by nucleosome sliding or ejection.

1.2.7. The mSWI/SNF complex and cancer

The chromatin remodeling complexes of the mSWI/SNF family have been widely implicated in human disease, including certain roles identified in type 2 diabetes[446], viral infections such as HIV[272,356] or hepatitis B virus[447], and immunological-related disorders such as Crohn's disease[448]. However, the two main groups of human illnesses with a wider observed contribution and relevance of the mSWI/SNF complexes, by much difference, are neurodevelopmental disorders and cancer.

The important role of mSWI/SNF transcriptional regulation in the correct development of the nervous system[104,109] explains the relationship of abnormalities in this chromatin remodeler with the first mentioned group of diseases. Indeed, germline mutations in genes encoding BAF, PBAF and ncBAF subunits have been associated to different neurodevelopmental disorders, eminently the Coffin-Siris syndrome, which is characterized by a cognitive delay of different degrees in combination with different congenital anomalies, including malformations of the phalanx, facial features, muscle tone, heart and genitourinary and gastrointestinal tracts, among others[449]. Heterozygous deleterious mutations of mSWI/SNF subunits related to this syndrome have been identified in *SMARCB1*, *ARID1A*, *ARID1B*, *ARID2*, *SMARCA4*, *DPF2*, *SMARCC2* and *SMARCE1*[450–454]. Mutations or low expression of different subunits have also been observed in Coffin-Siris-related neurodevelopmental disorders such as Nicolaides–Baraitser syndrome (NCBRS), Hirschsprung's disease or Kleefstra syndrome, as well as implicated in intellectual disability,

schizophrenia and autism spectrum disorders, being *ARID1B* the most relevant subunit altered in these cases[109,455]. On the other side, and more importantly for this doctoral thesis, mSWI/SNF complexes have been related during the last two decades to a great amount of oncologic diseases in different ways: by (i) the identification of recurrent mutations in mSWI/SNF subunits in a wide range of cancer types, with a rate comparable to classical tumor suppressors; by (ii) the detection that loss or genomic aberrations involving some of its subunits in certain cancers act as key tumor initiating and driving events; or by (iii) the discovery of multiple oncogenic properties of mSWI/SNF in transformed cells, revealing new therapeutic opportunities for the treatment of cancer[107,108].

Frequent inactivating mutations and loss of mSWI/SNF subunits in cancer

Early studies shortly after the discovery of the human SWI/SNF complex already reported a loss of expression of both catalytic subunits (SMARCA2/BRM and SMARCA4/BRG1) in different cancer cell lines, such as the SW13 adrenal cortex carcinoma and the C33 cervix carcinoma cell lines. Moreover, re-expression of the catalytic subunit exerted tumor suppressive effects on these cancer cells through the retinoblastoma (Rb) protein-mediated cell cycle blockage[456–459], suggesting its putative role as tumor suppressor in cancer cells. Loss of SMARCA4/BRG1 expression associated to recurrent mutations were detected in multiple cancer cell lines representative of different origins such as breast, lung, pancreas or prostate cancer [460–463], and these loss of expression and recurrent mutations were also found in patient samples of different tumor types, such as lung[464,465], gastric[466], oral[467] and skin[468] cancers. Posterior research continually increased the amount of cancer cell lines identified with loss or decreased expression of BRG1[469], and mutations in multiple subunits other than BRG1 were also discovered in different cancers, from the mutational loss of SMARCB1 in rhabdoid tumors[470] to the high frequency of ARID1A loss of expression, even higher than that of BRG1 loss, in several tumor types and cell lines, including breast and kidney carcinomas[471]. These initial studies marked the starting point, but the number of reports reporting recurrent mutations in subunits of the complex has exploded over the past two decades, as can be seen in Table 5, where published reports of tumor suppressive evidences attributed to mSWI/SNF subunits are listed, whether by recurrent inactivating mutations, recurrent loss of expression or functional experimental evidences of tumor suppressive functions.

Table 5: Tumor suppressive mSWI/SNF subunits in different human cancers. For each subunit and cancer type it is shown whether if recurrent inactivating mutations in tumor samples, loss of expression in tumors or functional experimental evidence supporting a tumor suppressive role have been reported.

Subunit	*Cancer type*	*Recurrent mutations*	*Loss of expression*	*Functional evidence*
SMARCA4	Pancreatic cancer	✓	✓	✓
	Lung cancer	✓	✓	✓
	SCCOHT	✓	✓	✓
	Oral cancer	✓	✓	
	Medulloblastoma	✓		
	Mesothelioma	✓		
	Neuroblastoma	✓		
	Urothelial carcinoma		✓	
	Esophageal carcinoma		✓	
	Skin carcinomas		✓	
	Gynecologic cancers			✓
	Retinoblastoma			✓
SMARCA2	Lung cancer		✓	✓
	SCCOHT		✓	✓
	Urothelial carcinoma		✓	
	Gastric cancer		✓	
	Skin carcinomas		✓	
	Esophageal		✓	
ARID1A	Ovarian cancer	✓	✓	✓
	Endometrial cancer	✓	✓	✓
	Pancreatic cancer	✓	✓	✓
	Gastric cancer	✓	✓	✓
	Lung cancer	✓	✓	✓
	Cervical cancer	✓	✓	✓
	Renal carcinoma	✓	✓	✓
	Colorectal	✓	✓	✓
	Hepatocellular carcinoma	✓	✓	✓
	Esophageal carcinoma	✓	✓	
	Neuroblastoma	✓	✓	
	Burkitt lymphoma	✓		
	Thyroid cancer	✓		
	Oligodendroglioma	✓		
	Breast cancer		✓	
ARID1B	Pancreatic cancer	✓	✓	✓
	Neuroblastoma	✓		
	Ovarian cancer	✓	✓	
	Endometrial cancer	✓	✓	
	Thyroid cancer	✓		
	Hepatocellular carcinoma	✓		✓
	Medulloblastoma			✓
ARID2	Hepatocellular carcinoma	✓	✓	✓
	Lung cancer	✓	✓	✓
	Thyroid	✓		
	Pancreatic cancer	✓		
	Mesothelioma	✓		
	Colorectal	✓		
PBRM1	Renal carcinoma	✓	✓	✓
	Mesothelioma	✓		
	Pancreatic cancer	✓		
SMARCB1	MRT	✓	✓	✓
	ATRT	✓	✓	✓
	Epithelioid sarcoma	✓	✓	
	MPNST	✓	✓	
	Myeloid leukemia	✓		✓
	Synovial sarcoma		✓	
	Thyroid	✓		
BCL7A	Non-Hodgkin lymphoma	✓		
	Multiple myeloma	✓		
SMARCC1	Ovarian cancer		✓	✓
	Colorectal cancer		✓	✓
	Prostate cancer			✓
BRD7	Ovarian cancer			✓
	Lung cancer			✓
	Digestive track tumors		✓	✓
SMARCE1	Breast cancer		✓	
SMARCD3	Breast cancer		✓	✓

SCCOHT means 'Small Cell Carcinoma of the Ovary, Hypercalcemic Type"; *MRT* means 'Malignant Rhabdoid Tumor'; *ATRT* means 'Atypical Teratoid/Rhabdoid Tumor'; *MPNST* means 'Malignany Peripheral Nerve Sheath Tumor'.

References: SMARCA4[462–465,467,468,472–480,481–487,488–492]; SMARCA2[466,468,479–481,488,489,493–495]; ARID1A[463,471,474,496–503,504–511,512–519,520–528,529–536,537–546]; ARID1B[474,487,500,531,537–539,544,547–552]; ARID2[486,504,513,525,531,544,553–559]; PBRM1[463,486,560–562]; SMARCB1[470,544,563–569,570–573]; BCL7A[574,575]; SMARCC1[576,577]; BRD7[578–581]; SMARCE1[582]; SMARCD3[583].

Indeed, the integration of all the data collected from genomic studies across samples from many different tumor origin in a meta-analysis published in 2013[232] shed light into the generalized relevance of the alterations of mSWI/SNF subunits in cancer. This study provided one of the most relevant facts regarding the role of mSWI/SNF complexes in human cancer: up to 19.6% of patient tumor samples from 44 different genomic analyses presented a missense, nonsense or insertion-deletion mutation in at least one subunit of the mSWI/SNF complex, suggesting a general role of this chromatin remodelers in tumorigenesis. The highest mutational rates were found in colorectal cancer, clear-cell ovarian cancer, renal cell carcinoma, hepatocellular carcinoma, medulloblastoma, acute-myeloid leukemia, and Burkitt lymphoma. In this meta-analysis[232], *ARID1A* was the most mutated subunit, followed by *SMARCA4*, *ARID1B*, *ARID2* and *PBRM1*, all of which showed mutational frequencies higher than the background mutational rate in two or more tumor types, revealing them as 'driver' tumorigenic mutations rather than 'passenger'. The majority of these mutations were found in heterozygosity, but around 14% of cases showed mutations in two or more different subunits, and authors hypothesized that compound heterozygosity effects among the mutations of different components may be the explanation behind the functional driver tumorigenic potential. If considering the whole complex as a single functional agent, these findings put mSWI/SNF complex at the same level in importance as classical pan-cancer tumor suppressors such as *TP53, PTEN* or *CDKN2A*, or oncogenes such as *PIK3CA*, *KRAS* or *CTNNB1* (β-catenin). In fact, a higher mutational rate was only detected for *TP53*, to which mSWI/SNF mutation frequency was comparable. *TP53* and mSWI/SNF mutations were mutually exclusive in different tumor types, such as colorectal and gastric cancers, which was interpreted as one more proof in favor of the driver role of these mutations. Finally, mSWI/SNF subunits were the most prevalently mutated genes among the different epigenetics regulators analyzed, such as Polycomb repressing complex, histone deacetylases or the other families of ATP-dependent chromatin remodelers.

The most frequently mutated subunit across multiple cancer types is *ARID1A*, which was initially found to be lost in many cancer cell lines, even more frequently than BRG1[471], and genomic approaches revealed the high frequency of inactivating mutations of this gene in different tumors. Its tumor suppressive role is remarkable in gynecological malignancies, being mutated in over 40% of endometrioid and clear cell ovarian carcinomas present[496–498], strongly correlating with loss of expression of the protein[496,499]. Similar results were obtained for other gynecological malignancies such as uterine endometrioid cancer, in which mutations[502] and loss

of expression[503] raised up to similar levels (~40% of cases), as well as in cervical cancer (~25% of cases)[517,518]. In these gynecological malignancies, its tumor suppressive role has been functionally validated[501,519], and the mutational loss of *ARID1A* has been suggested to be an oncogenic driver through the upregulation of the pro-survival PI3K-AKT signaling pathway[499]. In line with this, *ARID1A* mutations have been found to be concomitant with oncogenic PIK3CA mutations in these types of cancers[232,584]. Recurrent mutations in *ARID1A* associated with loss of expression and with functionally relevant tumor suppressive functions have been also found in pancreatic cancer[463,504], gastric cancer[507,508], lung cancer[512,513], renal cell carcinoma[520,521], colorectal cancer[524,525] and hepatocellular carcinoma[531] among others (Table 5). Interestingly, loss of ARID1A has been related to different tumorigenic traits, depending on the cancer type, including cell proliferation induction and apoptotic inhibition in lung, colorectal and gastric cancers[511,516,526] and the activation of epithelial-mesenchymal transition and invasiveness in several cancer types, such as pancreatic[505], gastric[510], renal[523] and colorectal[528] cancers, as well as neuroblastoma[540,542]. Recurrent mutations together with evidence of tumor suppressive functions have been also reported for neuroblastoma[537–542] and esophageal carcinoma[535,536]. Furthermore, in other types of tumors, such as Burkitt lymphoma, thyroid cancer or oligodendroglioma, frequent mutations are found[543–545], without further information about its relevance; and, on the other side, evidence of decreased expression of ARID1A have been reported in breast cancer cells[471,546] but no recurrent inactivating mutations have been reported until today.

Intriguingly, *ARID1B*, the paralogous *ARID1A* counterpart, has been shown to be much less mutated in cancer[232], revealing lower functional relevance in the tissues of origin of these cancers, that could be explained whether by non-completely overlapping functions of these two paralogues, or by a tendency towards higher expression of ARID1A to the detriment of ARID1B in tissues in general. Nevertheless, recurrent mutations and loss of expression of *ARID1B* have been reported in some cancers: in ovarian and endometrial cancers, a subset of patients show concomitant loss of ARID1A and ARID1B, and inactivating mutations of *ARID1B* have been found in these samples[500]. Recurrent *ARID1B* mutations have been also identified in genomic analyses of pancreatic cancer[548], neuroblastoma[487,537–539] and thyroid cancer[544], and tumor suppressive functions without reported mutations in patient samples have been found in hepatocellular carcinoma[551] and medulloblastoma[552], in both of them associated to the transcriptional control of specific sets of cancer-related genes.

SMARCA4/BRG1 is the second most frequently mutated subunit of the mSWI/SNF complex in human cancer. Its relevance as tumor suppressor is of especial interest in pancreatic and lung cancers. While somewhat frequent inactivating mutations in *SMARCA4* gene have been reported in up to 11% pancreatic cancer samples[463,472], in lung cancer, however, *SMARCA4* somatic mutations are sporadic[465]. Nevertheless, loss of protein expression is a more frequent event for both pancreatic (~50% of cases)[463,473,474] and lung (~30%)[464] cancers, and this trait has been related to poor prognosis. The driving tumor suppressive role of SMARCA4/BRG1 has been validated for both cancers[475,476] and attributed to the aberrant chromatin organization resulting from the loss of this subunit. Recurrent mutations in *SMARCA4* have also been reported in medulloblastoma, in this case only in the molecular subgroup defined by aberrations in the β-catenin pathway, and it has been proposed that the role of BRG1 as coactivator of the pathway may be the reason behind this relationship of concomitance[232,483–485]. *SMARCA4* gene has been found mutated also in mesothelioma[486], neuroblastoma[487] and oral cancer[467]; and lost without reported mutations in urothelial, esophageal and skin carcinomas[468,488,489], related to advanced tumor stages. Some tumor suppressive functions without observation of recurrent mutations or loss have been reported in retinoblastoma[492] and in gynecological malignancies, in the case of the latter ones based on the observation of breast and uterine tumor generation in heterozygous BRG1 mutant mice[490,491].

In the case of the other paralogue ATPase subunit *SMARCA2/BRM*, almost no significant mutations have been found in the genomic analysis performed on several tumor types[232]. However, in some cancers, loss of BRM expression has been reported in different tumors, such as lung cancer[493], in which silencing through promoter DNA hypermethylation has been described as a driving event in lung cancer progression[494]. Loss of BRM is also reported in gastric[466] and esophageal[489,495] cancers, with correlation with poor survival as well. Interestingly, concomitant loss of BRM and BRG1 has been reported in a considerable percentage (10%) of lung cancers, representing a patient subset of worse prognosis[464]. This concomitant tumor suppressive role has also been proposed for BRG1 and BRM in skin carcinomas[468]. The reason behind the higher prevalence of BRG1 mutations and loss in human cancers in comparison with BRM may be the greater functional relevance in a wide variety of tissues and developmental stages of the first one, a hypothesis sustained on the fact that BRM has been determined to be neither essential[585] nor expressed in key developmental steps such as in early embryonic pluripotent cells[218], in contrast with the essential functions of BRG1 in ESCs[586].

PBAF subcomplex-specific subunits have been also reported to be recurrently mutated or lost in different cancer types. In fact, *ARID2* and *PBRM1* are among the most frequently and widely mutated mSWI/SNF subunits[232]. *ARID2* inactivating mutations associated to loss of expression have been frequently detected in hepatocellular carcinoma[531,553–555], in which it has been demonstrated to suppress proliferation[556] and pro-metastatic[555] genes through transcriptional control. *ARID2* is also frequently mutated[513,557] and lost[558] in non-small cell lung cancers, through its role as transcriptional regulator of proliferation and metastasis genes, but also through its important DNA repair functions[558]. *ARID2* inactivating mutations are also recurrent in mesothelioma[486], pancreatic[504], thyroid[544] and colorectal[525,559] cancers. In the case of *PBRM1*, mutations have been detected in mesothelioma[486] and pancreatic cancer[463], but its role as frequently mutated tumor suppressor is of special relevance in clear cell renal carcinoma, in which it is found highly mutated (41% of cases)[560] and its loss of expression associated to poor prognosis[561]. PBRM1 has been seen to act in renal cancer by binding to acetylated p53 through one of its bromodomains and assisting the transcriptional functions of this tumor suppressor[562]. Remarkably, a type of familial renal cell carcinoma has been related to *PBRM1* germline mutations[449].

Mutations in the ATPase-associated subunit *BCL7A* have also been found to be significantly recurrent but restricted to a specific group of diseases, namely hematologic malignancies[232]. Concretely, *BCL7A* mutations have been detected in approximately 20% of non-Hodgkin lymphomas[574] and multiple myelomas[575]. Different tumor suppressive functions and downregulated expression associated to poor prognosis have been associated to other different mSWI/SNF subunits, including SMARCC1, BRD7, SMARCE1 and SMARCD3, in certain tumors (Table 5), but cancer-related mutations are rarely found in their corresponding genes, and are considered unlikely oncogenic drivers.

Interestingly, almost all mSWI/SNF mutations in cancer are found in heterozygosis, what could reflect a dose-dependent tumor suppressive functions of these specific subunits. Approximately a 14% of tumors carrying mSWI/SNF mutations present two or more heterozygous mutations in two or more different subunits, and it has been suggested that, due to the functional commitment of these group of genes, mutations in only one copy of multiple subunits may produce an effect of compound heterozygosity and compromise the functions of the complex, allowing this way to manifest the tumor suppressive role of these mutations[232]. However, most

of these mutations are strongly associated to the complete expression loss of the subunit, meaning that a second-hit must be conducing to loss of heterozygosity (LOH), probably through mutations, deletions or epigenetic inactivation of the remaining copy. This reinforces the adaptive advantage for cancers cells provided by the complete loss of these specific subunits, acting through the tumor suppressor pattern of classical mutated genes such as *TP53* or *RB*[107].

Specific mSWI/SNF aberrations define rare tumors

Although not representing a big proportion of the cancer cases with mSWI/SNF mutations, certain rare pediatric or juvenile cancers are of special interest due to the essential relevance of concrete aberrations involving subunits of the complex. Indeed, these malignancies are not just tumors with high frequency rates of mutations in specific subunits, but rather neoplasms defined by these aberrations, for the diagnose of which is necessary the identification of the specific mSWI/SNF subunit alteration.

First, small cell carcinoma of the ovary, hypercalcemic type (or SCCOHT) is a very rare type of ovarian cancer with early age of onset, 24 years in average, with patient ranging from 9 to 43 years, and has poor survival expectancy, with approximately half of the patients dying within the first 2 years after diagnose[587]. The vast majority (~90%) of this type of tumors show a complete loss of SMARCA4/BRG1 protein expression strongly associated to inactivating mutations[478,479] (Table 5). *SMARCA4* loss is attributed the bi-allelic gene inactivation through homozygous deleterious mutations, or heterozygous mutations followed by LOH events, although some cases of BRG1 protein loss with heterozygous genetic profiles are reported, probably due to epigenetic repression of the remaining copy[479]. Interestingly, concomitant loss of SMARCA2/BRM paralogue is detected in almost all cases[480], but no *SMARCA2* mutations have been associated to this phenomenon (Table 5). The oncogenic driver relevance of BRG1 and BRM loss have been proved for SCCOHT, and re-expression of the catalytic subunit of the complex exerts tumor suppressive effects on SCCOHT cells[481], by activating an epithelial-like transcriptomic signature that is lost upon BRG1/BRM inactivation[482]. The high sensitivity and specificity of this aberrant loss of expression of the mSWI/SNF ATPase subunits in SCCOHT, as well as its functional driving properties, has made BRG1/BRM loss a defining and fundamental trait used for the diagnose of this type of rare tumors[481].

On the other hand, SMARCB1 subunit is rarely mutated in the wide range of highly prevalent cancer types in which mSWI/SNF mutations are found. Nevertheless, SMARCB1 alterations are highly specific and of crucial relevance in a certain type of rare pediatric tumors known as malignant rhabdoid tumors (MRT) and atypical teratoid/rhabdoid tumors (ATRT), two closely related embryonic tumors of uncertain origin[588]. These tumors are highly aggressive and mostly appear at early ages in infants or children under 10 years, being the age of onset remarkably short, with cases reported within the two first months of life[589]. The difference between MRT and ATRT is the anatomical localization: MRT are extra-cranial and appear in varied localizations such as kidneys or soft tissues[590], while ATRT are tumors of the central nervous system (CNS)[591]. SMARCB1 loss of expression has been observed in the practical totality of these two types of tumors[563], associated to bi-allelic inactivation of the gene through different mutations or genomic deletions[470,566], being again a highly specific and sensitive defining trait used for the final diagnose of these neoplasms.

The functional consequences of losing SMARCB1 have been widely studied in rhabdoid tumors[563]: *SMARCB1* heterozygous mutant mice spontaneously develop rhabdoid tumors[564] and re-expression of SMARCB1 promotes cell cycle arrest of cells through p16^{Ink4a} activation[565], a relevant tumor suppressor that induces senescence[592]. Moreover, SMARCB1 loss has been shown to activate the expression of cyclin D1, allowing the progression of the cell cycle[593,594], as well as the activity of certain embryonic developmental pathways widely related to cancer such as Hedgehog/Gli1[595] or Wnt/β-catenin[596] pathways. Recent advances confirmed the molecular function of SMARCB1 in the mSWI/SNF complex as the key subunit for proper nucleosome binding[229]. It has been shown that tumorigenic loss of SMARCB1 does not produce an structural disassembly of the complex, but rather generates aberrant remaining complexes[155,597] unable to exert the antagonistic role of BAF and PBAF complexes against the repressing activity of Polycomb complexes[228], to which some of the oncogenic features gained from SMARCB1 loss have been attributed[598].

SMARCB1 loss is also recurrent in ~90% of epithelioid sarcomas[599], a rare mesenchymal malignancy of adolescents and young adults[568], in which big deletions affecting one copy and silencing of the remaining one through uncertain mechanisms are reported[600]. Recurrent SMARCB1 loss is also found in schwannoma and other malignant peripheral nerve sheath tumors (MPNST)[567,569], as well as in some myeloid leukemias[570,571]. Interestingly, some sporadic

rhabdoid tumors have been reported with SMARCA4 loss, instead of SMARCB1[601,602], and molecular analyses have revealed the great similarities between SCCOHT and rhabdoid tumors, mostly attributed to the strong functional link of these two genes. Some authors have even proposed the consideration of SCCOHT as 'MRT of the ovary', due to the molecular link through mSWI/SNF subunit aberrations[603,604]. Moreover, rhabdoid tumor predisposition syndrome, which causes one third of MRTs, are mainly inherited through *SMARCB1* germline heterozygous mutations, or by *SMARCA4* mutations in rare cases[449], which include SCCOHT as one of the clinical manifestations. Other predisposition syndromes caused by mSWI/SNF mutations are certain types of schwannomatosis and MPNSTs, caused by germline mutations of *SMARCB1*, or some familial cases of meningiomas attributed to *SMARCB1* or *SMARCE1* mutations[449].

Finally, another relevant rare cancer with defining mSWI/SNF aberrations is synovial sarcoma. It is rare soft tissue sarcoma manifested in both children and adults that arises from mesenchymal primitive progenitors. that appears near articulations, and with a current survival rate at 5-years after diagnose of 60-75%[605]. Interestingly, the recurrent mSWI/SNF alteration found in these tumors is not inactivating mutations or loss of expression, but rather a genomic rearrangement generating an oncogenic aberrant subunit variant. It has been known for long time that the driving oncogenic event is the aberrant fusion protein SS18-SSX caused by the translocation between the p arm of chromosome X and the q arm of chromosome 18, in the practical totality of synovial sarcoma cases[606–608].

Later, SS18 was revealed as a component of the mSWI/SNF complexes by its association with the catalytic subunits[267,268], concretely being a BAF-specific subunit[245]. Recent research has demonstrated the detrimental effects that the assembly of this aberrant fusion protein onto BAF complex has on its structural integrity: it impedes the correct incorporation of SMARCB1 subunit, generating a similar oncogenic effect as the SMARCB1 loss of rhabdoid tumors[269,270]. Interestingly, these studies suggested that the oncogenic consequences of this aberrant functions are based in the loss of function of the lost BAF complexes, but also in the gain of function of the SMARCB1-free aberrant complexes, which change genomic occupancy and reactivate pluripotency genes previously repressed by Polycomb repressing complexes, such as *SOX2*[269,270]. Interestingly, reduced SMARCB1 expression has been reported in synovial sarcomas (Table 5), most probably due to the destabilization of this protein upon the assembly of the aberrant SS18-SSX onto BAF complexes[572,573].

Oncogenic functions of mSWI/SNF subunits in human cancer

Paradoxical findings were already obtained in the initial studies regarding the role of mSWI/SNF complex subunits in oncologic diseases. Although the clear contribution of inactivating mutations and loss of function of concrete mSWI/SNF subunits strongly supports the tumor suppressive role of this chromatin remodeling complex in a wide variety of different tumors, increasing amounts of scientific literature support that the expression and activity of certain mSWI/SNF subunits is essential for the tumorigenesis and tumor progression of multiple cancer types (Table 6), revealing these proteins as interesting targets for hypothetical epigenetic therapies against cancer.

Table 6: Oncogenic mSWI/SNF subunits in different human cancers. For each subunit and cancer type it is shown whether if protein overexpression in tumor samples or functional experimental evidence supporting an oncogenic role have been reported, with the corresponding references.

Subunit	*Cancer type*	*Overexpression*	*Functional*
BRG1	Melanoma	✓ 609	✓ 610–615
	Acute myeloid leukemia		✓ 616–618
	Colorectal cancer	✓ 619	✓ 619,620
	Prostate cancer	✓ 621	✓ 622,623
	Breast cancer	✓ 624	✓ 625,626
	Hepatocellular carcinoma	✓ 627	✓ 627
	Gastric cancer	✓ 628	
	Medulloblastoma		✓ 629
	Neuroblastoma	✓ 630	✓ 630
	Glioblastoma	✓ 631	✓ 631
SMARCE1	Breast cancer	✓ 632	✓ 632–634
	Prostate cancer	✓ 635,636	✓ 635,636
	Ovarian cancer	✓ 637	✓ 637
	Gastric cancer	✓ 638	✓ 638
ACTL6A	Head and neck squamous cell carcinoma	✓ 639	✓ 639
	Esophageal carcinoma	✓ 640	✓ 640
	Rhabdomyosarcoma	✓ 641	✓ 641
ARID1A	Urothelial carcinoma	✓ 642	
	Hepatocellular carcinoma	✓ 534	✓ 534
ARID1B	Urothelial carcinoma	✓ 643	
SMARCC1	Prostate cancer	✓ 644	
DPF1/3	Glioma	✓ 645	✓ 645
SMARCD1	Hepatocellular carcinoma	✓ 646	✓ 646

Intriguingly, one of the most prevalently mutated subunits, SMARCA4/BRG1, is also the subunit for which more oncogenic properties have been described in a variety of tumors. Increased protein expression of BRG1 without genomic alterations was early reported in gastric cancers, and correlated with advanced stages[628]. In colorectal cancer, high protein levels of BRG1 have also been reported in patient samples[619] and a relevant oncogenic activity of BRG1 has been reported as transcriptional co-activator of β-catenin, a relevant oncogene in this type of tumors[620], and as activator of the cell cycle regulator cyclin D1 through the activation of the PI3K-AKT pathway[619]. Similar findings have been made in prostate cancer, in which aberrant increased expression of BRG1 is associated to tumorigenic and invasiveness traits[621], and it has been proposed as a therapeutic target[623]. Interestingly, although high levels of SMARCA2/BRM were also associated to oncogenic potential[621], other functional analyses have revealed that BRM exerts strong anti-proliferative effects in prostate cancer cells[622], indicating functional differences between both catalytic paralogues.

Oncogenic properties of BRG1 have been widely studied in melanoma. In this type of malignant cutaneous tumors, BRG1 has been found overexpressed in patient samples[609] and demonstrated to be crucial for the transcriptional activation of genes essential for melanoma oncogenic traits, by assisting the functions of the transcription factor MITF[610,611], an oncogene aberrantly overexpressed and with a central role in melanoma tumorigenesis that controls certain sets of genes essential for melanoma initiation, progression and plasticity[647]. Moreover, MITF-independent oncogenic functions have been also attributed to BRG1 in melanoma[612], including enhancement of invasive capacities[613] and transcriptional regulation of ultraviolet (UV)-inducible genes[614,615]. Oncogenic properties of BRG1 were also found essential for acute myeloid leukemia maintenance[616,617], together with other subunits of the complex including SMARCD2 and DPF2[618], a dependency not seen in healthy myeloid progenitors[617], suggesting a general oncogenic and aberrant activity of the complex gained in this kind of cancer potentially exploitable for a targeted therapy. BRG1 has also been found overexpressed and essential for breast cancer proliferation[624–626] as well as in hepatocellular carcinomas[627]. These oncogenic properties of BRG1 have been also found in tumors of the nervous system, both intra-cranial, such as glioblastoma[631] or medulloblastoma[629], in which BRG1 modulates transcriptional networks in the Hedgehog pathway dependent molecular subtype; and in extra-cranial neural tumors, namely neuroblastoma, in which our group found that BRG1 overexpression was

associated to poor prognosis and advanced disease stages, and that it controls the expression of key relevant gene sets related to survival and cell death pathways[630].

Besides BRG1, other different mSWI/SNF subunits have been also determined to play oncogenic roles in diverse malignancies. For instance, numerous studies have found oncogenic properties in SMARCE1/BAF57 subunit in breast cancer. Concretely, SMARCE1 has been demonstrated to be critical co-activator of estrogen receptors in these tumors[633], but also to positively regulate other oncogenic traits such metastatic potential[632,634]. This subunit exerts oncogenic and pro-metastatic roles also in prostate[635,636], ovarian[637] and gastric[638] cancers, and has been proposed as a potential therapeutic target for the treatment of these types of tumors.

Another oncogenic mSWI/SNF subunit is ACTL6A/BAF53, which was described in early studies as a transcriptional co-activator of the pan-cancer oncogene *MYC*[648]. Genomic amplification of *ACTL6A*, related to poor prognosis and increased proliferation through YAP pathway activation, has been described in head and neck squamous cell carcinoma[639], and in esophageal carcinomas[640]. Moreover, increased expression of this subunit contributes to the incomplete myogenic differentiation termination, a crucial hit for the initiation of rhabdomyosarcoma, a rare soft tissue sarcoma of the infancy[641]. Hints of oncogenicity have also been found for some other subunits. For example, high protein levels of ARID1A and ARID1B have been associated with poor outcomes of urothelial carcinoma[642,643]; SMARCC1 overexpression has been correlated with aggressive clinicopathological traits of prostate cancer[644]; DPF1 and DPF3 are functionally relevant for the maintenance of glioma cells stemness[645]; and SMARCD1 is overexpressed in hepatocellular carcinoma and promotes proliferation through activation of the mTOR signaling pathway[646].

While some of these oncogenic subunits, such as ACTL6A or DPF1/3, are different from the tumor suppressive ones explained before, surprisingly, some of the tumor suppressive mSWI/SNF components shown to be mutated or lost in specific tumors exert opposed functionalities by being essential for tumor maintenance and proliferation in other cases. This phenomenon gets strikingly interesting in the case of some subunits found to exert these two opposed roles in the same tumor type. BRG1 shows these kind of discrepancies in neuroblastoma, in which mutations in a small subset of patients (2.5%) are found[487], but it is known to control relevant oncogenic pathways at the transcriptional level[630]. Moreover, heterozygous mutations of BRG1 in mice promote breast cancer apparition[490,491], but high levels

of this protein have been related to poor prognosis in human samples[624,625]. Similar discrepancies have been observed from SMARCC1 in prostate cancer[577,644] and SMARCE1 in breast cancer[582,632–634].

Despite the apparent contradiction of these findings, the current evidence-based certainty of the high combinatorial complexity provided by numerous paralogue families and the tissue-specificity produced by multiple interplays with transcription factors and histone marks, among other agents, should prevent us from being puzzled by the discovery of unexpected functions in different oncologic scenarios. Indeed, although being a Herculean effort, current research is getting to reconcile these two apparently irreconcilable properties of the complex. For example, BRG1 is highly mutated in medulloblastoma[483–485] but it also exerts oncogenic roles in the same tumor[629]. However, this discrepancy is easily resolved because the molecular subtypes in which BRG1 has these two roles are different: as explained before, BRG1 mutations accumulate in the subtype with aberrations in the β-catenin pathway, whereas BRG1 has oncogenic properties in the medulloblastoma subtype associated to hyper-activated Hedgehog signaling; this reflects the context and pathway dependent functions of the mSWI/SNF complex. An interesting and elegantly explained case is the one of ARID1A in hepatocellular cancer, in which Sun and colleagues[534] described a context-dependent dual role of this subunit, acting as an oncogene that induces the formation and initiation of the tumor, but behaving as tumor suppressor in later stages of the disease, promoting when lost the metastatic spread of cancer cells.

mSWI/SNF mutations offer therapeutically exploitable synthetic lethalities

One of the most interesting findings about mSWI/SNF complexes in cancer is the identification of multiple and specific vulnerabilities of cancer cells with losses or mutations affecting the complex. In many cases, cancer cells with loss of certain subunits have been observed to strongly depend whether on remaining subunits of the complex (intra-complex dependencies), or on other related molecular mechanisms or pathways that may be exposed as weaknesses of cancer cells when mSWI/SNF function is altered (extra-complex dependencies). These relationships of synthetic lethality have been widely studied and proposed as an unprecedented opportunity for the targeted and high-precision treatment of tumors with mSWI/SNF complex alterations[345,649,650].

On the one hand, different intra-complex vulnerabilities have been described during the last two decades. Interestingly, the most well studied synthetic lethalities of this kind correspond to pairs of mutually exclusive paralogues, namely BRG1 with BRM, and ARID1A with ARID1B. Studies on lung cancer demonstrated that cells from tumors with loss of BRG1, whether by mutation or silencing, depended on BRM compensation for proper maintenance of proliferation and tumor growth capacities, whereas BRG1-retaining lung cancer cells were insensitive to BRM inhibition[651], proposing for the first time the exploitation of an intra-complex synthetic lethality as a therapeutic strategy. This BRG1 loss-dependent BRM vulnerability has been repeatedly confirmed in different BRG1-altered tumor types including lung, endometrium, ovary and esophageal cancers[495,652–654], and it depends on the ATPase functions of BRM, and not on its bromodomain[655]. Interestingly, biochemical studies have demonstrated the structural integrity of a BRM-containing fully assembled complexes in BRG1-depleted tumor cells[652], and that cells not simply depend on BRM activity, but on the whole functional integrity of this remaining complex, as demonstrated by similar synthetic lethalities at inhibiting the core subunit SMARCB1[653]. These findings reveal the partly redundant and partly divergent functions of BRG1 and BRM paralogues: a first hit involving loss of BRG1 might be driving tumorigenesis through loss of BRG1-specific tumor suppressive functions and/or gain of BRM-specific oncogenic ones, which renders cancer cells vulnerable to a second hit of BRM inhibition, that might fully suppress mSWI/SNF complex activities, causing detrimental effects on proliferation, viability and other oncogenic traits of cancer cells.

The other well studied intra-complex synthetic lethality is the dependency of ARID1A-altered cancer cells on ARID1B expression, in a similar way as BRG1 and BRM. This interplay between these two BAF subcomplex specific and essential interchangeable paralogues was first reported for ARID1A-lost ovarian clear cell adenocarcinoma[656,657] and further validated in other tumors such as colorectal cancer[658,659]. In the case of these subunits, the theory of 'partially redundant, partially specific' functions was validated at the chromatin remodeling level, revealing that ARID1A has more relevant specific functions of transcriptional control in normal conditions, which can be relied on ARID1B when mutated, conferring a specific vulnerability on the second one in those tumors[660]. How ARID1A loss provides adaptive advantage to cancer cells if their essential functions can be replaced by ARID1B is still an unanswered and open question.

Other dependency interplay between different mSWI/SNF subunits, that could be classified as 'inter-complex' synthetic lethality rather than 'intra-complex', is the vulnerability of SMARCB1-defficient tumors, such as MRT and ATRT, to the inhibition of the ncBAF complex-specific subunit BRD9. Indeed, this interplay between SMARCB1 and BRD9 was already determined before BRD9 was discovered as part of a non-canonical mSWI/SNF complex[661]. Today, it is known that ncBAF complexes, which in normal conditions lack of SMARCB1, are the less perturbed complexes in SMARCB1-deficient tumors and have crucial roles in controlling a transcriptional program essential for cancer cell proliferation and viability by maintaining the transcriptional activity on genes where canonical complexes have been displaced from, whether by SMARCB1 loss in MRT or ATRT, or by the incorporation of SS18-SSX fusion protein in synovial sarcoma[296]. This molecular interplay makes SMARCB1-deficient rhabdoid tumors specifically vulnerable to ncBAF-targeted therapies such as the pharmacological inhibition of BRD9[297]. Interestingly, this study reinforces the previously commented molecular similarities of rhabdoid tumors with synovial sarcoma, which has also been proposed as one rare tumor potentially benefited from BRD9-targeted therapies[662].

Besides the already mentioned interdependent vulnerabilities between components of the mSWI/SNF complex, few other synthetic lethalities between mSWI/SNF subunits have been found. Of especial interest is the systematic analysis performed by Schick and colleagues[663] using ovarian cancer as a model, in which they systematically inactivated through mutations 22 subunits of the complex, and interrogated by knockdown of every other subunit for new synthetic lethalities that would have gone unnoticed until then. By this approach, they validated the already known BRG1/BRM and ARID1A/ARID1B functional interactions, and revealed new synthetic lethalities involving another pair of paralogues, SMARCC1 and SMARCC2, but also between non-homologous subunits, such as SMARCA4 and ARID2, and SMARCA4 and ACTB. Nevertheless, this study highlighted the higher robustness and conservation among different cancer types of paralogue synthetic lethality in comparison with that of non-homologous subunits.

Beyond the complex, many molecular mechanisms and signaling pathways have been shown to be key vulnerabilities of cancer with alterations in mSWI/SNF subunits. For example, loss of certain subunits confers specific sensitivity to the inhibition of EZH2, the histone methyltransferase of Polycomb repressing complex 2[664], including tumors with loss of BRG1 and

BRM such as SCCOHT or lung cancer[664–666], ovarian carcinomas with ARID1A loss[667] or the SMARCB1-deficient malignant rhabdoid tumor[598,668]. The proposed rationale behind this interaction is the studied antagonism between mSWI/SNF activators and PRC repressors, being the latter responsible for carrying oncogenic functions when mSWI/SNF is mutated[598]. However, resistance to EZH2 inhibitors has been reported in mSWI/SNF altered tumors, and some authors have proposed a triple combination with the anti-apoptotic protein BCL2 inhibitors[669].

Inhibition of other epigenetic regulators has also been proposed for the treatment of this variety of tumors. Bromodomains inhibitors targeting the family of BET proteins, which includes the widely studied transcriptional regulator BRD4, have been proposed for the treatment of ovarian clear cell carcinoma with *ARID1A* mutations[670], but little rational is provided for this combinatorial effect, and the authors hypothesized that the down-regulation of ARID1B after BET inhibitors treatment should be the determinant event causing the anti-proliferative effect. Tumors with different mSWI/SNF subunit alterations have also been proved to be especially sensitive to HDAC inhibitors. Such is the case of the HDAC6 inhibitors[671] or pan-HDAC inhibitors[672] for the treatment of ovarian cancers with *ARID1A* mutations. Particularly, ARID1A loss promotes the reactivation of HDAC6, which deacetylates p53, inhibiting its pro-apoptotic functions[671]. The use of HDAC inhibitors in *ARID1A*-mutated ovarian cancer has been also tested with promising results in combination with anti-PD-L1 immunotherapy in this type of cancer[673]. Other epigenetic drugs have been shown to exert similar effects, such as histone demethylases inhibitors, which show efficient and specific anti-tumor activity against lung cancer or SCCOHT cells with BRG1 loss[674].

Beyond epigenetics, DNA damage through concrete classical chemo- or radiotherapy has been shown to produce anti-tumor synergism with BRG1[675,676] and ARID2[677] loss in pancreatic and hepatocellular carcinoma, respectively. This effect is probably related to the genomic stability role of PBAF complex during mitosis[275]. Of note, inhibition of the synthesis route of the antioxidant glutathione has synergistic effects on *ARID1A*-mutated gastric and ovarian cancers[678,679]. Moreover, different key molecular mechanisms related to different DNA repair events and cell cycle checkpoints have been identified as interesting vulnerabilities of mSWI/SNF deficient cancers and have been proposed as therapeutic targets. The relevant role of mSWI/SNF complexes in DNA repair make ARID1A-defficient tumors sensitive to inhibitors of key DNA repair regulators and associated cell cycle checkpoints, such as PARP[680,681], ATM[682]

or ATR[682,683]. Other pathways with similar effects upon inhibition on tumors with mSWI/SNF alterations include certain cell cycle regulators such as Aurora Kinase A[684] or CDK4/6[685,686]; or the inhibition of oxidative phosphorylation, which links SMARCA4 deficiency with higher oxygen consumption in lung cancer[687]. Finally, mSWI/SNF mutations have been lately found to be markers of response to certain immunotherapies in some highly malignant tumors such as pancreatic cancer[548].

The study of these synthetic lethalities is currently under intensive research, and some of these findings have already been translated into clinical trials, concretely those involving inhibitors already tested for other uses. As reviewed by Chabanon and colleagues[688], different clinical trials with mSWI/SNF alterations as inclusion criteria are currently ongoing: EZH2 inhibitors are being tested for SMARCB1-deficient, SS18-SSX translocation and SMARCA4-mutated cancer patients; PARP inhibitors for SMARCB1- and ARID1A-deficient tumors; and ATR and BRD4 inhibitors for *ARID1A*-mutated tumors. Further development of inhibitors of the different pathways mentioned before and of mSWI/SNF subunit-targeted drugs will increase the amount of clinical trials exploring the therapeutic exploitability of the synthetic lethalities offered by mSWI/SNF alterations in cancer.

1.2.8. mSWI/SNF-targeting drugs

The especial relevance of mSWI/SNF in a disease with such an impact as cancer, and the existence of key intra-complex vulnerabilities that can be exploited for therapeutic purposes, has accelerated during the last decade the development of different chemical compounds aimed at targeting and inhibiting the function of the complex through different mechanisms of action (Table 7).

The most numerous type of mSWI/SNF inhibitors are bromodomain inhibitors. Within this chromatin remodeler, there are several bromodomain-containing subunits: the constitutive ATPases SMARCA2/BRM and SMARCA4/BRG1, the PBAF-specific BRD7 and PBRM1, and the ncBAF-specific BRD9. An explosion of research on bromodomain inhibitors came after the success in the generation of the first compound targeting the BET family proteins BRD2, BRD3 and BRD4[96], able of displacing them from chromatin. Since then, multiple bromodomain inhibitors against all the bromodomain-containing mSWI/SNF subunits with different levels of

specificity have been developed and characterized. The first ones were PFI-3, inhibitor of BRG1/BRM and PBRM1 subfamily VIII bromodomains[689] and LP99, dual inhibitor of BRD7 and BRD9, closely related proteins of the bromodomain subfamily IV[690]. Since then, additional inhibitors have been developed with more specific selectivity for PBRM1[691,692], BRM[693] and BRD9[694–696]; as well as other multiple-bromodomain mSWI/SNF inhibitors, such as BRM/BRG1/PBRM1 pan-inhibitors[697,698] or more efficient BRD7/BRD9 dual inhibitors[696,699]. Nevertheless, mSWI/SNF bromodomains have been determined to be accessory elements with no crucial relevance for the chromatin remodeling *per se*, but rather be genomic targeting appendixes, what causes that bromodomain inhibition does not exert the anti-proliferative effects expected from synthetic lethality studies[655]. Therefore, additional inhibitors targeting the catalytic activity or the structural integrity of the complex should be generated in order to be able to exploit these intra-complex vulnerabilities.

Table 7: mSWI/SNF-targeting drugs, sorted by mechanism of action.

Inhibitor type	*Name*	*Target subunit*	*Reference*
Bromodomain inhibitor	PFI-3	BRG1, BRM, PBRM1 (fifth BD)	689
	Compound 12	PBRM1 (fifth BD)	691
	LM146	PBRM1 (second and fifth BDs)	692
	LP99	BRD7/9	690
	BI-7273	BRD7/9	696,699
	BI-9564	BRD9	696
	I-BRD9	BRD9	695
	Compound 26	BRG1, BRM, PBRM1 (fifth BD)	697
	DCSM06-05	BRM	693
	Compound 27	BRD9	694
	Inhibitor 22	BRG1, BRM, PBRM1 (all BDs)	698
PROTAC	ACBI1	BRG1, BRM, PBRM1	700
	dBRD9	BRD9	701
	VZ185	BRD7, BRD9	702
ATPase inhibitor	BRM014	BRG1, BRM	703
Transcriptional repression inhibitor	BRD-K98645985	ARID1A	704

Abbreviations: *BD* means 'bromodomain'.

A few compounds with different mechanisms of action have also been developed. For instance, an inhibitor of the ATPase activity of the complex was identified and characterized by high-throughput screening of chemical binding to the catalytic center of BRG1/BRM, already validated *in vivo* to exert the synthetic lethalities expected in BRG1-mutated tumors[703]. With a different approach, Marian and colleagues[704] developed an *in vivo* reporter of the repressing activity of ARID1A for the identification of non-toxic compounds targeting this property of the complex, in order to reverse the latency of genomic-integrated HIV. The resulting compound is a macrolactam compound that does not alter neither the ATPase activity nor the structural integrity of the complex, but has been shown to physically interact with ARID1A and displace the complex from chromatin. Although targeting a previously untargeted subunit, the effects of this strategy does not differ from the chromatin displacement exerted by bromodomain inhibitors, and the same limitations explained before may be also found for this compound for cancer synthetic lethalities exploitation.

Finally, the latest generation of mSWI/SNF-targeted drugs are based on the targeted degradation of proteins through the recruitment of ubiquitin ligase for their proteosomal degradation. This system, known as PROTAC (proteolysis targeting chimera), allows the physical interaction of the target protein and the ubiquitin ligase through a single small molecule formed by two modules of affinity to both proteins joined by a bridge[705]. Degrader PROTAC molecules have been developed against BRG1/BRM/PBRM1, by recruiting the E3-ubiquitin ligase to their closely related family VIII bromodomains, with great efficacy and selectivity[700]. Successful generation of PROTAC degraders has been also achieved for BRD9 degradation[701] as well as for dual degradation of BRD7 and BRD9[702]. The main advantage of this strategy is that the inhibition is produced by the complete degradation of the protein, producing the same effect as transcriptional silencing, and abolishing all functions of the targeted protein, overpassing the limited effect of bromodomain inhibitors or other compounds of similar mechanisms of action. Today, PROTAC degraders are the mSWI/SNF inhibitors more likely to promote structural disruption of the complex.

To this date, no protein-protein interaction inhibitor for the structural destabilization and disassembly of the mSWI/SNF complex has been developed.

1.3. **mSWI/SNF complex as therapeutic target in neuroblastoma**

1.3.1. Neuroblastoma

Molecular alterations of epigenetic regulators are even more relevant in cancers appearing in the childhood than in adults[63]. Pediatric cancers are rare diseases if considered separately, but together they constitute the main cause of pediatric death by disease in developed countries[706]. The social impact of this heterogeneous group of diseases has caused to focus humungous efforts on its research, making the current survival rate at 5 years of pediatric cancer patients noticeably higher than in adults. However, the improvement of this survival indicator has stalled in 80% during the last 20 years, making further research essential for the welfare of all pediatric cancer patients[706,707]. Moreover, child and adult tumors show deep differences in origin and clinical behavior, urging the study of pediatric cancers as independent biological entities and the development of specific therapies[708].

The most prevalent childhood cancers are the hematological malignancies, followed by tumors of the central nervous system (CNS) (Figure 12). Third is neuroblastoma, an embryonal neoplasia that stands out as the most common extracranial solid tumor of the infancy[709], representing the 7% of cancers yearly diagnosed in patients aged from 0 to 14 years[706,707]. Neuroblastoma accounts for 12-15% of pediatric cancer-related deaths[710], representing nowadays a clinical challenge in pediatric oncology departments of hospitals around the world. Translational research on molecular and biological features of this tumor is still a must for the identification of new diagnostic, prognostic and therapeutic tools for the improvement of life expectancy and welfare of neuroblastoma patients.

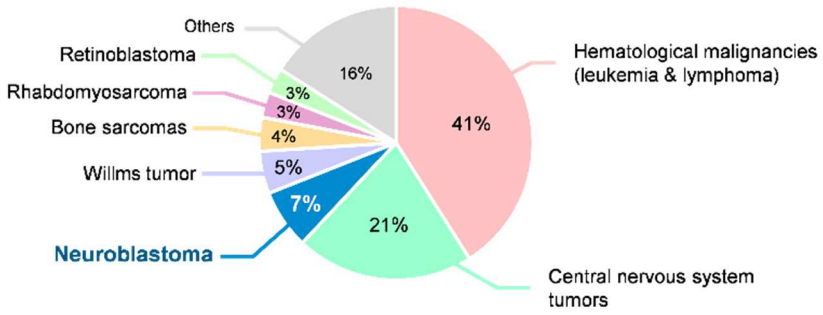

Figure 12: Frequency of each of the main groups of pediatric cancers. Contribution to the pediatric cancer incidence rate for patients aged 0-14 years is represented as percentage. Based on Ward *et al.* 2014[707].

Developmental origins of neuroblastoma

Neuroblastoma is an embryonal neural tumor occurring outside of the CNS, concretely in the sympathetic component of the peripheral nervous system[709]. It is classified as embryonal due to its proposed and widely accepted cell of origin: these tumors are thought to arise from sympathoadrenergic progenitors derived from neural crest cells that fail to fully differentiate during embryonic development[711]. Neural crest is a temporal cell aggrupation formed during gastrulation, at 3-5 weeks of human pregnancy, between the newly formed neural tube and the ectoderm, by a group of cells that delaminate from the neural tube (Figure 13). These are pluripotent cells that will later undergo long distance migration to varied corporal locations coupled to differentiation processes into different types of tissues, which are relevant for the respective destinations. Neural crest-derived tissues include craniofacial bones, melanocytes, adrenal chromaffin cells and cells of the sympathetic peripheral nervous system, being the latter the ones believed to originate neuroblastoma. These subset of neural crest cells, called trunk neural crest cells, perform a dorsolateral migration process for the formation of different structures of the peripheral nervous system, including sympathetic ganglia and the adrenal gland. These are the two main primary sites where neuroblastoma appears[711,712].

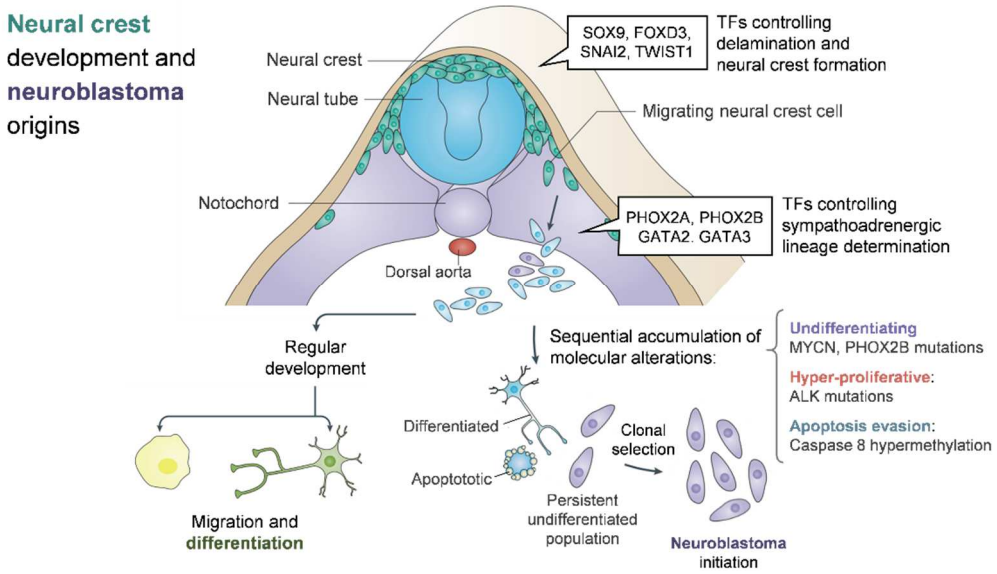

Figure 13: Neural crest development and neuroblastoma origins, adapted from Marshall *et al.* (2014)[712] and Matthay *et al.* (2016)[713]. Neural crest cells migration and differentiation is regulated by specific core transcription factors (TFs) and epigenetic events. Multiple aberrations involving these regulatory networks have been implicated in neuroblastoma origins by avoiding terminal differentiation, inducing hyperproliferation and evading apoptotic processes.

Neural crest formation and differentiation-coupled migration of neural crest progenitors is a complex multi-step process with a tight and delicate molecular signaling control that involves the communication between different cell populations through extracellular gradients of growth and transforming factors, such as BMP, Wnt or Notch signaling pathways. The activation of these pathways triggers the determination of the neural crest progenitors from a subpopulation of the neural tube, which leads to their delamination through epithelial-mesenchymal transition (EMT) mechanisms, and finishes with the migration to different locations and the final step of terminal differentiation. Multiple key transcriptional regulators of pluripotency (MYC) and EMT (SOX9, FOXD3, SNAI2, TWIST1) play critical roles during the initial neural crest induction and delamination steps, but need to be progressively shut down throughout the process, whereas adrenergic determination transcriptional programs must be activated through transcription factors like PHOX2B or GATA2/3. Errors in the correct signaling and achievement of each of these steps before neural crest cells complete the differentiation process have been proposed, based on multiple evidences, to contribute to neuroblastoma initiation[711].

Molecular alterations

The developmental origin of neuroblastoma is reflected in the molecular alterations driving its tumorigenesis and progression. Recurrent driving mutations are found in those key regulators of the differentiation process from neural crest precursors to sympathoadrenergic cells. For example, loss-of-function dominant negative mutations in *PHOX2B* gene, one of the transcription factors that is key in the determination of the adrenergic lineage differentiation, has been determined to be an early event in neuroblastoma origins[714,715], and autosomal dominant germline mutations of incomplete penetrance have been related to neuroblastoma predisposition, in the rare hereditary cases reported (1-2% of all neuroblastoma cases)[716].

Multiple chromosomal aberrations have been associated with the prognosis of neuroblastoma patients. The most frequent and relevant driving segmental chromosomal alterations are the loss of chromosome arms 1p and 11q[717–719], whether by deletion or by LOH, and the gain of 17q[720,721]. These alterations are frequent in the poorest prognostic neuroblastoma patients, and have been included in the guidelines for assessing risk stratification of the patients. In fact, neuroblastomas are characterized at the genetic level by the high prevalence and bad prognosis association of segmental chromosomal alterations in comparison to punctual mutations in genes[722]. Interestingly, the total chromosomal content (ploidy) is also associated with the

prognostic of the patients but, in this case, aberrations such as hyperploidy have been associated with a better prognosis in comparison with those tumors with diploid genomes but with segmental aberrations[723].

However, the most relevant chromosomal aberration in neuroblastoma is the genomic amplification of *MYCN*. Neuroblastomas are considered *MYCN*-amplified when more than 10 copies of this oncogene are detected, although it is usually found in hundreds[724]. It gives rise to an abnormal hyper-expression of MYCN protein, member of the MYC family of pluripotency-related transcription factors[725]. It is present in 20-30% of neuroblastomas[726], and implies the immediate classification of patients as high risk[713]. *MYCN* amplification has been widely shown to be a potent oncogenic driver of neuroblastoma. MYCN is expressed in neural progenitors of the CNS during regular development, but barely expressed in neural crest cells, in which a transient peak of expression is observed during dorsolateral migration[711]. It is proved that an abnormal misexpression of MYCN in neural crest precursors produces an aberrant maintenance of a transcriptional program that avoids its terminal differentiation, promoting pluripotency-like features such as increased proliferation, self-renewal, cell plasticity and migration capacities[727]. This aberrant overexpression, together with alterations avoiding cell death or cycle blockage, such as *TP53* mutations, has been proved to be a driving event in neuroblastoma origins[728]. Therapeutic targeting of MYCN is still a challenge under intensive research[729].

The second most recurrently mutated gene in neuroblastoma is the *anaplastic lymphoma* kinase (*ALK*) gene[538], encoding a tyrosine kinase receptor involved in developmental processes of the nervous system. Gain of function mutations in this gene are found in ~10% of neuroblastoma cases, including copy number gain and activating point mutations[730,731]. Hyper-activation of this receptor triggers the activation of the pro-survival and oncogenic MAP kinase pathway, among others, and is proved to be a relevant neuroblastoma initiating event[732,733]. Moreover, ALK germline mutations are found in more than 50% of neuroblastoma familial cases[734].

Despite the already mentioned low rate of point mutations in neuroblastomas, different recurrent mutated genes are currently known. Such is the case of *ATRX*, which encodes a SWI/SNF remotely-related chromatin remodeler thought to act as a histone chaperone[735], and shows loss of function mutations in 10% of cases, with higher frequency in adolescent patients (>14 years)[736]. Another example are mutations in the promoter of the telomerase gene (*TERT*), a well-known oncogenic driver in several cancers, which enhance its expression[737].

Clinical presentation and diagnose

Neuroblastoma is a pediatric cancer of early apparition, being the majority of patients diagnosed at ages between 0 and 4 years and with the average onset age at 19 months[710]. Indeed, it is the most common tumor diagnosed in the infancy (i.e. in patients aged 1 year or less)[738]. In fact, age at diagnosis is one important prognostic factor: a cutoff of 18 months of age is used for patient risk classification, with older patients showing a poorer prognosis and a higher susceptibility to developing metastatic disease[713].

Neuroblastoma most common primary tumor site is the adrenal gland medulla, in 47% of the cases, followed by sympathetic ganglia located at the abdominal (24%) or thoracic (15%) cavities (Figure 14). Adrenal gland neuroblastomas are mainly unilateral, with less than 1% of cases arising in both glands. Other less frequent primary tumor sites are the pelvis or the neck[739]. However, and probably due to its developmental origins, neuroblastomas have a high metastatic potential, with a 50% debuting with already formed metastasis[740]. The most frequent sites of neuroblastoma metastases are bone marrow (in 74% of metastatic cases), bone (61%), distant lymph nodes (35%) and liver (18%). Metastases in lungs, skin and CNS have been reported but are less frequent (<5% of metastatic cases)[739].

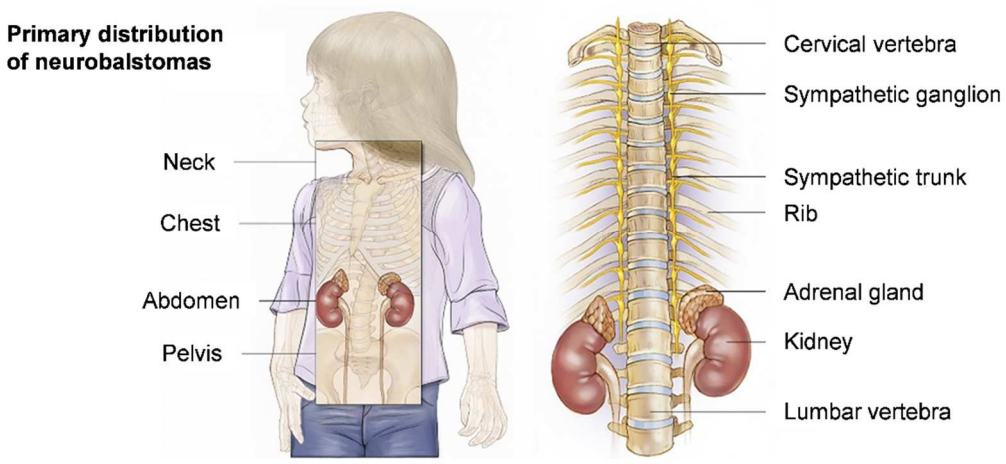

Figure 14: Main neuroblastoma primary tumor locations at the sympathetic peripheral nervous system. Extracted from cancer.net (American Society of Clinical Oncology, 2005).

Neuroblastoma is a heterogeneous disease that can manifest as from localized tumors to systemic metastatic disease. The International Neuroblastoma Staging System (INSS) has been the classical consensual criteria to classify neuroblastoma patients according to the progression of the disease. It classified each case in stages 1, 2, 3 or 4, with progressive increase of metastatic dispersion: from the localized and resectable primary tumors of stage 1 neuroblastomas, to the systemic metastatic dispersion of stage 4 tumors (Table 8)[741]. Nevertheless, a recent actualization has improved the classification of neuroblastoma patients into pretreatment risk groups (International Neuroblastoma Risk Group, INGR), in order to facilitate the comparison between clinical trials. This stratification is done based on the tumor features before surgery and treatment, and includes a new staging system (International Neuroblastoma Risk Group Staging System, INGRSS), which substitutes the INSS, and is based on image-defined risk factors (IDRF), namely radiological imaging diagnosis. INGRSS stages are L1, L2, M and MS (Table 8)[742].

The localization and stage of the primary tumor and/or metastatic lesions determine the symptomatology of the patients. Primary tumor at adrenal glands or abdominal cavity can produce abdominal distension; and, if located in paraspinal ganglia, can produce spinal cord compression. However, metastatic disease cause more severe and varied symptoms, depending on the organs affected, which include bone pain, fever, weight loss or anemia[713].

Table 8: INSS and INRGSS stages description, based in Brodeur *et al.* (1993)[741] and Monclair *et al.* (2009)[742].

System	*Stage*	*Description*
INSS	1	Localized tumor, complete surgical excision. No metastasis. No lymph node invasion.
	2a	Localized tumor, incomplete surgical excision. No metastasis. No lymph node invasion.
	2b	Localized tumor, complete or incomplete surgical excision with invasion to regional lymph nodes.
	3	Unresectable primary tumor. Unilateral or midline with abdominal infiltration, or unilateral localized with metastasis to distant lymph nodes.
	4	Any primary tumor with metastasis to distant lymph nodes or any other organ, except of 4S.
	4S	Localized primary tumor, <1 year, metastasis in skin, liver or bone marrow with <10% of tumor involvement.
INRGSS	L1	Localized tumor in one body compartment not involving vital structures.
	L2	Loco-regional tumor with one or more image-defined risk factors.
	M	Distant metastatic disease.
	MS	Distant metastatic disease, < 18 months, metastasis in skin, liver or bone marrow.

Neuroblastoma diagnosis combines imaging and symptomatic evidence together with laboratory blood and pathological analyses[713]. From the histopathologic perspective, neuroblastomas are composed of two different cellular components: neuroblasts or ganglionic cells, which are the tumor cells *per se,* and a variable population of Schwann cells forming what is called the Schwannian stroma. This stroma is of uncertain origin: while some authors claim that is composed from Schwann cells from healthy tissues, other have reported them to be also derived from a common tumor progenitor[743,744]. Neuroblastomas are pathologically classified depending on the percentage of Schwannian stroma and grade of morphological differentiation into three distinct categories: neuroblastoma, ganglioneuroblastoma and ganglioneuroma, from less to more differentiated. The latter two are highly differentiated and delimited tumors, with a high content of Schwannian stroma (>50%), and are considered the benign forms of neuroblastoma[713].

Neuroblastomas, as the malignant and less differentiated pathological category, are further classified according to cellular differentiation signs into undifferentiated, poorly differentiated and differentiating, as part of the routine prognostic assessment[745]. Undifferentiated or poorly-differentiated states are recurrently observed in aggressive and therapy resistant neuroblastomas, and are strongly associated to high-risk patients[746].

By contrast, neuroblastoma is believed to be the oncologic disease with the highest regression rate by spontaneous differentiation[747], which is of special interest in a subset of patients with advanced metastatic disease, classified as 4S by the INSS, or as MS by the INRGSS (Table 8). These are infant patients with metastases in skin, liver or bone marrow, that undergo spontaneous regression related to a massive cell death of undifferentiated neuroblasts. This phenomenon was reported to happen in a 2% of diagnosed neuroblastomas, but population screenings suggest that this rate may be higher, since spontaneous regression may be hiding the apparition of several cases of disseminated neuroblastomas that go unnoticed by the clinical practice[748]. Several hypotheses have been proposed to explain these cases, including the action of the immune system at some point of the early development, or the induction of telomere-induced senescence. In both cases, the absence of a second or third oncogenic hit might be the reason behind neuroblastoma spontaneous regression[749].

Risk stratification and clinical management

After clinical and pathological diagnosis, and before the treatment, neuroblastoma patients are classified in different risk groups based on the progression of the disease and molecular alterations, for the adjudication of specific treatment regimens. These pre-treatment risk groups, according the INRG system, are very-low, low, intermediate and high risk patients. The criteria for classification of patients on each group is shown in Table 9. Neuroblastoma risk groups were defined from a cohort of 8800 patients classified according to the features of groups of patients with 5-year event-free survival ranges of >85% (very-low), 75-85% (low), 50-75% (intermediate) and <50% (high risk)[742]. The practice has shown that very-low, low and intermediate risk groups present an overall survival rates higher than 90%[750]. High-risk patients, however, represent the main clinical challenge, showing an average overall survival at 5 years below 50%[750], and groups patients with most of the poor prognostic features: older than 18 months, stage M, and unfavorable molecular alterations such as MYCN amplification, segmental chromosomal alterations and diploid genomes[713].

Table 9: INRG risk group stratification system. Extracted from Matthay *et al.* 2016[713].

Risk group	*INRG stage*	*IDRFs in primary tumor*	*Age (months)*	*Histology*	*Differentiation grade*	*MYCN status*	*Genomic profile*	*Ploidy*
Very low	L1	Absent	Any	GNBn, NB	Any	–	Any	Any
	L1/L2	Any	Any	GN, GNBi	Any	–	Any	Any
Low	L2	Present	<18	GNBn, NB	Any	–	Fav.	Any
	L2	Present	≥18	GNBn, NB	Differentiating	–	Fav.	Any
	MS	Any	<12	Any	Any	–	Fav.	Any
Intermediate	L2	Present	<18	GNBn, NB	Any	–	Unfav.	Any
	L2	Present	≥18	GNBn, NB	Differentiating	–	Unfav.	Any
	L2	Present	≥18	GNBn, NB	Poorly/undiff.	–	Any	Any
	M	Any	<18	Any	Any	–	Any	Hyperdiploid
	M	Any	<12	Any	Any	–	Unfav. and/or diploid	
	MS	Any	12-18	Any	Any	–	Fav.	Any
	MS	Any	<12	Any	Any	–	Unfav.	Any
High	L1	Absent	Any	GNBn. NB	Any	+	Any	Any
	L2	Present	≥18	GNBn, NB	Poorly/undiff.	+	Any	Any
	M	Any	12-18	Any	Any	–	Unfav. and/or diploid	
	M	Any	<18	Any	Any	+	Any	Any
	M	Any	≥18	Any	Any	Any	Any	Any
	MS	Any	12-18	Any	Any	–	Unfav.	Any
	MS	Any	<18	Any	Any	+	Any	Any

Abbreviations: GNBn, 'Ganglioneuroblastoma nodular'; GNBi, 'Ganglioneuroblastoma intermixed'; GN, 'Ganglioneuroma'; NB, 'Neuroblastoma'; Undiff., 'Undifferentiated'; Fav. and Unfav., 'Favourable' and 'Unfavourable', respectively (presence or absence of segmental chromosome alterations).

Very-low and low-risk groups are treated with surgery alone, and a limited chemotherapeutic intervention is only indicated in case of patients with symptomatic or progressive disease[751], or when the primary tumor is unresectable[752]. Some patients, especially infants younger than 6 years, can even remain only under observation without any intervention[753]. Intermediate-risk patients receive a routine moderate inductive chemotherapy consisting in two to eight cycles of a carboplatin, cyclophosphamide, doxorubicin and etoposide combination[754], prior to surgical resection of the tumors. However, the impossibility of surgical resection and chemotherapy treatment alone reduces survival rate of this group from 90 to 70%[755].

High risk neuroblastoma are the group of patients receiving the most aggressive treatment regime (Table 10). In Europe, induction chemotherapy is administered following the indications of SIOPEN (International Society of Pediatric Oncology European Neuroblastoma), which determines a specific combination of therapeutics called 'rapid COJEC'[756]. Nearly at the end of or right after induction therapy, surgical resection is performed when possible, followed by consolidation therapy, consisting in high-dose myeloablative chemotherapy (i.e. that kills bone marrow cells) coupled to autologous hematopoietic stem cell transplantation, obtained and preserved during the final cycles of induction therapy, to repopulate bone marrow [757]. In Europe, SIOPEN directions establish a consolidation myeloablative therapy of busulfan and melphalan[758]. Consolidation therapy also includes radiotherapy to the primary tumor bed[757]. Finally, treatment of minimal residual disease is applied with the differentiating agent 13-*cis*-retinoic acid (RA) or with immunotherapy, consisting of antibodies against the neuroblastoma-specific ganglioside surface marker GD_2[759].

Table 10: Risk group-based treatment regimens established in Europe following SIOPEN directions[754-756].

Risk group	*Induction therapy*	*Surgery*	*Consolidation therapy*	*Minimal Residual Disease treatment*
Very low		✓		
Low		✓		
Intermediate	Carboplatin Cyclophosphamide Doxorubicin Etoposide	✓		
High	**Rapid COJEC**: Cisplatin (C) Vincristine (O) Carboplatin (J) Etoposide (E) Cyclophosphamide (C)	✓	**BuMel** (Myeloablative): Busulphan Melphalan **Radiotherapy**	**Isotretinoin** (13-*cis*-retinoic acid) **Dinutuximab** (anti-GD_2)

Nevertheless, relapse occurs in more than 50% of high-risk neuroblastoma patients, due to acquirement of resistance to classical chemo and radiotherapy. This group of patients show fatal prognostic, with a 5-year survival rate that drops to 20%, or below in patients that relapse earlier[760,761]. Today, there is not an established and consensus second line of treatment for neuroblastoma patients, although combinations of multiple high-dose chemotherapeutics are usually given. It is for these patients for which clinical trials with new therapeutic agents, combinations or regimens are crucial. Multiple targeted directed therapies have been tested or are still currently being tested, to overcome the resistance to standard-of-care therapeutics, including CDK4/6, ALK, PARP and BET inhibitors, and more recently some immunotherapy strategies[762].

1.3.2. Epigenetic alterations in neuroblastoma

Given the embryonal origin of neuroblastoma, and how alterations in relevant molecular signaling processes of neural crest determination and sympathoadrenergic differentiation play a role in neuroblastoma oncogenesis, it is not surprising that epigenetic mechanisms, which are essential for correct lineage determination and differentiation during development, are altered and relevant for the tumor initiation and progression of neuroblastoma. In fact, oncogenic epigenetic alterations have been found in neuroblastoma cells at the three epigenetic signaling levels (reviewed in[763]): DNA hyper- and hypo-methylation; the formation of oncogenic super-enhancers defined by aberrant histone mark patterns; the existence of non-coding RNAs with oncogenic or tumor suppressive functions; and the identification of multiple epigenetic regulators as putative therapeutic targets for neuroblastoma treatment.

DNA methylation in neuroblastoma

Regarding DNA methylation, hyper-methylation of certain tumor suppressor genes has been recurrently described. For example, abnormal methylation of the CpG island at caspase 8 promoter is found in the most aggressive neuroblastoma patients, concretely in 68% of MYCN amplified cases[764]. This adaptive silencing of caspases, which are proteases crucial in the triggering and execution of programmed cell death, or apoptosis, might be preventing cell death through activation of tumor suppressive mechanisms such as p53, acting as a secondary oncogenic hit. Hyper-methylation takes part in the silencing of multiple other genes with known

pro-apoptotic functions, such as the receptors of the extrinsic apoptotic pathway TRAILRs[765,766]. Promoter hyper-methylation has also been found in the promoters of neuroblastoma putative tumor suppressor genes such as *CAMTA1*, *CHD5* and *KIF1B*, which are located at 1p36, a region with recurrent LOH associated to poor prognosis[767]. Some have proposed this mechanism as a complementary silencing mechanism of the remaining chromosome copy at 1p36 LOH neuroblastomas[763]. On the other side, global hypo-methylation was has been also described in neuroblastoma cells , not only restricted to intergenic sites and promoting genomic instability, as reported for many other tumors[51–53], but also in several promoter and distal *cis* regulatory elements, driving the overexpression of oncogenic genes, such as the cell cycle regulator cyclin D1[768]. Whether hyper- or hypo-, the truth is that global DNA methylation patterns are altered in neuroblastoma, and some of these global changes are associated to clinicopathological features and have prognostic value[769–771].

Histone marks and super-enhancers in neuroblastoma

The generation of driving oncogenic super-enhancers that control and potentiate the transcriptional status of specific gene expression programs relevant for tumor initiation and progression has been repeatedly reported in neuroblastoma[58,772]. For example, a specific polymorphism in an intragenic sequence of the *LMO1* gene causes the apparition of a super-enhancer that aberrantly activates *LMO1*expression through aberrant hyper-activation by GATA transcription factors binding[773]. Phenomena like this example are not isolated events, and occur genome-wide in neuroblastoma cells, without the need of genetic polymorphisms. On the one hand, two different phenotypes related to the differentiation status of neuroblastoma cells, adrenergic or mesenchymal, have been defined by the transcriptional changes produced by super-enhancers defined by the activating acetylated H3K27 and controlled by developmental transcription factors[58]. This interesting data supports the idea that epigenetic errors blocking terminal differentiation are key and driving events in neuroblastoma genesis. More recently, analysis of super-enhancers, also defined by H3K27ac, in human neuroblastoma samples[772] has shown the control of several oncogenic factors relevant for neuroblastoma, such as *MYCN*, *ALK* or *CCND1* (cyclin D1) under these regulatory elements. Moreover, a clear clustering of the patients according to their super-enhancer landscape has been determined, generating super-enhancer signatures according to *MYCN* status and risk group, which are strongly associated to clinicopathological parameters. These epigenetic landscapes correlate with previously known

transcriptional circuitries regulated by core transcription factors[774] that also define different grades of differentiated phenotypes: for example, GATA3 transcriptional network is relevant for noradrenergic cells, while the FOS/JUN one is for neural crest-like ones[775].

Non-coding RNA in neuroblastoma

The role of non-coding RNAs as epigenetic regulators in neuroblastoma is still understudied. Research on non-coding transcripts in neuroblastoma has been practically limited to their correlation with clinicopathological parameters in order to generate lncRNA based prognostic tools. That is the case, for example, of SNHG1 lncRNA, associated to poor prognosis[776] or of a 24-lncRNA prognostic signature generated by Pandey and collaborators[777] able to discriminate between high- and low-risk neuroblastomas. This study also showed that the lncRNA NBAT-1 (Neuroblastoma-Associated Transcript 1) acts as a tumor suppressor in neuroblastoma by binding to the Polycomb family repressive epigenetic regulator PRC2 and inhibiting the expression of oncogenes. Other chromatin associated non-coding transcript, MALAT1, exerted a functional role, in this case oncogenic, by upregulating AXL tyrosine kinase receptor and increasing neuroblastoma invasiveness[778].

Epigenetic regulators as therapeutic targets in neuroblastoma

The deregulation of epigenetic signals suggests an abnormal function of epigenetic regulators in neuroblastoma, whether writers, erasers, readers or remodelers. Indeed, many of these regulators have been proposed as therapeutic targets for the treatment of neuroblastoma (reviewed in [70]). Multiple pathogenic mutations on epigenetic regulators were detected in a recent genomic analysis of 283 neuroblastoma samples, with mutations on 33 different epigenetic regulators found in up to 20% of samples, and mapping to functional domains in 8.4% of cases, being the most recurrent *ATRX*, *SMARCA4*, *MLL3* and *ARID1B* mutations[487]. These recurrent alterations of epigenetic regulators unveil interesting therapeutic opportunities in neuroblastoma. For instance, DNMTs, overexpressed in high-risk neuroblastoma, can be targeted by the hypomethylating agent 5-aza-2'-deoxycytitidine, resulting in anti-proliferative and pro-differentiation effects[779,780] and reversion of resistance to chemotherapeutics[781,782]. However, early phase clinical trials of this agent in combination with chemotherapy revealed strong toxicities, as reported for other malignancies. HDAC have been also long studied in neuroblastoma, and the use of multiple inhibitors targeting this numerous family of epigenetic

regulators, such as vorinostat, have shown multiple and varied anti-tumor effects, from preventing angiogenesis to sensitizing to radiotherapy[70].

Besides writers and erasers, therapeutically exploitable oncogenic roles for epigenetic readers have been detected in neuroblastoma cells, concretely for bromodomain-containing proteins. For instance, the BET protein BRD4 inhibitor JQ1 exerts anti-proliferative effects on neuroblastoma cells and, importantly, reduces MYCN levels, a crucial 'undruggable' neuroblastoma driver[783,784]. In the case of the epigenetic remodelers, genes of two different ATP-dependent chromatin remodeling complexes, *CHD5* and *ARID1A*, are located in the 1p36 chromosome, the deletion or LOH of which is recurrent in high-risk neuroblastoma patients, and is a marker of poor prognosis[718]. CHD5 forms part of a nucleosome remodeling and deacetylation (NuRD) epigenetic repressive complex[785] with functional relevance in nervous system development[786], and its loss has been functionally proved to be a determinant driver in a *MYCN*-independent manner[541,787]. Concretely, CHD5 exerts its tumor suppressing function through the transcriptional repression of cell cycle progression genes[788].

1.3.2. The mSWI/SNF complex in neuroblastoma

Epigenetic signaling writing, erasing and reading must be translated into chromatin condensation states to have functional consequences, and the mSWI/SNF chromatin remodeling complex is one of the main effectors in this sense. Therefore, it is easy to expect that in such an epigenetic-altered cancer as neuroblastoma this remodeler has a relevant role. Indeed, interesting studies giving insights on the functions of mSWI/SNF in neuroblastoma have been appearing during last years, basically focused on the BAF-specific structural paralogues ARID1A and ARID1B, and in the ATPase subunit SMARCA4/BRG1.

Early studies already detected a recurrent truncated form of ARID1A in neuroblastoma samples[789]. Genomic analysis of different neuroblastoma patient cohorts have detected frequent pathogenic deletions and truncating or point mutation in both *ARID1A* and *ARID1B* genes. Sausen and collaborators[538] were the first ones to detect mutations in these genes in a genomic analysis of 71 neuroblastoma samples. Up to 11% (8 out of 71) of cases showed point mutations or deletions in one of these two genes, and one of the cases showed mutations in both genes (Figure 15). If considering together these two almost functionally identical

paralogues, *ARID1A/B* genes were the third most recurrently mutated genes in neuroblastoma patient samples, only after *MYCN* and *ALK* alterations. Remarkably, patients with *ARID1A/B* mutations were determined to have a reduced survival expectancy in comparison with *ARID1A/B* wild-type neuroblastoma patients.

Independent studies have corroborated frequent mutation of these two subunits in neuroblastoma[487,537] and its association to poor prognosis[537]. Interestingly, neuroblastoma is the only tumor in which *ARID1B* is as much recurrently mutated as *ARID1A*, and in these studies with even higher frequency. *ARID1A/B* mutations have been also detected in circulating tumor DNA in 3 out 11 (27%) advanced metastatic stage neuroblastoma cases[539]. Moreover, *ARID1A* is located in 1p36, a recurrently lost chromosome arm in high-risk neuroblastomas, and it has been described as one of the main driving tumor suppressors that explain the poorer prognosis of 1p36-LOH neuroblastomas, by exerting potentiated oncogenic effects in combination with *MYCN* amplification[541].

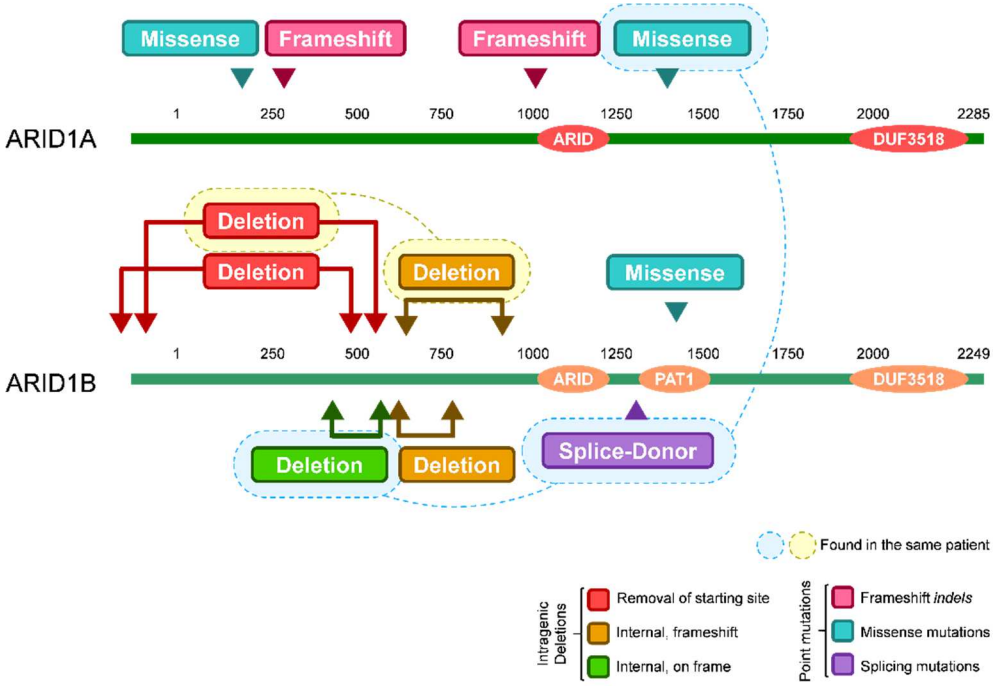

Figure 15: Genetic alterations found by Sausen *et al.* (2013)[538] in *ARID1A* and *ARID1B* genes by means of genomic analyses of neuroblastoma samples. Graph shows the location of the mutation in the amino acid sequence of the proteins. Protein domains ARID, DUF3518 (unknown function) and PAT1 are indicated.

Different studies have shed some light on the tumor suppressive functional mechanism of *ARID1A/B* that may be explaining its recurrent mutations in neuroblastoma. ARID1A was reported to be upregulated upon RA treatment, and to participate in the anti-tumor effects of this differentiating agent through the repression of telomerase (*TERT*) transcriptional expression by genomic binding and recruitment of the SIN3A transcriptional repressor, a mechanism already reported for different cancers[790]. ARID1B was showed to inhibit WNT/β-catenin signaling pathway, leading to differentiated phenotypes when inhibited[791], what reinforces the functional role of this paralogue in nervous system development that could explain its specific greater importance in neuroblastoma in comparison with other tumors.

In a 2020 study, Shi and colleagues[540] showed that homo- or heterozygous knockout of *ARID1A* increases neuroblastoma penetrance in a *MYCN*-driven zebrafish model, as well as tumor volume through hyperplasia of sympathoadrenergic precursors during development. In this study, partial or complete loss of *ARID1A* also increased the migrating and invasive capacities of the NGP human neuroblastoma cell line by promoting adrenergic-to-mesenchymal transition, an effect that had already been reported before[542]. They also showed that after ARID1A depletion, ARID1B-complexes were structurally intact, and corroborated in neuroblastoma one of the intra-complex synthetic lethalities already assessed in other tumors: the proliferative dependency on ARID1B of ARID1A-mutated cells. However, they did not deepen into the substitutive role of ARID1B regarding its molecular functions and genomic repositioning after ARID1A loss, nor the phenotypic effects of the complete depletion of the ARID1 paralogue family and BAF structural disruption.

On the other side, SMARCA4/BRG1 ATPase subunit has been also studied in neuroblastoma. A genomic analysis in 2018[792] found few *SMARCA4* gene point mutations in the most aggressive subset of stage M neuroblastoma patients. Later, recurrent *SMARCA4* gene mutations were detected in 2.5% of cases in a recent genomic analysis of 283 neuroblastoma samples[487], together with *ARID1B* and *ARID1A* mutations. Eight alterations were found: 6 point mutations with pathogenic prediction, one focal deletion and one complete deletion. Three samples presented double events affecting both copies. This study also found in one of the samples double deleterious events in the PBAF-specific PBRM1 subunit, and less recurrent sporadic alterations in *ARID2*, *SMARCA2*, *SMARCC1* and *SMARCD3* genes.

These inactivating mutations of *SMARCA4* gene in a subset of neuroblastoma patients are in contrast with results from our group published in 2016[630], in which the catalytic subunit SMARCA4/BRG1, but not its counterpart SMARCA/BRM, mRNA and protein expression levels correlated with poor prognosis and advanced stages in neuroblastoma patient samples. It was also determined that this subunit controlled a transcriptional program involving key regulators of cell survival and apoptotic pathways, suggesting an oncogenic functional role. Therefore, inhibition of the BRG1-dependent mSWI/SNF catalytic activity was proposed as a potential therapeutic strategy to overcome resistance in high-risk neuroblastoma patients.

The above explained current state in the field of research of mSWI/SNF remodeling complex in neuroblastoma presents large knowledge gaps and even contradictions, and deeper investigations into the functional role and biological value of the mSWI/SNF chromatin remodelers in neuroblastoma are needed. Indeed, these ambiguous and somewhat contradictory results, far from demotivating research efforts, pose a major scientific challenge and encourage the deeper study of this epigenetic regulator in a pediatric tumor with urgent needs for novel therapies.

2. **HYPOTHESIS** AND **OBJECTIVES**

I don't know just where I'm going
But I'm gonna try for the kingdom, if I can

Heroin
The Velvet Underground
The Velvet Underground & Nico
1967

Widespread metastatic dissemination and resistance to therapy are the main clinical challenges for the cure of relapsed high-risk neuroblastoma patients. Discovery and exploitation of neuroblastoma vulnerabilities by research on its biology and molecular alterations, leading to new therapies targeting signaling pathways and molecular mechanisms responsible for its aggressiveness, are needed to overcome the therapy resistance acquired by tumor cells in this subset of patients. Indeed, a proposed therapeutic strategy that has become increasingly common in recent years for the treatment of refractory tumors is multi-targeted therapy. It consists in the use at once of multiple targeted therapies to inhibit or activate different pathways or mechanisms that might be cooperating for the survival and progression of cancer cells, in order to avoid compensation effects when only inhibiting one.

The study of epigenetic regulators with altered functions in tumors and its therapeutic targeting opens the possibility of exploiting their genome-wide transcriptional control and revert aberrant cancer gene expression programs, which involve genes related to different cancer-relevant oncogenic pathways and biological functions. Through this mechanism, an epigenetic therapy with a single pharmacological agent designed for the inhibition of a key epigenetic writer, eraser, reader or remodeler, should ideally have the same effect on multiple pathways as the individual targeting of each of them separately with different drugs in a multi-targeted therapy (Figure 16). Moreover, the possible off-target epigenetic changes promoted in non-tumor cells would be reversible, reducing the probability of long-term side effects, another advantage in comparison with classical DNA-damaging chemo and radiotherapies.

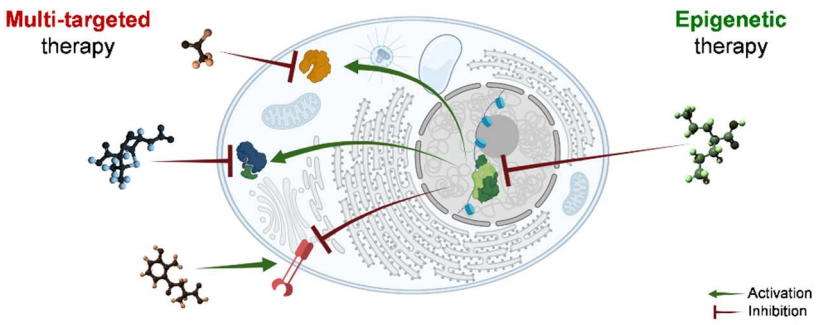

Figure 16: The multi-targeted aspect of epigenetic therapy, in comparison with classical multi-targeted therapies.

An interesting epigenetic regulator to study in neuroblastoma is the mSWI/SNF chromatin remodeling complex. As exposed in the introduction, there is a lack of knowledge and conflicting information regarding its functions in neuroblastoma, two facts that by themselves already justify the need for deeper investigations. In addition, previous work from our group attributed oncogenic properties to one of the catalytic subunits of the mSWI/SNF complex, the ATPase SMARCA4/BRG1.

Relevant functions of these remodelers in neuroblastoma cells can be guessed from the fact that specific epigenetic landscapes are crucial for neuroblastoma tumor phenotypes. Therefore, we hypothesized that, being mSWI/SNF complexes essential effectors of epigenetic signaling, they mediate the phenotypic consequences and maintenance of these particular chromatin states and oncogenic transcriptional programs in neuroblastoma cells.

Therefore, a systematic analysis in neuroblastoma cells of the mSWI/SNF complex as a whole, and not of its subunits as independent entities, is needed in order to corroborate our hypothesis, to fully understand its functions and to evaluate a possible epigenetic therapy focused on this chromatin remodeler. With this main purpose, four leading objectives were defined for the development of this thesis:

1. To assess the presence and composition of mSWI/SNF complexes in neuroblastoma cells.
2. To determine the biological relevance of mSWI/SNF complexes in neuroblastoma.
3. To determine the biological processes transcriptionally controlled by the mSWI/SNF complex in neuroblastoma.
4. To develop a therapeutic strategy to target the mSWI/SNF complex.

3. **MATERIALS** AND **METHODS**

Quién pudiera escoger
Sus armas al nacer
Y no enloquecer
Bajo el enroque cruel

Cuello Isabelino
Medalla
Medalla
2019

3.1. **Cell lines and tissue culture**

Five different neuroblastoma cell lines were used during the course of this work: SK-N-BE(2), SH-SY5Y, SK-N-AS, CHLA-90 and IMR-32 cell lines. Cell line features are listed in Table 11. SK-N-AS, SH-SY5Y and IMR-32 cell lines were purchased from American Type Culture Collection (ATCC, Manassas, VA, USA); SK-N-BE(2) cell line was procured from the Public Health England Culture Collection (Salisbury, UK); and CHLA-90 cell line was obtained from the Children's Oncology Group Cell Culture and Xenograft Repository (Lubbock, TX, USA). All neuroblastoma cell lines were cultured, as suggested by Children's Oncology Group Cell Culture and Xenograft Repository, in Iscove's modified Dulbecco's medium (IMDM, Gibco, Amarillo, TX, USA), supplemented with 20% heat-inactivated fetal bovine serum (FBS; South America Premium, Biowest, Nuaillé, France), 1% insulin-transferrin-selenium supplement (Gibco), 100 U/mL penicillin, 100 µg/mL streptomycin (Gibco), and 5 µg/mL plasmocin (InvivoGen, San Diego, CA, USA). The human embryonic kidney cell line HEK293T was purchased from ATCC and cultured in Dulbecco's modified Eagle's medium (DMEM, Gibco), supplemented with 10% heat-inactivated FBS, 100 U/mL penicillin, 100 µg/mL streptomycin, and 5 µg/mL plasmocin.

All cultures were maintained at 37 °C in a 5% CO_2 saturated atmosphere, and biannually tested for mycoplasma contamination. All cell lines grew in adhesion as monolayer. Before reaching confluence, cells were rinsed once with phosphate-buffered saline (PBS; Hyclone Laboratories, Logan, UT, USA) and detached using 0.05% trypsin (Gibco) or non-enzymatic cell dissociation buffer (Gibco), collected with fresh medium, centrifuged for 3 minutes at 800 rpm, resuspended and cultured in new plates or flasks with fresh medium.

Table 11: Neuroblastoma cell lines molecular features and clinical parameters of the patients of origin, extracted from ExPASy's Cellosaurus database[793].

Cell line	*Lesion of origin*	*Stage*	*MYCN status*	*TP53 status*
SK-N-BE(2)	Bone marrow metastasis	4	Amplified	Mutated
SH-SY5Y	Unknown	4	Non-amplified	Wildtype
IMR-32	Bone marrow metastasis	4	Amplified	Wildtype
SK-N-AS	Bone marrow metastasis	4	Non-amplified	Mutated
CHLA-90	Bone marrow metastasis	4	Non-amplified	Mutated

Cell counting was performed by mixing a 10 µl sample of cell suspension with 10 µl of 0.4% trypan blue and loading 10 µl of the mixture onto Cell Counting slides (NanoEntek, Seoul, South Korea); viable cell number was determined using Cell Counter EVE (NanoEntek).

For cell line storage, cells were cryopreserved in FBS with 10% dimethyl sulfoxide (DMSO) by slow freezing using an isopropanol freezer container at -80ºC, prior to immersion into liquid nitrogen. Resuscitation of frozen cells was performed by rapid thawing at 37ºC, dilution of cells into fresh medium, centrifugation, resuspension and plating in fresh medium.

3.2. **Lentiviral shRNA vectors production and transduction**

Silencing pLKO.1-puro plasmids carrying shRNA against different proteins were purchased from Sigma-Aldrich (St. Louis, MO, USA) Mission shRNA repository (Table 12). DNA vectors were transformed into bacterial Library Efficiency DH5α Competent Cells (Invitrogen, Waltham, MA, USA) by the heat-shock method following manufacturer's recommendations. Briefly, aliquots of competent cells were thawed on ice and mixed with 1-50 ng of plasmid DNA, incubated 20 minutes on ice, heated 45 seconds at 42ºC and placed back on ice for 2 minutes more. After heat-shock, bacteria were diluted 1:10 in S.O.C. Medium (Invitrogen) and plated on LB agar (Invitrogen) plates with 100 µg/mL ampicillin (Sigma-Aldrich). Resulting bacterial colonies were used for culture amplification by inoculation in lysogeny broth (LB) medium (Sigma-Aldrich) with ampicillin 100 µg/mL. Plasmids were extracted using midi (Plasmid Midi Kit, Qiagen, Hilden, Germany) or maxiprep (NucleoBond Xtra Maxi EF, Macherey-Nagel, Allentown, PA, USA) plasmid DNA extraction kits. Glycerol -80ºC stocks were prepared by mixing bacterial suspension with sterile glycerol in a 1:1 proportion. Plasmid DNA concentration was assessed by quantification with Nanodrop 2000 spectrophotometer (Thermo Scientific, Waltham, MA, USA).

Lentiviruses were generated in HEK293T cells using previously described methods[794,795]. One hundred mm plates were coated with 5 mL of 0.1% gelatin from bovine skin (Sigma-Aldrich) for 20 minutes at 37ºC before rinsing once with PBS. A total of 4 million HEK293T cells were plated on each gelatin-coated 100 mm plate. The day after, each HEK293T plate was transfected with a mixture of 12 µg of the specific shRNA plasmid together with lentiviral helper vectors: 4 µg of envelope plasmid pMD2G and 8 µg of packaging plasmid psPAX2. Transfection was performed

using Lipofectamine 2000 (Invitrogen) following manufacturer's instructions. Briefly, the three plasmids together with 30 µl of Lipofectamine 2000 were mixed in 2 mL of OptiMEM (Gibco) and incubated for 20 minutes at room temperature. During this time, the medium of HEK293T cells was replaced by 6 mL of OptiMEM supplemented with 5% FBS. After incubation, the 2 mL of transfection mixture were added on each plate, gently shaken, and incubated at 37ºC for 6 hours; then, transfection mixture was replaced by fresh medium of the target cells, i.e. IMDM supplemented with 20% FBS for neuroblastoma cells. Two days after transfection, lentiviral supernatant was collected, centrifuged for 5 minutes at 1500 rpm to discard floating HEK293T cells, and passed through a 0.45 µm syringe filter (Fisher Scientific, Waltham, MA, USA). Lentiviral supernatants were frozen at -80ºC and stored until further use.

Table 12: shRNA target sequences and related information.

Target protein	*shRNA name*	*Sigma-Aldrich ID*	*Target sequence*	*Transcript accession*	*Position in transcript*	*Transcript region*
ARID1A	shARID1A #1	TRCN0000059088	CGGCTCACAATGAAAGACATT	NM_006015.6	5361 to 5381	CDS
	shARID1A #2	TRCN0000059089	GCCTGATCTATCTGGTTCAAT		2306 to 2326	CDS
	shARID1A #3	TRCN0000059090	CCTCTCTTATACACAGCAGAT		1721 to 1741	CDS
	shARID1A #4	TRCN0000059091	CCGTTGATGAACTCATTGGTT		7182 to 7202	CDS
	shARID1A #5	TRCN0000059092	GCAGCCAAACTATAATGCCTT		2822 to 2842	CDS
ARID1B	shARID1B #1	TRCN0000415830	TGGTCACGTTGGCCAACATTT	NM_017519.3	6587 to 6607	CDS
	shARDI1B #2	TRCN0000416443	GGGTTTGGCCCAGGTTAATAA		3846 to 3866	CDS
	shARID1B #3	TRCN0000436265	TGCTGTCTAGTGCATTCAAAG		7512 to 7532	3'-UTR
	shARDI1B #4	TRCN0000420576	GAAGATTAGAGGGTCACATAT		7293 to 7313	3'-UTR
ARID2	shARID2 #1	TRCN0000166160	CCGCTGAAATCATGTGGGTAT	NM_152641.4	7715 to 7735	3'-UTR
	shARID2 #2	TRCN0000162164	CCAGCGTGAAATGTATCCATT		6902 to 6922	3'-UTR
	shARID2 #3	TRCN0000166264	CGTACCTGTCTTCGTTTCCTA		1059 to 1079	CDS
	shARID2 #4	TRCN0000166321	CCTCCTTCAAACTCAGGGAAA		4044 to 4064	CDS
	shARID2 #5	TRCN0000166359	CCGACTAACAGCTGCCTTAAT		5435 to 5455	CDS
SMARCC1	shSMARCC1 #1	TRCN0000297368	CCCACCACATTTACCCATATT	NM_003074.4	704 to 724	CDS
	shSMARCC1 #2	TRCN0000278033	GCTATGATACTTGGGTCCATA		812 to 832	CDS
	shSMARCC1 #3	TRCN0000277971	CCTAGCTGTTTATCGACGGAA		177 to 197	CDS
	shSMARCC1 #4	TRCN0000278029	GCTCTCTTGGTTGAGACACAA		2785 to 2805	CDS
	shSMARCC1 #5	TRCN0000015630	GCTATGATACTTGGGTCCATA		812 to 832	CDS
SMARCC2	shSMARCC2 #1	TRCN0000015702	CGCAGTGAAAGCTAAGCACTT	NM_003075.5	2629 to 2649	CDS
	shSMARCC2 #2	TRCN0000329883	TCACTAAACTGCCGATCAAAT		240 to 260	CDS
	shSMARCC2 #3	TRCN0000329808	CCCAACAAATGCTCAACTTTC		1686 to 1706	CDS
	shSMARCC2 #4	TRCN0000015701	CCAAACTACTAGGGAAATTAA		471 to 491	CDS
	shSMARCC2 #5	TRCN0000329885	GCCTGTCTCGACCTAACATTT		429 to 449	CDS
Non-Silencing Control		SHC002	CAACAAGATGAAGAGCACCAA	No human or mouse target		

CDS means 'Coding Sequence'; 3'-UTR means '3'-Untranslated Region'.

Transduction of neuroblastoma cell lines with lentiviral particles was performed by seeding 5 × 10^5 neuroblastoma cells (SK-N-BE(2) or SH-SY5Y) in 60 mm plates with lentiviral supernatant diluted in IMDM 20% FBS medium at different dilutions, depending on the cell line. A balance between sufficient transduction rates and viral toxicity was empirically assessed for each cell line. SK-N-BE(2) cells were transduced with lentiviral supernatant diluted 5 times in single transduction experiments, and 3 times in combination experiments; whereas SH-SY5Y cells were transduced with 10 times diluted lentiviral supernatant in single transduction experiments, and 5 times in combination experiments. The next day after seeding and transduction, lentiviral supernatant was replaced by fresh medium. Transduced cells were maintained in culture, and used at the time points indicated in the different experiments. If needed, selection of transduced cells was performed making use of the puromycin resistance cassette included in pLKO.1-puro vectors, by treatment with 1 µg/mL puromycin (Sigma-Aldrich), at least 48 hours after transduction, and until control non-transduced cells were completely dead.

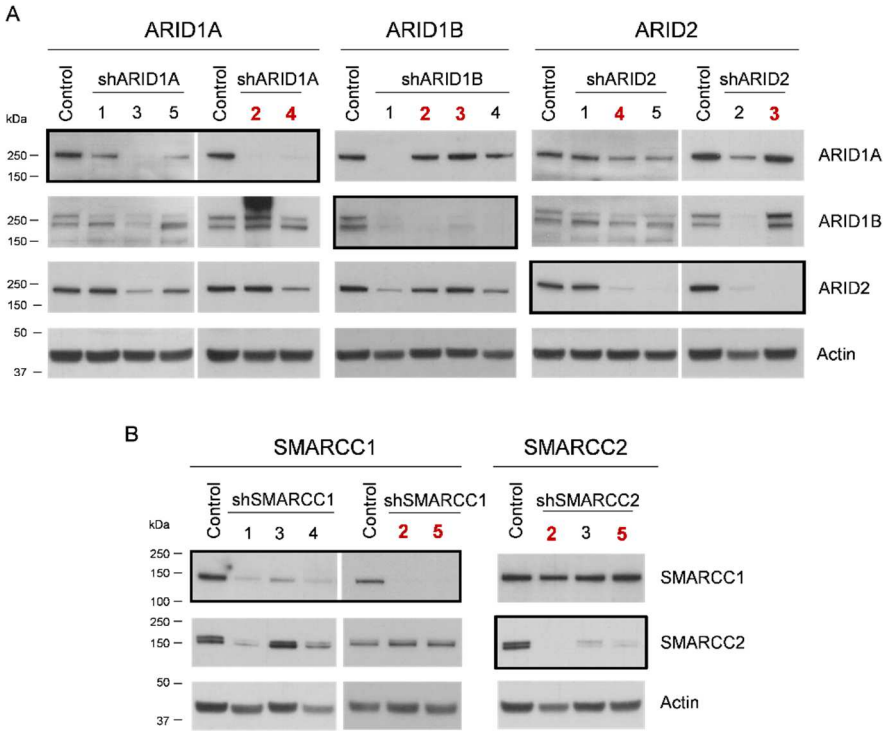

Figure 17: Validation of shRNAs against mSWI/SNF subunits in neuroblastoma cells. SK-N-BE(2) were transduced with different lentiviral vectors carrying shRNAs against the indicated subunits, or with a non-silencing negative control. After transduction, cells were left grow for 96 hours, prior collection and lysis for western blot analysis of ARID1A, ARID1B and ARID2 (**A**), or of SMARCC1 and SMARCC2 (**B**) protein levels, using actin as loading control. Bold dark-red marked numbers indicate the shRNA chosen for functional experiments. Framed panels indicate each shRNA-target protein.

Between four and five shRNA with different target sequences were acquired for each target protein to knockdown, and their efficacy and specificity was assessed before selecting the two shRNAs with a better profile for both parameters. This was especially important because shRNAs targeting mSWI/SNF paralogue family members, such as ARID1A, ARID1B and ARID2, or SMARCC1 and SMARCC2, showed frequent off-target paralogue targeting (Figure 17). Negative controls used were pLKO-Non-Silencing Control (Table 12), expressing a non-targeting shRNA, or pLKO-empty, not expressing any shRNA, acquired from AddGene repository (Plasmid #8453; Watertown, MA, USA). When performing combination transduction experiments, double concentration of control lentiviral supernatant was used to compensate viral doses, and in the case of single inhibition in these experiments, control lentiviral supernatant was added to the specific shRNA of each condition to equate the amount of lentiviral supernatant in all the samples.

3.3. **Proliferation assays**

Proliferation assays of neuroblastoma cell lines were performed by seeding of 8×10^4 transduced or non-transduced cells per well in 24-well plates. For treatments with ACBI1 or *cis*ACBI1, acquired from the public OpnME repository of molecules for research (Boehringer Ingelheim, Ingelheim am Rhein, Germany), compounds were resuspended upon arrival in DMSO at 10 mM, and diluted in 100 µL of medium before added to the cells 24h post-seeding, at the indicated concentrations. Between 72 and 96 hours later, proliferation was assessed by crystal violet staining. Briefly, medium was aspirated and cells were fixed with 1% glutaraldehyde (Alfa Aesar, Haverhill, MA, USA) for 20 minutes at room temperature. Glutaraldehyde was aspirated, cells were rapidly rinsed once with PBS and stained with 0.5% crystal violet (Sigma-Aldrich) for 20 minutes at room temperature. Crystal violet excess was removed by vigorous rinsing with distilled water. Stained cells were left air-dry and the next day crystals were dissolved in 500 µl of 15% acetic acid, 100 µl of which were placed in 96-well plates for the absorbance analysis at 590 nm in an Epoch microplate spectrophotometer (Biotek, Winooski, VT, USA). Percentage of proliferation was calculated normalizing the absorbance values of each condition to their respective controls in each experiment.

3.4. **Western blot analysis**

Determination of protein levels in cultured cell lines or in tissues from mouse models were performed by western blot analyses. From *in vitro* experiments, cells were harvested from plates at the indicated time points, centrifuged for 5 minutes at 1500 rpm, rinsed once with 1 mL of PBS, and pelleted again. After PBS aspiration, pellets were immediately used for protein extraction, or stored at -80ºC for posterior lysis. Cell pellets were lysed by resuspension in 5-10 times their volume of RIPA lysis buffer (Thermo Scientific) supplemented with EDTA-free Protease Inhibitor Cocktail (Roche, Basel, Switzerland) and Phosphatase Inhibitor Cocktails 2 and 3 (Sigma-Aldrich). In the case of frozen tissues, pieces of 2 to 5 mm diameter were immersed in 200 to 500 µl of the same buffer, and each fragment was disrupted with 20 ceramic beads with a Bead Ruptor 12 (Omni, Kennesaw, GA, USA), using one cycle of agitation of 20 seconds at a speed of 5 m/s. In both cases, samples were incubated for 20 minutes on ice to allow cell lysis, prior to debris precipitation by maximum speed centrifugation (i.e. 13300 rpm) at 4ºC for 15 minutes. Supernatant fraction (i.e., soluble cell lysates) was collected and pellet discarded. Protein concentration in µg/µl of cell lysates was quantified with DC protein assay (Bio-Rad, Hercules, CA, USA), a Lowry-modified absorbance-based protein quantification method, using a standard curve of 0.5 to 5 µg Bovine Serum Albumin (BSA) (Bio-Rad).

For western blot analysis, 30 µg of each protein sample were mixed with NuPAGE LDS sample buffer (Invitrogen), with volumes adjusted to 30 µl using RIPA buffer, and heated at 70ºC for 10 minutes. Samples were then loaded onto precasted NuPAGE 4-12% Bis-Tris polyacrylamide gels (Invitrogen) and run for 1 hour and 30 minutes, approximately, at constant 150 V, in NuPAGE MES sodium dodecyl sulfate (SDS) running buffer (Invitrogen), using an XCell SureLock Novex Mini-Cell electrophoresis system (Invitrogen). Precision Plus Protein Dual Color Standards (Bio-Rad) was added as molecular weight marker, using 5 µl per well, with final volume adjusted to 30 µl with NuPAGE LDS sample buffer diluted in RIPA. Next, proteins were transferred onto methanol-activated and distilled water-washed polyvinylidene fluoride (PVDF) membranes (GE Healthcare Life Sciences, Piscataway, NJ, USA), using a wet/tank blotting system (Bio-Rad). PVDF membrane and polyacrylamide gel were sandwiched with two Whatman filter papers (GE Healthcare Life Sciences) and one sponge on each side, and transfer was performed at constant 110 V at 4ºC under agitation for 2 hours and 30 minutes in cold transfer buffer consisting in 25 mM Tris, 192 mM Glycine and 20% methanol.

Membranes were then briefly washed in tris-buffered saline (20 mM Tris, 150 mM Sodium Chloride) with 0.1% Tween 20 (Sigma-Aldrich) (TBS-T), and blocked for 1 hour in 5% Albumin Bovine Fraction V (BSA; NZYTech, Lisbon, Portugal) or 5% non-fat dried milk (PanReac AppliChem ITW Reagents, Castellar del Vallès, Spain) diluted in TBS-T. A quick TBS-T wash was performed prior overnight incubation with primary antibodies diluted in 5% BSA or 5% milk TBS-T (Table 13). The next day, membranes were washed three times for 5 minutes with TBS-T before incubation for 1 hour with horseradish peroxidase (HRP)-conjugated secondary antibodies diluted in 5% BSA or 5% milk TBS-T, depending on the primary antibody. After 5 additional TBS-T washes of 5 minutes, proteins were detected by incubation with Enhanced Chemiluminescence (ECL) (GE Healthcare Life Sciences), a luminol-based HRP substrate, and posterior exposure to X-ray films (Fujifilm, Tokyo, Japan), which were developed with a Curix 60 X-ray film automatic processor (Agfa, Mortsel, Belgium). Developed films were marked and digitalized by scanning.

Table 13: List of antibodies used for Western Blot analyses.

Target protein	*Origin*	*Dilution*	*Reference*	*Company*
Primary antibodies				
SMARCA4/BRG1	Mouse monoclonal	1:1000 in 5% BSA	sc-17796	Santa Cruz Biotechnology
PBRM1	Mouse monoclonal	1:1000 in 5% milk	AMAb90690	Sigma-Aldrich
SMARCB1/hSNF5	Mouse monoclonal	1:1000 in 5% milk	sc-166165	Santa Cruz Biotechnology
ARID1A	Mouse monoclonal	1:1000 in 5% milk	sc-32761	Santa Cruz Biotechnology
ARID1B	Mouse monoclonal	1:500 in 5% milk	ab57461	Abcam
DPF2	Rabbit monoclonal	1:1000 in 5% milk	ab134942	Abcam
BRD7	Mouse monoclonal	1:1000 in 5% milk	sc-376180	Santa Cruz Biotechnology
BRD9	Rabbit polyclonal	1:500 in 5% milk	A303-781A-T	Bethyl Laboratories
SMARCC1/BAF155	Mouse monoclonal	1:1000 in 5% milk	sc-32763	Santa Cruz Biotechnology
SMARCC2/BAF170	Rabbit monoclonal	1:1000 in 5% milk	#12760	Cell Signaling Technology
Cyclin D1/CCND1	Rabbit monoclonal	1:10000 in 5% BSA	ab134175	Abcam
Phosphorylated-Rb	Rabbit monoclonal	1:1000 in 5% BSA	#8516	Cell Signaling Technology
CASP3 (Full length)	Rabbit polyclonal	1:2000 in 5% BSA	#9662	Cell Signaling Technology
CASP3 Cleaved	Rabbit monoclonal	1:500 in 5% BSA	#9664	Cell Signaling Technology
PARP	Rabbit polyclonal	1:2500 in 5% BSA	#9542	Cell Signaling Technology
LOXL2	Rabbit polyclonal	1:1000 in 5% milk	NBP1-32954	Novus Biologicals
Integrin β3/ITGB3	Rabbit monoclonal	1:1000 in 5% BSA	#13166	Cell Signaling Technology
Integrin α9/ITGA9	Mouse monoclonal	1:1000 in 5% BSA	H00003680-M01	Abnova
SMARCA2/BRM	Mouse monoclonal	1:500 in 5% milk	sc-17828	Santa Cruz
Actin	Mouse monoclonal-HRP	1:20000 in 5% BSA	sc-47778 HRP	Santa Cruz
Secondary antibodies				
Rabbit IgG	Goat polyclonal-HRP	1:10000 in 5% BSA or milk	A0545	Sigma-Aldrich
Mouse IgG	Rabbit polyclonal-HRP	1:10000 in 5% BSA or milk	A9044	Sigma-Aldrich

Headquarters: Santa Cruz Biotechnology, Dallas, TX, USA; Abcam, Cambridge, UK; Bethyl Laboratories, Montgomery, TX, USA; Cell Signaling Technology, Danvers, MA, USA; Novus Biologicals, Centennial, CO, USA; Abnova, Taipei, Taiwan.

3.5. **Co-immunoprecipitation and Mass Spectrometry**

Affinity purification of mSWI/SNF complexes from neuroblastoma cell lines for proteomic analysis was performed by co-immunoprecipitation of SMARCA4/BRG1 subunit. SK-N-BE(2) and SH-SY5Y cells were grown in three 150mm dishes for each biological replicate until 80-90% confluence, and subcellular fractionation protocol was performed. Briefly, cells were scraped in cold subcellular fractionation buffer (10 mM PIPES pH 6.8, 300 mM sucrose, 50 mM sodium chloride, 1 mM EDTA, 0.5% Triton X-100 (Sigma-Aldrich)) supplemented with EDTA-free Protease Inhibitors Cocktail, and incubated for 20 minutes on ice before centrifugation at 720 xG for 5 minutes. Supernatants containing cytosolic fractions were discarded and nuclei-containing pellets were resuspended in immunoprecipitation (IP) lysis buffer (50 mM Tris pH 7.5, 300 mM NaCl, 2 mM EDTA, 10% glycerol, 0.1% SDS, 1% Triton X-100) supplemented with protease inhibitors. Nuclei were lysed by incubation on ice for 30 minutes and centrifuged at 13300rpm for 20 minutes to discard cell debris. Nuclear lysate supernatant was collected and protein quantified with the same method used for western blot analyses. For each co-immunoprecipitation reaction, 500 µg of nuclear lysates were pre-cleared with 10µL of Protein A-Sepharose beads (Sigma-Aldrich) and 1 µg of Normal Rabbit IgG (Sigma-Aldrich) in IP buffer. Pre-cleared lysates were incubated overnight at a concentration of 1 µg/µL with 5 µg of Rabbit monoclonal anti-BRG1 antibody (ab110641, Abcam) or Normal Rabbit IgG, before addition of 25 µL of Protein A-Sepharose beads and incubation for 2 hours. Beads were then washed three times with 200 mM Ammonium Bicarbonate (ABC; Sigma-Aldrich) and resuspended in 6 M urea (GE Helthcare Life Sciences) diluted in 200mM ABC. For protein reduction, 10mM dithiothreitol (Sigma-Aldrich) in 200mM ABC was added and incubated for 1 hour at 37ºC with shaking. Iodoacetamide (Sigma-Aldrich) at 20 mM in 200 mM ABC was added for alkylation, and samples were incubated for 30 minutes at room temperature with shaking in darkness. Digestion with 1 µg of sequence-grade trypsin (Promega, Madison, WI, USA) was performed overnight at 37ºC with constant shaking. Beads were pulled-down and samples were acidified with 20 µL of 100% formic acid. For sample desalting, C18 reverse phase UltraMicroSpin columns were used (The Nest Group, Inc., Ipswich, MA, USA). Columns were conditioned with methanol and equilibrated twice with 5% formic acid. Samples were loaded twice into the columns, washed twice with 5% formic acid and eluted with 50% acetonitrile in 5% formic acid before drying using a SpeedVac concentrator (Thermo Scientific).

Samples were resuspended and resolved by liquid chromatography prior to analysis by mass spectrometry. Proteomics analyses were performed in the Proteomics Unit of Centre for Genomic Regulation/Pompeu Fabra University (CRG/UPF, Barcelona, Spain). Samples were analyzed by LC-MS/MS using a 60-min gradient in an Orbitrap Velos Pro mass spectrometer (Thermo Scientific). As a quality control, BSA controls were digested in parallel and ran between each of the samples to avoid carryover and assess the instrument performance. Samples were searched against SP_Human database, using the search algorithm Mascot v2.6[796]. Peptides were filtered based on false discovery rate (FDR) and only peptides showing an FDR lower than 5% were retained. Interactome analysis of SMARCA4/BRG1 in SK-N-BE(2) and SH-SY5Y cells was performed using Significance Analysis of INTeractome (SAINT), a software package for scoring protein-protein interactions based on label-free quantitative proteomics data (i.e., spectral counts) in co-immunoprecipitation/mass spectrometry experiments. SAINT allowed to select bona fide interactions and remove nonspecific interactions in an unbiased manner[797].

3.6. **Cell transfection with siRNA**

For siRNA knockdown, sets of four custom siRNA duplexes against each targeted protein (i.e. ARID1A and ARID1B) with [dT][dT] overhangs were purchased from Sigma-Aldrich, based on validated target sequences extracted from literature, or designed *in silico* using the Invitrogen Block-iT RNAi Designer (Table 14). Block-iT fluorescent siRNA control (Invitrogen) was used as negative control. Stock of siRNA were resuspended at 20 µM in nuclease-free water (Invitrogen) and stored in small aliquots (10 µL) at -80ºC.

Table 14: siRNA target sequences and related information.

Target protein	*siRNA name*	*Target sequence*	*Transcript accession*	*Position in transcript*	*Transcript region*	*Reference*
ARID1A	siARID1A #1	GCCTGATCTATCTGGTTCAAT	NM_006015.6	2306 to 2326	CDS	798
	siARID1A #2	CCTCTCTTATACACAGCAGAT		1721 to 1741	CDS	798
	siARID1A #3	GCCAGACTCCATATTACAA		1786 to 1804	CDS	Self-designed
ARID1B	siARID1B #1	ACCATGAAGACTTGAACTTAA	NM_017519.3	2501 to 2521	CDS	551
	siARDI1B #2	CTCTCTGGTTGCATCTGTC		7209 to 7227	CDS	791
	siARID1B #3	AAGCAAATTGACTTTAAAGAA		7598 to 7618	3'-UTR	551
	siARDI1B #4	GCCGAATTACAAACGCCATAT		4620 to 4640	CDS	791

CDS means 'Coding Sequence'; 3'-UTR means '3'-Untranslated Region'.

Neuroblastoma cell lines were transfected with siRNAs using Lipofectamine 2000, following the manufacturer's instructions. For each 60 mm plate of neuroblastoma cells, 3.75 µL of each 20 µM siRNA stock and 10 µL of Lipofectamine 2000 were mixed in 1 mL of OptiMEM and incubated for 20 minutes at room temperature. In the meanwhile, SK-N-BE(2) or SH-SY5Y cells were prepared at a concentration of 2.5 × 10^5 cells/mL in neuroblastoma tissue culture medium without antibiotics. Cells were reversely transfected by seeding 5 × 10^5 cells (2 mL of the cell suspension) in 60 mm plates with 1 mL of the incubated mixture of siRNA (25 nM final concentration) and Lipofectamine 2000. Plates were incubated overnight at 37ºC, and when cells were attached (~16 hours later), transfection mixture was replaced by fresh antibiotic-containing culture medium. When performing combination transfection experiments, 25 nM siRNA was used for each protein to maintain silencing performance, rising total siRNA concentration to 50 nM. Therefore, concentration of negative control siRNA was doubled to 50 nM, to compensate doses, and in the case of single inhibition in these experiments, negative control siRNA was added to the specific siRNA of each condition to equate siRNA concentrations to 50 nM in all the conditions. As in the case of shRNAs, all acquired siRNAs against ARID1A and ARID1B were first tested and validated by western blot to check their silencing efficacy and specificity on these highly similar proteins (Figure 18). The siRNAs with a more specific silencing profile together with less deleterious observable effects on neuroblastoma cells were the ones selected for the following experiments. In this case, siARID1A #1 and siARID1B #1 were the chosen ones.

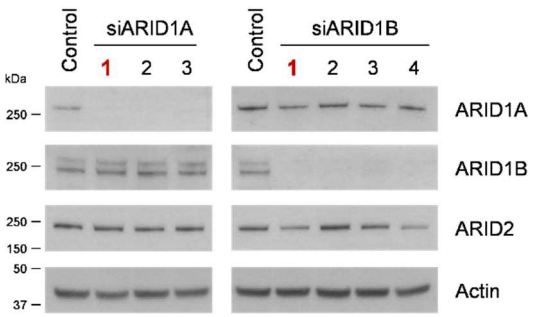

Figure 18: Silencing validation of siRNAs against ARID1A and ARID1B in neuroblastoma cells. SK-N-BE(2) were transfected with the indicated siRNAs against ARID1A and ARID1B, or with a negative control siRNA and, 96 hours post-transfection, cells were harvested and the levels of ARID1A, ARID1B and ARID2 were analyzed by western blot. Actin was used as loading control. Bold dark-red marked numbers indicate the siRNAs chosen for functional experiments.

Proliferation assay methods with siRNAs were performed differently than with shRNAs or the different inhibitors used in the rest of the experiments, due to the transient silencing effects of siRNAs. Transfection of the RNA product instead of an integrative DNA element, as in the case of shRNA lentiviral vectors, makes the silencing dependent on the cytoplasmic permanence of the siRNA molecules, the working concentration if which is diluted upon cell proliferation. Thus, in highly proliferative cells such as the SK-N-BE(2) and SH-SY5Y neuroblastoma cell lines, these effects become transient and lost in ~1 week. Therefore, in order to capture all the differences in proliferation produced by siRNA-mediated knockdown of the studied proteins, proliferation was assessed by viable cell trypan blue-based cell counting, using a Cell Counter EVE, of the total amount of cells transfected in 60 mm plates after 1 week of transfection. These cells were only manipulated at day 4 after transfection to split them (1:2) into a new 60 mm plate to avoid over-confluence. At this point, knockdown efficiency was confirmed by western blot. With this method, we were able to detect any delay in proliferation produced since the beginning of the transfection experiment and accumulated for 1 week after.

3.7. **RNA-sequencing transcriptomic analysis**

RNA-sequencing was performed to assess genome-wide transcriptional levels in comparison between shRNA-mediated ARID1A and/or ARID1B knockdown SK-N-BE(2) cells and a Non-Silencing Control. RNA extraction was performed at 72 hours post-transduction of 2.5×10^5 SK-N-BE(2) transduced in 6-well multi-well plates in biological triplicates with Non-Silencing Control, two different shRNAs against ARID1A (#2 and #4), two shRNA against ARID1B (#2 and #3), and two different combinations of shRNAs against each protein (shARID1A#2 and shARID1B #3, or shARID1A #4 and shARID1A #2). Cells were scraped in 500 µL of Qiazol lysis buffer (Qiagen) and total RNA was extracted using the miRNeasy mini extraction kit (Qiagen), following the manufacturer's instructions. An additional in-column step of DNAse I treatment (Qiagen) was performed for 10 minutes at room temperature to minimize the contamination with genomic DNA. Total RNA was eluted in 20 µL of nuclease-free water, fluorescently quantified using Qubit RNA HS Assay (Invitrogen) and quality checked by analysis with RNA 6000 Nano Assay on a Bioanalyzer 2100 (Agilent, Santa Clara, CA, USA). All samples contained enough material (> 1 µg) of high RNA quality (RNA integrity number (RIN) of 10 out of 10 for all samples).

Library preparation and sequencing was performed at the National Center of Genomic Analyses (CNAG-CRG, Barcelona, Spain). The RNA-Seq libraries were prepared following the TruSeq Stranded mRNA LT Sample Prep Kit protocol (Illumina, San Diego, CA, USA) and sequenced on NovaSeq 6000 (Illumina). RNA-seq reads were mapped against human reference genome (GRCh38) using STAR software version 2.5.3a[799] with ENCODE parameters. Genes were quantified using RSEM version 1.3.0[800] with default parameters and annotation file from GENCODE version 34. Differential expression analysis was performed with DESeq2 v1.26.0 R package[801] using a Wald test to compare control and problem samples. Differentially expressed genes were those with *P*-value adjusted < 0.05 and absoludte fold-change (FC) > 1.5, or more restrained thresholds, when indicated. Functional enrichment analysis of Hallmarks gene set collections from MSigDB database were performed using Gene Set Enrichment Analysis (GSEA) software[802,803]. Heatmaps were generated by normalizing the normalized counts of each gene by the average counts of the gene in all conditions, and $\log_2$ transformation. This value was represented in a color gradient Heatmap using Microsoft Office Excel (Microsoft Corporation, Redmond, WA, USA) and TM4's Multiple Experiment-Viewer MeV[804] softwares.

3.8. **Flow cytometry cell cycle assay**

Cell cycle assays were performed by the propodium iodide method. In this assay, DNA content of single cells is determined by flow cytometry analysis of permeabilized and propidium iodide-stained cell suspensions, in order to assess the percentage of cells at the different stages of the cell cycle in a determined moment in a culture, with the aim of observing changes referable to cell cycle blockade events. Propidium iodide is a dye only fluorescent when binding to DNA that is widely used to label and quantify genomic DNA in permeabilized and fixed pools of cells, allowing the calculation of proportion of cells in G_1 (DNA content of n), G_2/M (2n) and S phases (between n and 2n), on the base on the fluorescence signal intensity. SK-N-BE(2) and SH-SY5Y transduced cells were fixed 96 h after transduction in 70% ice-cold ethanol overnight at -20°C, at a density of 10^6 cells/mL. Fixed cells were washed twice with PBS and resuspended in a staining solution containing 15 µg/mL propidium iodide (Sigma-Aldrich), 1.14 mM sodium citrate (Sigma-Aldrich), and 0.3 mg/mL RNase A (PanReac AppliChem ITW Reagents) in PBS at a density of 10^6 cells/mL. Cells were incubated at room temperature (20–25°C) in the staining

solution for at least 30 minutes prior to analysis of propidium iodide intensity on single cells using a FACSCalibur flow cytometer (BD Biosciences, Franklin Lakes, NJ, USA) at the Flow Cytometry facility of Vall d'Hebron Institute of Research (UAT, VHIR, Barcelona, Spain). Flow cytometry results were analyzed using the FlowJo v10.8 Software (BD Biosciences).

3.9. **Cell death assays**

3.9.1. Hoechst staining

The determination of apoptosis through the observation of nuclear condensation and/or fragmentation was performed by staining neuroblastoma cells with Hoechst 33342 (Sigma-Aldrich), a fluorescent DNA dye. It is cell and nuclear penetrant without the need of fixation and/or permeabilization, and it does not affect cell viability in the short term. When binding to adenosine-thymidine rich regions of genomic DNA it becomes highly fluorescent, being excited by ultraviolet light (maximal excitation wavelength of 350 nm) and emitting blue fluorescent light (maximal emission wavelength of 461 nm).

Hoechst staining assays were performed on neuroblastoma living cells on tissue culture, which were plated in 24-well plates (8×10^4 cells/well). Twenty-four hours later, cells were stained with 0.05 mg/ml Hoechst 33342 by addition on the same plate of the fluorescent dye and incubation for 30 minutes at room temperature. Stained nuclei were observed and photographed under ultraviolet fluorescence microscopy.

3.9.2. Fluorescence cell death assay

CellTox Green Cytotoxicity Assay (Promega) kit was used for the determination of cell toxicity involving permeabilization of cell membrane and releasing of free genomic DNA. This kit uses a non-cell penetrant DNA-binding fluorescent dye, that becomes fluorescent when binding to DNA released by dying cells whose plasmatic membrane is compromised, exciting at 485–500 nm, and emitting at 520–530nm. Transduced neuroblastoma cells were seeded on black opaque 96-well plates (2×10^4 cells/well). Twenty-four hours later, the CellTox reaction was performed on these same plates by addition of the fluorescent dye, following the manufacturer's protocol. Cell lysis solution included in the kit was used as a positive technical

control of cell death. Fluorescence was measured using an Appliskan (Thermo Scientific) microplate reader. Fluorescence signal was normalized against each control.

3.10. **Adhesion assay**

Cell adhesion assays were performed to determine the adhesion dynamics of neuroblastoma cells to culture plate surfaces coated with collagen, an abundant component of the extracellular matrix. First, 96-well culture plates were pre-coated with poly-D-lysine, which are chemically synthesized artificial amino acid chains widely used in tissue culture for the attachment to culture-treated plastic surfaces of cells or molecules of the extracellular matrix. We pre-coated tissue culture plates with these polymers in other to assure the attachment of the posterior collagen coating to the surface of the plates.

Poly-D-lysine stock (Sigma-Aldrich) stored at -20ºC at 50 mg/mL in ultrapure water was diluted to 0.5 mg/mL in water, and 50 µL per well were placed on 96-welll plates, and incubated at 37ºC for 20 minutes. Next, poly-D-lysine suspension was aspirated and 50 µL of rat tail collagen V (Corning Inc., Corning, NY, USA) at 80 µg/mL diluted in 0.02 M acetic acid was added to the plates and left to fully evaporate overnight on the biosafety cabinet. After evaporation of the solvent, wells were rinsed twice with PBS and once with culture medium.

Adhesion dynamics was assessed by seeding 4×10^4 transduced neuroblastoma cells in 100 µL per well in these collagen-coated 96-well plates, and performing a time course of 5 minute intervals of cell aspiration, rapid PBS rinsing, PBS aspiration and fresh medium addition. Time points ranged from 0 minutes to 25 minutes after cell plating, using 6 replicate wells for each time point. The cells remaining in the wells after this, considered to be collagen-adhered, were left to fully attach to plates for 8 hours, a period of time in which differences in proliferation were no detectable by crystal violet staining. Plates were then fixed with 1% glutaraldehyde and stained with crystal violet (see section 3.3). Adhesion percentage was calculated by normalizing the absorbance values of each condition against the values of their respective controls on each experiment. Empty wells were used as a negative control (= 0% adhesion) and seeded cells without aspiration (4×10^4 cells /well) as a positive control (=100% adhesion).

3.11. **Invasion assay**

Invasion assays were performed using poly-D-lysine and collagen coated 8.0 µm pore size transwell inserts (Corning) placed on 24-well plates. Neuroblastoma cells were seeded 96 hours post-transduction in the upper chamber of each collagen-coated transwell with culture medium without FBS nor Insulin-Transferrin Selenium, at a concentration of 10^5 cells per 100 µL. The lower chambers (wells of 24-well plates) were filled with 700 µL 20% FBS and Insulin-Transferrin Selenium supplemented culture medium, to create a chemo-attracting gradient to induce neuroblastoma cell invasion through the collagen matrix. Cells were left to invade overnight (16 hours) at 37ºC. The next day, cells remaining in the upper chamber were removed using a PBS-wet cotton swab, and cells migrated to the lower surface of the membrane were fixed with 4% paraformaldehyde (Sigma-Aldrich) for 15 minutes at room temperature, washed with PBS and stained with crystal violet. Crystal violet excess was removed by rinsing of transwells with abundant distilled water. Stained invading cells were imaged by bright field microscopy. Invasion was quantified by diluting crystals with 200 µL of acetic acid on the lower chamber of each transwell, and incubation for 10 minutes with vigorous shacking. An aliquot of 100 µL of acetic acid-diluted crystal violet of each replicate was placed in 96-well plates for absorbance analysis at 590 nm in an Epoch microplate spectrophotometer. The absorbance values of each condition were normalized against the values of their respective controls on each experiment to assess the percentage of invasion.

3.12. **Phalloidin staining and immunofluorescence**

To visualize and quantify morphological changes involving neuroblastoma cells cytoskeleton and stress fibers, actin filaments were stained with the Phalloidin dye. A total of 2×10^5 cells per well were seeded in collagen-coated glass cover slips in 24-well plates and grown for 2 days. Next, cells were rinsed twice with PBS and fixed with 4% paraformaldehyde for 10 minutes at room temperature. Cells were washed three more times in PBS and incubated in glycine 0.1 M in PBS at room temperature for 5 minutes under soft agitation. After 2 more washes with PBS, cells were permeabilized with 0.1% Triton X-100 in PBS at room temperature. Two more washes with PBS were performed prior blocking with 3% BSA in PBS for 60 minutes at room temperature under soft agitation. After one more wash with PBS, cover slips were incubated with the staining

solution containing phalloidin-iFluor 594 (Abcam) diluted according manufacturer's instructions, monoclonal Anti-β-Tubulin–FITC (Sigma-Aldrich) 1000-times diluted and DAPI 10 µ/mL (Invitrogen) in 3% BSA in PBS, for 1 hour at room temperature under soft agitation, in a dark wet chamber. After 3 final washes with PBS, cover slips were mounted onto microscopy slides using ProLong Diamond Antifade Mountant (Invitrogen), and visualized with a ZEISS LSM 980 confocal microscope (Oberkochen, Germany). Ten random fields were acquired for each biological replicate and processed using ImageJ software. Number of cells per field was counted using DAPI staining of nuclei, and area stained with phalloidin and anti-tubulin was calculated. Tubulin-positive area percentage was used as a reference of the surface occupied by the main body of the cell, whereas area percentage of actin filaments protruding from this main body was considered as a quantification measure of stress-fiber protrusions. Thus, quantification of filamentous actin protrusions for each field was performed by calculating the percentage of tubulin-free phalloidin area per cell, by subtracting the tubulin area percentage to the phalloidin area percentage.

3.13. **Luciferase assay**

To control the effects of the combined shARID1A and shARID1AB transduction on the expression of the luciferase reporter gene used to track metastatic growth *in vivo*, luciferase activity was measured *in vitro* in SK-N-BE(2) stably transduced with lentiviral FLUC vector (named SK-N-BE(2)-FLUC hereafter).

We made use of the Dual-Glo Luciferase Assay System (Promega). Different numbers of SK-N-BE(2) viable cells (1.25, 2.5 and 5 × 10^5 per well) previously transduced with either control shRNA or shARID1A and shARID1B were seeded per well 120 hours after transduction in white opaque 96-well plates. Cell lysis and luciferase reactions were performed following the manufacturer's recommendations. Luminescence was measured using an Appliskan microplate reader. Luciferase signal was linearly correlated to the number of viable cells, confirming the reproducibility and feasibility of the technique and the results.

3.14. **Mouse models**

Experimental procedures involving animals were performed at the Rodent Platform of the Laboratory Animal Service of Vall d'Hebron Institute of Research (LAS, VHIR, Barcelona, Spain). All animal protocols were reviewed and approved according to regional Institutional Animal Care and Ethical Committee of Animal Experimentation.

3.14.1. Long-term neuroblastoma metastatic mouse model

SK-N-BE(2) cells were derived from a bone marrow metastatic lesion of a *MYCN* amplified neuroblastoma case. When injected by tail vein into immunosuppressed mice, in what is called metastatic, or pseudo-metastatic, model, generates liver metastases in 100% of injected mice, and bone marrow metastases in about 80%[805], representing an interesting model for the study of initiation and progression of these two kinds of clinically-relevant neuroblastoma metastatic lesions. Generation of this model was performed by intravenous injection of 2×10^5 SK-N-BE(2)-FLUC cells in 200 µL of PBS into 5-week old Fox Chase SCID beige mice (Charles River, Wilmington, MA, USA). This mouse strain was developed by intercross of C.B-17 SCID/SCID to C57BL/6 bg/bg mice, and carries both autosomal recessive SCID and *beige* mutations, which produce severe combined immunodeficiency affecting both the B and T lymphocytes, and defective natural killer (NK) cells, respectively.

Mice were monitored at two levels. On the one hand, luciferase activity contained in the stably transduced FLUC lentiviral reporter vector was used for *in vivo* bioluminescence imaging (IVIS) at the indicated time points. Mice were anesthetized by isoflurane inhalation and intraperitoneally injected with D-luciferine (Invitrogen). Luciferase signal was acquired using an IVIS SpectrumCT *In Vivo* Imaging System (PerkinElmer, Waltham, MA, USA), and visualized and quantified using Living Image Software 4.5.2 (Perkin Elmer). Average photon counts from same-duration expositions were calculated for the whole body of each mouse and normalized by extraction of background signal. Quantification was corrected by the luciferase signal change factor calculated as described in section 3.14. On the other hand, mice were routinely monitored for symptomatology such as suffering signs or apparition of palpable metastatic lesions, marking the ending point of the experiment for the individual mouse, which was euthanized. This follow-up also allowed the performance of survival analyses between groups.

3.14.2. Short-term neuroblastoma metastatic mouse model

For the monitoring of the early metastatic arrival and colonization of SK-N-BE(2) neuroblastoma cells into the liver, SK-N-BE(2)-FLUC cells were stained with CellTrace FarRed Cell Proliferation Kit (Invitrogen) following manufacturer's instructions. This flow cytometry dye is a stable cytoplasmic dye that dilutes with cell division, allowing the monitoring of proliferation of a certain bulk cell culture since the moment that they are stained, by following the decrease on time of FarRed intensity by means of flow cytometry. This helped us to compare the rates of proliferation between conditions of the cells arriving at early stages to the liver in metastatic models. SK-N-BE(2)-FLUC were detach and stained at 1 µL of dye in 1 mL of 1 million cell suspension in PBS for 20 minutes at 37ºC. Five times the staining volume of culture media was added to stop the staining, incubated for 5 minutes at 37ºC. Cells were pelleted and resuspended in PBS for intravenous injection.

A total of 2 million Cell Trace-stained SK-N-BE(2)-FLUC cells were injected per animal intravenously in 5-week old Fox Chase SCID beige mice. At days 4 and 7 after injection, mice were euthanized and livers were collected in culture media. Livers were mechanically dissociated and each one incubated with 5 mL of 10 mg/mL Collagenase Type I (Gibco) in culture medium under agitation at 37ºC. Next, each homogenate containing one dissociated liver was filtered through a 100 µm cell strainer (Corning), diluted in 10 mL of PBS and centrifuged for 10 minutes at 1500 rpm. Supernatant was discarded and pellet resuspended in 5 mL erythrocyte lysis buffer (Qiagen) and incubated for 10 minutes on ice. Homogenates were centrifuged again for 5 minutes at 1500 rpm, pellets resuspended in 10 mL of PBS and filtered again through a 100 µm cell strainer. After one more centrifugation and PBS wash step, the resulting single cell suspension containing a mix of mouse hepatocytes and human neuroblastoma cells was counted using an Eve cell counter.

Human cell population was enriched with the Mouse Cell Depletion Kit, following manufacturer's instructions, using one purification LS column for each liver in a QuadroMACS magnetic cell separator (Miltenyi Biotec, Bergisch Gladbach, Germany). The resulting eluates were pooled in pairs of livers from the same experimental conditions to increase the detection performance of neuroblastoma cells by flow cytometry, and purified for a second round with Mouse Cell Depletion Kit using an additional LS column. Final purified pooled cell eluates were

resuspended in 200 µL of PBS, stained with SYTOX Blue fluorescent viability marker (Invitrogen), and analyzed using a FACS Fortessa flow cytometer for mCherry, FarRed and SYTOX Blue detection at the Flow Cytometry facility of Vall d'Hebron Institute of Research.

Flow cytometry results were analyzed using the FlowJo v10.8 Software (BD Biosciences). Among the viable and single cell population, mCherry positive and FarRed positive were identified as human neuroblastoma cells, in contrast with the residual mouse hepatocytes, negative for these markers. Number of invading neuroblastoma cells was normalized by the total of events in millions reported for living and single cells for each sample. Cell Tracer proliferation rate was assessed from the average FarRed intensity for the human neuroblastoma population.

3.15. **ARID1A druggability analysis and high throughput virtual screening**

Virtual analyses for the identification of small molecules able to disrupt BAF intra-complex protein-protein interactions were performed by Nostrum Biodiscovery (Barcelona, Spain), a joint spin-off company of the Barcelona Supercomputing Center (BSC-CNS) and the Institute for Research in Biomedicine of Barcelona (IRB Barcelona), that uses modeling technologies that combine structure and ligand-based simulations with artificial intelligence algorithms for drug design.

Druggability analysis of ARID1A protein was first performed making use of the nucleosome-bound human BAF complex tri-dimensional structure (PDB code: 6LTJ). Initial examination revealed three inter-subunit interactions, with SMARCD1, SMARCB1 and SMARCA4. In order to characterize these protein-protein interactions and assess their druggability, different algorithms such as Fpocket and SiteMap were used[806,807]. These tools are widely used to identify cavities and predict druggable pockets based on geometric algorithms. The orientation of the side chains involved in the potential binding sites was considered and optimized when deemed necessary. All the possible predicted pockets were scored and ranked using an empirical scoring function, a mathematical model that combined pocket properties such as volume, hydrophobicity, hydrophilicity and others key properties. Combining the analysis of the predicted druggability score with the cryo-TEM complex structures, the most probable pockets that located within protein-protein interaction sites between ARID1A with its partner proteins

were depicted. Sequence alignment between ARID1A and ARID1B was performed to check the degree of sequence conservation on the amino acids involved in these pockets between these two paralogues using Clustal Omega[808].

The two most promising interface-located pockets in ARID1A were identified and selected for Virtual Screening (VS) campaign using a library of commercially available compounds extracted from the ZINC database[809], a small molecule database composed of ~7.5 million compounds. All Virtual Screening calculations were carried out with Schrödinger´s Glide 2018-2 version[810]. The protein receptor grids for docking simulation were generated at the center of the pocket. Hierarchy VS was employed using the high throughput virtual screening (HTVS) protocol as the first docking step on the ZINC database. The second screening was done on the top 50,000 docking poses of the previous HTVS step, using the Standard Precision (SP) scoring function, which has more exhausted ligand conformational sampling and more accurate scoring functions. Finally, the top 500 ranked-compounds were filtered with the molecular properties required for nucleus membrane crossing, which are MW ≤ 450, number of H-bond donor ≤ 4, number of H-bond acceptor ≤ 8, PSA ≤ 140 and cLogP ≤ 4.5. Then the docking poses of selected compounds were manually examined to finalize the selection of the most promising compounds. A set of ~40-50 inhibitor candidates were delivered and proposed for experimental testing for each pocket.

3.16. **Functional screening of BAF disruptor candidates**

A total of 50 BAF disruptor candidates resulting from the virtual screening were acquired in 1 mg quantities from the following chemical companies: Enamine (Riga, Latvia), Ambinter (Orléans, France), Chemspace (Riga, Latvia) and Chembridge (San Diego, CA, USA). Upon arrival, lyophilized compounds were resuspended in DMSO at a concentration of 20 mM. For proliferation screening, SK-N-BE(2) cells were seeded at a concentration of 5,000 cells in 100 µL of medium per well in 96-well plates. The next day, 50 µL of medium with diluted compounds at 150 µM was added, giving a final concentration of 50 µM. For each biological replicate, six wells were used as technical replicates for each compound. For each 96-well plate, 3 columns of 6 wells distributed along the plate were treated with DMSO as negative control. After 96 hours of incubation at 37ºC, plates were fixed with glutaraldehyde 0.1%, rinsed with PBS and

stained with crytal violet, as detailed in section 3.4. Crystals were dissolved in 100 µL of 15% acetic acid, and read at 590 nm on in an Epoch microplate spectrophotometer. Proliferation for each compound was assessed by normalizing to the average of the three DMSO columns of its respective plate. Proliferation effects were expressed as log_2 fold change against control.

Dose-response proliferation experiments with BDC-D07 were performed under the same conditions of volumes, numbers of cells and timings, but changing concentrations to the indicated serial dilutions. Half inhibitory concentrations (IC_{50}) were calculated using GraphPad Prism 6 (GraphPad, San Diego, CA, USA), setting the maximum of the curves at 100% of vehicle-normalized proliferation percentage, and the minimum over 0%.

3.17. **Statistical analyses**

Unless otherwise stated, graphs represent the average of three independent replicates, and standard error of the mean (S.E.M.) is represented by error bars. Statistical significance was determined using GraphPad Prism 6 Software, and unless otherwise stated two-tailed Student's *t*-test was used for comparisons between two conditions, and one or two way-ANOVA followed by Sidak's test for multiple comparisons.

4. **RESULTS**

Still don't know what I was waiting for
And my time was running wild
A million dead end streets
And every time I thought I'd got it made
It seemed the taste was not so sweet

Changes
David Bowie
Honky Dory
1971

4.1. **Degradation of the mSWI/SNF chromatin remodeling complex catalytic subunit is not sufficient to impair neuroblastoma proliferation**

In order to elucidate the contribution of the mSWI/SNF complex to the oncogenic capacity of neuroblastoma cells, we first aimed at inhibiting the catalytic ATPase activity of the complex, which is relevant for active chromatin remodeling[199,811–813]. The catalytic function of the complex relies on SMARCA2 and SMARCA4 subunits, also known as BRM and BRG1, respectively. These are a pair of highly similar (>70%) and mutually exclusive homologues that are present in all three complex variants BAF, PBAF and ncBAF (Figure 19A)[198,200,215]. Therefore, full ablation of the catalytic functions of the different mSWI/SNF complexes should include the inhibition of these subunits.

Recently, a PROTAC degrader molecule, ACBI1, was generated for the post-translational silencing by directed proteolysis of BRG1 and BRM proteins. ACBI1 targets the acetyl-histone binding bromodomains of both proteins and recruits an E3-ubiquitin ligase for their proteosomal degradation. Due to the bromodomain-oriented design of the molecule, PBRM1 is also degraded by ACBI1, but at a lesser extent[700]. Thus, we proceeded to assess the effects of catalytic subunit inhibition in neuroblastoma, using cell proliferation as initial readout.

Proliferation assays were performed using two different neuroblastoma cell lines representative of patient molecular heterogeneity[710]: SK-N-BE(2) cell line, which is *MYCN* amplified and *TP53* mutated, and SH-SY5Y, which is *MYCN* non-amplified and *TP53* wild type[814–816]. Treatment of these two cell lines with ACBI1 for 96 hours did not had any effect on neuroblastoma proliferation, while post-transcriptional silencing of BRG1 using a shRNA lentiviral vector caused a dramatic decrease in proliferation (Figure 19B), as reported before by our group[630]. Western blot analysis confirmed the degradation of BRG1 and PBRM1 by ACBI1, as well as the shRNA silencing of BRG1 (Figure 19C).

With the aim of finding and explanation to clarify this discrepancy between the results obtained with these two silencing technologies, the structural integrity of the complex was monitorized by checking the protein levels of other non-catalytic structural subunits, both ubiquitous (SMARCB1) or subtype-specific (ARID1A/B and DPF2 from BAF, and BRD7 from PBAF). Due to their high commitment towards the complex, when physical interactions are lost and subunits disassemble, their stability is compromised and are rapidly removed by proteasomal

degradation[214,817]. This property has eased us to monitor the integrity of the complex by checking the total protein levels of the subunits. As shown in Figure 19C, ACBI1 degradation did not cause significant changes in the levels of these subunits. Nevertheless, a general and marked decrease was observed for all and each of the mentioned subunits after shRNA silencing.

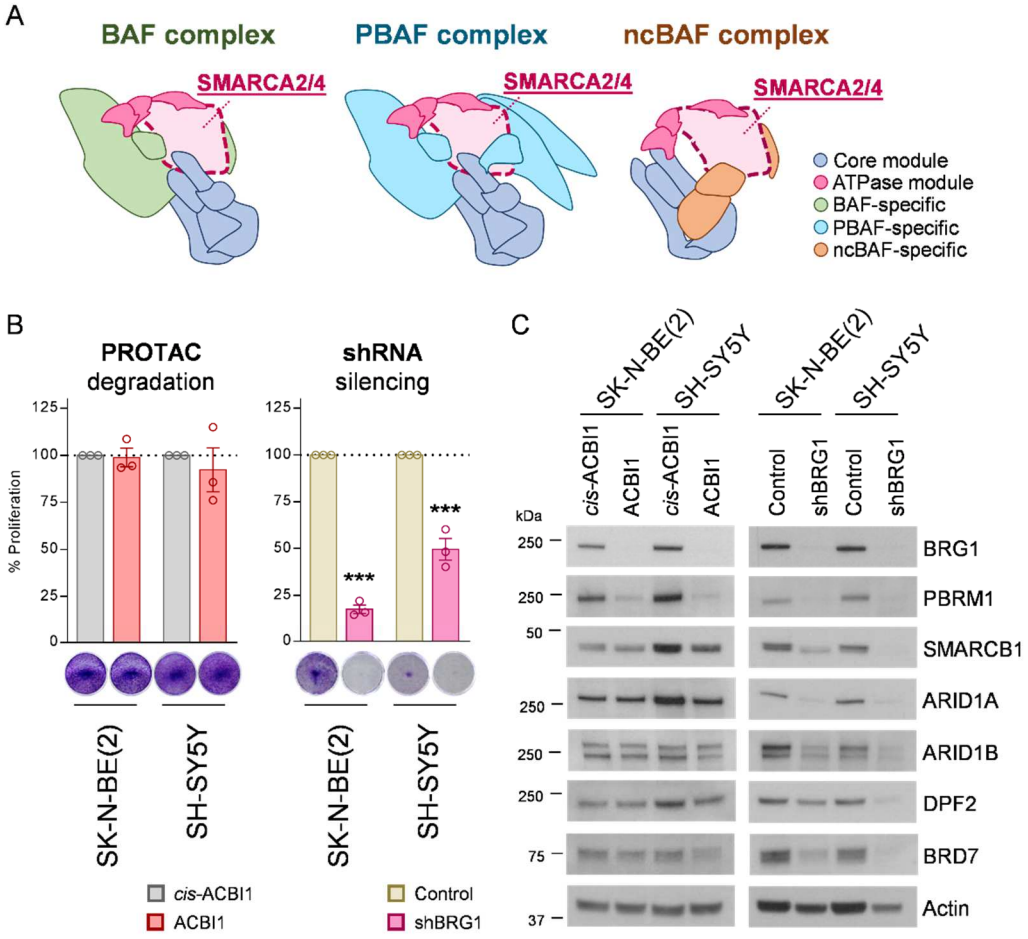

Figure 19: Inhibition of mSWI/SNF ATPase subunits in neuroblastoma cells. **A.** Schematic representation of the catalytic subunits –SMARCA2 (BRM) and SMARCA4 (BRG1)– on each mSWI/SNF complex subtype. The silencing the two paralogues is one strategy of inhibiting all three complexes at once. **B**. Proliferation assays with neuroblastoma cell lines seeded in 24-well plates and grown for 96 hours. Cells were treated with ACBI1 or its negative control *cis*-ACBI1, at 1 µM. For shRNA silencing, cells were transduced 72 hours before seeding with a shRNA against BRG1 (shBRG1) or a shRNA control. Proliferation was assessed by crystal violet quantification and normalized with its respective control. **C**. Protein expression analysis of multiple mSWI/SNF subunits in neuroblastoma cells treated with ACBI1 1 µM, or transduced with shBRG1, for 96 hours before western blot detection of the indicated proteins. *** means $P < 0.001$.

These effects on subunit stability pointed to a loss of structural integrity after the inhibition of the catalytic subunit using RNA interference methods that is not produced with PROTAC degradation, and that could be explaining the phenotypic inconsistencies found in proliferation between both silencing tools. On the base of this evidence, we hypothesized that the structural integrity of the mSWI/SNF complex, and not its catalytic activity, was relevant for neuroblastoma proliferation, and redirected our investigations accordingly.

4.2. **BAF complex structural integrity is required for neuroblastoma proliferation**

4.2.1. Neuroblastoma cells contain fully assembled BAF, PBAF and ncBAF subcomplexes

In order to assess the relevance of the mSWI/SNF complex structural integrity for the proliferative capacities of neuroblastoma cells, we decided to perform a complete and systematic analysis of the presence of the different complex subtypes, their composition and their specific contribution to neuroblastoma proliferation.

We first performed a proteomic analysis of the complex by co-immunoprecipitation (co-IP) of the catalytic subunit SMARCA4/BRG1 followed by mass spectrometry identification of its interactors on nuclear extracts of SK-N-BE(2) and SH-SY5Y neuroblastoma cell lines. BRG1 was chosen as bait because of its ubiquity in all three complex variants[215], which ensured the maximum capacity of detection of any expressed and functional subunit assembled to any complex variant in these cells. As shown in Figure 20, all known subunits of the three mSWI/SNF complex variants, corresponding to the common core and ATPase modules, as well as the BAF, PBAF and ncBAF specific subunits, were significantly enriched in BRG1 co-IP in comparison to IgG negative control in both cell lines. This indicates the presence and complete subunit composition of all of the three variants. Remarkably, all members of each family of paralogues (e.g., DPF1, DPF2 and DPF3) were detected, showing the deep and wide detection capacity of this technical approach.

Besides the known dedicated subunits, six non-mSWI/SNF proteins were also detected in both neuroblastoma cell lines: ACTA1 and ACTG1, which are actin-α and γ[818]; HSPA5 or BiP, an endoplasmic reticulum (ER) chaperone[819]; KPNA2, a nuclear protein import regulator[820]; PCBP2, an RNA oligonucleotide binding protein[821]; and RPL10A, a ribosomal protein[822].

A

	SK-N-BE(2) FoldChange vs IgG	SK-N-BE(2) BFDR	SH-SY5Y FoldChange vs IgG	SH-SY5Y BFDR	
SMARCB1	330	< 0.01	68.5	< 0.01	Core
SMARCC1	356	< 0.01	54.38	< 0.01	
SMARCC2	1003.33	< 0.01	34.09	< 0.01	
SMARCD1	636.67	< 0.01	803.33	< 0.01	
SMARCD2	473.33	< 0.01	513.33	< 0.01	
SMARCD3	393.33	< 0.01	456.67	< 0.01	
SMARCE1	22.78	< 0.01	21.27	< 0.01	
ACTB	6.5	< 0.01	4.26	< 0.01	ATPase
ACTL6A	523.33	< 0.01	563.33	< 0.01	
ACTL6B	73.33	< 0.01	476.67	< 0.01	
BCL7A	210	< 0.01	273.33	< 0.01	
BCL7B	66.67	< 0.01	80	< 0.01	
BCL7C	76.67	< 0.01	73.33	< 0.01	
SMARCA4	**79.17**	**< 0.01**	**72.13**	**< 0.01**	
ARID1A	1436.67	< 0.01	211	< 0.01	BAF
ARID1B	1013.33	< 0.01	1126.67	< 0.01	
DPF1	106.67	< 0.01	230	< 0.01	
DPF2	416.67	< 0.01	67.5	< 0.01	
DPF3	40	< 0.01	200	< 0.01	
SS18	116.67	< 0.01	126.67	< 0.01	
SS18L1	100	< 0.01	136.67	< 0.01	
ARID2	85	< 0.01	41	< 0.01	PBAF
BRD7	500	< 0.01	496.67	< 0.01	
PBRM1	963.33	< 0.01	1153.33	< 0.01	
PHF10	263.33	< 0.01	270	< 0.01	
BICRA	170	< 0.01	233.33	< 0.01	ncBAF
BICRAL	133.33	< 0.01	170	< 0.01	
BRD9	93.33	< 0.01	176.67	< 0.01	
ACTA1	5.04	< 0.01	3.65	< 0.01	Non SWI/SNF proteins
ACTG1	6.33	< 0.01	4.19	< 0.01	
HSPA5	76.67	< 0.01	106.67	< 0.01	
KPNA2	15	< 0.01	15.67	< 0.01	
PCBP2	5.5	< 0.01	4	0.01	
RPL10A	8	0.01	6.5	0.01	

B

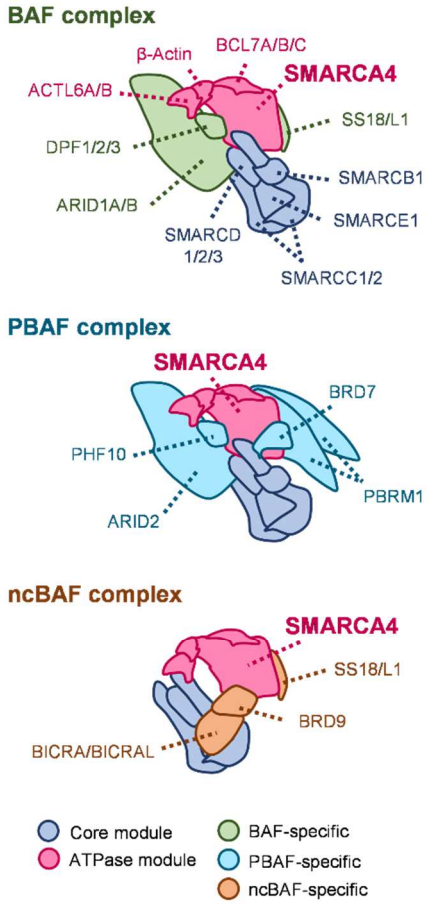

C

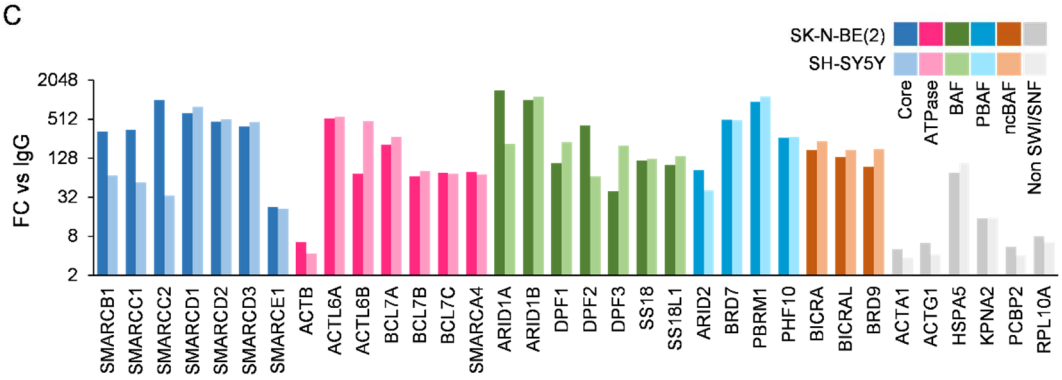

Figure 20: Mass spectrometry identification of mSWI/SNF complexes and composition in SK-N-BE(2) and SH-SY5Y neuroblastoma cell lines by SMARCA4/BRG1 co-immunoprecipitation. **A**. Proteins significantly enriched in SMARCA4/BRG1 co-immunoprecipitates compared to normal IgG control in both cell lines, using a cutoff value of Bayesian False Discovery Rate (BDFR) < 0.05. Fold Change of average spectrum counts with respect to IgG control and BFDR are shown. **B.** Schematic representation of the mSWI/SNF subunits detected by mass spectrometry. **C**. Graphical representation of the spectral counts Fold Change (FC) quantification of the detected proteins in both cell lines.

These results reveal and support the complete structural integrity of BAF, PBAF and ncBAF complexes as well as their coexistence in neuroblastoma cell lines.

4.2.2. Only specific disruption of BAF complex inhibits neuroblastoma proliferation

Different functions associated to distinct genomic occupancies and controlled transcriptional networks have been associated to the different variants of mSWI/SNF complexes[228,247,248,823]. Therefore, the coexistence of all the complexes in neuroblastoma cells might be misleading or masking subtype-specific functions relevant for these cells when the activity of the three of them is inhibited at once.

For this reason, we decided to analyze the effects of the specific structural disruption of each subtype on the proliferation of neuroblastoma cells. We resorted to the previous knowledge generated and published about the intricate mSWI/SNF assembly process[215] and consulted the pathway of each complex variant, with the aim of silencing the key subunit necessary for the final assembly of each variant. As shown in Figure 21A, the key subunits for the final assembly of BAF complex were the pair of mutually exclusive paralogues ARID1A and ARID1B; for PBAF complex assembly, ARID2; and for ncBAF, BRD9. Specific silencing of these proteins was done using lentiviral vectors carrying shRNA against each of them; or, in the case of BRD9, using a PROTAC degrader molecule (dBRD9)[701].

When each of these specific inhibitions were performed on SK-N-BE(2) and SH-SY5Y neuroblastoma cell lines, only the silencing of the two subunits necessary for BAF complex integrity, ARID1A and ARID1B, caused a significant and consistent reduction in the proliferation of both cell lines, whereas assembly disruption of PBAF through ARID2 silencing, or of ncBAF through BRD9 degradation, did not cause significant nor consistent effects on proliferation (Figure 21B). ARID1A and ARID1B are BAF-specific interchangeable homologue subunits[213] that, although some functional non-overlapping genome occupancies and functions have been reported[660,798,824–827], can replace each other at the structural level when one of them is lost[658,660,798,826–828]. Therefore, the full assembly disruption of the BAF complex needs to be achieved by simultaneous silencing of both proteins. Interestingly, single inhibition of the two proteins caused partial effects on proliferation in comparison to the dual inhibition, in which the effects on proliferation where maximum. Western blot analysis confirmed the correct and

specific knockdown or degradation of the target proteins for each silencing tool, but also the specific destabilization of each of the three complexes, by monitoring the levels of subtype-specific reporter subunits: DPF2 as BAF-stability reporter subunit, BRD7 as PBAF reporter and BRD9 as ncBAF reporter (Figure 21C).

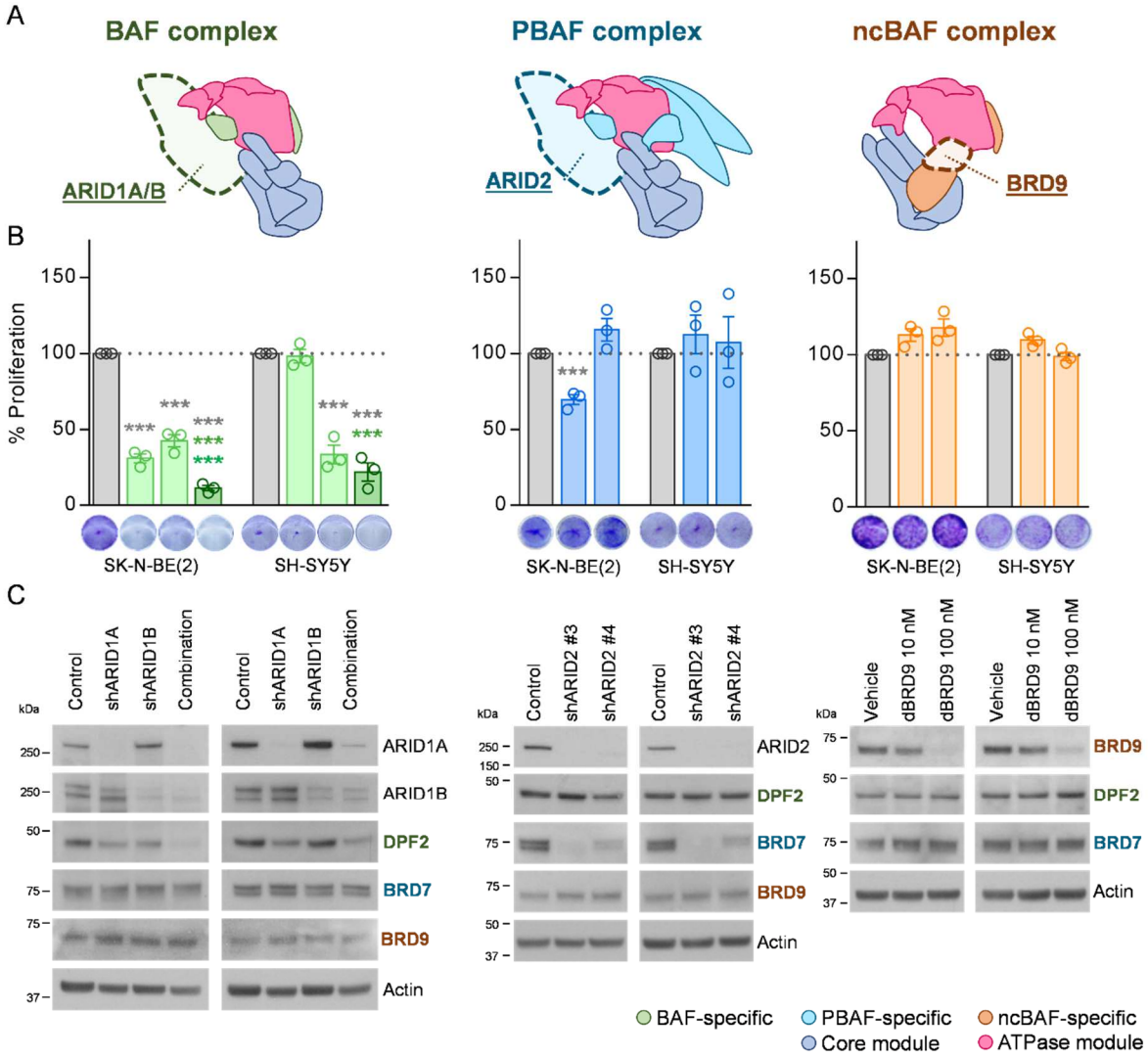

Figure 21: mSWI/SNF subtypes specific disruption in neuroblastoma cells. **A**. Schematic representation of the key subtype-specific subunits selected for silencing. **B**. Proliferation assays with neuroblastoma cell lines seeded in 24-well plates and grown for 96 hours, 72 hours after transduced with shRNA against specific proteins or a shRNA control. For BRD9 degradation, cells were treated with dBRD9 or vehicle at the indicated doses. Proliferation was assessed by crystal violet quantification and normalized with its respective control. **C**. Protein expression analysis of multiple mSWI/SNF subunits in neuroblastoma cells transduced with shRNA or treated with dBRD9 for 96 hours before western blot detection of the indicated proteins. *** means $P < 0.001$.

As expected, these reporter subunits suffered a dramatic decrease in protein levels after silencing of the key subunit of their respective complex, while the levels of the other reporters remained stable. Thus, BAF complex disruption through ARID1A/B silencing decreased only DPF2 levels, while BRD7 and BRD9 remained the same. PBAF disruption through ARID2 only promoted BRD7 destabilization, and not affected DPF2 and BRD9 levels. In the same way, BRD9 degradation did not cause any effect on DPF2 and BRD7 levels.

The partial effects on proliferation by single inhibition of ARID1A and ARID1B proteins, respectively, was further confirmed by using two shRNAs with different target sequences for each subunit (Figure 22A). In addition, with the aim of validating the results with a different silencing tool, the effects of BAF disruption on neuroblastoma proliferation were confirmed by transfection of siRNAs against the two proteins, with different target sequences from those of shRNAs (Figure 22B).

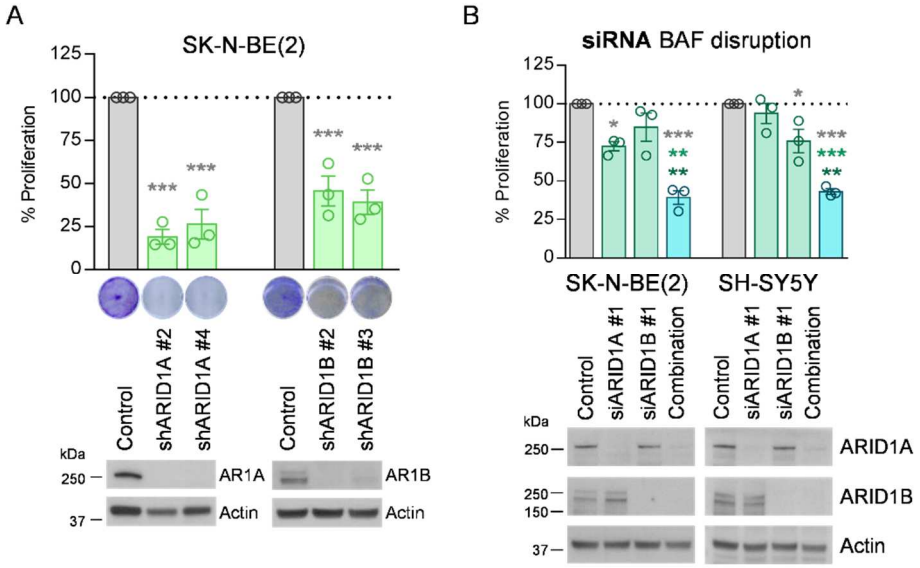

Figure 22: Validation of BAF complex disruption effects on proliferation of neuroblastoma cells. **A**. Knockdown of ARID1A and ARID1B with two different shRNA lentiviral vectors for each protein in SK-N-BE(2) cells. Graph shows proliferation assays of cells seeded in 24-well plates 72 hours after transduction and grown for 96 hours. Proliferation was assessed by crystal violet quantification and normalized with the shRNA control. Lower, knockdown validation by western blot of the target proteins 96 hours after transduction. **B.** Knockdown of ARID1A and ARID1B separately or in combination, by transfection of siRNAs in with SK-N-BE(2) and SH-SY5Y cells. Graph shows proliferation analysis of cells transfected in 60-mm plates and grown for one week before trypsinizing and viable cell counting using trypan blue. Proliferation was normalized with the siRNA control. Lower, validation by western blot of the target proteins 96 hours after transfection. * means $P < 0.05$; ** means $P < 0.01$; *** means $P < 0.001$. Abbreviations: *AR1A*, ARID1A; *AR1B*, ARID1B.

Returning to the initial hypothesis that it is the structural integrity of the mSWI/SNF complex – concretely of BAF complex–, and not its ATPase activity by itself, what is relevant for neuroblastoma proliferation, we postulated that the complete structural disintegration of all three variants at once, including the BAF complex, should reproduce the same phenotypic effects observed after specific BAF disruption.

In order to perform this full ablation of the complex in neuroblastoma cells, we designed an experimental approach based again on the mSWI/SNF assembly tree. The first two subunits necessary for the initiation of the core module assembly, before ramifications to the different subtypes, are the pair of homologues SMARCC1 and SMARCC2. These two subunits are not mutually exclusive, but rather dimerize, forming both homodimers and heterodimers (Figure 23A). Indeed, the dimerization of SMARCC subunits is the necessary starting point for the whole assembly process[215]. Hence, we performed single and dual silencing of both proteins using two different shRNAs for each one on neuroblastoma cells.

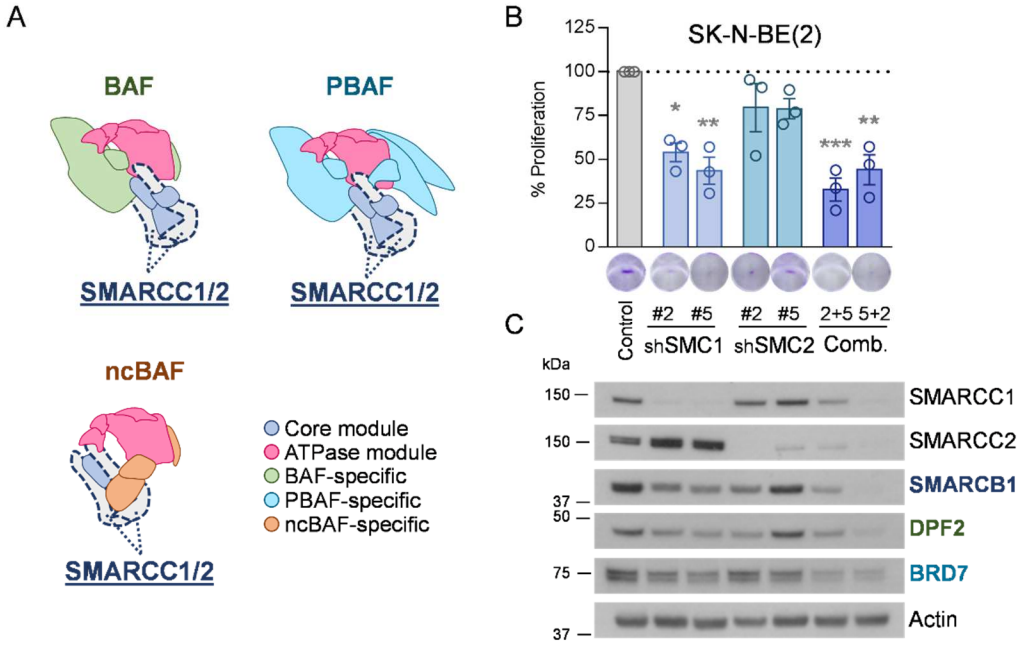

Figure 23: Full assembly disruption of the mSWI/SNF complex in neuroblastoma cells. **A**. Schematic representation of the experimental approach, showing the key core subunits selected for silencing. **B**. Proliferation assay of SK-N-BE(2) cells transduced with shRNAs agains SMARCC1 (shSMC1) and SMARCC2 (shSMC2), separately or in combination (Comb.). Cells were seeded 72 hours after transduction in 24-well plates and grown for 96 hours. Proliferation was assessed by crystal violet quantification and normalized with the shRNA control. **C**. Western blot analysis of the target proteins and other mSWI/SNF subunits 96 hours after transduction. * means $P < 0.05$; ** means $P < 0.01$; *** means $P < 0.001$.

As expected, simultaneous silencing of both proteins produced a decrease in neuroblastoma proliferation (Figure 23B). Interestingly, only single inhibition of SMARCC1, and not of SMARCC2, had also effects on proliferation, what might be indicating that the functional relevance on proliferation relies more on SMARCC1 rather than on SMARCC2. Protein level analysis of multiple mSWI/SNF members, including the core module subunit SMARCB1, showed a general decrease in the subunit protein levels (Figure 23C), even in the single silencing, confirming the full destabilization of the complex.

Altogether, these results indicate that, among the three coexistent and fully assembled mSWI/SNF complexes found in neuroblastoma cells, only the structural integrity of BAF complex is relevant for neuroblastoma cell proliferation.

4.3. **BAF complex controls a large cancer-related transcriptional network in neuroblastoma cells**

4.3.1. Combined silencing of ARID1A and ARID1B is necessary for complete modulation of BAF transcriptional network in neuroblastoma cells

The remarkable reduction in proliferation observed after BAF complex disruption through ARID1A and ARID1B silencing encouraged us to delve into the study of the detailed functions of this chromatin remodeler in neuroblastoma biology. Given its specialized role as transcriptional coactivator –or corepressor in certain cases– of large sets of genes[302,331,332,346] through chromatin opening at promoters and other *cis*-regulatory elements[333,339,340], the most straightforward way and with most detection power to identify any function of the BAF complex relevant for neuroblastoma oncogenic properties was the determination of the network of genes whose expression is under BAF control in these cells by means of genome wide analyses.

Transcriptome analysis of SK-N-BE(2) neuroblastoma cells after the disruption of BAF complex by silencing of ARID1A and ARID1B with two different shRNA for each protein was performed by RNA sequencing (RNA-Seq), detecting hundreds of transcripts whose expression was modulated after the simultaneous knockdown of both subunits (Figure 24A).

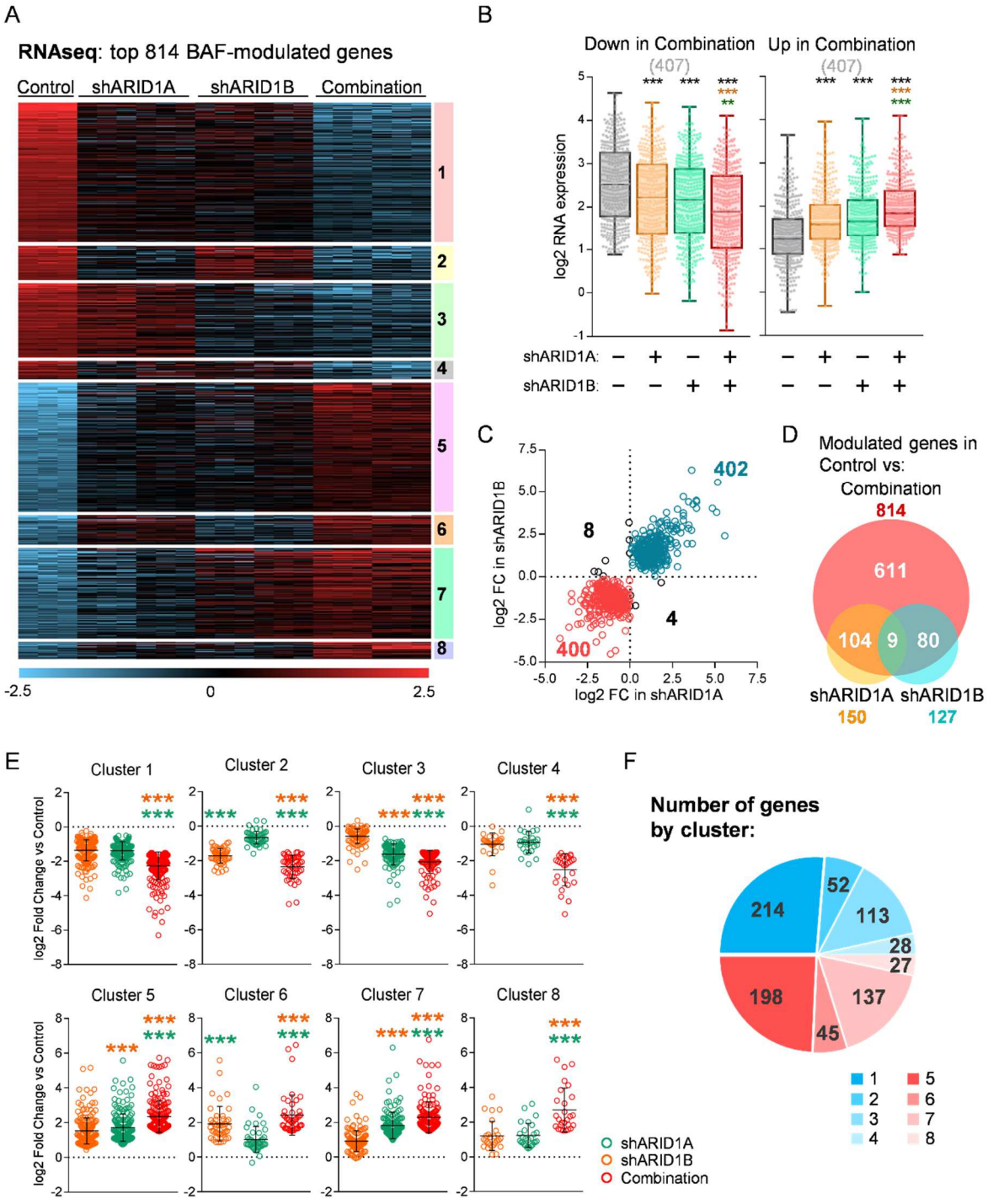

Figure 24. *See figure legend on next page.*

We also analyzed the gene expression changes produced by the single inhibition of the two proteins separately and compared it with those of the combined silencing. The average expression levels of those genes modulated after BAF full disruption were observed to undergo a less accentuated modulation after single inhibitions (Figure 24B), although these genes were modulated in the same directions by both proteins separately (Figure 24C). Remarkably, under the same cutoff values, the set of genes modulated by the combined silencing (814 genes) was significantly wider than those modulated by ARID1A (150) and ARID1B (127) alone (Figure 24D). The majority of the genes modulated in these last two groups were also modulated after full BAF disintegration, but little overlap was found between them.

Additionally, sorting of BAF-modulated genes according to their behavior after single inhibition let us classify them into 8 different clusters (Figure 24A and E): genes modulated in both single inhibitions (clusters 1 and 5, down- and up-regulated transcripts, respectively); genes only modulated in ARID1A single inhibition (clusters 2 and 6); genes only modulated in ARID1B single inhibition (clusters 3 and 7); and genes not significantly modulated in either of the two single inhibitions (clusters 4 and 8). Cutoff criteria used for considering a gene to be modulated or not in the single inhibitions was an adjusted *P*-value of 0.05. The comparison between the single and combined knockdowns within these clusters revealed that, in all of them, average expression levels were again more strongly modulated after full BAF disruption compared to the single inhibitions, even in the cases in which those genes were modulated by only one of the proteins alone (Figure 24E). Indeed, the majority of these 814 BAF-modulated genes (50.61%) belongs to clusters 1 and 5, meaning that they are partially controlled by ARID1A and ARID1B separately, but modulated in a more pronounced and complete way after simultaneous inhibition (Figure 24F).

Figure 24: Simultaneous knockdown of ARID1A and ARID1B in SK-N-BE(2) neuroblastoma cells exerts synergistic effects on BAF-controlled transcriptional network. **A**. Heatmap of RNA-Seq relative expression of the top modulated genes after BAF-disruption, using a cutoff of log_2 Fold Change > 1.5 or < -1.5, and adjusted *P*-value < 0.001. Two shRNAs for each protein (shARID1A, shARID1B) and two combinations of shRNA for both proteins were analyzed. Samples were sorted by experimental group and genes by single inhibition behavior-based clusters. Color gradient represents log_2 transformed normalized counts relativized for each gene. **B**. Gene expression levels comparison of 814 BAF-modulated transcripts, split in down- or up-regulated, among experimental groups. Graph represents the log_2 transformed RNA-Seq normalized counts for each gene. **C**. Scatter plot comparing the expression fold change (FC) with respect to control of the 814 BAF-modulated transcripts between single ARID1A and ARID1B inhibitions. **D**. Venn diagram of modulated genes in the three experimental conditions (shARID1A, shARID1B and Combination) using cutoff values of log_2 Fold Change > 1.5 or < -1.5, and *P*-adjusted < 0.001. **E**. Comparison of expression fold changes against control among experimental groups of BAF-modulated genes split in single inhibition behavior-based clusters. **F**. Pie chart representing the proportion of BAF-modulated genes included in each cluster. ** means $P < 0.01$; *** means $P < 0.001$.

In brief, these analyses make evident the significant impact of BAF complex assembly disruption at the transcriptomic level in neuroblastoma cells, and show the synergistic effects of the simultaneous inhibition of ARID1A and ARID1B on the transcriptome of these cells, in terms of both gene network extension and intensity of gene expression modulation

4.3.2. BAF complex controls transcriptional expression of cell cycle progression and epithelial mesenchymal transition genes in neuroblastoma

Once ascertained that the specific disintegration of BAF complex produced a significant impact on neuroblastoma transcriptome, the next step was to carry out the functional annotation of the BAF-modulated transcriptional network. The purpose of this was to determine the main biological processes affected by this deregulation not only with the aim of giving explanation to the observed effect on proliferation, but also of discovering other relevant cancer-related modulated pathways that could have gone unnoticed by only using proliferation as phenotypic readout, and could be interesting from a therapeutic point of view. For this functional annotation, gene set enrichment analysis (GSEA) was performed. This algorithm uses the whole list of genes ranked by expression change in a comparison between experimental groups and determines the enrichment of pre-established gene sets related to concrete biological processes and pathways in either of the two conditions[802,803]. The initial analysis interrogated the collection of fifty biological hallmarks from the public Molecular Signatures Database (MSigDB)[802,829,830] on the RNA-Seq expression comparison between control and the combined inhibition of ARID1A and ARID1B, in order to find the main pathways modulated after BAF-disruption.

As shown in Figure 25A, 47 out of 50 hallmarks were determined to be enriched in the control in comparison to BAF-depleted samples, and 18 of them with a False Discovery Rate (FDR) smaller than 0.05 (Figure 25B). This means that these signatures are significantly repressed at the transcriptional level after BAF disruption. Among them, gene sets related to epithelial mesenchymal transition and cell cycle progression (i.e., E2F targets, G_2-M checkpoint, mitotic spindle) had the highest normalized enrichment scores (NES), drawing our attention because of the great importance of these pathways in cancer[831] (Figure 25C). In contrast, the only three signatures enriched in BAF-disrupted cells were not statistically significant (Figure 25D and E).

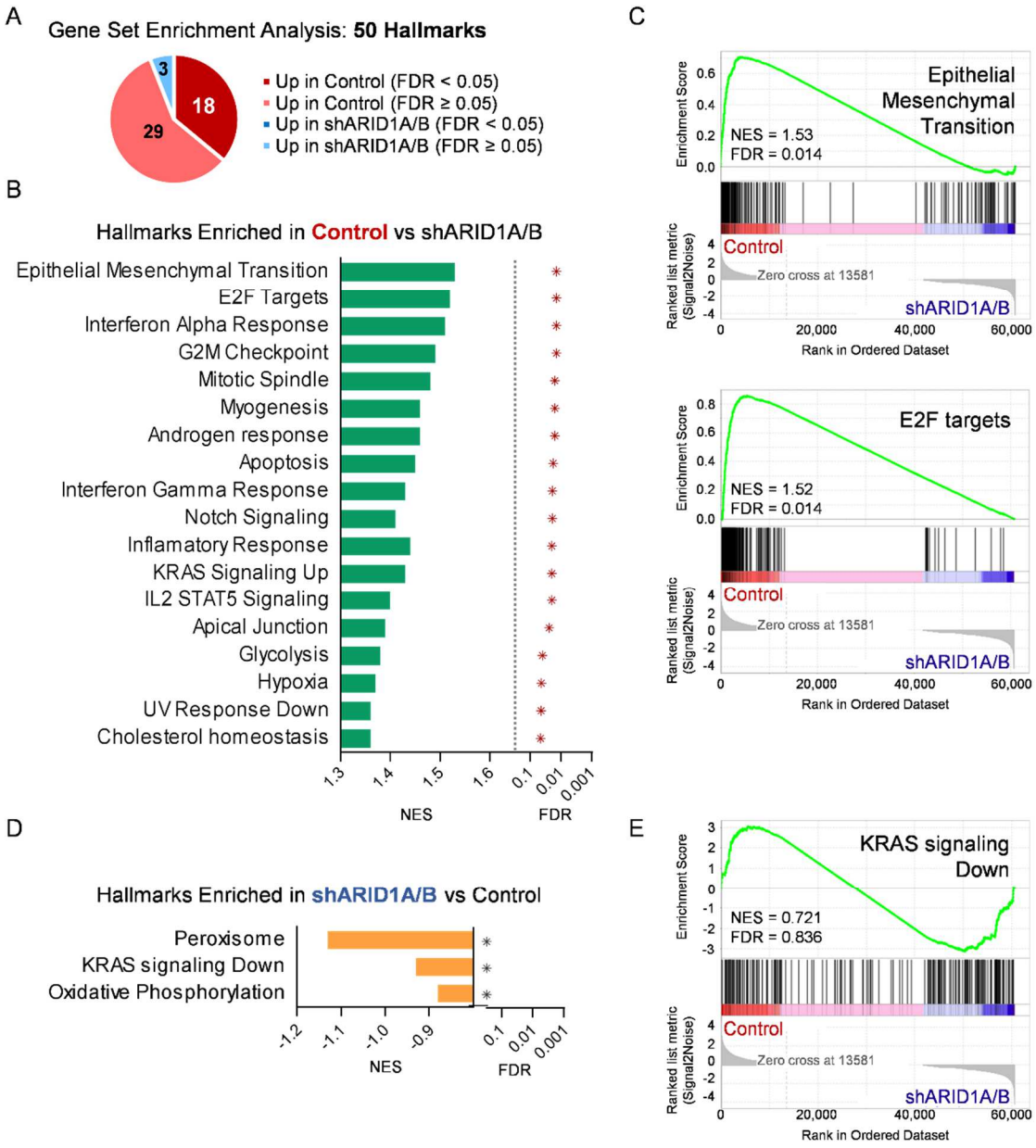

Figure 25: BAF disruption in neuroblastoma modulates cell cycle progression and epithelial-mesenchymal transition transcriptional signatures. **A**. Pie chart review of gene set enrichment analysis of 50 hallmarks from MSigSB on RNA-Seq expression data from SK-N-BE(2) comparing control against combination of shARID1A and shARID1B (shARID1A/B). **B**. Normalized Enrichment Score (NES) and False Discovery Rate (FDR) of the 13 gene sets significantly enriched in control. **C**. Enrichment plots of two of the gene sets most enriched in the control versus combined inhibition of ARID1A and ARID1B, Epithelial Mesenchymal Transition and E2F targets, consisting of 200 genes each one. **D**. NES and FDR of the 3 gene sets in enriched in shARID1A/B cells versus control. **E**. Example enrichment plot of one of the non-enriched gene sets, KRAS Signaling Down, consisting of 200 genes.

In summary, the results of analyzing the transcriptional program of neuroblastoma cells after the assembly disruption of BAF complex validated this chromatin remodeler as a relevant transcriptome regulator in these cells; it also revealed that, in order to obtain the complete functional consequences of its disruption, both key subunit homologues –ARID1A and ARID1B– must be targeted; and guided our next investigations towards the functional validation of the cancer-related pathways found to be controlled by the complex.

4.4. **BAF complex disruption promotes neuroblastoma cell cycle arrest**

As shown before, gene set enrichment analysis of neuroblastoma cell line SK-N-BE(2) transcriptome data after BAF-disruption revealed a decreased in gene signatures related to different cell cycle checkpoints. Concretely, these were signatures of E2F targets, G_2-M checkpoint and mitotic spindle genes. E2F proteins are a family of transcription factors that play an essential role in the progression of cell cycle from G_1 to S phase. E2F proteins are usually inactivated by the binding of hypo-phosphorylated Rb protein. During G_1 to S transition, the complex formed by cyclin D1 and CDK4/6 phosphorylates Rb protein, liberating E2F transcription factors and allowing the transcriptional expression of the genes necessary for cell cycle progression at that point (i.e., proteins of the replication fork and DNA polymerases, among others)[832–834]. On the other side, G_2-M and mitotic spindle genes are relevant at a later point of the cell cycle, and include not only the mechanic machinery necessary for chromosome condensation and segregation, but also important regulatory proteins implicated in the DNA-damage checkpoint[835–837].

As shown in Figure 26A and B, the vast majority of the BAF-modulated genes belonging to these cell cycle-related enriched gene sets were down-regulated after the disruption of the complex in neuroblastoma cells. Indeed, key regulators of both transitions were pronouncedly repressed: G_2-M transition regulators such as Chk1 (CHEK1), Wee1, CDK1 or Aurora B kinase (AURKB); and G_1-S proteins like DNA polymerases (POLA2, POLE), replication fork proteins (MCM3, MCM4), E2F family members (E2F2, E2F8) and cyclin D1 (CCND1). The repression of genes related to these two different cell cycle points could be explained by an arrest in the G_1 phase, which would cause that most genes only expressed in S, G_2 and M phases had a reduced expression.

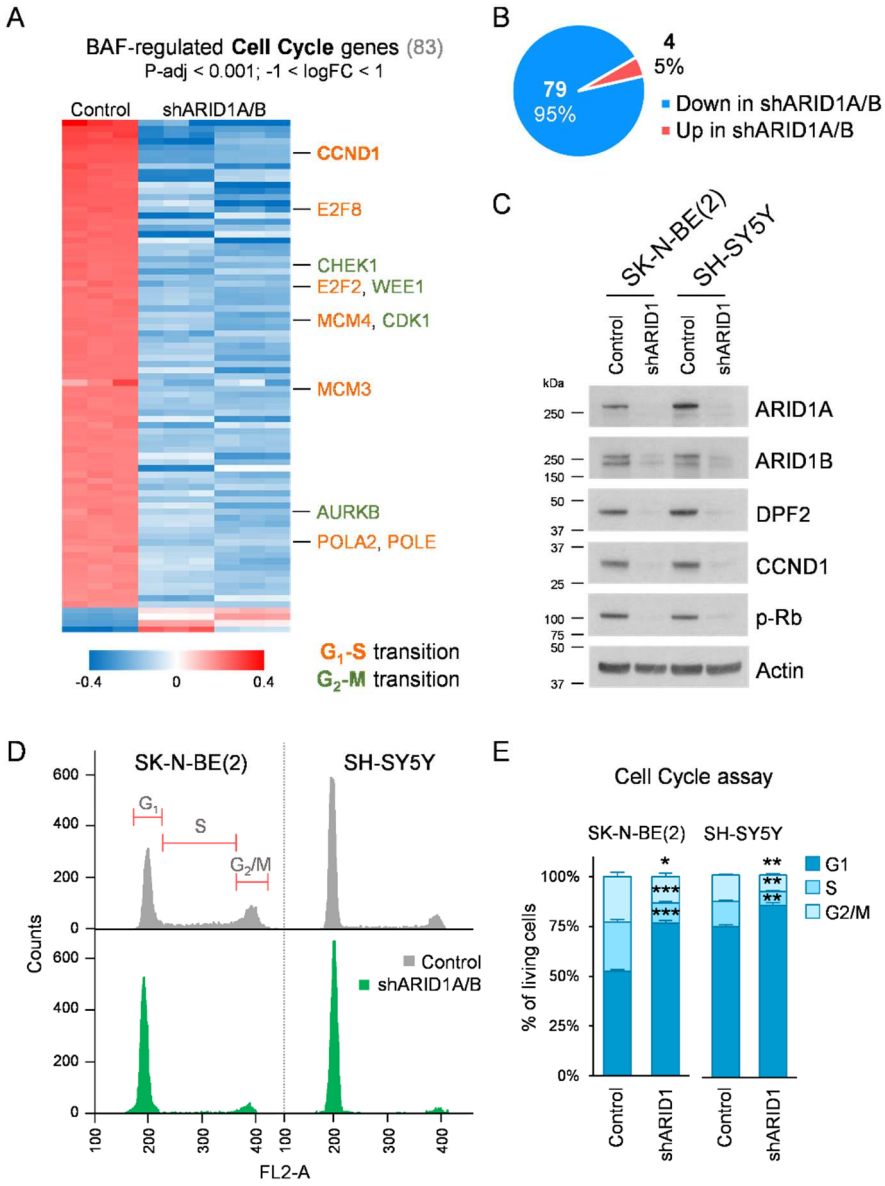

Figure 26: BAF complex disruption produces G_1 phase blockade in neuroblastoma cells through modulation of key cell cycle regulators. **A**. Heatmap representing relative expression of those genes included in E2F targets, G_2-M checkpoint and mitotic spindle hallmarks from MSigDB, and were found to be modulated after BAF-disruption using the indicated cutoff. Color gradient represents RNA-Seq normalized counts relativized for each gene and log_2 transformed. **B**. Pie chart representing the proportion of cell cycle-related BAF-modulated genes up or down-regulated after BAF disruption. **C**. Cyclin D1 (CCND1) and phosphorylated Rb (p-Rb) western blot analysis of BAF-disrupted cells, at 96 hours after transduction with shARID1A and shARID1B, or control shRNA. DPF2 was analyzed for monitoring the destabilization of the BAF complex. **D**. Flow cytometry cell cycle assay by propodium iodide staining at 96 hours after transduction with shARID1A and shARID1B, or control shRNA. DNA content is represented in the X axis of the histograms. **E**. Quantification and comparison of the different cell cycle phase populations detected by flow cytometry. * means $P < 0.05$; ** means $P < 0.01$; *** means $P < 0.001$.

Western blot analysis revealed a strong decrease of cyclin D1 protein levels in SK-N-BE(2) and SH-SY5Y cells after BAF disruption, and a concomitant reduction in the phosphorylation of Rb (Figure 26C), reinforcing our hypothesis. Finally, flow cytometry cell cycle analysis by propidium iodide staining showed a clear increase in the percentage of cells in G_1 phase and a reduction of the S and G_2/M phases in both cell lines, fully confirming the G_1 arrest after BAF complex disruption (Figure 26D and E). Cell cycle arrest was not accompanied by cell death, since no signs of apoptotosis were observed in the long term (i.e., >1 week after transduction) neither by means of cleavage activation of the caspase 3 (CASP3) apoptotic effector or of its substrate PARP (Figure 27A) nor by detection of condensed and fragmented chromatin (Figure 27B). To discard other cell death, we performed an independent cell death assay that measures the amount of released DNA after cell membrane permeabilization. Again, the disruption of the BAF complex did not reveal any sign of cell death involving membrane pemeabilization (Figure 27C). Therefore, we concluded that the decrease in proliferation observed after BAF disruption was related to the strong cell cycle arrest, without the contribution of cell death.

These results prove that the disruption of the BAF complex promotes G_1 phase arrest in neuroblastoma cells, explaining the decrease in proliferation, and validating the findings on cell cycle signatures obtained by whole transcriptome analysis of BAF-disrupted cells.

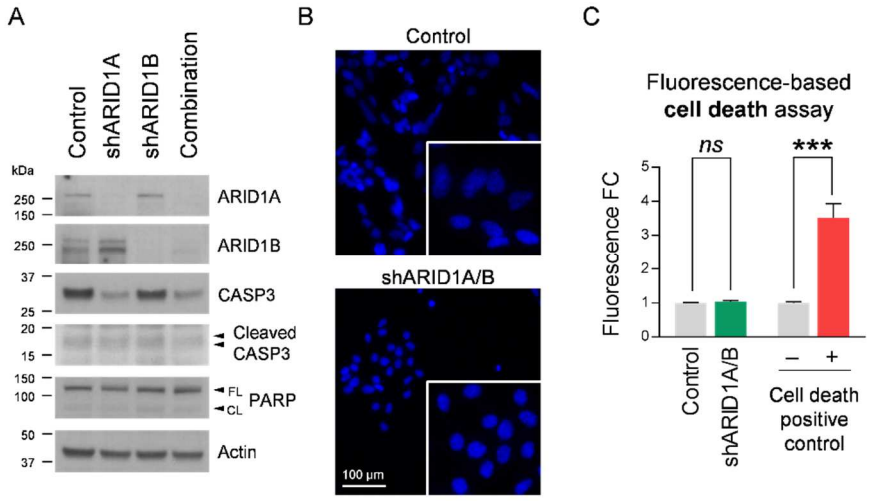

Figure 27: BAF complex disruption does not trigger cell death in SK-N-BE(2) neuroblastoma cells. **A**. Western blot analysis of the full length (FL) and cleaved (CL) forms of caspase 3 (CASP3) and PARP, 10 days after transduction with shARID1A/B. **B**. Representative fluorescence images of Hoechst stained SK-N-BE(2) cells at the same time point. **C**. Fold change (FC) fluorescence based cell toxicity assay of SK-N-BE(2) at the same time point, using CellTox kit (Promega). Lysis solution from the kit was used as cell death positive control. *ns* means 'non-significant'; *** means $P < 0.001$.

4.5. **BAF disruption promotes the repression of metastasis-related gene signatures**

4.5.1. BAF disruption promotes the repression of the neuroblastoma mesenchymal phenotype gene signature

The most enriched hallmark found in control with respect to BAF-disrupted cells in the transcriptome analysis was epithelial-mesenchymal transition (EMT) (Figure 25B). EMT comprises a series of inter- and intracellular reversible changes that include reduced cell-cell adhesion and increased motility, affinity for extracellular matrix (ECM) and capacity of invasion, regulated by an intricate network of cross-talking pathways ending in transcriptional changes[838–841]. EMT is crucial for the correct completion of normal embryonic development, but numerous EMT-related mechanisms have been reported to be relevant for many cancer types' invasiveness and metastasis initiation[842–844]. The non-epithelial origin of neuroblastoma cells makes them not able to undergo EMT, strictly speaking. However, it has been proposed to classify them into adrenergic or mesenchymal cell lineages on the base of their transcriptional and epigenetic profile[58]. These lineages have characteristic phenotypes: mesenchymal phenotype consist in neural crest-like undifferentiated cells, with higher invasive potential and drug resistance, in contrast to the more differentiated and less invasive and drug sensitive phenotype of adrenergic cells. Mesenchymal neuroblastoma transcriptional signature is highly similar to that of the neural crest cells and includes many classical EMT regulators[58,845,846].

We decided to interrogate this neuroblastoma mesenchymal phenotype transcriptional signature, consisting of 485 genes, on the RNA-Seq data from BAF-depleted neuroblastoma cells. In concordance with our previous results, the mesenchymal signature was significantly enriched in control in comparison with BAF-depleted cells (Figure 28A). When looking at the BAF-modulated mesenchymal phenotype genes, using the indicated cutoff, all of them were down-regulated after assembly disruption of BAF complex through simultaneous silencing of ARID1A and ARID1B (Figure 28B). Interesting key mesenchymal genes were found repressed, standing out *LOXL2*, *SNAI2*, *CDH11* and integrins αV (*ITGAV*) and α4 (*ITGA4*). LOXL2 is a lysyl oxidase with an epigenetic role in EMT as transcriptional co-repressor. It deaminates the trimethylated lysine 4 of histone 3 (H3K4me3) activation mark and is recruited by the Snail family of transcriptional factors (SNAI1, SNAI2, SNAI3) to the promoters of their target genes[847–849]. Snail factors are central regulators of EMT that act as transcriptional repressors of epithelial phenotype genes, such as E-cadherin, whose downregulation is one EMT hallmark[842,850].

Interestingly, the family member Slug (SNAI2) is part of the neuroblastoma mesenchymal signature, and is also one of the BAF-modulated mesenchymal genes (Figure 28B). Another repressed mesenchymal gene after BAF disruption was cadherin 11 (*CDH11*), which is also one of the neuroblastoma mesenchymal signature genes. Cadherins are transmembrane proteins that mediate cell-cell interactions and are key in EMT. As mentioned before, some of them are crucial for the maintenance of the epithelial phenotype, but other cadherins are implicated in the mesenchymal phenotype[851,852]. CDH11 is one of these mesenchymal cadherins[853] and it is a type-II cadherin, which promote lower cell-to-cell adhesion[854]. Interestingly, CDH11 plays an important developmental role by allowing neural crest cells to detach from neural tube and undergo EMT[855,856] and its expression has been associated with invasion and metastasis in multiple tumor types[857–860]. Western blot validated the repression of LOXL2 in SK-N-BE(2) cells after BAF disruption (Figure 28C). SH-SY5Y, which are paradigmatic adrenergic phenotype cells, did not expressed detectable basal levels of LOXL2, as expected. These results illustrate the putative transcriptional control of mesenchymal genes through BAF complex in mesenchymal neuroblastoma cells.

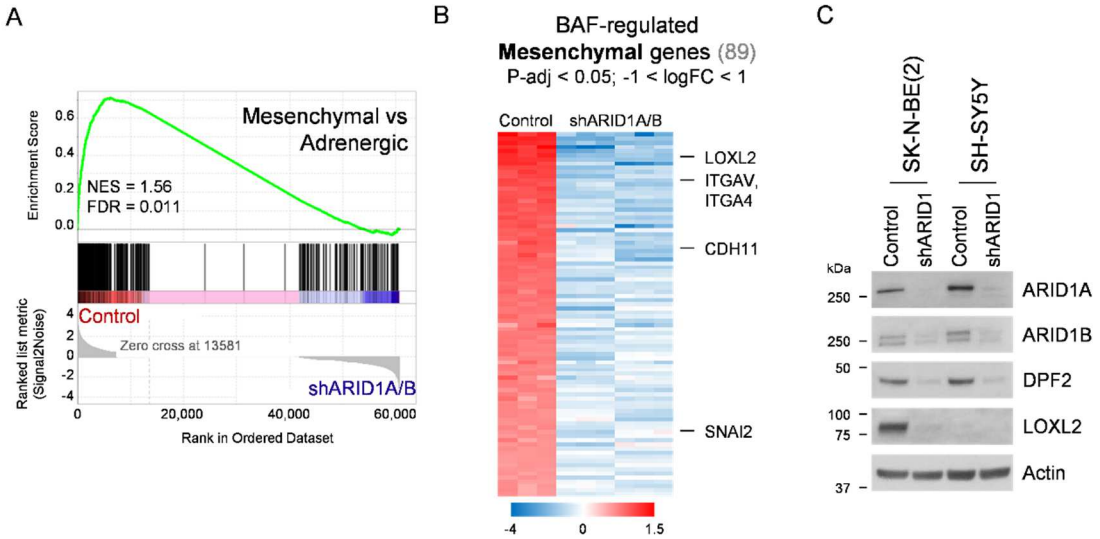

Figure 28: BAF complex disruption causes the repression of the neuroblastoma mesenchymal phenotype gene signature. **A**. Enrichment plot of the neuroblastoma mesenchymal phenotype gene signature on RNA-Seq control *vs.* BAF-depleted SK-N-BE(2) cells. Normalized Enrichment Score (NES) and False Discovery Rate (FDR) are indicated. **B**. Heatmap of the relative expression of genes included in EMT hallmark from MSigDB or in neuroblastoma mesenchymal signature[63] modulated after BAF-disruption with the indicated cutoff. Color gradient represents log_2 transformed normalized counts relativized for each gene. **C.** Western blot validation of mesenchymal protein LOXL2 repression after BAF disruption, 96 hours after transduction with shARID1A and shARID1B (shARID1) lentiviral particles.

4.5.2. BAF disruption promotes an extensive repression of the integrin gene family in neuroblastoma cells

Among all the mesenchymal phenotype genes downregulated after inhibition of BAF complex, a specific family of proteins caught our attention due to the elevated number of members found to be down-regulated: the integrin gene family. Integrins are ECM interaction transmembrane proteins which act as sensors of external stimuli and transducers of signals into the cells, but also as mechanical effectors of processes like migration and invasion, given their ability to adhere to multiple ECM components, such as collagen, fibronectin or laminin[861].

Gene set enrichment analysis of transcriptional signatures related to the activation of integrin signaling and related-proteins showed a clear repression of these groups of genes after assembly disruption of the BAF complex in neuroblastoma cells (Figure 29A). Intriguingly, the same analysis for the whole family of integrins, consisting of 26 members, showed a clear and significant enrichment of this group of genes in control in comparison with BAF-depleted neuroblastoma cells (Figure 29B). Particularly, 12 out of these 26 members were found significantly modulated after BAF depletion, being 11 down-regulated and only one (ITGB4) up-regulated (Figure 29C), indicating a wide repression in the expression of the members of this gene family when the structural integrity of BAF complex is compromised in neuroblastoma cells. Interestingly, those BAF-modulated integrins showed an incomplete down-regulation when single inhibition of ARID1A or ARID1B was analyzed, in comparison with the modulation levels obtained after combined silencing (Figure 29D). These results highlight again the need of simultaneous inhibition of both proteins for full achievement of BAF inhibition functional consequences.

Among the modulated integrins, both α- and β-integrins were found (Figure 29E). Integrins have full functional activity when they form dimers, which must be composed by one subunit of each subfamilies, α and β[862]. The two most repressed integrins found in neuroblastoma cells after BAF complex inhibition were integrins β3 and α9 (ITGB3 and ITGA9, respectively), both of them previously implicated in cancer, and particularly in metastatic processes[863,864]. Western blot analysis validated the reduction on protein expression levels of these two members after BAF complex disruption in SK-N-BE(2) and SH-SY5Y cells (Figure 29F).

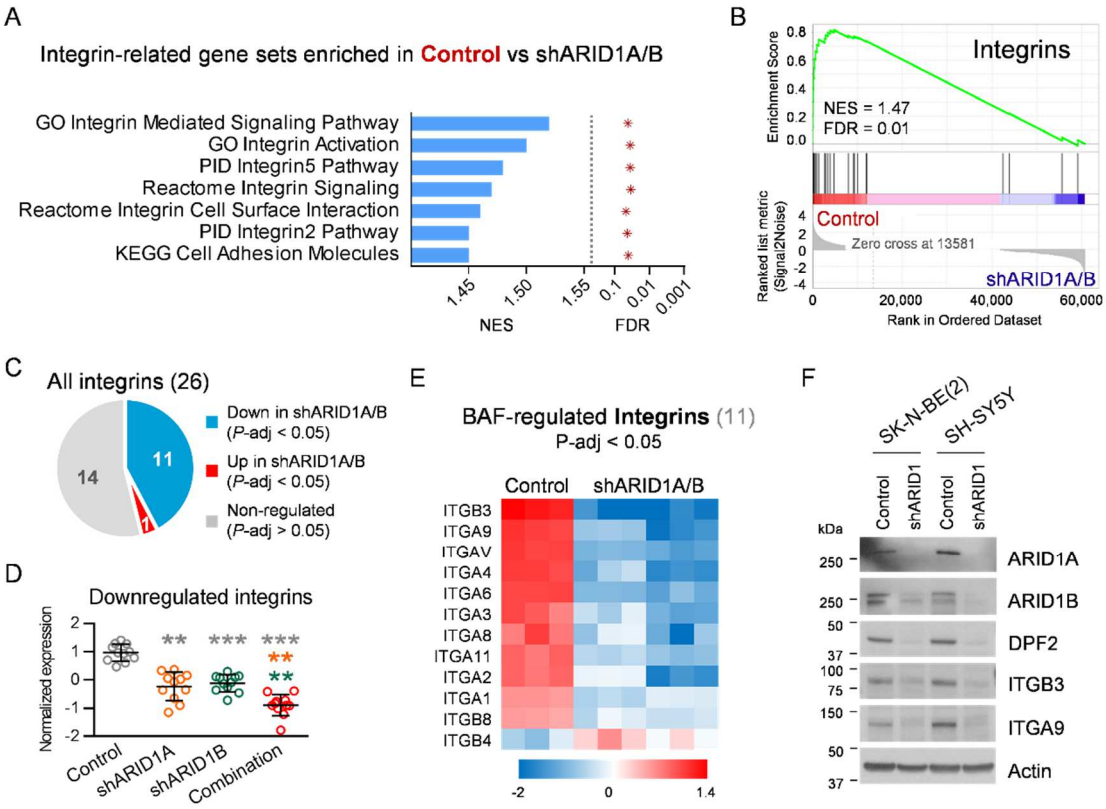

Figure 29: BAF complex disruption produces an extensive modulation of the integrin gene family expression in neuroblastoma cells. **A**. Normalized Enrichment Score (NES) and False Discovery Rate (FDR) of the 5 integrin-related gene sets significantly enriched in RNA-Seq expression data of control compared to BAF-depleted SK-N-BE(2) cells. **B**. Enrichment plot of the 26 existing human integrins. NES and FDR are indicated. **C**. Pie chart of the proportion of human integrins down-, up- or non-regulated by BAF complex. **D**. Normalized expression of the 11 repressed integrins after BAF inhibition after single or combined silencing of ARID1A and ARID1B. **E**. Heatmap representing relative expression of BAF-modulated integrins. Color gradient represents RNA-Seq normalized counts relativized for each gene and log_2 transformed. **F**. Validation of integrins β3 (ITGB3) and α9 (ITGA9) repression after BAF complex inhibition, using DPF2 as complex-stability reporter. ** means $P < 0.01$; *** means $P < 0.001$.

The drastic modulation of important mesenchymal phenotype regulators and a large family of proteins such as the integrins, both of them widely implicated in invasiveness and metastatic potential of cancer cells, unveiled a putative oncogenic role of the BAF chromatin remodeling complex in neuroblastoma beyond proliferation, which was possible to identify thanks to the genome wide analysis of transcriptional changes produced by its specific disruption.

4.6. **BAF complex structural integrity is necessary for neuroblastoma metastasis formation and progression**

4.6.1. BAF complex disruption blocks ECM adhesion, invasiveness and stress fiber formation of neuroblastoma cells *in vitro*

Given the impact of BAF disruption observed at the transcriptome level of neuroblastoma cells on pathways and gene families related to ECM adhesion, motility and invasion, we decided to validate if this transcriptional reprogramming manifested itself as functional phenotypic effects associated to these metastasis-related capabilities.

First, and due to the observed broad inhibition of integrins, we wanted to asses if there was a change in the affinity of neuroblastoma cells to components of the ECM. We decided to perform *in vitro* experiments of adhesion to collagen since, among all the known substrates to which integrins are able to bind, collagen is one of the more ubiquitous integrin ligands, and it is also one of the most abundant ECM components[865]. Seeding upon a collagen matrix of SK-N-BE(2) or SH-SY5Y neuroblastoma cells transduced with either control shRNA or the combination of shRNAs against ARID1A and ARID1B, and posterior aspiration and washing after short periods of time –from 5 to 25 minutes–, let us monitorized the kinetics of affinity of these cells to collagen. Ablation of BAF complex produced a drastic reduction in the attachment dynamics of neuroblastoma cells to the matrix (Figure 30A), indicating a clear reduction of their affinity and capacity of adhesion to collagen. Next, we examined the effects on motility and invasiveness by transwell assays with a collagen barrier. Concordantly with our previous results, the inhibition of the BAF complex reduced the capacity of both SK-N-BE(2) and SH-SY5Y neuroblastoma cells to pass through the collagen barrier (Figure 30B and C), for a period of time –16 hours– at which differences could not be explained by different proliferation rhythms between experimental conditions. Finally, confocal microscopy of actin filaments by phalloidin staining of neuroblastoma cells was performed to monitor changes in the cell prolongations that mediate motility (i.e., stress fibers)[866]. BAF complex depletion produced a clear change in neuroblastoma cell morphology to a rounded shape without prolongations (Figure 30D). Quantification of cell prolongations was performed by calculating the phalloidin positive area sticking out of the main cell body defined by tubulin signal. For both cell lines, this quantification confirmed the observable morphological changes (Figure 30E and F).

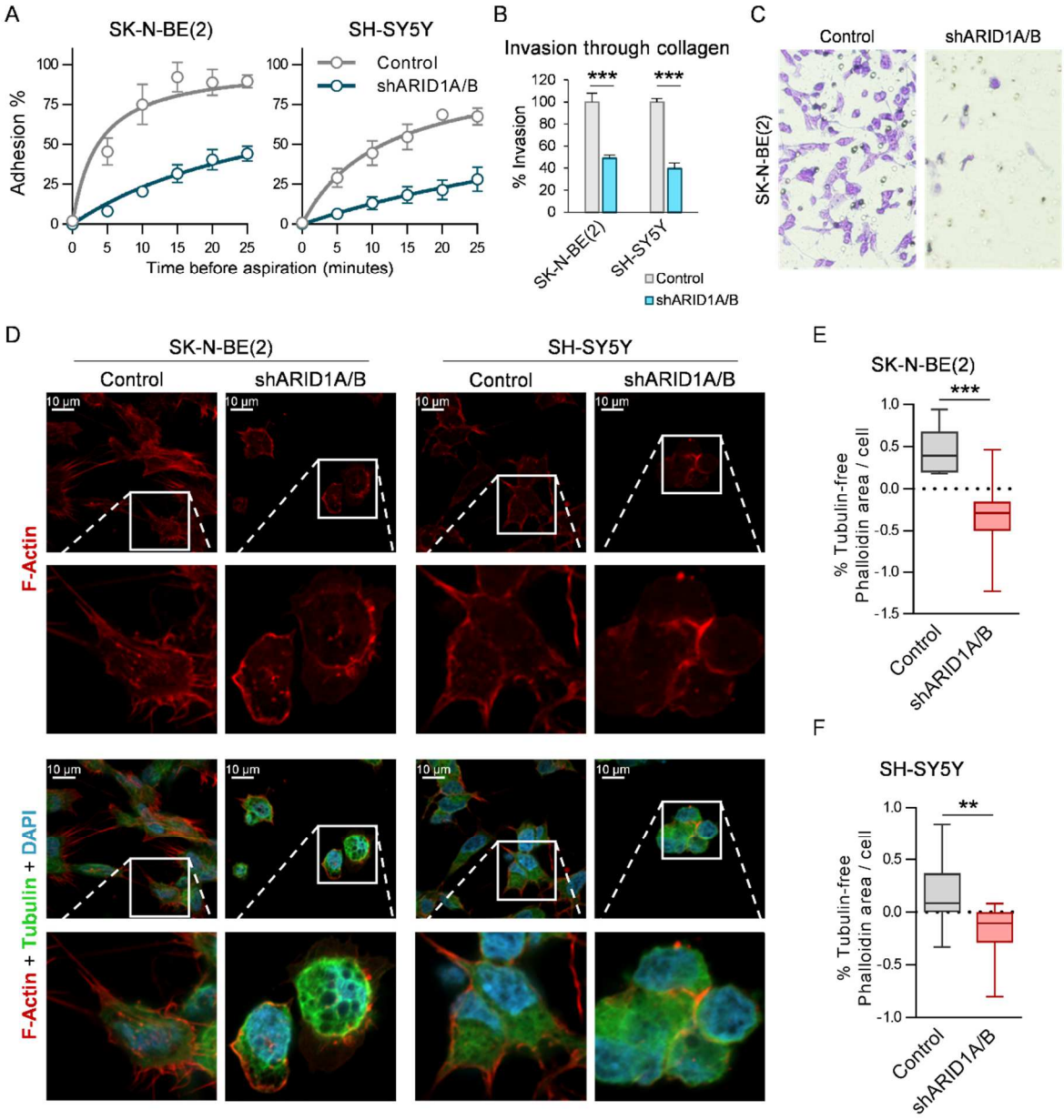

Figure 30: BAF complex disruption reduces ECM adhesion and invasion *in vitro*, and causes drastic morphological changes and destruction of stress fibers in neuroblastoma cells. **A**. Adhesion assays by seeding 40,000 cells upon collagen-coated 96-well plated. Cells were aspirated and rinsed at the indicated time points after seeding. When remaining cells were fully attached after 8 hours, plates were quantified using crystal violet staining, normalizing to non-aspirated cells. **B**. Invasion assay with collagen-coated transwell. A total of 200,000 cells were seeded and let migrate for 16 hours, before removing the non-migrated cells from the upper chamber and quantification by crystal violet staining. **C**. Representative microscopy pictures of crystal violet stained migrated cells. **D**. Confocal microscopy representative pictures of neuroblastoma cells stained with phalloidin (F-Actin), anti-tubulin antibody and DAPI. **E** and **F**. Quantification of SK-N-BE(2) and SH-SY5Y, respectively, tubulin-free phalloidin area per cell. Ten fields per biological replicate were analyzed. ** means $P < 0.01$; *** means $P < 0.001$.

Altogether, BAF complex disruption was validated to promote in neuroblastoma a functional repression of metastasis-related cell properties *in vitro* that included affinity and adhesion to collagen, as well as motility and invasion through this component of the ECM. Finally, clear changes in the morphological phenotype that led to loss of stress fibers were observed, highly likely related to the decrease in motility.

4.6.2. BAF disruption impairs neuroblastoma metastasis formation and growth *in vivo*

Given all the *in vitro* evidence showing the relevance of BAF complex structural integrity on metastasis-related cell properties, we decided to assess the effects of disrupting the assembly of this chromatin remodeler in the formation and progression of metastasis of neuroblastoma in an *in vivo* mouse model. We used SK-N-BE(2) cells transduced with a lentiviral vector encoding the firefly luciferase (FLUC) reporter gene that helped us to monitor *in vivo* metastasis growth and localization. These cells were intravenously injected in the tail vein of immunosuppressed SCID beige mice 72 hours after transduction with lentiviral vectors containing shRNAs against both ARID1A and ARID1B proteins, or the empty vector, and animals where monitored for the following weeks by *in vivo* luminescence imaging and followed-up for signs of macrometastases for differential survival analysis (Figure 31A). In order to avoid a possible confounding factor related to different reporter signal between control and ARID1A/B depleted cells, we analyzed the effects on luminescence signal *in vitro* of these cells after the disruption of the BAF complex. Interestingly, double inhibition of ARID1A and ARID1B reduced the luminescence signal per viable cell, being approximately ~2.516 times lower than in control cells (Figure 31B). Metabolic differences or changes in chromatin accessibility –since lentiviral vectors are integrative– may be explaining this difference, which however seems to remain stable and to linearly correlate with the number of viable cells. Therefore, we decided to use this luminescence signal correction ratio for the *in* vivo quantification of luciferase signal.

Corrected luminescence signal one hour after injection showed injected cells only in the lungs (Figure 31C) and no quantitative difference was observed between experimental groups at this time point (Figure 31D), technically validating the injection of the same number of viable cells on the bloodstream of the mice. Lung is not a classical neuroblastoma metastasis target organ, so we deduced that the accumulation of neuroblastoma cells right after tail vein injection was due to the mechanical barrier found by the cells in this organ.

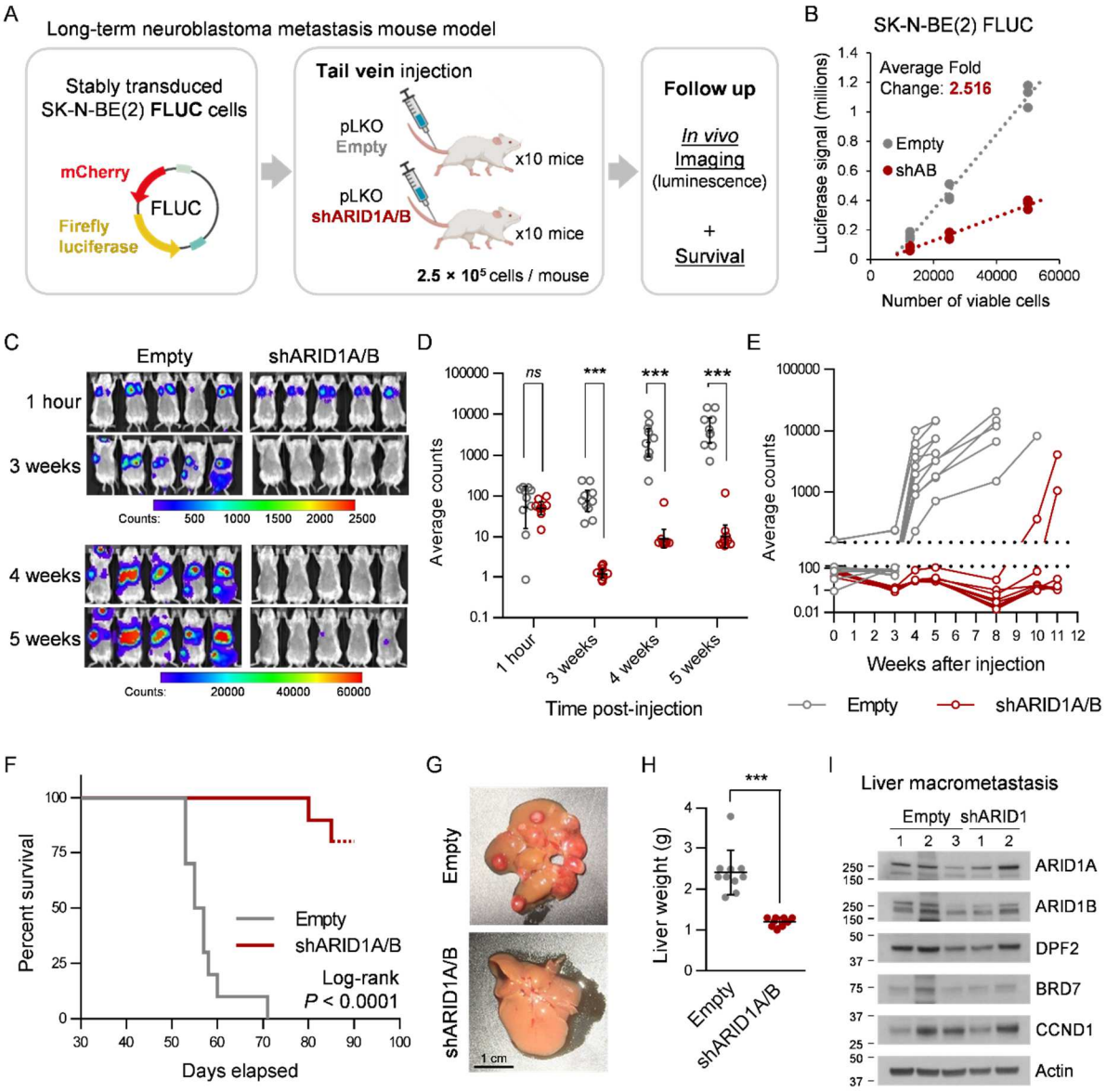

Figure 31: BAF complex disruption inhibits metastasis formation *in vivo* and extends the survival of metastatic neuroblastoma mouse models. **A.** Experimental design of the long-term neuroblastoma metastasis mouse model. **B**. *In vitro* luciferase assay comparing luminescence signal of different numbers of pLKO-empty or pLKO-shARID1A/shARID1B (shARID1A/B or shAB) transduced SK-N-BE(2) FLUC viable cells. **C**. Representative *in vivo* luminescence images of 5 mice per group at the indicated time points. Scale bar represents luminescence counts. **D**. Luminescence quantification, expressed in average counts, and comparison between experimental groups at the indicated times post-injection. **E**. Individual mice luminescence quantification follow-up through the entire experiment. **F**. Kaplan-Meier survival plot comparing Empty or shARID1A/B cells-injected mice- Log-rank test was performed to assess statistical significance. **G**. Representative images of mice livers of both groups showing multi-foci macrometastases in the empty group. **H**. Comparison between groups of liver weight at the moment of euthanize. **I.** Protein levels analysis of the indicated proteins of 3 empty-vector and 2 shARID1A/B liver macrometastases, by western blot. *ns* means 'non-significant' (P > 0.05); *** means $P < 0.001$.

In vivo weekly imaging starting from 3 weeks after injection showed the disappearance of cells from the lungs and a sustained increased in luminescence signal in empty vector-transduced SK-N-BE(2) neuroblastoma cells-injected mice. In this group, metastatic foci were found in liver of all mice, in the leg bone marrow in 8 out of 10 mice, and sporadically in thoracic and neck lymph nodes. On the other side, BAF-depleted cells through ARID1A and ARID1B silencing (shARID1A/B), did not form detectable macrometastases in the majority of the mice; only two developed liver metastases, with delay in comparison with the control group, as they were only detectable from week 5 after injection, while bigger metastases were already found in control mice at week 3 (Figure 31C-E).

Hepatic metastases were usually the first to appear and the biggest to grow, causing the first signals of suffering on the animals. With the aim of avoiding it, at the moment liver macrometastases were palpable, mice were taken out of the study and euthanized. This symptomatology follow-up allowed us to analyze the effects of BAF disruption on the survival of the different groups of mice. In accordance with the clear differences observed by luciferase imaging, while control mice showed a median survival time of 56 days after injection, 8 of the mice injected with BAF-depleted cells did not manifested any metastasis-related symptomatology, coinciding with the lack of luminescence foci, and survived until the end of the experiment, and 2 of them –those that developed delayed hepatic metastases– survived until days 80 and 85 after injection. Altogether, survival was significantly extended when BAF complex assembly was disrupted in tail vein-injected neuroblastoma cells (Figure 31F). In accordance with these results, necropsy of the mice only showed clear multi-foci liver macrometastases in the empty vector group, while livers of the BAF-disrupted cells injected mice were found clean of lesions (Figure 31G), except from those 2 who developed delayed metastases, which consisted in only one focus each one. This result was further supported by a marked difference in liver weight between groups (Figure 31H).

As the effect of BAF disruption abolished in most cases metastasis formation, end point western blot validation of the knockdown was not possible for all the cases. However, we were able to compare the two delayed metastases formed in shARID1A/B group with 3 of the control group macrometastases, finding no signals of neither ARID1A nor ARID1B silencing, destabilization of BAF complex by DPF2 levels, or down-regulation of cyclin D1 (Figure 31I). These results suggest that these two delayed macrometastases formed in the BAF-disrupted group of mice might be

originated by cells that evaded silencing of both proteins, possibly a remainder of cells inefficiently transduced with pLKO-shRNA lentiviral vectors. This reinforces the impact of BAF-complex disruption on metastasis formation and progression observed in this experiment, as it means that the only two metastases that could be formed after disruption of the complex did it through evasion of the silencing technique.

4.6.3 BAF disruption hampers the early arrival and colonization of neuroblastoma metastatic cells

The reduction in metastasis formation and growth observed after BAF disruption in the long-term neuroblastoma metastatic mouse models could be explained merely as the result of the decrease in proliferation exerted by this inhibition on neuroblastoma cells, since the depletion of the complex was already produced before cells were injected, and therefore before macrometastases could be formed by sequential cycles of cell division.

For these reasons, we decided to monitor the early stages of the hepatic metastasis process of neuroblastoma cells, in order to determine if BAF complex had effects on the initial arrival and maintenance of metastatic cells, or only in the posterior metastasis growth by affecting proliferation. Then, we performed a short-term metastasis *in vivo* experiment, schematized in Figure 32A, in which early detection and quantification of human neuroblastoma cells at 4 and 7 days after injection of SK-N-BE(2)-FLUC cells, transduced either with the empty vector or with shARID1A/B, was performed by flow cytometry using the fluorescent mCherry protein encoded in the reporter vector FLUC. Moreover, cells were stained prior injection with a fluorescent proliferation tracing dye, to monitor the proliferation rate of these cells on the base of the dilution of the dye and its consequent decrease of fluorescence signal.

This double fluorescent marking assured us the clear identification of the human neuroblastoma cell population and its discrimination from the residual mouse hepatocyte population in the processed liver cell suspensions from the injected mice (Figure 32B). Empty vector-transduced SK-N-BE(2) cells were detected in the liver in a ratio of 10,000 positive events per million at 4 days post-injection. However, in the liver of mice injected with BAF complex-disrupted (shARID1A/B) cells, a drastic reduction, of about a 10-fold, was already observed at this early time point (Figure 32B and C).

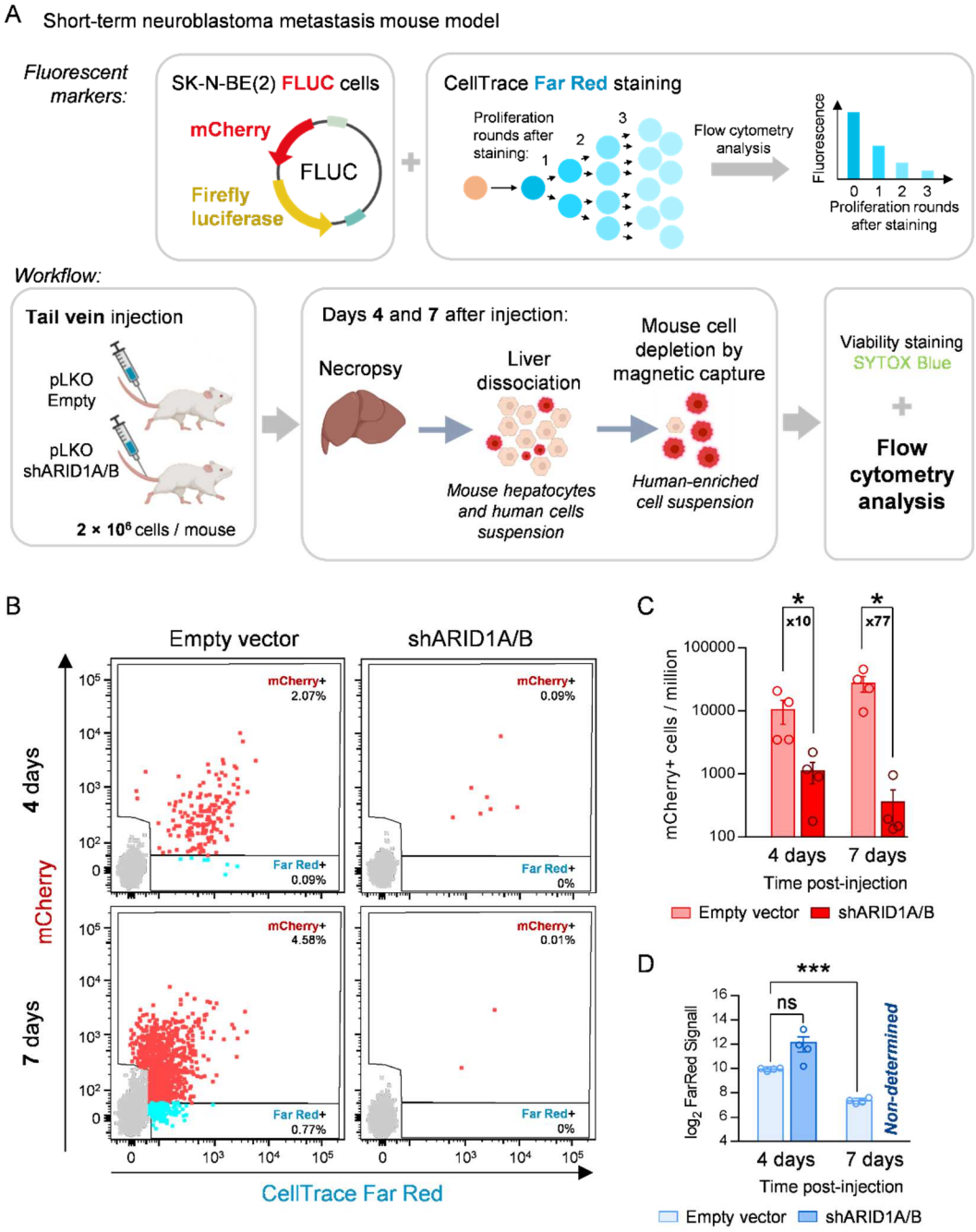

Figure 32: BAF disruption hampers the early arrival and colonization of metastatic neuroblastoma cells to liver. **A**. Experimental design of the short-term neuroblastoma metastasis mouse model performed with SK-N-BE(2) cells. **B**. Representative flow cytometry plots of each experimental condition and time point, showing mCherry positive (mCherry+) and FarRed positive/mCherry negative (FarRed+) single living cell populations. **C**. Quantification of detected mCherry positive cells, expressed in events per million of living single cells (parent gate). * means $P < 0.05$ in Mann-Whitney's test. Fold change between conditions are indicated. **D**. Average FarRed intensities assessed, when possible, for the mCherry+ population of each experimental group. *** means $P < 0.001$ and *ns* means 'non-significant'.

Remarkably, no significant differences on the signal from the proliferation tracer were detected at this time point between both groups (Figure 32D). This indicates that the strong decrease in the number of mCherry positive cells could unlikely be attributed to differences in proliferation rates at this time point. In fact, even if the observed trend to a higher retention of the FarRed dye in shARID1A/B was real (< 2 division cycles), the difference in the proliferation tracer could not explain a 10-fold drop in the number of metastatic neuroblastoma cells. Therefore, the reduction in number of neuroblastoma cells at this time point when BAF complex is disrupted is probably not completely due to a delay in the proliferation rate.

In addition, at day 7 post-injection, an expected increase in the number of positive cells was observed in the control (Figure 32B and C), concomitant with a marked decrease in the signal of the proliferation tracer (Figure 32D). This results strongly supports the idea that between 4 and 7 days, newly arrived metastatic cells have already started populating the tissue by proliferating. However, BAF-disrupted cells maintained the low numbers at this time point, reaching almost undetectable levels. These low number prevented us from quantifying the intensity of the proliferation tracer, by not getting three samples with at least 5 positive events. Nevertheless, these results show that, in contrast with the control, the few BAF depleted cells that had reached the liver at day 4 had not increased in number by proliferating at day 7, thereby avoiding the early colonization of the liver.

These results suggest that BAF disruption has additional effects on neuroblastoma metastasis initiation besides proliferation, probably through reducing the arrival, invasion and/or posterior survival of neuroblastoma cells on the metastatic niche. Indeed, this indicates that BAF complex depletion has two probable combined effects on the metastatic process: it reduces the number of living cells arriving to the liver and/or surviving in the early steps of metastatic invasion; and also blocks the proliferation of the few cells that have been able to arrive.

To sum up, the findings obtained through transcriptome analyses made us investigate the role of BAF complex structural integrity in the metastatic process of neuroblastoma, leading to the discovery that BAF disruption causes a strong detrimental effect on neuroblastoma metastasis at very early stages, by reducing the arrival and invasion of cells to the metastatic site (i.e., liver), which is later magnified by a strong blockade of proliferation. The combination of these effects prevents the formation and growth of macrometastases and expands the survival of metastatic neuroblastoma mouse models.

4.7. **Virtual screening identifies 85 small molecule candidates to disrupt BAF complex**

The phenotypic consequences of BAF complex assembly disruption on neuroblastoma proliferation and metastasis formation reported before uncovered the therapeutic potential of this way of modulation of this chromatin remodeler for the treatment of this type of tumor. Unfortunately, the attempts of BAF complex pharmacological inhibition have been few and focused on bromodomain targeting[689] or ATPase activity inhibition[703]. Some inhibitors have been developed from functional reporter screenings, without full evidence of the targeting mechanism[704]. Therefore, this strategy of inhibition is nowadays not developed enough and still a pending task. On the other hand, the therapeutic use of RNA interference for the specific silencing of target proteins is a potential strategy being developed for tumors such as neuroblastoma[867], but the current state of the art of these technologies is still not sufficiently developed for easily silencing two proteins simultaneously in this type of cancer. The biggest obstacle for the generation of structure-based reasoned inhibitors has been the lack of structural information of the assembled BAF complex until 2020, when two independent studies assessed by high resolution electron microscopy the structure of the nucleosome-bound full assembled complex, with great consistence between them[258,259]. These structures also corroborated the map of intra-complex interactions previously determined by cross-linking mass spectrometry[215,258], where ARID1A, and concretely its ARM-domains contained in the C-terminal part of the protein, concentrates a great part of the interactions with other complex subunits, suggesting that ARID1 proteins act as relevant structural scaffolds of the complex.

4.7.1. ARID1A protein contains two potentially druggable pockets at ARID1A/SMARCA4 and ARID1A/SMARCD1 interaction surfaces

Taking advantage of the newly generated knowledge, we decided to make use of this structural information to identify possible druggable pockets on the surface of ARID1A and ARID1B that could be targeted to block key interactions with other subunits and interrupt the assembly of the BAF complex, an unprecedented inhibition strategy. Druggability analysis was performed on the surface of ARID1A contained in the 6TLJ Protein Data Bank (PDB) structure of nucleosome-bound complex (Figure 33A), using two different pocket identification algorithms.

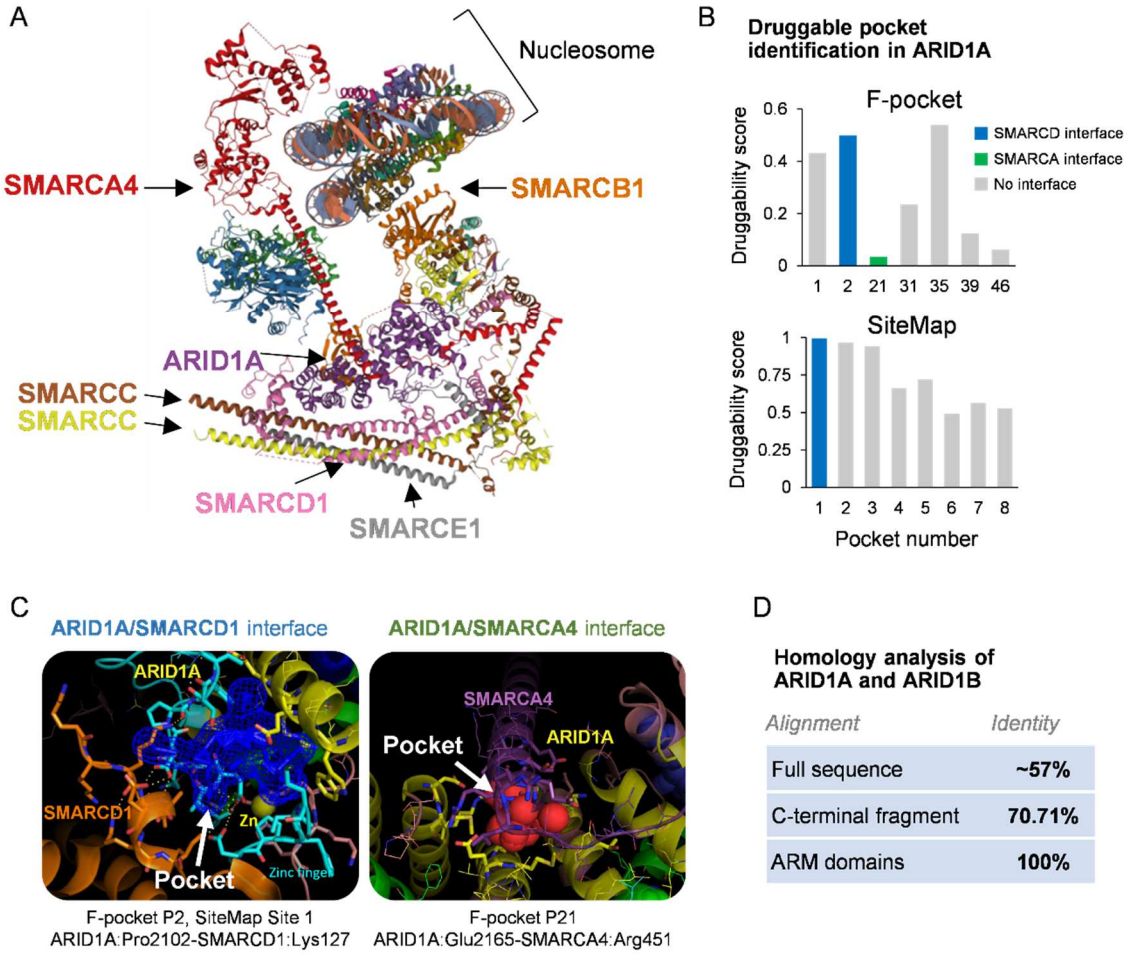

Figure 33: Druggability study of ARID1A. **A**. Tridimensional structure of nucleosome-bound assembled BAF complex, from 6TLJ. Representative picture was extracted from Protein Data Bank (PDB). Relevant components are indicated with color code. **B**. Druggability scores of *bona fide* pockets for each algorithm. Pocket 2 from F-pocket and pocket 1 from SiteMap are coincident. **C**. Representative images of the two pockets found in interaction sites of ARID1A surface. **D**. Homology analysis of ARID1A and ARID1B. Identity percentages are shown of different alignments on various parts of the proteins.

Examination of those pockets with highest druggability score revealed two of them located at surfaces of interaction with SMARCD1 and SMARCA4/BRG1 subunits, belonging to core and ATPase modules, respectively. ARID1/SMARCD interface pocket was predicted by both algorithms, while ARID1/SMARCA interface pocket was only predicted by F-pocket (Figure 33B and C).

As reported before, to obtain the complete functional consequences of BAF inhibition in neuroblastoma cells, full structural disruption of the complex must be produced by simultaneous inhibition of ARID1A and ARID1B homologues. Homology analysis of the two proteins showed a high similarity percentage concentrated in the C-terminal fragment, and maximum at the ARM domains (Figure 33D). Moreover, the amino acids involved in the two identified pockets belong to ARM domains and are conserved in both proteins. We therefore concluded that, although the druggability analysis was performed on ARID1A surface, small molecules targeting these two pockets with high probability will bind to ARID1B too.

4.7.2. Virtual screening identifies 85 candidate molecules targeting the two ARID1A pockets

With the aim of maximizing the probability of finding a small molecule acting as a structural disruptor of the BAF complex assembly, we used the two pockets previously found in ARID1A surface for a high-throughput virtual screening (HTVS) of molecules. The ZINC database was used, which is a virtual library of 7.5 million commercially available 'drug-like' compounds[809]. These compounds were tested for its fitness in both ARID1/SMARCD and ARID1/SMARCA pockets.

The virtual screening consisted in a multi-step process (Figure 34A). A first HTVS was performed, resulting in 100.000 filtered molecules. Second, Standard Precision (SP) scoring function was performed, which has a more exhausted ligand conformational sampling and more accurate scoring functions. The resulting top 500 molecules from the second step were further filtered with the molecular properties required for nucleus membrane crossing (detailed in Figure 34A). Finally, the docking poses of the selected compounds were manually examined to finalize the selection of the most promising compounds. The virtual screening of small molecules generated a list of 85 BAF-disruptor candidate compounds, 46 identified in the ARID1/SMARCD interaction surface pocket and 39 in the ARID1/SMARCA one. A final prioritization score was determined for each compound, from 1 to 3, from less to more priority (Figure 34B).

In summary, the druggability analysis of ARID1A revealed the presence of two different interaction surface-located pockets potentially druggable with 85 candidate molecules.

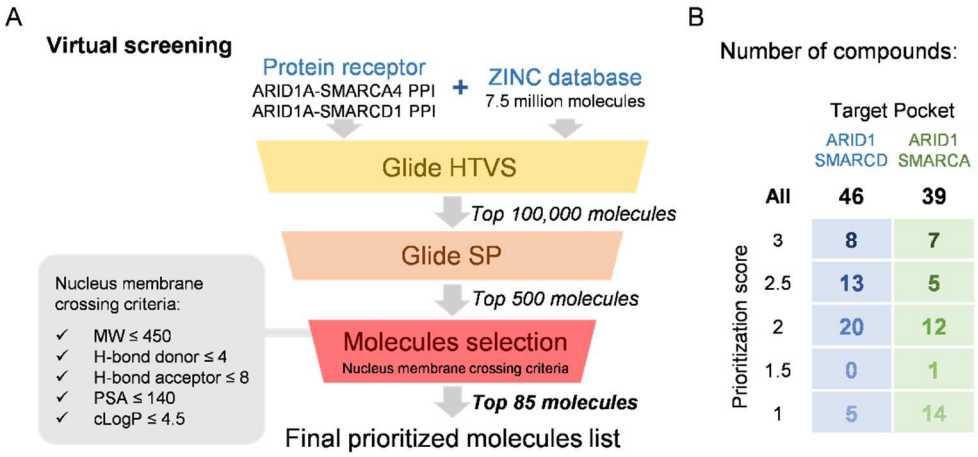

Figure 34: Virtual screening of small molecules targeting ARID1A/SMARCA4 and ARID1A/SMARCD1 interface pockets. **A**. High-throughput virtual screening (HTVS) of ZINC database molecules in ARID1A pockets flowchart. **B**. Final number of resulting molecules for each pocket, broken down by prioritization score.

4.8. **Four BAF disruptor candidates inhibit neuroblastoma proliferation**

4.8.1. Screening of 50 BAF disruptor candidates reveals 4 anti-proliferative compounds

To narrow down the list of BAF complex disruptor candidates (BDC), we decided to test the effects of these compounds on the proliferation of neuroblastoma cells. This functional screening readout method was chosen, despite all its drawbacks, because of the clear effects that RNA interference-mediated disruption of the complex showed on neuroblastoma cell lines' proliferation, and the practical simplicity and reproducibility of the technique. Although many chemically promising compounds might be discarded by this method because of different reasons (e.g., they are not efficiently cell-penetrating), it allowed us to narrow down our list to those which are able to arrive to the cell nucleus, bind to ARID1A/B, disrupt the assembly of the complex and exert the phenotypic consequences on proliferation.

Forty-eight compounds were commercially available from companies proposed by ZINC database, and 2 of them were asked for custom synthesis (Figure 35A). We prioritize the acquirement of these two molecules because of their high score (3), but also because of the features of SMARCD interface pocket: it was predicted with high confidence by both algorithms and it is an interaction site of ARID1A/B with the core module, whose inhibition, in our opinion,

has more probability of affecting BAF structural integrity than the disruption of the interaction with SMARCA4, the ATPase subunit. The rest of the compounds were out-of-stock, and custom synthesis of all of them would have implied a time-consuming unreasonable increase in the cost-to-benefit ratio of the discovery phase. For this reason, only those with higher probabilities of targeting the complex were ordered whether or not in stock. We acquired a total of 50 compounds and tested their effects on proliferation at 50 µM for 96 hours on a single dose, in SK-N-BE(2) neuroblastoma cells, using vehicle (DMSO) treated cells as normalizing control (Figure 35B).

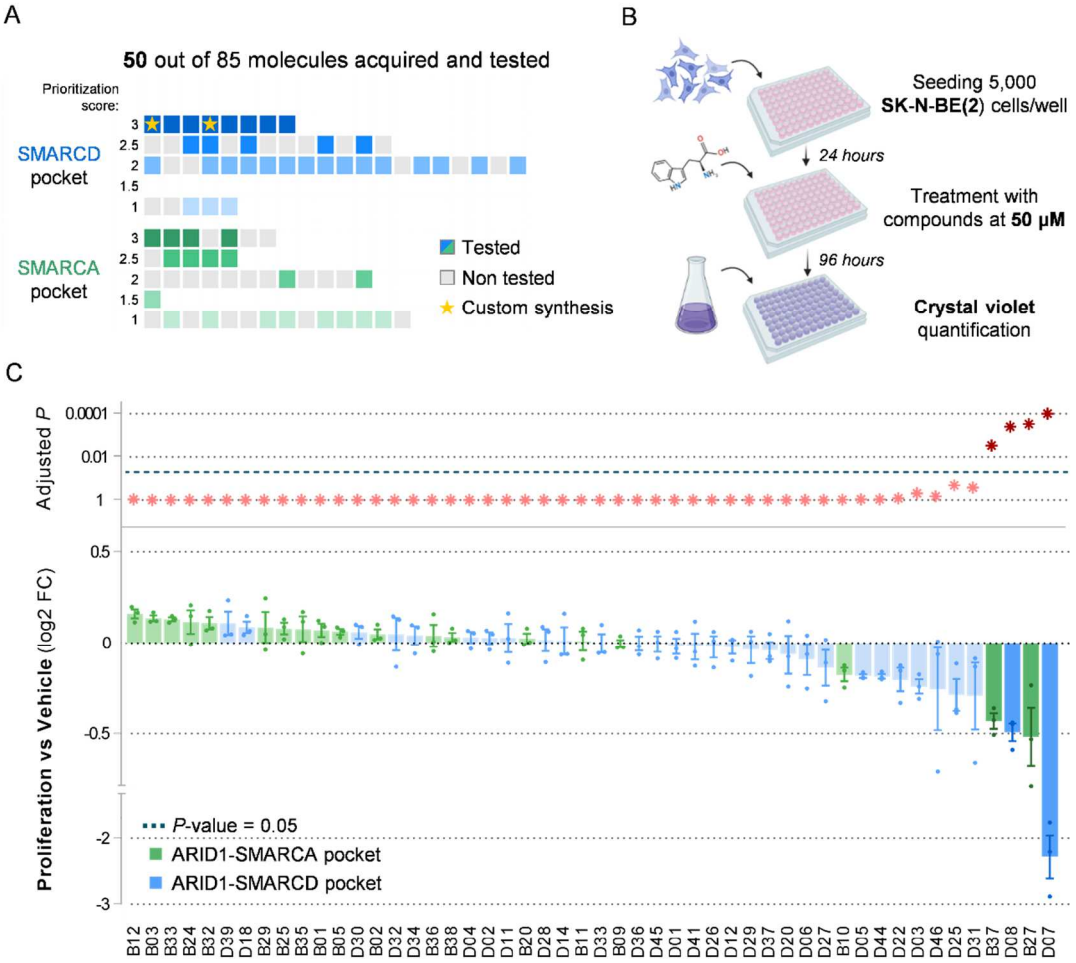

Figure 35: Proliferation screening of 50 BDCs in neuroblastoma cells. **A**. Schematic representation of the tested compounds. **B**. Experimental design of the proliferation screening. **C**. Proliferation Fold Change (FC) and adjusted *P*-value for each compound.

We selected a concentration of 50 µM as a compromise between the fact that these molecules were not optimized from a pharmacological point of view, preventing us from expecting high levels of stability and pharmacokinetics from them; and the need of discarding the molecules without any effects at high doses in order to narrow down the list of candidates. Based on the concentration needed for other nuclear protein-protein interaction inhibitors, the half maximal inhibitory concentrations (IC_{50}) of which easily arrive to the µM order of magnitude[868], we decided that 50 µM was a high dose within the range of reasonable pharmacological concentrations for tissue culture treatment.

Proliferation screening revealed a significant reduction in proliferation by four of the BDC compounds (Figure 35C). Two of these compounds, D07 and D08, targeted the SMARCD1-interaction pocket, and the other two, B27 and B37, the SMARCA4-interaction pocket.

4.8.2. Functional and biochemical characterization of four BAF disruptor screening hits

The four molecules that were able to reduce the proliferation of neuroblastoma cells were further characterized. While D07 and D08 ARID1/SMARCD pocket candidate molecules were among the 3-scored prioritization group, B27 and B37 ARID1/SMARCA pocket candidates had only a prioritization score of 1. Among all 4 compounds, D07 was the one to exert the most potent anti-proliferative effects, reducing proliferation below 25% with respect to vehicle-treated cells after 96 hours of treatment at 50 µM (Figure 36A), and having a great impact on cell morphology, causing a clear change to round-shape. On the other hand, compounds B27, D08 and B37 had a more modest impact on proliferation with the same conditions, with an average reduction on cell proliferation below 30%, and not having any sensible effects on cell morphology.

To discard off-target toxicities, we decided to check if the decrease in proliferation obtained with the treatment of neuroblastoma cells with these molecules was concomitant with any effect on the protein stability of the components of the BAF complex. We hypothesized based on our RNA interference-mediated BAF disruption results that, according to the planned mechanism of action of blocking the assembly of the complex through inhibition of ARID1A/B with other subunits, a destabilization of the subunits assembling after ARID1A/B incorporation should be detected by means of total protein levels assessment, indicating the reaching of the intended

target. Western blot analysis did not show any relevant change in BAF-specific DPF2 subunit after treatment with B27, D08 and B37 compounds. However, we did observe a reduction in DPF2 levels, as well as in SMARCB1/SNF5 core module member, after treatment with D07 (Figure 36B). Of note, PBAF-specific BRD7 subunit, did not show such decrease. We also reported a clear reduction in the levels of cyclin D1, one of the previously reported key cell cycle regulators modulated by BAF complex in neuroblastoma cells.

Finally, a dose-response characterization of D07 was performed in 5 different neuroblastoma cell lines to assess its pharmacological kinetics. D07 showed similar dose-response profiles for these molecular-heterogeneity representative neuroblastoma cell line panel (Figure 36C), and a half maximal inhibitory concentration (IC_{50}) of between 40 and 125 µM, being the low-cycling CHLA-90 cells the more resistant and SK-N-BE(2) the more sensitive (Figure 36D).

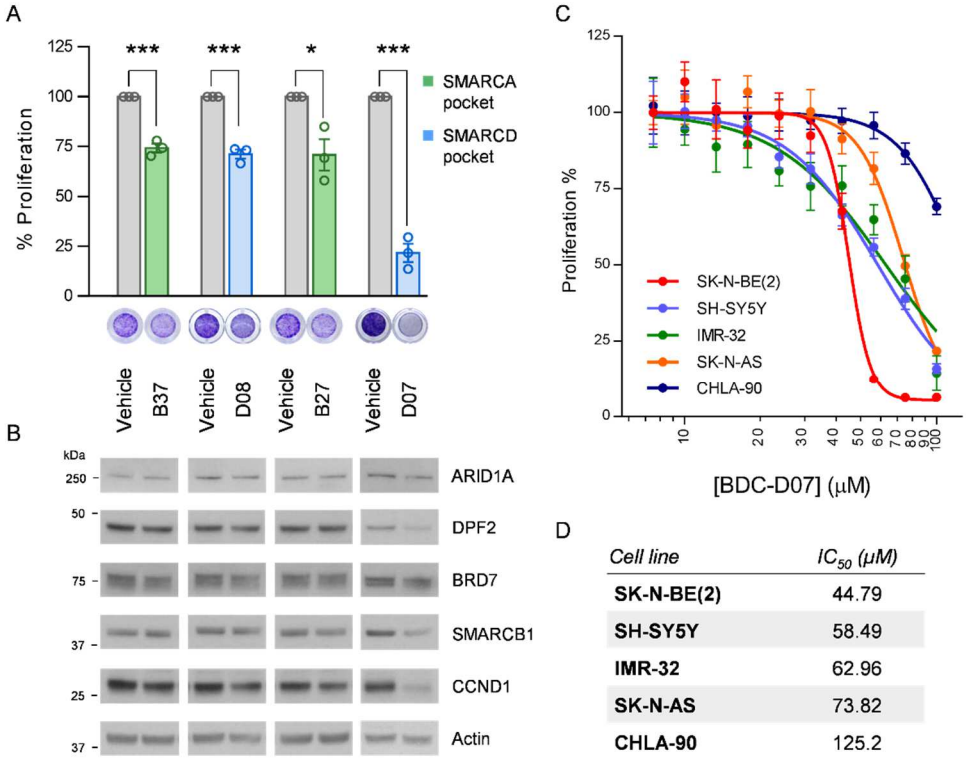

Cell line	IC_{50} (µM)
SK-N-BE(2)	44.79
SH-SY5Y	58.49
IMR-32	62.96
SK-N-AS	73.82
CHLA-90	125.2

Figure 36: Characterization of the four proliferation screening hits. **A**. Proliferation effect of BDCs B37, D08, B27 and D07 on SK-N-BE(2) neuroblastoma cells treated for 96 hours at 50 µM, expressed in percentage with respect to vehicle-treated cells, assessed by crystal violet staining. **B**. Western blot analysis of mSWI/SNF subunits and cell cycle effectors in SK-N-BE(2) cells after 72 hours of treatment at 50 µM with each compound. **C**. D07 dose-response curves of in a panel of five neuroblastoma cell lines, assessed by crystal violet staining. **D**. Half maximal inhibitory concentration (IC_{50}) of D07 in five neuroblastoma cell lines. * means $P < 0.05$; *** means $P < 0.001$.

In summary, four different BAF disruptor candidate molecules targeting ARID1 surface sites of interaction with other subunits, identified by druggability study of ARID1A and high-throughput virtual screening, were found to inhibit neuroblastoma proliferation *in vitro*. One of them, D07, which showed the most pronounced anti-proliferative effect, produced a reduction in the levels of some BAF complex subunits, thereby suggesting on-target effects and destabilization of the complex. These results will open a whole new research line for the generation, optimization and validation of new first-in-class BAF complex small molecule inhibitors.

5. **DISCUSSION**

I can't escape it
I'm never gonna make it out of this in time
I guess that's just fine
I'm not there quite yet
My thoughts, such a mess
Like a little boy
What you runnin' for?

Hard to fight what I can't see
Not trying to build no dynasty
I can't see beyond this wall
But we lost this game so many times before

At The Door
The Strokes
The New Abnormal
2020

5.1. **Specific dependency of neuroblastoma cells on BAF structural integrity**

Aberrant epigenomes are behind relevant neuroblastoma tumor phenotypes[58,772], which need molecular effectors, including chromatin remodelers, to translate epigenetic signals into specific chromatin states. Mutations in subunits of the mSWI/SNF chromatin remodeling complex have been found in ~11% of neuroblastoma patient samples[537,538], a remarkably high mutation frequency in these pediatric tumors, which are characterized by low point mutations rates[722]. In addition, previous empirical data had pointed towards a possible oncogenic role of this chromatin remodeling complex in neuroblastoma, since its main catalytic subunit SMARCA4/BRG1 was associated with poor prognostic clinical parameters and shown to control oncogenic pathways in neuroblastoma cell lines[630]. This body of evidence made us focus on and deepen into the study of the mSWI/SNF chromatin remodeling complex as a functionally relevant epigenetic regulator in neuroblastoma. Thus, we designed an experimental approach for the systematic and holistic study of the presence, composition and biological role of the different mSWI/SNF complexes in neuroblastoma cells by proteomic analyses and loss of function experiments, with the aim of assessing their potential as targets for a new epigenetic therapy for neuroblastoma.

Integral proteomic characterization of mSWI/SNF complexes in neuroblastoma cells had not been reported before. Determining the presence and structural integrity of the different subtypes of mSWI/SNF complexes was definitely needed if a complete study of these chromatin remodelers was to be performed in this type of pediatric tumors. Our choice was to isolate all possible assembled complex subtypes existing in neuroblastoma cell lines by co-immunoprecipitation and posterior mass spectrometry analysis, using the ATPase subunit SMARCA4/BRG1, present in all known mSWI/SNF variants, as bait. SMARCA4/BRG1 is highly expressed in all neuroblastoma cell lines, in comparison with the low and limited expression of SMARCA2/BRM paralogue counterpart[630]. Our results indicate that neuroblastoma cells contain the full composition of the three described subtypes of mSWI/SNF complexes, with proteomic detection of all of their known subunits. The tangible and comparable protein levels of all the subtype-specific subunits (Figure 20) strongly suggest the presence and structural integrity of these subcomplexes in neuroblastoma cells. This assumption is done on the basis that the high levels of commitment to the complex have been demonstrated to make mSWI/SNF subunits especially vulnerable to destabilization and proteasomal degradation when physically separated

from the rest of the complex[817]. Indeed, the experiments of subcomplex-specific destabilization through silencing of key structural subunits presented in this thesis corroborate this model. For instance, the structural disruption of BAF complex by combined silencing of ARID1A and ARID1B promoted a decrease in the levels of BAF-specific and committed subunits at the protein level, and not of PBAF or ncBAF-specific subunits; and the same effect was also reported in PBAF and ncBAF specific disruption experiments (Figure 21). Nevertheless, BAF-specific protein downregulation after complex disruption was not concomitant with a decrease in the transcriptional levels of the corresponding genes, as assessed by RNA-Seq transcriptome analysis (Figure 37A). Indeed, the majority of mSWI/SNF subunits were not transcriptionally modulated after ARID1A and ARID1B combined silencing, and those significantly modulated were with very discreet fold changes. Only DPF1 and BCL7A were clearly down and upregulated, respectively, besides the shRNA targets ARID1A and ARID1B. This indicates that changes at the protein level, such as the marked decreased in DPF2 levels (Figure 37B), are not produced by a global transcriptional control by BAF complex itself of its own subunits, in a hypothetical positive feedback loop, and points towards a more than probable protein destabilization followed by proteasomal degradation. These data supports the idea of the presence of fully assembled BAF, PBAF and ncBAF complexes in neuroblastoma cells, as well as of their structural disintegration after the knockdown of key subunits.

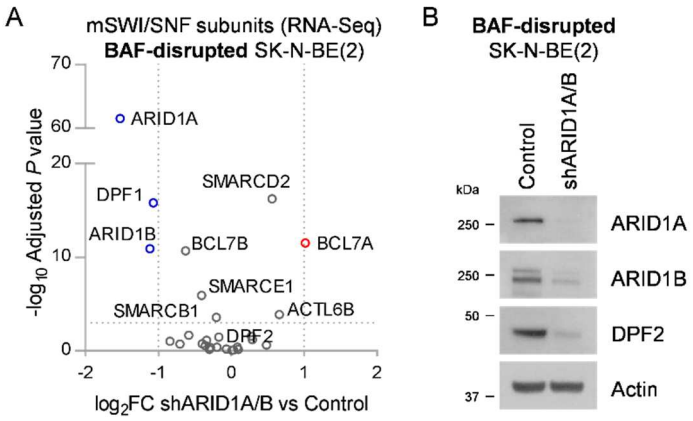

Figure 37: Intra-complex expression effects of BAF complex disruption. **A**. Vulcano plot showing Fold Change (FC) and adjusted *P* value of mSWI/SNF subunits RNA expression after BAF disruption by ARID1A/B silencing (RNA-Seq data). **B**. Western blot analysis of BAF-specific DPF2 subunit levels after BAF disruption through combined silencing of ARID1A and ARID1B.

Of note, a set of non-mSWI/SNF proteins were found bound to SMARCA4/BRG1 in the proteomic approach. We attributed the identification of the α and γ-actin variants (ACTA1, ACTG1) to their similarity with the β-actin (ACTB1) belonging to the complex, and the apparition of a ribosomal protein as a common mass spectrometry contaminant frequently detected in proteomic approaches[869] due to their numerous gene copies and high expression. However, two interesting putative regulators were consistently found in both cell lines: the endoplasmic reticulum (ER) chaperone BiP (HSPA5) and the nuclear transport regulator karyopherin α2 (KPNA2). The observed interaction of these regulatory proteins with BRG1, and probably with other members of the complex, suggests alternative mechanisms for targeting the action of the complex through protein destabilization at the ER level or by blockage of nuclear transportation. Indeed, previous reports have assessed the impact of nuclear shuttling regulatory systems of different mSWI/SNF subunits in the modulation of the activity of the complex[870–872], some of them involving karyopherins[873], revealing an interesting mechanism with potential value as an indirect mSWI/SNF targeting strategy.

Loss of function experiments were our choice for the functional study of mSWI/SNF complexes in neuroblastoma cells. Nevertheless, and due to their multiprotein and multifunctional aspects, the inhibition of the activity of these ATP-dependent remodeling complexes is not a trivial task, and the different strategies that can be used to achieve it vary not only in the mechanism of action of the inhibitory method, but also in the targeted subunit or group of subunits to inhibit. For example, one option could be the inhibition of concrete functions such as the ATPase catalytic activity or bromodomain binding, making use of the different inhibitors developed for these purposes (Table 7). However, one of the main features and also an evolutionary meaning of this multiprotein complex, like many other protein macromolecular complexes such as ribosomes or spliceosomes, is the concentration in time and space of multiple and varied molecular processes for the completion of a multistep process[107]. In the case of mSWI/SNF complexes, this functional integration includes activities of characteristics as different as the genomic targeting through bromodomain-containing proteins, the nucleosome-binding properties of SMARCB1 and the SnAc domains of SMARCA2/4, or the ATP-dependent DNA translocation performed by the catalytic subunits. Therefore, if a holistic analysis of the functions of this complex through its full repression was to be performed, the inhibition of only one of these activities had many chances to not unveil all the roles of this complex in neuroblastoma. This has been already observed in the incapacity of exploiting cancer synthetic lethalities using

bromodomain inhibitors[655]. Moreover, this kind of activity-specific inhibitors are not designed to produce a depletion of the protein, which stands out as the only strategy that ensures the inhibition of any possible subunit function, even of activities of unstudied domains.

The results presented in this thesis support these considerations: the inhibition through targeted proteasomal degradation of ATPase subunits with the PROTAC degrader ACBI1, did not have effects on proliferation in neuroblastoma cell lines. On the other hand, the structural destabilization of the complex, leading to a generalized decline in the protein levels of mSWI/SNF subunits, produced a clear decline in the proliferative capacities of neuroblastoma cells. This structural destabilization was first observed when making use of a shRNA silencing tool against the BRG1/SMARCA4 subunit. This is a ubiquitous subunit present in all three known variants of the complex, but can be substituted by its paralogue SMARCA2/BRM, if expressed. Although protein expression of BRM is detected at low levels in neuroblastoma cell lines, and completely undetectable in some of them[630], it is expressed in both SK-N-BE(2) and SH-SY5Y neuroblastoma cell lines, the two main neuroblastoma models used in this thesis. Inhibition of BRG1 through shRNA silencing promoted an increase on BRM protein levels (Figure 38A), being one of the few mSWI/SNF subunits not deleteriously affected by the structural destabilization promoted by shBRG1, and the only one reported to increase its levels. This compensation effect had already been reported for SMARCA2/4 in inhibition experiments[874]. We attribute this upregulation to the increased availability of subunits released from BRG1-depleted complexes, to which BRM can bind without the competition of BRG1. The rise in the number of BRM-containing complexes would reduce the number of BRM free polypeptides, and increase the global protein levels through its stabilization, through the already mentioned regulatory system of mSWI/SNF subunit levels, based on the binding-associated stability[817]. This effect reinforces the idea that the deleterious effects on neuroblastoma proliferation are not related to the ATPase activity of the complex, since the spontaneous upregulation and incorporation of an alternative ATPase subunit after BRG1 knockdown did not rescue the deleterious effects on proliferation. Moreover, BAF disruption through ARID1A/B silencing did not affect SMARCA4/BRG1 protein levels (Figure 38B), most probably due to its structural independence as a separate module, further supporting the ATPase independence of the mSWI/SNF proliferative dependency of neuroblastoma cells.

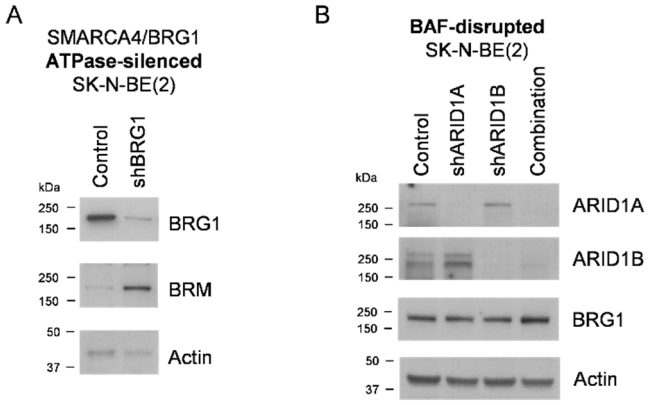

Figure 38: Structural effects of mSWI/SNF complex perturbations on ATPase subunits. **A**. Western blot showing the effects of SMARCA4/BRG1 knockdown on SMARCA2/BRM protein levels. **B**. Western blot showing the effects of ARID1A and ARID1B combined silencing on SMARCA4/BRG1 protein levels.

The ATPase activity is not only relevant, but even a defining trait of the SWI/SNF complexes, widely named with the title 'ATP-dependent', which were indeed historically discovered in *D. melanogaster* and in humans by the identification of the catalytic subunits. The relevance of the hydrolysis of ATP as energetic source to execute the physical tension needed for altering nucleosome states by disrupting the tight binding between DNA and histone octamers is undoubtable, as explained in the introduction of this thesis. Multiple mutations affecting the ATP hydrolysis have been shown to impair the proper chromatin remodeling activities of the complex[811,813,875], and recent research also found that ATPase activity is also necessary for other functions such as the active search of targets throughout the chromatin[876] or the release of the complex and conclusion of the remodeling process[812,876]. Naturally, this led us to think that the inhibition of ATPase activity was synonymous of full inhibition of the activity of mSWI/SNF complexes. However, as demonstrated by our results, that assumption was far from reality. The structural destabilization of the complex, whether by shRNA-mediated BRG1 silencing (Figure 19), or by assembly disruption of the whole complex through SMARCC paralogues inhibition with the same silencing method (Figure 23), was observed to exert clear phenotypic effects consisting in a reduction in the proliferative capacities of neuroblastoma cells, not produced by the specific degradation of the ATPase subunits, which did neither cause these structural effects upon the complex. These results strongly suggest ATPase-independent functions of the complex relevant at least for proliferation in neuroblastoma cells.

These results may be surprising, but do not represent a rarity on this research field. In fact, SWI/SNF complexes have been determined to exert part of their genome-wide functions in an ATPase-independent manner in a series of previous research reports. An early 1996 publication already reported that human mSWI/SNF complexes were able to maintain the altered partially-unfolded states of nucleosomes, leading to increased access to transcription factors, without the need for ATPase activity. Catalytic activity was seen to be essential for the change from regular nucleosome configuration to the altered state, indicating that it is only essential for the active initiation of a chromatin remodeling event, rather than for its maintenance[877]. This has functional consequences affecting the genome-wide gene expression control functions of the complex. For example, the catalytic activity of *Drosophila* BRM, which does not have an interchangeable paralogue, has been determined to be dispensable for the expression control through promoter chromatin remodeling of almost half of SWI/SNF controlled genes[878,879], and these genes belong to differential biological pathways and had different promoter configurations, with specific enriched DNA motifs, when compared to those controlled by ATP-dependent functions. Subsets of genes transcriptionally controlled by mSWI/SNF complexes in an ATPase-independent manner has also been reported in human cells[353].

One possible explanation extracted from these evidences is that an interplay of mSWI/SNF complexes with additional transcriptional cooperators or antagonists might be conditioning the need for ATPase activity. For instance, the presence of an opposition force promoting chromatin condensation and gene repression at the same genomic sites where mSWI/SNF complexes are counteracting these effects by generating chromatin accessibility, could make necessary the active action of the complex through ATP hydrolysis. Chromatin remodeling by mSWI/SNF is a dynamic process[880,881], and in a plausible scenario in which chromatin opening by mSWI/SNF and closing by a repressor are constantly intercalated, the output chromatin state of this equilibrium would be determined by that chromatin remodeler winning in the average time during which its effects on chromatin accessibility are maintained. This would imply the need of constantly initiating chromatin remodeling events by mSWI/SNF complex in order to counteract the opposing repressing force, with the consequential necessity of ATP hydrolysis[877], a scenario that would define ATPase-dependent SWI/SNF-regulated genes. On the contrary, the absence of an opposing repressing force of such characteristics would make mSWI/SNF complex only necessary for the maintenance of the open chromatin state, which is thought to be, at least in some cases, ATPase independent[877], making the catalytic activity dispensable and defining a set

of ATP-independent SWI/SNF-regulated genes. While the inhibition of ATPase activity would only affect the first set of groups, the structural disintegration of the complex would affect both. This model could explain the dispensability of the ATPase activity in the proliferation dependency of neuroblastoma cells on the mSWI/SNF complex.

These are mere hypotheses that open, again, encouraging research lines. A candidate with many possibilities to perform this role of chromatin repressing opposing force determining the need of ATPase activity from SWI/SNF complexes are Polycomb Repressing Complexes (PRC), a group of well-known epigenetic repressors that antagonize the transcriptional activation functions of mSWI/SNF complexes[882]. Indeed, co-localization and genomic occupancy competition between these two complexes have been described in detail[382,880], and there is evidence for thinking that mSWI/SNF ATPase activity could be necessary to oppose Polycomb repressing effects. For example, Polycomb eviction from chromatin by mSWI/SNF complexes is a dynamic process that requires ATP consumption in human cells[883]. Other work found that only a part of SWI/SNF functions rely on its antagonism with PRC in *C. elegans* development, discovered by ATPase inhibition, while the remaining functions were only manifested after complete removal of the complex, and were independent of PRC[884]. Moreover, loss of SMARCB1 in ATRT has been shown to not immediately involve gene repression in genes occupied by Polycomb, since the residual ATPase activity of co-localized mSWI/SNF complexes is sufficient to oppose this contrary regulation. Indeed, this interplay led to an explanation for the specific vulnerability of ATRT on mSWI/SNF ATPase subunits, related to their residual opposition to Polycomb repression[885]. All these recent findings shed light to the mSWI/SNF-Polycomb antagonism, and the probable relevance of the ATPase activity of the first one in this interplay.

Despite the presence of BRM, the silencing of BRG1 with shRNA in our neuroblastoma models, produced a drastic effect on the stability of many other members of the complex, including core (SMARCB1), BAF-specific (DPF2) and PBAF-specific (BRD7) subunits (Figure 19). This is a counterintuitive effect: while simultaneous ablation of three subunits (two ATPase homologues and PBRM1) did not have structural effects on the complex, the inhibition of only one subunit with a RNA interference silencing tool did. A clear and empirically-demonstrated explanation to this interesting observation is beyond the experimental scope of this thesis. Nevertheless, different ideas have passed through our minds, generating hypotheses of what may be happening. What is more probable is that these divergent effects are not due to the different

targeted subunits. The fact that ACBI1 simultaneously targets three complex subunits (BRG1, BRM and PBRM1) and the shRNA only one (BRG1), should increase the chances that the former had a phenotypic effect on cells over the latter, but our empirical findings show the opposite. However, the intrinsic differences on the mechanism of silencing of both methods may be behind these differential effects.

On the one hand, proteasomal degradation of BRG1, BRM and PBRM1 with ACBI1 is achieved after translation, due to the specific features of PROTAC degraders. Of note, this degradation can be induced on already-assembled subunits. In fact, mSWI/SNF subunits are highly committed to the complex, and its separate existence is limited to the period of time that it takes for them to be synthesized from the mRNA in the cytoplasm, and to be transported to the nucleus for its assembly into the complex, what minimizes the proportion of free mSWI/SNF subunits in the cell. Therefore, one could not expect the fast dynamics of effective degradation observed with the treatment of ACBI1 on the levels of its target subunits, if only degradation of separated subunits was being produced. Because of this, ACBI1 must be promoting the degradation of BRG1, BRM and PBRM1 polypeptides already incorporated in ATPase assembled modules or fully assembled complexes.

On the other hand, the mechanism of BRG1 silencing through shRNA is radically different: it is a post-transcriptional and pre-translational method of silencing that inhibits the synthesis of new polypeptides by degradation of the mRNA transcript, what makes this silencing method certainly unable to promote the depletion of already assembled subunits. Although ATPase module has functional and structural autonomy[215,216], on the base of our empirical data we hypothesized that the pre-translational inhibition of BRG1 subunit, and the impossibility of assembly of new polypeptides into the ATPase module and the rest of the complex, have structural consequences in the whole assembly, which are not produced when BRG1, BRM and PBRM1 are degraded after its proper incorporation.

In summary, as an explanation for the paradoxical results presented in Figure 19, we hypothesize that the loss of newly incorporating BRG1 subunits to the mSWI/SNF complex may have structural consequences leading to destabilization, whereas the degradation of already bound BRG1, BRM and PBRM1 subunits may not. Nevertheless, this are mere assumptions that open encouraging new lines of research on the biochemical and structural features of this complex, and urge the need of deeper investigations.

In any case, these results led us to investigate the relevance of the structural integrity, instead of the ATPase activity alone, of mSWI/SNF complexes in neuroblastoma proliferation, and we confirmed these effects by full disintegration of the complex (Figure 23), and specific disintegration of each complex subtype (Figure 21), revealing BAF complex as solely responsible for this deleterious effects on neuroblastoma proliferation. The main functional difference of the three mSWI/SNF complex variants, as explained in the introduction, is their genomic occupancy and set of genes under their transcriptional control[228,247,248,823]. Therefore, the fact that only the structural integrity of BAF complexes was relevant for neuroblastoma proliferation suggested that the reported deleterious effects were probably produced by the set of genes under the specific and exclusive transcriptional control of this complex subtype. Thus, we continued our investigations by interrogating the BAF-specific transcriptional network of neuroblastoma cells to find the effectors of neuroblastoma proliferative dependency on the structural integrity of BAF complex, and to determine additional oncogenic features controlled by BAF complex that may had remained uncovered by only using proliferation as oncogenic readout.

5.2. **BAF controls neuroblastoma cell cycle: epigenetic regulation of cyclin D1**

The analysis of genome-wide transcriptional changes after the specific structural disruption of BAF complex assembly clearly reflected at the gene expression level what we had previously reported in proliferation assays: the most pronouncedly modulated groups of genes when BAF depletion was performed were those related to the progression of the different phases of cell cycle. Concretely, we detected a decrease of those transcripts which are upregulated when cells transition from phase G_1 to S (E2F targets) and also those arising during G_2 phase and the transition to mitosis (G_2/M checkpoint, mitotic spindle genes). Altogether, these results clearly pointed towards a G_1 cell cycle blockade that was confirmed by flow cytometry analyses (Figure 26). The strong modulation of these sets of genes should not lead to hastily affirm that these genes are directly modulated by the BAF complex in neuroblastoma cells, since indeed some other agents causing a G_1 arrest of the same characteristics would have a similar impact on the transcriptome of neuroblastoma cells, due to the cell cycle-related gene expression network controlled by key transcription factors, such as the E2F family, whose action is restrained to certain cell cycle phases[832–834]. Nevertheless, these transcriptomic insights on cell cycle

progression genes affected by BAF disruption served us to fully characterize and give a sense to the observed decline in proliferation. Moreover, some interesting key cell cycle regulators which had already been implicated in neuroblastoma oncogenic features were observed downregulated in this analysis, suggesting that these could potentially be directly modulated by BAF complex, establishing a causative link between the chromatin remodeling events and the arrest on G_1 phase after ARID1A and ARID1B inhibition. Among them, cyclin D1 (CCND1) caught our attention.

Cyclin D1 is a well-known oncogenic protein specifically relevant for neuroblastoma. Its biological function consists in the binding to cyclin-dependent kinases 4 and 6 (CDK4/6) to promote the phosphorylation of Rb, which releases E2F family transcription factors, activating the transcriptional program that leads to the initiation of the S phase of cell cycle[886]. Therefore, cyclin D1 is an important key regulator of cell cycle progression and proliferation, with relevant roles in different cancers, and more specifically in neuroblastoma cells, which have sensibly higher levels of dependency for this protein in comparison with many other tumor types[772]. High CCND1 levels in neuroblastoma have been related to dedifferentiated and, therefore, more aggressive tumors, and resistance to the differentiating agent RA[887,888]. Moreover, multiple anti-proliferative drugs and tumor suppressive microRNAs repress CCND1 protein expression in neuroblastoma[889–892]. CCND1 overexpression has been related to genomic aberrations in neuroblastoma leading to gain of gene copies[893,894], but its transcriptional hyper-activation has also been described without the need of segmental chromosomal alterations, through the action at its *cis* regulatory DNA elements of transcription factors such as the stemness-related GATA3[895], relevant for neural crest development and sympathoadrenergic lineage determination[896,897].

Interestingly, epigenetic deregulation of *CCND1* gene has been described. For instance, aberrant hypo-methylation of its promoter has been detected[768], a more than plausible mechanism of overexpression adaptively selected for its driving oncogenic advantages. Moreover, search of super-enhancers using the activation mark H3K27ac in neuroblastoma patient samples have recently raised the importance of epigenetic regulation of *CCND1* in neuroblastoma[772]. Three super-enhancers conserved among neuroblastoma tumor samples and cell lines are strongly associated to *CCND1* gene and mediate its overexpression. Interestingly, these are among the most active super-enhancers found in neuroblastoma, and

they are also implicated in the binding of transcription factors that control core regulatory circuits of neuroblastoma implicated in both mesenchymal and adrenergic phenotypes. For example, in mesenchymal cells, footprints for different mesenchymal-related transcription factors in these regulatory regions were found, and *CCND1* expression was proved to be regulated by mesenchymal-related transcription factors such as FOSL2; however, adrenergic neuroblastoma cells also presented footprints for adrenergic-related transcription factors in these three super-enhancers, and some of them, such as MEIS2 or GATA3, were functionally confirmed to control *CCND1* expression through these regulatory elements. These findings reinforced CCND1 as an important and wide neuroblastoma therapeutic target, and also highlighted the importance of its epigenetic upregulation in neuroblastoma cell lines regardless of their lineage phenotype, which could be reflecting the specific dependency of neural crest cells on cyclin D1 regulation of cell cycle for the proper delamination process in the initial steps of its formation[898]. This developmental regulation may be inherited by the derived oncogenic neuroblastoma cells independently of the phenotypic stage at which they arrive, since active super-enhancer regulation of *CCND1* expression may be maintained by both early mesenchymal or later adrenergic transcription factors of core regulatory circuits.

Our results indicate that the specific disruption of the BAF chromatin remodeling complex produce a drastic reduction on CCND1 protein levels, which are concomitant with a decrease in proliferation and blockade in G_1 phase of cell cycle. Association of CCND1 levels with the activity of mSWI/SNF complex has previously been reported in other cancers, but in contradictory ways. For instance, BRG1 was shown to inhibit its expression in breast cancer cells, leading the loss of this ATPase subunit to increased levels of CCND1 and proliferative capacities[376]. ARID2 was found in hepatocellular carcinoma to have similar repressive effects on the *CCND1* gene[556]. An interesting case is the one of ATRT, in which loss of SMARCB1 subunit was correlated to an overexpression of this cell cycle-related protein[899], but this mSWI/SNF aberration was recently functionally associated with the loss of cyclin D1 and dependency of ATRT cells on its associated kinases CDK4/6[900]. Nevertheless, the functions of mSWI/SNF complexes are strongly conditioned by the epigenetic landscape of the different lineages, which are, by definition, different among them since they have different needs on gene expression. Therefore, a differential functionality of these chromatin remodelers in tumors from dissimilar developmental origins are expected.

Given the highly specialized and conserved role of mSWI/SNF complexes in the functional translation of epigenetic signals into chromatin states that allow the action of regulatory proteins, we considered a possible direct transcriptional regulation of *CCND1* by these remodelers through *cis* regulatory elements. Indeed, such epigenetic signals could be the abundant histone acetylation detected in distal regulatory elements like lineage-specific super-enhancers, which are found to be dependent in a majority of cases on the action of mSWI/SNF chromatin remodelers for the proper regulatory performance of these *cis* elements on their target genes[352]. Therefore, a plausible hypothesis would be that mSWI/SNF mediate the regulatory activity of some of the three widely conserved *CCND1* neuroblastoma super-enhancers, probably by allowing the binding of the multiple transcription factors mentioned before. The conservation between mesenchymal and adrenergic phenotypes would also support this model, since strong downregulation of CCND1 was observed in a paradigmatic adrenergic neuroblastoma cell line (SH-SY5Y), but also in SK-N-BE(2) cells (Figure 26), which show mesenchymal features, such as strong expression of LOXL2, a mesenchymal hallmark. Moreover, the decrease of proliferation concomitant with CCND1 downregulation was observed only when depleting BAF complexes, and not when doing it with PBAF or ncBAF variants. BAF complexes are preferentially localized at distal regulatory elements in comparison with the other two variants, which are preferentially located at promoters. This BAF complex trait is one more point in favor of the model in which this mSWI/SNF subtype controls the expression of *CCND1* gene by promoting the chromatin states required at its associated super-enhancers for the hyper-activation of this gene, which is essential for neuroblastoma proliferation. This model would open the possibility of exploiting the neuroblastoma-specific dependency on CCND1 by reverting its lineage-inherited epigenetic programming through the alteration of the chromatin state of its super-enhancers by BAF complex disruption.

Our results robustly support that the structural integrity of BAF complex is essential for proper cell cycle progression. Some authors have attributed a general proliferative dependency of cells on mSWI/SNF complexes and have speculated that it is due to its collaboration with topoisomerases during DNA replication, which leads to a DNA topological crisis that blocks cell cycle and reduces proliferation when mSWI/SNF complexes are inhibited[108]. However, ablation of SWI/SNF complex was demonstrated in *C. elegans* to have proliferation consequences prior entrance in S phase, indicating that the causative events on proliferation are transcriptional, or at least non-related to DNA replication[884]. Moreover our results in neuroblastoma cells showed

a decrease in the proportion of cells at S phase after disruption of the complex. In addition, we were able to attribute the anti-proliferative effects to only one complex subtype, BAF complexes, and the main difference among these variants is their genomic occupancy and the consequent controlled transcriptional network. Altogether, we considered most likely that reduction in proliferation was related to a transcriptome regulatory event rather than to replicative stress. Indeed, the clear modulation of a key cell cycle regulators such as CCND1, with relevant implication in neuroblastoma proliferative capacities, reinforced these considerations.

5.3. **BAF control of mesenchymal genes: a link to neural crest development**

Epithelial-mesenchymal transition (EMT) comprises a series of inter- and intracellular reversible changes that include a decrease in cell-cell adhesion and an increase of motility and affinity for and invasion through extracellular matrix (ECM), regulated at the molecular level by an intricate network of cross-talking pathways in response to internal and external stimuli ending in a specific transcriptional program mainly controlled by the Snail proteins SNAI1, SNAI2 and SNAI3 [838–841]. EMT is important for the correct completion of normal embryonic development at different stages, but it has been also widely demonstrated to be a relevant process for cancer progression, since numerous EMT-related mechanisms have been reported to be essential for the invasiveness and metastasis initiation of many cancer types[843,844]. Remarkably, increasing evidence is showing the implication of epigenetic regulation in these transcriptional events occurring during EMT, with special detail on histone marks. For example, the methylation status of histone H3 on lysine 4, a mark of bivalent chromatin, cooperates in the transcriptional regulation by SNAI proteins, which fits in the quick and reversible changes observed in EMT[901,902]. However, its effects at the level of chromatin remodeling have not been fully investigated, although some functions on invasiveness and regulation of some EMT proteins have been described for CHD chromatin remodelers[902].

An important developmental point in which EMT is crucial is the formation of neural crest, composed of mesenchymal cells, from epithelial cells of the neural tube. The mesenchymal cells of the neural crest have high migration capacities that allow them populate a great variety of tissues along the organism while completing their differentiation process. Neuroblastoma cells are thought to arise from these mesenchymal neural crest cells that at different developmental

points fail to complete their differentiation process into fully differentiated adrenergic cells[711]. This may be the developmental explanation for the recent epigenetic-based classification of neuroblastoma cells into adrenergic or mesenchymal cell lineages, with more or less undifferentiated phenotypes, respectively. In fact, the mesenchymal neuroblastoma transcriptional signature shows high similarity to that of neural crest cells, and shares many genes with the classical EMT regulators[58]. Moreover, adrenergic to mesenchymal transition have been reported in some scenarios, regulated by known pathways (i.e., Notch, Wnt, SWI/SNF mutations)[540,845,846], suggesting a putative regression of partially differentiated adrenergic neuroblastoma cells back to more mesenchymal undifferentiated states in response to determined oncogenic inputs. Interestingly, the different transcriptional signature between mesenchymal and adrenergic phenotype was found to be related to different super-enhancers controlling part of the cell type-specific genes, and mesenchymal phenotype super-enhancers as well as the associated transcriptional circuit also had great coincidence with those of neural crest cells[58,772]. This suggests an important epigenetic factor regulating these two phenotypes and probably the transition between them; moreover, the differential super-enhancers have been associated to different chromatin accessibility states related to the expression control by mesenchymal or adrenergic-specific transcription factors[772], strongly suggesting that chromatin remodeling events are involved in these epigenetic events and are probably relevant for the functional execution of the gene activation effects of these super-enhancers.

The results presented in this thesis suggest that the functional executor of chromatin remodeling events that link the epigenetic signals (i.e., histone acetylation) of neuroblastoma mesenchymal super-enhancers to the binding of specific transcription factors and activation of downstream genes might be the BAF chromatin remodeling complex. Upon specific disruption of this mSWI/SNF subtype, one of the top downregulated gene signatures observed in the transcriptomic profile of neuroblastoma cells was that corresponding to EMT hallmark. Since EMT is strictly not plausible in neuroblastoma cells, we tested our results with the neuroblastoma-specific homologous mechanism, and checked the behavior of the mesenchymal transcriptional signature, previously established by transcriptional comparison of mesenchymal neuroblastoma cell lines against cell lines of adrenergic phenotype[58], and a significant downregulation of this signature was also observed. Moreover, transcriptional repression of key elements of this signature, also relevant for EMT processes in other cancers,

was observed. Among them, relevant neuroblastoma-mesenchymal hallmark genes such as *SNAI2*, *CDH11* and *LOXL2* caught our attention.

SNAI2, also known as Slug, is one of the master transcriptional regulators involved in the transcriptional programming of mesenchymal phenotypes. Interestingly, SNAI2 is relevant for the EMT process that marks the initiation of neural crest formation. Its inhibition has been reported to impair the proper development of this embryonal structure, as well as to block the migration capacities of neural crest-derived cells and the proper development of the derived tissues in *Xenopus tropicalis*[903,904] and chick embryos[905]. Moreover, SNAI2 expression is silenced during the process of neural crest cells migration and differentiation[906]. Although this relevance in initial steps of neural crest formation was not observed in mouse embryos[907], specific expression of SNAI2 in mesenchymal cells of neural-crest origin is detected during mouse development[908]. What is more interesting, SNAI2 expression in neuroblastoma cells has been associated to the maintenance of an undifferentiated phenotype and to the resistance to treatment with RA, and its downstream transcriptional signature correlates with poor prognosis in neuroblastoma patient samples[909], findings that reflect the developmental origin of neuroblastoma cells, which aberrantly retain the expression neural crest mesenchymal factors that facilitate the blockade of differentiation and maintenance of migratory traits.

On the other side, a similar role has been reported for cadherin 11 (CDH11), also known as osteoblast (OB) cadherin, one of the neuroblastoma mesenchymal signatures hallmarks, in the process of neural crest formation[910]. CDH11 is relevant for the loss of cell-cell adhesion needed during the initial EMT process leading to delamination of neural crest precursors from the neural tube[855], as well as for collective and directed migration of neural crest-derived cells[911]. CDH11 expression not only reduces cell-cell interactions, but also binds to components of the extracellular matrix, an interaction relevant for cell migration[912]. Oncogenic properties of this transmembrane protein in multiple different tumor types such as gastric, pancreatic or oral cancers[913–915] have been reported, including the potentiation of invasiveness and migratory capacities, but also the interaction with microenvironment and with the immune system. In the case of CDH11, however, no functional evidence of oncogenic functions have been reported yet in neuroblastoma.

The transcriptomic profile of neuroblastoma cells after BAF depletion shows a significant reduction in the mRNA levels of both *SNAI2* and *CDH11*, but we could not corroborate these

results at the protein levels because of the impossibility of detection of basal levels of these two proteins by our means of protein expression analysis (i.e., western blot). The reason of this might be either a technical question regarding the convenience of the used lysis buffer, the adequacy of western blot procedures for these proteins, or the performance of the primary antibodies; or real basal low levels, or total silencing, of these two proteins in the two neuroblastoma cell lines tested. For CDH11, previous works observed expression in all neuroblastoma cell lines tested[916], suggesting a probable technical issue in our experimental set. Nevertheless, the regulation at the transcriptional level of these genes, which are modulated by mesenchymal-associated super-enhancers, reveals a plausible relevant regulation of these key mesenchymal regulators through BAF complex that may be conserved among different neuroblastoma cell lines and tumors, independently of the final expression pattern of these two proteins, which depend on other layers of epigenetic control at the promoter, and of post-transcriptional and post-translational regulation, that may vary among neuroblastoma cases.

Nevertheless, we did corroborated the reduction in the protein expression of the mesenchymal regulator LOXL2, which was previously reported at the transcriptional level. LOXL2 is a lysine oxidase that plays an important role in EMT by acting as an extracellular matrix remodeler, but also as an epigenetic regulator that cooperates in the determination of mesenchymal transcriptional programs[847,848]. Relevant LOXL2 functions in EMT and related processes such as metastatic spreading have been widely reported in breast cancer[917,918], and LOXL2 inhibitors have been recently developed and proposed as therapeutic agents for these kind of gynecological malignancies[919]. Moreover, its role as epigenetic regulator has also been proved to have oncogenic relevance in these type of tumors[920]. Nevertheless, LOXL2 has not yet been implicated either in the regular EMT process during neural crest development, or in the oncogenic properties of neuroblastoma cells. However, this protein is also one of the neuroblastoma mesenchymal signature genes[58], and our western blot analyses confirmed its down-regulation only in SK-N-BE(2) cells. In SH-SY5Y cells, the other neuroblastoma cell line used in the experiments of this thesis, no basal expression was observed, in full concordance with the fact that this one is a paradigmatic adrenergic cell line. SK-N-BE(2), however, have a more ambiguous phenotype. Although in the initial classification of neuroblastoma cell lines, SK-N-BE(2)-C cell line, which is derived from SK-N-BE(2), was classified into the adrenergic lineage on the base of its transcriptional profile[58], the difference between mesenchymal and adrenergic lineages is a continuum with intermediate states between the pure adrenergic and

mesenchymal edges. This may be a reflection of the continuous, and not discrete, nature of the EMT and subsequent differentiation processes that neural crest cells undergo during development, which may derive in different degrees of differentiation in the resulting neuroblastomas, and therefore, in different combinations of mesenchymal or adrenergic markers, depending on the case. Our results prove that one relevant mesenchymal marker, LOXL2, is highly expressed in a neuroblastoma cell line previously classified as adrenergic, and is repressed after BAF depletion, suggesting a plausible mechanism of epigenetic regulation through distal *cis* elements by these chromatin remodeler on mesenchymal phenotype markers.

Altogether these results reveal a clear modulation of neuroblastoma mesenchymal genes after BAF depletion that could be explained by the action of this chromatin remodeler at the super-enhancers of these genes, by translating epigenetic signals into active chromatin states. This regulation could be exploited for the therapeutic transcriptional repression of these genes, when expressed, on multiple neuroblastoma cells, not only those purely mesenchymal, for the reversion of the highly invasive and resistant neuroblastoma mesenchymal phenotype.

5.4. **BAF complex links chromatin remodeling and metastasis in neuroblastoma**

Metastatic spreading is one of the major challenges in the clinical management of neuroblastoma patients. Widespread systemic dispersion mainly to bone marrow, bone and liver is presented in M and MS stages of the disease, determining the symptomatology and prognosis of these patients. While MS neuroblastomas undergo spontaneous regression by massive cell death and/or differentiation, M stage neuroblastomas represent a vast majority (~90%) of newly diagnosed high-risk cases, and >70% of relapsed cases, whose 5-year survival rate drops to dramatic levels below 20%[761,921]. Therefore, the study of the molecular mechanisms that allow neuroblastoma cells to migrate, invade and survive in the blood stream, as well as to colonize, adapt to and populate each metastatic niche, is essential for the development of new therapeutic strategies against the formation and progression of metastasis, and thus for the improvement of the survival rate of high-risk metastatic neuroblastoma patients.

Among the downregulated mesenchymal genes in SK-N-BE(2) cells after BAF disruption, two genes, *ITGAV* and *ITGA4*, belonged to the gene family of integrins. This family of ECM-binding transmembrane proteins caught our attention due to their proved special relevance in several

cancer types for processes that involve interaction with the ECM such as migration and invasion, which are crucial in multiple steps of the metastatic process[861]. On the cytoplasmic membrane, integrins form dimers, which are composed by one subunit of each of the two existing subfamilies, integrins α and β. These integrin dimers act as sensors of external stimuli and transducers of signals into the cells, but also as mechanical effectors through adhesion to multiple ECM components, such as collagen, fibronectin, vitronectin or laminin[861]. In neuroblastoma, implication of integrins in processes relevant for metastasis has been described. For example, integrin β1, one of the most abundant subunits and present in the majority of integrin dimers, has been shown to confer different oncogenic properties to neuroblastoma cells, mostly related to migratory capacities[922,923]. Similar roles in metastatic neuroblastoma have been attributed to other integrins, such as integrin α4[924]. In fact, downstream integrin signaling mediated by the focal adhesion kinase (FAK) has been reported to be critical for the metastasis of neuroblastoma cells to the liver[925], suggesting a generalized dependency of neuroblastoma cells on these group of proteins, and its activation through binding to ECM ligands, for the metastatic process.

Nevertheless, other studies have reported anti-oncogenic functions of certain integrins in neuroblastoma cells, mostly related to the differentiation process, such as de necessity of integrin β1 for proper RA-induced differentiation and neurite outgrowth[926], or the anti-invasiveness effects of integrin α1[927]. This multi-functional nature is probably the consequence of the high number and heterogeneity of members of this family, which gets more complicated when the multiple different ligands of the ECM come into play. For example, collagen is an ECM component for which neuroblastoma cells have high integrin-mediated affinity[928], and this interaction, through integrins α1, α3, αv, β1 and β3 has been demonstrated to be crucial for neuroblastoma cells to avoid the apoptotic cell death stimulated by non-adherent conditions[929]. On the other side, binding to vitronectin through integrin αv promoted a decrease in proliferation[930], and the interaction to this same ECM component through αvβ5 dimers is essential for RA-induced differentiation[931]. These multiple roles are probably the reflection of the implication of integrins in the proper developmental steps that involve interaction with ECM during development of neural crest-derived tissues, including migration and differentiation.

The transcriptomic analyses presented in this thesis show that, after BAF disruption, 11 out of the 26 human integrins were significantly downregulated at the transcriptional level in SK-N-

BE(2) cells, and a generalized repression of genes related the integrin mediated signaling pathway was observed by means of gene set enrichment analysis, indicating functional downstream consequences of the repression of this gene family (Figure 29). The rest of the family, although non-significantly modulated under the restrictive statistical parameters used in our analyses, showed a tendency to a decreased expression, and only 4 members were overexpressed (Figure 29B). We validated at the protein level the top two modulated integrins after BAF disruption, integrins α9 (ITGA9) and β3 (ITGB3), which were expressed in SK-N-BE(2) cells, but also in the adrenergic SH-SY5Y cell line, and confirmed the strong repression of these two proteins in both neuroblastoma cell lines. These results led us to hypothesize that BAF complex may act as a putative master transcriptional regulator of adhesion surface proteins through chromatin remodeling at their *cis* regulatory elements.

When testing the functional consequences of this repressive event, BAF disruption exerted a marked decrease in the affinity of both neuroblastoma cell lines for collagen, an important neuroblastoma integrin ligand. This loss of affinity was concomitant with a reduction of the capacity of both cell lines to invade and migrate through a collagen matrix *in vitro*, and with a clear reduction in the formation of stress fibers, actin structures crucial for cell migration[866]. Although further analyses will corroborate or discard the putative contribution of integrin repression to these phenotypic effects, it served us as a starting point to extend our investigations beyond the anti-proliferative effects of BAF disruption, and to assess its phenotypic effects related to the metastatic process.

Indeed, whether through integrin repression or not, the results of *in vivo* metastatic models presented in this thesis show that BAF disruption in neuroblastoma cells represses metastatic formation and progression, widely extending the survival of mice. When focusing at the early events of metastasis, BAF disruption reduced the arrival and colonization of neuroblastoma cells to liver, in concordance with the strong phenotypic effects previously shown *in vitro*. Although the growth suppression of the macrometastases in the long term metastatic mouse model presented in Figure 31 could be explained only by the abrupt cell cycle G_1 arrest promoted by BAF disruption in neuroblastoma cells, the results presented in the short term metastatic model shown in Figure 32 suggest that there is a strong decrease in the invasion and early colonization of the liver by neuroblastoma cells. This decline, of about a 10-fold decrease, in the number of neuroblastoma cells detected at day 4 after injection cannot be explained by differences in

proliferation at this time point, since flow cytometry proliferation tracing showed small and non-significant differences between both conditions in the retention of the tracing dye at this time point. After 7 days, a marked increase in the numbers of cells from the control group, concomitant with a strong decrease in the proliferation marker, magnified the difference with BAF-disrupted cells, whose detection did not increase at this time point, and even dropped to derisory numbers of events. These results strongly suggest a combinatorial effect of decreased initial invasion and colonization, with a posterior strong cell cycle blockage that amplifies the initial differences, resulting in a clear reduction in the initiation and progression of liver and bone marrow metastasis, materialized in the long term survival extension of mice as shown in Figure 31.

Altogether, these results highlight the importance of BAF complex structural integrity in the initiation and progression of the neuroblastoma metastatic process, probably through the wide modulation at the transcriptional level of integrins, among other metastasis-related genes. Indeed, the possible future validation of the BAF complex as a master transcriptional regulator of the gene family of integrins could be exploited as a therapeutic opportunity to perform a general targeting of this metastasis-relevant group of proteins through its transcriptional repression by epigenetic reprograming. In fact, pharmacological inhibition of different integrins have been proposed and tested for the treatment of neuroblastoma, such as integrin avβ3 dimers inhibitors[932,933], both subunits showing a clear downregulation in neuroblastoma cells after BAF disruption. This reinforces the appealing of a pharmacological transcriptional repression of these set of genes, further complemented with other anti-tumor effects such as the cell cycle arrest, through BAF complex structural disruption, for the treatment of metastatic neuroblastoma.

5.5. **Pharmacological BAF disruptors for the treatment of neuroblastoma**

The phenotypic effects observed in neuroblastoma cells after BAF structural disruption suggest a potential therapeutic intervention for the transcriptional modulation of both, cell cycle and metastasis-related genes especially relevant in neuroblastoma. Nevertheless, the molecular tools mainly used in this thesis to interrupt the assembly of this chromatin remodeler complex (i.e., shRNA and siRNA), although essential and useful for the proof of concept of its therapeutic

potential in *in vitro* and *in vivo* neuroblastoma models, have very few options to be tested and used as therapeutic agents in the real clinical practice in a reasonable near future. Therefore, if the therapeutic potential of BAF structural destabilization was to be translated into preclinical and clinical settings in a short or middle term, the discovery or development of pharmacological small molecules that mimic the effects of our molecular biology tools on BAF complex is essential.

Regrettably, as explained in the introduction, the current available mSWI/SNF inhibitors mainly act by inhibiting the activity of certain functions related to specific domains contained in a subset of subunits, such as bromodomain or ATPase inhibitors, which probably would not have the expected effects on the base of the ATPase-independent features of the neuroblastoma-relevant BAF complex roles discovered in this thesis. Different PROTAC degraders have also been developed, but these molecules only target specific subunits, and do not promote a structural disruption of the complex, essential to achieve the desired phenotypic effects, also shown by our results.

To this date, no small molecules discovered or designed for producing a structural disruption of any of the human mSWI/SNF complex have been reported. The publication in 2020 of two different high resolution electronic microscopy tridimensional structures of human BAF complexes, however, was a turning point in this sense, since these studies validated and deeply detailed the tangle of intra-complex interactions formed between the subunits of this complex. These interactions, on the base of the stepwise sequential and specific incorporation of subunits inherent of the assembly process, are crucial for the proper final formation of the three mSWI/SNF complex subtypes. Indeed, blocking one of these interactions should have many chances of impairing the assembly sequence, since the incorporation of a specific subunit would be inhibited, impeding the binding of the subsequent subunits and the completion of the full assembly.

The relevance of protein-protein interactions in the structural formation of BAF complex led us to think that identifying small molecules able to inhibit interactions of ARID1A and ARID1B subunits, which we validated to be structural keys of this subcomplex, with other members of the complex, impeding the correct incorporation of these subunits into the forming complex, should impede the posterior assembly of the rest of the BAF complex subunits, mimicking the structural effects obtained when silencing both proteins with molecular biology tools (Figure

39). Indeed, ARID1A and ARID1B have been proposed, on the base of strong evidence coming from crosslink-mass spectrometry and tridimensional molecular structure determination, as relevant structural scaffolds that accumulate an important proportion of intra-complex protein-protein interactions in its C-terminal domain, concretely in what have been called ARM domains. For these reasons, we decided to explore the druggability potential of ARID1A and ARID1B surfaces for the identification of druggable pockets located at protein-protein interaction sites, for the posterior discovery of candidate molecules able to bind to those pockets and inhibit the corresponding interactions.

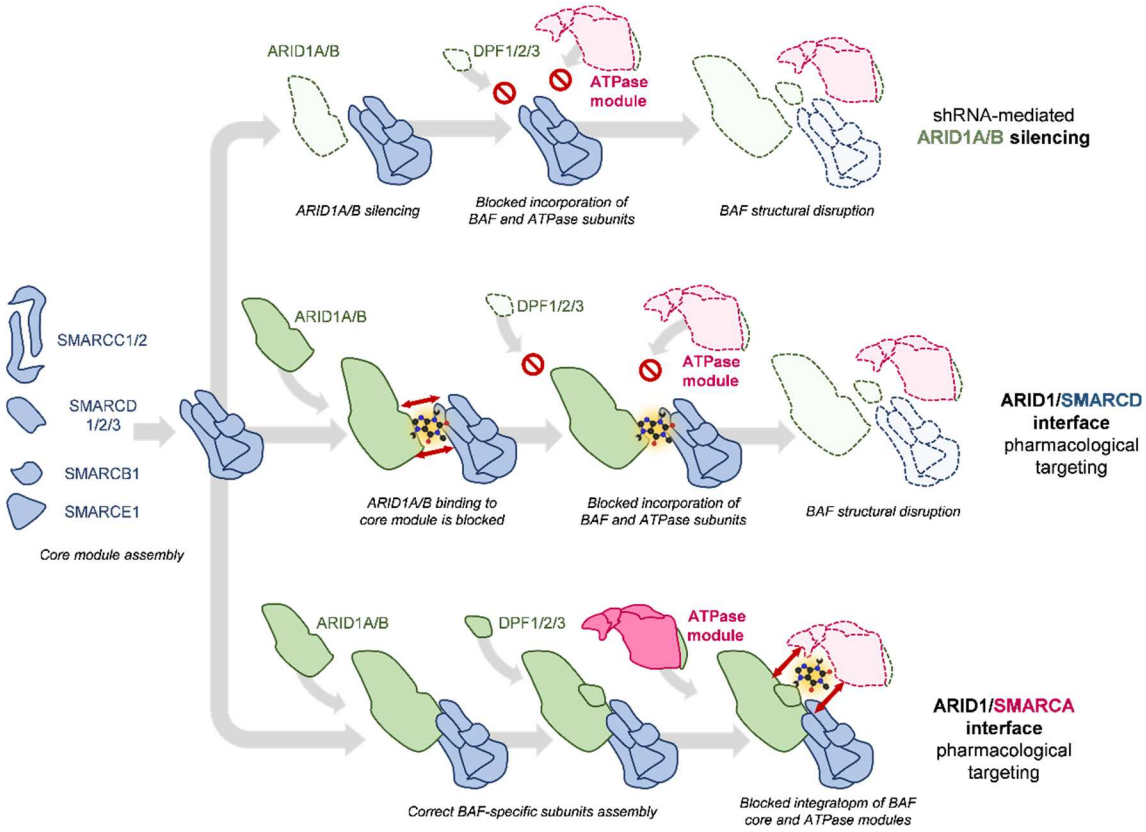

Figure 39: Hypothesized mechanisms of action on the BAF complex assembly process of ARID1/SMARCD and ARID1/SMARCA interfaces-directed BAF disruptor candidates (BDC), in comparison with the shRNA-mediated silencing of ARID1A and ARID1B subunits.

These druggability analysis and high-throughput virtual screening were performed on the tridimensional structure of ARID1A, which was the only ARID1 paralogue family member with available tridimensional structural information inside the complex, since it was the one contained in the reconstituted nucleosome-bound human BAF complex used for the determination of 6LTJ structure. However, as detailed by our transcriptomic analysis comparing single and combined silencing of these two paralogues, the inhibition of both ARID1A and ARID1B has synergistic effects on the modulation of the BAF transcriptomic program in neuroblastoma cells, which is only fully achieved when both proteins are simultaneously silenced. We assumed that small molecules targeting only one of these two subunits would have the same effect of the single silencing with molecular biology tools. Therefore, we analyzed the level of similarity between these two proteins in order to predict the reproducibility of the results obtained from ARID1A structure in ARID1B. The high sequence homology that ARID1A and ARID1B present, which is magnified in the C-terminal fragment, and maximized in the ARM domains, assured us that performing these analyses only in ARID1A would have high probabilities that the results were applicable to its paralogous counterpart ARID1B. Indeed, the amino acids involved in the two pockets used for high-throughput virtual screening of candidate small molecules were conserved among both proteins, maximizing the chances of the desired double targeting through these potential disrupting molecules.

In silico analyses of BAF-contained ARID1A structure identified two potentially druggable pockets on its surface coincident with surfaces of interaction with other BAF subunits: SMARCD1 and SMARCA4/BRG1, respectively. SMARCD1, together with its mutually exclusive and highly similar paralogues SMARCD2 and SMARCD3, belongs to the initial core module of the complex, and this interaction might represent an anchorage point of ARID1A/B relevant for the incorporation of these initial BAF-specific subunits into the shared initially assembled core modules, and therefore for the determination of the BAF-complex assembly branch and subsequent incorporation of the specific BAF subunits, including DPF2, and complete formation of these complex subtype. On the other side, an interaction between ARID1A/B and SMARCA4/BRG1, and probably its paralogue SMARCA2/BRM, has more chances of having structural relevance on other steps of the BAF assembly branch, concretely in the final incorporation of the ATPase module into partially formed BAF complexes (Figure 39). These considerations led us to think that the ARID1/SMARCD interface pocket would have more chances of reproducing the effects of ARID1A/B shRNA-mediated silencing, making it a more

promising druggable site for the structural disruption of the BAF complex. On the other side, inhibiting the interaction of already assembled ARID1A/B with SMARCA ATPases, rather than having these structural effects, would probably inhibit the integration of BAF-specific core module with the ATPase module, and effect with high probabilities of having similar effects as the ATPase PROTAC degrader ACBI1, which we validated to not be sufficient for neither structurally destabilizing the complex, nor for exerting anti-proliferative effects on neuroblastoma cells. Nevertheless, we performed the virtual screening of small molecules using both pockets in order to maximize the discovery performance of our approach.

Indeed, the most promising molecule in this preliminary analysis of BAF disruptor candidates, with strongest effect on proliferation and showing hints of BAF complex structural destabilization, called BDC-D07, was identified on the ARID1/SMARCD interface pocket screening. Nevertheless, the initial functional screening of these molecules presented in this thesis represents only a starting point for the development of first-in-class structural disruptors of the BAF chromatin remodeling complex. Our approach showed that only relatively high concentrations (i.e., a single dose of 50 µM for 96 hours) had effects on proliferation, with half inhibitory concentrations on the same range of concentrations for five different neuroblastoma cell lines in the case of BDC-D07. Although some clues of on-target effects for this compounds can be inferred from the reduction at the protein level of different BAF complex subunits, off-target effects cannot be ignored. Indeed, further characterization of this compound on healthy cells such as fibroblasts, and on BAF-independent cell lines from other origins, will be performed to check its toxicity and specificity profiles. Moreover, this first high-throughput screening has been performed for the identification of small molecule structures that serve as starting point for the generation of derived molecular families rationally refined from a structural chemistry point of view, generated by manually examination of the interaction of these molecules with the corresponding pockets, to increase binding efficacy and specificity. For this, future collaboration with research groups specialized in pharmacological chemistry will be essential.

On the other side, the functional screening design on neuroblastoma cultured cells may represent a too restrictive filter for these molecules. Some chemically promising candidates able to bind the desired target and block the corresponding interaction might have been gone unnoticed because of low chemical stability on the culture medium; low penetrance into neuroblastoma cells through the plasmatic membrane, or into the nucleus through the nuclear

envelope; or low chemical stability on the intra-cellular environment, among other possible explanations. Therefore, we are not discarding the initial list of candidate molecule and aim at performing an alternative *in vitro* screening with purified BAF complexes and some type of structural stability reporter, based, for instance, on fluorescence-based protein-protein interaction detection methods, such as fluorescence resonance energy transfer (FRET), a system that has already been successfully used in similar *in vitro* protein-protein interaction screenings[934–936].

Altogether, the initial results presented in this thesis for the identification of a BAF disruptor candidate able to reproduce the BAF-specific structural destabilization achieved by ARID1A and ARID1B combined silencing, represent an encouraging first step in a new whole research line in our group. Taking advantage of the knowledge generated by this thesis, the further development of BAF disrupting small molecules, will not only putatively represent a plausible option for the treatment of neuroblastoma, but also an unprecedented strategy of BAF inhibition through structural destabilization that will be helpful in the general study of this chromatin remodeling on basic and applied research.

5.6. **Potential toxicities and undesired effects of a BAF-targeted therapy**

We cannot ignore the possible toxic effects of inhibiting an epigenetic regulator of such developmental relevance as the BAF chromatin remodeling complex for the treatment of a pediatric disease. As explained in detail in the introduction, the importance of mSWI/SNF complexes on embryonal development rely on their cooperation in the functional execution and maintenance of lineage-specific transcriptional programs. Mouse models have shown that knockout of mSWI/SNF key subunits such as BRG1 exert pre-implantation lethalities, due to the relevant pluripotency maintenance of the specific variant of the complex called esBAF[218,586], but also other complex variants such as ncBAF[248]. Nevertheless, it has also been demonstrated that this essentiality is maximum in these extremely initial developmental steps, and becomes less accentuated in more committed and differentiated cell lineages, such as fibroblasts, the proliferation of which is not affected by the status of the mSWI/SNF complex[218]. For example, studies of the oncogenic effects of BRG1 in acute myeloid leukemia have shown that only neoplastic cells depend on the activity of the mSWI/SNF complex, while healthy bone marrow

progenitors do not[617], suggesting an specific dependency of cancer cells on the activity of this chromatin remodeler, at least in this scenario.

Nevertheless, we do not forget the massive amounts of data supporting a tumor suppressive role of these complex in multiple human cancers. Although it is mainly described by the presence of inactivating mutations only in one paralogue, which could be compensated by the replacement of the remaining counterpart, different functional evidence suggests an initiating role of the loss of mSWI/SNF activity in different tumors. For example, a recent report showed that ARID1A and ARID1B double knockout in mice promoted tumorigenesis in skin, liver and endometrium, raising the cautions regarding the BAF-directed cancer therapies aimed at exploiting the intra-complex synthetic lethalities identified between different pairs of mSWI/SNF proteins[826]. Nevertheless, the functional differences between the completely and irreversible genetic ablation of two genes and the temporal and reversible pharmacological binding inhibition of their corresponding coding proteins are evident. Indeed, a point in favor of a small-molecule protein-protein interaction inhibition-based BAF structural disruption therapeutic strategy would be the reversibility of the effects on the possible affected healthy tissues, since these molecules are initially designed and thought to bind the desired pockets through electrostatic interactions.

However, these issues and concerns must be addressed by further validation studies of the potential toxicities on healthy cells *in vitro* and on animal models. Indeed, dealing with side effects is a day-to-day challenge in cancer therapy research, and multiple research lines are focused on the generation of strategies that help in the minimization of these toxicities. For example, the encapsulation of drugs into nanoparticles, which serve to improve the distribution, stability and efficacy of the encapsulated agent, may also help to reduce the delivery of a BAF disruptor molecule into undesired healthy tissues if the containing nanoparticles are specifically directed to neuroblastoma cells, for example by decoration with antibodies or binding peptides against neuroblastoma specific surfaces markers.

Another way to overcome possible undesired toxicities on healthy cells and tissues of a BAF-disruption therapy for neuroblastoma treatment would be the administration by intratumoral injection of the hypothetical inhibitor, a strategy that has been recently adopted for reducing the systemic secondary effects of immunotherapies[937]. This type of administrations are usually not much pragmatic in general cancer treatment, since surgical resection of primary tumors is

often the first step, and in these cases, intratumoral injection of chemotherapy or targeted therapies are only possible in unresectable cases. However, in the case of high-risk neuroblastoma, patients are mainly treated with cycles of induction therapy prior surgical resection, opening a plausible therapeutic window for the intratumoral administration of a BAF-targeted therapy that would ideally induce a reduction in the growth of the primary tumor, but also of the metastatic capacities of neuroblastoma cells, before the surgical removal of the primary tumor.

To sum up, if a BAF complex-directed therapeutic strategy is to be developed for the treatment of high-risk metastatic neuroblastoma, the possible detrimental effects of BAF structural disruption must be assessed in healthy cells and tissues by means of standard preclinical toxicity analyses to assure the safety of the patients. However, multiple strategies should be tested to overcome these undesired effects, if detected, in order to exploit the potential benefits of this epigenetic therapy.

5.7. **Fitting together the paradoxical roles of ARID1A/B in neuroblastoma**

While previous studies on the ATPase subunit SMARCA4/BRG1 suggested oncogenic functions of the mSWI/SNF complex in neuroblastoma[630], functional evidence of tumor and metastasis suppressive roles have also been attributed to ARID1A in neuroblastoma in different studies[540,542], in addition to the recurrent inactivating mutations reported for these two genes in neuroblastoma[537,538]. However, although initially contradictory, the existence of this kind of discrepancies can be explained by paying attention to the structural and functional nature of the complex. As repeatedly explained, ARID1A and ARID1B are mutually exclusive paralogues with highly overlapping and redundant functions. This concrete feature was validated at the transcriptomic level by the results presented in this thesis, although a minority of genes seemed to be preferentially controlled by ARID1A or ARID1B-containing BAF complexes, respectively (Figure 24). The loss of one of these two subunits is structurally replaced by the other one, not generating a full disruption of the complex, as demonstrated by our results, but also by Shi and colleagues[540], who reported that after ARID1A depletion, ARID1B-complexes were structurally intact. Indeed, this study confirmed the intra-complex synthetic lethality already assessed between ARID1B and ARID1A in other tumors: ARID1B was essential for the proper proliferation

of ARID1A-mutated neuroblastoma cell lines. This, in addition to the detrimental effects produced by the simultaneous inhibition of ARID1A and ARID1B presented in this thesis, suggest a model in which the loss of one of these paralogues in neuroblastoma through recurrent mutations is structurally compensated by the remaining one, whereas the combined silencing uncovers a global transcriptional modulation that goes unnoticed when only inhibiting one.

Nevertheless, how this loss of ARID1A, compensated at the structural level through ARID1B replacement, provides neuroblastoma cells of novel oncogenic properties is an intriguing question, but hypotheses can be formulated from some pieces of evidence. On the one hand, Shi and colleagues[540] reported that ARID1A homozygous knockout altered the genomic occupancy of BAF complex by weakening some of its binding sites but strengthening many others, indicating a change in chromatin occupancy rather than a functional mSWI/SNF inhibition. Indeed, ARID1A depletion had similar effects on PBAF complexes, by general repositioning of the ARID2 subunits. Being ARID1A a BAF exclusive subunit, these findings suggest a subunit stoichiometry decompensation after ARID1A loss with oncogenic genome-wide repositioning consequences. On the other side, our results on ARID1A and ARID1B silencing show that the single silencing of either of the two produced an increase in the protein levels of the other ones (Figure 21), in a similar way as the interplay reported between BRG1 and BRM homologues when silencing the first one (Figure 38). We again attributed this compensation event to the stoichiometric regulation of mSWI/SNF subunit levels, meaning that the loss of competition between both paralogues for joining to the other subunits when one of them is depleted increases the amount of complexes containing the remaining one, raising its stability and therefore its total protein levels.

One possible consequence of this structural event would be an overcompensation effect on the genes preferentially controlled by the remaining subunit. If, for example, genes preferentially controlled by ARID1B-containing complexes were directly related to the metastatic potential of neuroblastoma cells, loss of ARID1A leading to an increase of ARID1B-containing complexes would probably lead to a higher activity of the BAF complex on the promoter or enhancers of these genes, maybe potentiating their expression and conferring reinforced metastatic or other oncogenic features to these cells. In addition, the total disruption of the complex by the inhibition of ARID1B in this scenario would totally block the expression of this ARID1B-preferential genes, but also of the shared ARID1A/B-controlled genes, which we demonstrated

to be the main group of BAF-controlled genes in neuroblastoma and to have relevant oncogenic features (Figures 24 and 25).

One loose end that can be extracted from our results is the fact that single inhibition of either ARID1A or ARID1B had partial effects on proliferation, although the full phenotypic effects were only observed after the combined silencing. This might be indicating that ARID1A and ARID1B have specific and non-redundant relevant functions on neuroblastoma cell lines affecting at least their proliferative capacity. However, this would contradict the already mentioned oncogenic capacities acquired when solely inhibiting ARID1A reported before[540,542]. However, an alternative explanation is that the functional compensation and rescue of the detrimental proliferative effects related to BAF complex functions in neuroblastoma is not immediate and requires the time that it takes the remaining subunit, whether ARID1A or ARID1B, to incorporate into new complexes and stabilize the released subunits that were previously forming the complex containing the silenced subunit, before re-stabilizing the transcriptional program controlled by BAF complex in neuroblastoma cells. In this period of time, before the full replacement of subunits, effects on proliferation might be already manifested and accumulated during the time course of our proliferation assays, explaining the partial reduction in proliferation observed after single ARID1A or ARID1B silencing (Figure 21). Further experiments of single subunit silencing with long term transduced cells, to allow the full replacement and stabilization of new BAF complexes will demonstrate or refute this hypothesis.

In any case, the model proposed here is fairly interesting, since it would help to explain and reconcile the contradictory evidences regarding the function of mSWI/SNF complexes observed in cancer in general. Moreover, it would prove that a therapeutic strategy targeting the structural integrity of the BAF complex in neuroblastoma would not only revert the gained oncogenic features obtained by enrichment of ARID1B or ARID1A remaining complexes on its preferential genes in *ARID1A* or *ARID1B* mutated tumors, respectively, but it would also affect the genes not affected by this asymmetrical overcompensation effect, which are the majority of BAF-controlled genes in neuroblastoma, and belong to relevant oncogenic processes. Indeed, this would make this therapeutic strategy appealing for the treatment not only of *ARID1A* or *ARID1B*-mutated tumors, but also for all cases of neuroblastoma, regardless of their mSWI/SNF mutational profile, expanding the therapeutic benefit of targeting the BAF complex beyond the known synthetic lethalities.

5.8. **Proposed model for the role and therapeutic potential of the BAF chromatin remodeling complex in neuroblastoma**

The results presented in this thesis support the conception that a therapeutic intervention consisting in the structural disruption of the BAF chromatin remodeling complex by blocking its assembly process by inhibiting ARID1A and ARID1B subunits, whether by gene silencing or through small molecule protein-protein interaction inhibitors that block their incorporation into the complex, would have potential benefits in the clinical management of neuroblastoma. We base our hopes on its therapeutic potential on the fact that this inhibition would epigenetically reprogram neuroblastoma cells to induce a decrease in proliferation in combination with an inhibition of metastasis formation and progression, highlighting the multi-targeted nature of epigenetic therapies exposed in the exposition of hypothesis and objectives of this thesis.

Pharmacological inhibition of cyclin D1-CDK4/6 complexes is being studied as a new therapeutic option for neuroblastoma[938] with many chances to reach the clinics. Also, the pharmacological targeting of integrin αvβ3 dimers has been very recently proposed for the treatment of neuroblastoma[932,933]. Both cyclin D1 (*CCND1*), and integrins αv and β3 (*ITGAV*, *ITGB3*) were transcriptionally repressed in neuroblastoma cells after BAF complex disruption. This reflects the benefits of a BAF-targeting therapy, in which the expression of relevant neuroblastoma therapeutic targets of interest related to different processes, such as cell cycle progression or metastasis, instead of inhibited by multiple individual molecules against each of them, would be transcriptionally repressed by the use of a unique therapeutic agent (Figure 40).

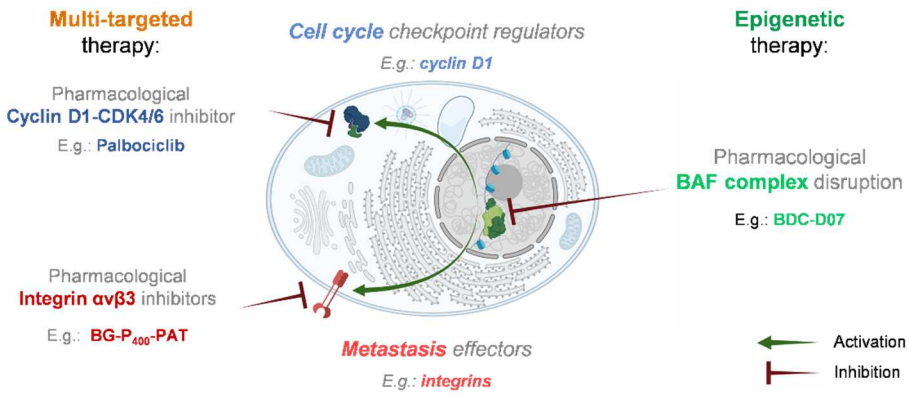

Figure 40: Proposed model for a BAF disruption-based epigenetic therapy for neuroblastoma, in contrast with a hypothetical multi-targeted therapy targeting the same signaling pathways.

6. **CONCLUSIONS**

That's all
I don't even think of you that often

Chelsea Hotel #2
Leonard Cohen
New Skin for the Old Ceremony
1974

First: Neuroblastoma cells contain the three fully assembled known mSWI/SNF chromatin remodeling complex subtypes, but only BAF complex structural integrity, and not its ATPase activity, is relevant for neuroblastoma proliferation.

Second: BAF complex structural disruption produces a wide transcriptional reprogramming in neuroblastoma cells that can only be completely achieved through the combined inhibition of its key structural subunits ARID1A and ARID1B, and not by the single inhibition of one out of these two mutually exclusive and redundant paralogues.

Third: The transcriptional reprograming produced by BAF complex structural disruption in neuroblastoma cells promotes a strong cell cycle arrest, the repression of mesenchymal phenotype genes, and a marked reduction of metastasis initiation and progression *in vivo*.

Fourth: ARID1A tridimensional structure contains two druggable pockets located at surfaces of interaction with other BAF complex subunits that can be potentially used to pharmacologically disrupt the assembly of the complex through protein-protein inhibition with small molecules, such as the candidate BDC-D07, which produces a destabilization of BAF complex subunits and reduces neuroblastoma proliferation.

Fifth: BAF complex structural disruption represents a novel strategy for the development of an epigenetic therapy for the treatment of high-risk metastatic neuroblastoma patients, which would combine in one single therapeutic agent the effects on multiple independent signaling pathways and molecular mechanisms, including cell cycle progression and metastatic invasion, through the chromatin remodeling-based epigenetic reprogramming of neuroblastoma cells.

7. **BIBLIOGRAPHY**

Forgiving who you are, for what you stand to gain
Just know that if you hide, it doesn't go away

I grieve in stereo, the stereo sounds strange
You know that if it hides, it doesn't go away

If I get out of bed, you'll see me standing all alone
Horrified on the stage, my little dark age

Little Dark Age
MGMT
Little Dark Age
2017

1. Wolpert, L. Do We Understand Development? *Science* **266**, 571–572 (1994).
2. Davidson, E. H. & Erwin, D. H. Gene Regulatory Networks and the Evolution of Animal Body Plans. *Science* **311**, 796–801 (2006).
3. Weinreb, C., Rodriguez-Fraticelli, A., Camargo, F. D. & M Klein, A. Lineage tracing on transcriptional landscapes links state to fate during differentiation. *Science* **367**, eaaw3381 (2020).
4. Gulati, G. S. *et al.* Single-cell transcriptional diversity is a hallmark of developmental potential. *Science* **367**, 405–411 (2020).
5. Kiefer, J. C. Epigenetics in Development. *Dev. Dyn.* **236**, 1144–1156 (2007).
6. Berger, S. L., Kouzarides, T., Shiekhattar, R. & Shilatifard, A. An operational definition of epigenetics. *Genes Dev.* **23**, 781–783 (2009).
7. Dillon, N. Heterochromatin structure and function. *Biol. Cell* **96**, 631–637 (2004).
8. Ahuja, N., Sharma, A. R. & Baylin, S. B. Epigenetic Therapeutics: A New Weapon in the War Against Cancer. *Annu. Rev. Med.* **67**, 73–89 (2016).
9. Hotchkiss, D. The quantitative separation of purines, pyrimidines, and nucleosides by paper chromatography. *J. Biol. Chem.* **175**, 315–332 (1948).
10. Arber, W. & Linn, S. DNA modification and restriction. *Annu. Rev. Biochem.* **38**, 467–500 (1969).
11. Bird, A. P. CpG-rich islands and the function of DNA methylation. *Nature* **321**, 209–213 (1986).
12. Holliday, R. The inheritance of epigenetic defects. *Science* **238**, 163–170 (1987).
13. Holliday, R. DNA Methylation and Epigenetic Mechanisms. *Cell Biophys.* **15**, 15–20 (1989).
14. Eden, S. & Cedar, H. Role of DNA methylation in the regulation of transcription. *Curr. Opin. Genet. Dev.* **4**, 255–259 (1994).
15. Duncan, C. G. *et al.* Dosage compensation and DNA methylation landscape of the X chromosome in mouse liver. *Sci. Rep.* **8**, 10138 (2018).
16. Wu, H. & Zhang, Y. Mechanisms and functions of Tet protein- mediated 5-methylcytosine oxidation. *Genes Dev.* **25**, 2436–2452 (2011).
17. Kornberg, R. D. Structure of chromatin. *Annu. Rev. Biochem.* **46**, 931–954 (1977).
18. Luger, K., Mäder, A. W., Richmond, R. K., Sargent, D. F. & Richmond, T. J. Crystal structure of the nucleosome core particle at 2.8 A resolution. *Nature* **389**, 251–260 (1997).
19. Piovesan, A. *et al.* On the length, weight and GC content of the human genome. *BMC Res. Notes* **12**, 106 (2019).
20. Sun, H. B., Shen, J. & Yokota, H. Size-dependent positioning of human chromosomes in interphase nuclei. *Biophys. J.* **79**, 184–190 (2000).
21. Krebs, J. E. & Peterson, C. L. Understanding 'active' chromatin: a historical perspective of chromatin remodeling. *Crit. Rev. Eukaryot. Gene Expr.* **10**, 1–12 (2000).
22. ALLFREY, V. G., FAULKNER, R. & MIRSKY, A. E. ACETYLATION AND METHYLATION OF HISTONES AND THEIR POSSIBLE ROLE IN THE REGULATION OF RNA SYNTHESIS. *Proc. Natl. Acad. Sci. U. S. A.* **51**, 786–794 (1964).
23. Pogo, B. G., Allfrey, V. G. & Mirsky, A. E. RNA synthesis and histone acetylation during the course of gene activation in lymphocytes. *Proc. Natl. Acad. Sci. U. S. A.* **55**, 805–812 (1966).
24. Sealy, L. & Chalkley, R. DNA associated with hyperacetylated histone is preferentially digested by DNase I. *Nucleic Acids Res.* **5**, 1863–1876 (1978).
25. Rice, J. C. & Allis, C. D. Histone methylation versus histone acetylation: new insights into epigenetic regulation. *Curr. Opin. Cell Biol.* **13**, 263–273 (2001).
26. Zhang, Y. & Reinberg, D. Transcription regulation by histone methylation: interplay between different covalent modifications of the core histone tails. *Genes Dev.* **15**, 2343–2360 (2001).
27. Justin, N., De Marco, V., Aasland, R. & Gamblin, S. J. Reading, writing and editing methylated lysines on histone tails: new insights from recent structural studies. *Curr. Opin. Struct. Biol.* **20**, 730–738 (2010).
28. Lavarone, E., Barbieri, C. M. & Pasini, D. Dissecting the role of H3K27 acetylation and methylation in PRC2

mediated control of cellular identity. *Nat. Commun.* **10**, 1679 (2019).

29. Kim, T. H. *et al.* A high-resolution map of active promoters in the human genome. *Nature* **436**, 876–880 (2005).
30. Bernstein, B. E. *et al.* A bivalent chromatin structure marks key developmental genes in embryonic stem cells. *Cell* **125**, 315–326 (2006).
31. Strahl, B. D. & Allis, C. D. The language of covalent histone modifications. *Nature* **403**, 41–45 (2000).
32. Turner, B. M. Histone acetylation and an epigenetic code. *Bioessays* **22**, 836–845 (2000).
33. Jenuwein, T. & Allis, C. D. Translating the histone code. *Science* **293**, 1074–1080 (2001).
34. Spicuglia, S. & Vanhille, L. Chromatin signatures of active enhancers. *Nucleus* **3**, 126–131 (2012).
35. Zhou, W., Wang, X. & Rosenfeld, M. G. Histone H2A ubiquitination in transcriptional regulation and DNA damage repair. *Int. J. Biochem. Cell Biol.* **41**, 12–15 (2009).
36. Rossetto, D., Avvakumov, N. & Côté, J. Histone phosphorylation: a chromatin modification involved in diverse nuclear events. *Epigenetics* **7**, 1098–1108 (2012).
37. Ntorla, A. & Burgoyne, J. R. The Regulation and Function of Histone Crotonylation. *Front. cell Dev. Biol.* **9**, 624914 (2021).
38. Dawson, M. A. & Kouzarides, T. Cancer epigenetics: from mechanism to therapy. *Cell* **150**, 12–27 (2012).
39. Buschbeck, M. & Hake, S. B. Variants of core histones and their roles in cell fate decisions, development and cancer. *Nat. Rev. Mol. Cell Biol.* **18**, 299–314 (2017).
40. Hsu, C.-J., Meers, O., Buschbeck, M. & Heidel, F. H. The Role of MacroH2A Histone Variants in Cancer. *Cancers (Basel).* **13**, (2021).
41. ENCODE Project Consortium. An integrated encyclopedia of DNA elements in the human genome. *Nature* **489**, 57–74 (2012).
42. Statello, L., Guo, C.-J., Chen, L.-L. & Huarte, M. Gene regulation by long non-coding RNAs and its biological functions. *Nat. Rev. Mol. Cell Biol.* **22**, 96–118 (2021).
43. Morlando, M., Ballarino, M. & Fatica, A. Long Non-Coding RNAs: New Players in Hematopoiesis and Leukemia. *Front. Med.* **2**, 23 (2015).
44. Hall, L. L. & Lawrence, J. B. The cell biology of a novel chromosomal RNA: chromosome painting by XIST/Xist RNA initiates a remodeling cascade. *Semin. Cell Dev. Biol.* **14**, 369–378 (2003).
45. Neve, B., Jonckheere, N., Vincent, A. & Van Seuningen, I. Long non-coding RNAs: the tentacles of chromatin remodeler complexes. *Cell. Mol. Life Sci.* **78**, 1139–1161 (2021).
46. Carter, S. B. Tissue homeostasis and the biological basis of cancer. *Nature* **220**, 970–974 (1968).
47. Rodríguez-Molinero, A., López-Diéguez, M. & Banegas, J. R. Tissue homeostasis and cancer. *Med. Hypotheses* **68**, 1333–1341 (2007).
48. Patel, S. A. & Vanharanta, S. Epigenetic determinants of metastasis. *Mol. Oncol.* **11**, 79–96 (2017).
49. Craddock, V. M. & Magee, P. N. Analysis of bases of rat-liver nucleic acids after administration of the carcinogen dimethylnitrosamine. *Biochem. J.* **100**, 724–732 (1966).
50. Silber, R. *et al.* Methylation of nucleic acids in normal and leukemic leukocytes. *Biochim. Biophys. Acta* **123**, 638–640 (1966).
51. Qu, G. Z., Grundy, P. E., Narayan, A. & Ehrlich, M. Frequent hypomethylation in Wilms tumors of pericentromeric DNA in chromosomes 1 and 16. *Cancer Genet. Cytogenet.* **109**, 34–39 (1999).
52. Xu, G. L. *et al.* Chromosome instability and immunodeficiency syndrome caused by mutations in a DNA methyltransferase gene. *Nature* **402**, 187–191 (1999).
53. Eden, A., Gaudet, F., Waghmare, A. & Jaenisch, R. Chromosomal instability and tumors promoted by DNA hypomethylation. *Science* **300**, 455 (2003).
54. Berman, B. P. *et al.* Regions of focal DNA hypermethylation and long-range hypomethylation in colorectal cancer coincide with nuclear lamina-associated domains. *Nat. Genet.* **44**, 40–46 (2011).
55. Feinberg, A. P. & Tycko, B. The history of cancer epigenetics. *Nature reviews. Cancer* vol. 4 143–153 (2004).

56. Chi, P., Allis, C. D. & Wang, G. G. Covalent histone modifications--miswritten, misinterpreted and mis-erased in human cancers. *Nat. Rev. Cancer* **10**, 457–469 (2010).

57. Zhao, S., Allis, C. D. & Wang, G. G. The language of chromatin modification in human cancers. *Nat. Rev. Cancer* **21**, 413–430 (2021).

58. Van Groningen, T. *et al.* Neuroblastoma is composed of two super-enhancer-associated differentiation states. *Nat. Genet.* **49**, 1261–1266 (2017).

59. Jiang, Y., Jiang, Y.-Y. & Lin, D.-C. Super-enhancer-mediated core regulatory circuitry in human cancer. *Comput. Struct. Biotechnol. J.* **19**, 2790–2795 (2021).

60. Mishra, K. & Kanduri, C. Understanding Long Noncoding RNA and Chromatin Interactions: What We Know So Far. *Non-coding RNA* **5**, (2019).

61. Tachiwana, H. & Saitoh, N. Nuclear Long Non-Coding RNAs as Epigenetic Regulators in Cancer. *Curr. Med. Chem.* **28**, 5098–5109 (2021).

62. Forbes, S. A. *et al.* COSMIC: mining complete cancer genomes in the Catalogue of Somatic Mutations in Cancer. *Nucleic Acids Res.* **39**, D945-50 (2011).

63. Gröbner, S. N. *et al.* The landscape of genomic alterations across childhood cancers. *Nature* **555**, 321–327 (2018).

64. Shekhawat, J. *et al.* Ten-eleven translocase: key regulator of the methylation landscape in cancer. *J. Cancer Res. Clin. Oncol.* **147**, 1869–1879 (2021).

65. Leonhardt, H., Page, A. W., Weier, H. U. & Bestor, T. H. A targeting sequence directs DNA methyltransferase to sites of DNA replication in mammalian nuclei. *Cell* **71**, 865–873 (1992).

66. Okano, M., Bell, D. W., Haber, D. A. & Li, E. DNA methyltransferases Dnmt3a and Dnmt3b are essential for de novo methylation and mammalian development. *Cell* **99**, 247–257 (1999).

67. Christman, J. K. 5-Azacytidine and 5-aza-2′-deoxycytidine as inhibitors of DNA methylation: mechanistic studies and their implications for cancer therapy. *Oncogene* **21**, 5483–5495 (2002).

68. Tsai, H.-C. *et al.* Transient low doses of DNA-demethylating agents exert durable antitumor effects on hematological and epithelial tumor cells. *Cancer Cell* **21**, 430–446 (2012).

69. Kaminskas, E., Farrell, A. T., Wang, Y.-C., Sridhara, R. & Pazdur, R. FDA drug approval summary: azacitidine (5-azacytidine, Vidaza) for injectable suspension. *Oncologist* **10**, 176–182 (2005).

70. Jubierre, L. *et al.* Targeting of epigenetic regulators in neuroblastoma. *Exp. Mol. Med.* **50**, 1–12 (2018).

71. Lin, H.-Y., Chen, C.-S., Lin, S.-P., Weng, J.-R. & Chen, C.-S. Targeting histone deacetylase in cancer therapy. *Med. Res. Rev.* **26**, 397–413 (2006).

72. Karagiannis, D. & Rampias, T. HDAC Inhibitors: Dissecting Mechanisms of Action to Counter Tumor Heterogeneity. *Cancers (Basel).* **13**, (2021).

73. Juergens, R. A. *et al.* Combination epigenetic therapy has efficacy in patients with refractory advanced non-small cell lung cancer. *Cancer Discov.* **1**, 598–607 (2011).

74. Brownell, J. E. & Allis, C. D. Special HATs for special occasions: linking histone acetylation to chromatin assembly and gene activation. *Curr. Opin. Genet. Dev.* **6**, 176–184 (1996).

75. Morimoto, T. *et al.* The dietary compound curcumin inhibits p300 histone acetyltransferase activity and prevents heart failure in rats. *J. Clin. Invest.* **118**, 868–878 (2008).

76. Wang, Y. *et al.* Targeting cancer epigenetic pathways with small-molecule compounds: Therapeutic efficacy and combination therapies. *Pharmacol. Res.* **173**, 105702 (2021).

77. Song, Y., Wu, F. & Wu, J. Targeting histone methylation for cancer therapy: enzymes, inhibitors, biological activity and perspectives. *J. Hematol. Oncol.* **9**, 49 (2016).

78. McLean, C. M., Karemaker, I. D. & van Leeuwen, F. The emerging roles of DOT1L in leukemia and normal development. *Leukemia* **28**, 2131–2138 (2014).

79. Dorrance, A. M. *et al.* The Mll partial tandem duplication: differential, tissue-specific activity in the presence or absence of the wild-type allele. *Blood* **112**, 2508–2511 (2008).

80. Sterling, J., Menezes, S. V, Abbassi, R. H. & Munoz, L. Histone lysine demethylases and their functions in

cancer. *Int. J. cancer* (2020) doi:10.1002/ijc.33375.

81. Shi, Y. *et al.* Histone demethylation mediated by the nuclear amine oxidase homolog LSD1. *Cell* **119**, 941–953 (2004).

82. Chang, B., Chen, Y., Zhao, Y. & Bruick, R. K. JMJD6 is a histone arginine demethylase. *Science* **318**, 444–447 (2007).

83. Fang, Y., Liao, G. & Yu, B. LSD1/KDM1A inhibitors in clinical trials: advances and prospects. *J. Hematol. Oncol.* **12**, 129 (2019).

84. Yang, G.-J., Ko, C.-N., Zhong, H.-J., Leung, C.-H. & Ma, D.-L. Structure-Based Discovery of a Selective KDM5A Inhibitor that Exhibits Anti-Cancer Activity via Inducing Cell Cycle Arrest and Senescence in Breast Cancer Cell Lines. *Cancers (Basel).* **11**, (2019).

85. Miyake, Y. *et al.* Identification of novel lysine demethylase 5-selective inhibitors by inhibitor-based fragment merging strategy. *Bioorg. Med. Chem.* **27**, 1119–1129 (2019).

86. Plch, J., Hrabeta, J. & Eckschlager, T. KDM5 demethylases and their role in cancer cell chemoresistance. *Int. J. cancer* **144**, 221–231 (2019).

87. Klose, R. J. & Bird, A. P. Genomic DNA methylation: the mark and its mediators. *Trends Biochem. Sci.* **31**, 89–97 (2006).

88. Taverna, S. D., Li, H., Ruthenburg, A. J., Allis, C. D. & Patel, D. J. How chromatin-binding modules interpret histone modifications: lessons from professional pocket pickers. *Nat. Struct. Mol. Biol.* **14**, 1025–1040 (2007).

89. Zeng, W., Ball, A. R. J. & Yokomori, K. HP1: heterochromatin binding proteins working the genome. *Epigenetics* **5**, 287–292 (2010).

90. Sanchez, R. & Zhou, M.-M. The PHD finger: a versatile epigenome reader. *Trends Biochem. Sci.* **36**, 364–372 (2011).

91. Wagner, E. K., Nath, N., Flemming, R., Feltenberger, J. B. & Denu, J. M. Identification and characterization of small molecule inhibitors of a plant homeodomain finger. *Biochemistry* **51**, 8293–8306 (2012).

92. Bhushan, B. *et al.* Investigations on small molecule inhibitors targeting the histone H3K4 tri-methyllysine binding PHD-finger of JmjC histone demethylases. *Bioorg. Med. Chem.* **26**, 2984–2991 (2018).

93. Zeng, L. *et al.* Mechanism and regulation of acetylated histone binding by the tandem PHD finger of DPF3b. *Nature* **466**, 258–262 (2010).

94. Filippakopoulos, P. & Knapp, S. The bromodomain interaction module. *FEBS Lett.* **586**, 2692–2704 (2012).

95. Boyson, S. P. *et al.* Functional Roles of Bromodomain Proteins in Cancer. *Cancers (Basel).* **13**, (2021).

96. Filippakopoulos, P. *et al.* Selective inhibition of BET bromodomains. *Nature* **468**, 1067–1073 (2010).

97. Vizán, P., Beringer, M., Ballaré, C. & Di Croce, L. Role of PRC2-associated factors in stem cells and disease. *FEBS J.* **282**, 1723–1735 (2015).

98. Clapier, C. R., Iwasa, J., Cairns, B. R. & Peterson, C. L. Mechanisms of action and regulation of ATP-dependent chromatin-remodelling complexes. *Nat. Rev. Mol. Cell Biol.* **18**, 407–422 (2017).

99. Lusser, A., Urwin, D. L. & Kadonaga, J. T. Distinct activities of CHD1 and ACF in ATP-dependent chromatin assembly. *Nat. Struct. Mol. Biol.* **12**, 160–166 (2005).

100. Reyes, A. A., Marcum, R. D. & He, Y. Structure and Function of Chromatin Remodelers. *J. Mol. Biol.* **433**, 166929 (2021).

101. Konev, A. Y. *et al.* CHD1 motor protein is required for deposition of histone variant H3.3 into chromatin in vivo. *Science* **317**, 1087–1090 (2007).

102. Murawska, M. & Brehm, A. CHD chromatin remodelers and the transcription cycle. *Transcription* **2**, 244–253 (2011).

103. Bao, Y. & Shen, X. SnapShot: Chromatin remodeling: INO80 and SWR1. *Cell* **144**, 158-158.e2 (2011).

104. Ronan, J. L., Wu, W. & Crabtree, G. R. From neural development to cognition: Unexpected roles for chromatin. *Nat. Rev. Genet.* **14**, 347–359 (2013).

105. Alfert, A., Moreno, N. & Kerl, K. The BAF complex in development and disease. *Epigenetics and Chromatin* **12**, 1–15 (2019).

106. Cenik, B. K. & Shilatifard, A. COMPASS and SWI/SNF complexes in development and disease. *Nat. Rev. Genet.* **22**, 38–58 (2021).

107. Kadoch, C. & Crabtree, G. R. Mammalian SWI/SNF chromatin remodeling complexes and cancer: Mechanistic insights gained from human genomics. *Sci. Adv.* **1**, 1–18 (2015).

108. Hodges, C., Kirkland, J. G. & Crabtree, G. R. The many roles of BAF (mSWI/SNF) and PBAF complexes in cancer. *Cold Spring Harb. Perspect. Med.* **6**, (2016).

109. Sokpor, G., Xie, Y., Rosenbusch, J. & Tuoc, T. Chromatin remodeling BAF (SWI/SNF) complexes in neural development and disorders. *Front. Mol. Neurosci.* **10**, 1–22 (2017).

110. Centore, R. C., Sandoval, G. J., Soares, L. M. M., Kadoch, C. & Chan, H. M. Mammalian SWI/SNF Chromatin Remodeling Complexes: Emerging Mechanisms and Therapeutic Strategies. *Trends Genet.* **36**, 936–950 (2020).

111. Haber, J. E. & Garvik, B. A new gene affecting the efficiency of mating-type interconversions in homothallic strains of Saccharomyces cerevisiae. *Genetics* **87**, 33–50 (1977).

112. Stern, M., Jensen, R. & Herskowitz, I. Five SWI genes are required for expression of the HO gene in yeast. *J. Mol. Biol.* **178**, 853–868 (1984).

113. Peterson, C. L., Kruger, W. & Herskowitz, I. A functional interaction between the C-terminal domain of RNA polymerase II and the negative regulator SIN1. *Cell* **64**, 1135–1143 (1991).

114. Peterson, C. L. & Herskowitz, I. Characterization of the yeast SWI1, SWI2, and SWI3 genes, which encode a global activator of transcription. *Cell* **68**, 573–583 (1992).

115. Yoshinaga, S. K., Peterson, C. L., Herskowitz, I. & Yamamoto, K. R. Roles of SWI1, SWI2, and SWI3 proteins for transcriptional enhancement by steroid receptors. *Science* **258**, 1598–1604 (1992).

116. Carlson, M., Osmond, B. C. & Botstein, D. Mutants of yeast defective in sucrose utilization. *Genetics* **98**, 25–40 (1981).

117. Neigeborn, L. & Carlson, M. Genes affecting the regulation of SUC2 gene expression by glucose repression in Saccharomyces cerevisiae. *Genetics* **108**, 845–858 (1984).

118. Abrams, E., Neigeborn, L. & Carlson, M. Molecular analysis of SNF2 and SNF5, genes required for expression of glucose-repressible genes in Saccharomyces cerevisiae. *Mol. Cell. Biol.* **6**, 3643–3651 (1986).

119. Estruch, F. & Carlson, M. SNF6 encodes a nuclear protein that is required for expression of many genes in Saccharomyces cerevisiae. *Mol. Cell. Biol.* **10**, 2544–2553 (1990).

120. Laurent, B. C., Treitel, M. A. & Carlson, M. The SNF5 protein of Saccharomyces cerevisiae is a glutamine- and proline-rich transcriptional activator that affects expression of a broad spectrum of genes. *Mol. Cell. Biol.* **10**, 5616–5625 (1990).

121. Happel, A. M., Swanson, M. S. & Winston, F. The SNF2, SNF5 and SNF6 genes are required for Ty transcription in Saccharomyces cerevisiae. *Genetics* **128**, 69–77 (1991).

122. Laurent, B. C., Treitel, M. A. & Carlson, M. Functional interdependence of the yeast SNF2, SNF5, and SNF6 proteins in transcriptional activation. *Proc. Natl. Acad. Sci. U. S. A.* **88**, 2687–2691 (1991).

123. Yoshimoto, H. & Yamashita, I. The GAM1/SNF2 gene of Saccharomyces cerevisiae encodes a highly charged nuclear protein required for transcription of the STA1 gene. *Mol. Gen. Genet.* **228**, 270–280 (1991).

124. Laurent, B. C. & Carlson, M. Yeast SNF2/SWI2, SNF5, and SNF6 proteins function coordinately with the gene-specific transcriptional activators GAL4 and Bicoid. *Genes Dev.* **6**, 1707–1715 (1992).

125. Cairns, B. R., Kim, Y., Sayre, M. H., Laurentt, B. C. & Kornberg, R. D. A multisubunit complex containing the SWI1/ADR6, SWI2/SNF2, SWI3, SNF5, and SNF6 gene products isolated from yeast. *Proc. Natl. Acad. Sci. U. S. A.* **91**, 1950–1954 (1994).

126. Côté, J., Quinn, J., Workman, J. L. & Peterson, C. L. Stimulation of GAL4 derivative binding to nucleosomal DNA by the yeast SWI/SNF complex. *Science* **265**, 53–60 (1994).

127. Peterson, C. L., Dingwall, A. & Scott, M. P. Five SWI/SNF gene products are components of a large multisubunit complex required for transcriptional enhancement. *Proc. Natl. Acad. Sci. U. S. A.* **91**, 2905–2908 (1994).

128. Sternberg, P. W., Stern, M. J., Clark, I. & Herskowitz, I. Activation of the yeast HO gene by release from multiple negative controls. *Cell* **48**, 567–577 (1987).

129. Kruger, W. & Herskowitz, I. A negative regulator of HO transcription, SIN1 (SPT2), is a nonspecific DNA-binding protein related to HMG1. *Mol. Cell. Biol.* **11**, 4135–4146 (1991).

130. Prelich, G. & Winston, F. Mutations that suppress the deletion of an upstream activating sequence in yeast: Involvement of a protein kinase and histone H3 in repressing transcription in vivo. *Genetics* **135**, 665–676 (1993).

131. Kruger, W. *et al.* Amino acid substitutions in the structured domains of histones H3 and H4 partially relieve the requirement of the yeast SWI/SNF complex for transcription. *Genes Dev.* **9**, 2770–2779 (1995).

132. Neigeborn, L., Rubin, K. & Carlson, M. Suppressors of SNF2 mutations restore invertase derepression and cause temperature-sensitive lethality in yeast. *Genetics* **112**, 741–753 (1986).

133. Neigeborn, L., Celenza, J. L. & Carlson, M. SSN20 is an essential gene with mutant alleles that suppress defects in SUC2 transcription in Saccharomyces cerevisiae. *Mol. Cell. Biol.* **7**, 672–678 (1987).

134. Hirschhorn, J. N., Brown, S. A., Clark, C. D. & Winston, F. Evidence that SNF2/SWI2 and SNF5 activate transcription in yeast by altering chromatin structure. *Genes Dev.* **6**, 2288–2298 (1992).

135. Knezetic, J. A. & Luse, D. S. The presence of nucleosomes on a DNA template prevents initiation by RNA polymerase II in vitro. *Cell* **45**, 95–104 (1986).

136. Lorch, Y., LaPointe, J. W. & Kornberg, R. D. Nucleosomes inhibit the initiation of transcription but allow chain elongation with the displacement of histones. *Cell* **49**, 203–210 (1987).

137. Han, M. & Grunstein, M. Nucleosome loss activates yeast downstream promoters in vivo. *Cell* **55**, 1137–1145 (1988).

138. Laurent, B. C., Yang, X. & Carlson, M. An essential Saccharomyces cerevisiae gene homologous to SNF2 encodes a helicase-related protein in a new family. *Mol. Cell. Biol.* **12**, 1893–1902 (1992).

139. Laurent, B. C., Treich, I. & Carlson, M. The yeast SNF2/SWI2 protein has DNA-stimulated ATPase activity required for transcriptional activation. *Genes Dev.* **7**, 583–591 (1993).

140. Logie, C. & Peterson, C. L. Catalytic activity of the yeast SWI/SNF complex on reconstituted nucleosome arrays. *EMBO J.* **16**, 6772–6782 (1997).

141. Utley, R. T., Côté, J., Owen-Hughes, T. & Workman, J. L. SWI/SNF stimulates the formation of disparate activator-nucleosome complexes but is partially redundant with cooperative binding. *J. Biol. Chem.* **272**, 12642–12649 (1997).

142. Whitehouse, I. *et al.* Nucleosome mobilization catalysed by the yeast SWI/SNF complex. *Nature* **400**, 784–787 (1999).

143. Jaskelioff, M., M. Gavin, I., Peterson, C. L. & Logie, C. SWI-SNF-Mediated Nucleosome Remodeling: Role of Histone Octamer Mobility in the Persistence of the Remodeled State. *Mol. Cell. Biol.* **20**, 3058–3068 (2000).

144. Dechassa, M. L. *et al.* SWI/SNF Has Intrinsic Nucleosome Disassembly Activity that Is Dependent on Adjacent Nucleosomes. *Mol. Cell* **38**, 590–602 (2010).

145. Brown, C. R., Mao, C., Falkovskaia, E., Law, J. K. & Boeger, H. In Vivo role for the chromatin-remodeling enzyme SWI/SNF in the removal of promoter nucleosomes by disassembly rather than sliding. *J. Biol. Chem.* **286**, 40556–40565 (2011).

146. Sudarsanam, P., Iyer, V. R., Brown, P. O. & Winston, F. Whole-genome expression analysis of Snf/Swi mutants of Saccharomyces cerevisiae. *Proc. Natl. Acad. Sci. U. S. A.* **97**, 3364–3369 (2000).

147. Cairns, B. R., Levinson, R. S., Yamamoto, K. R. & Kornberg, R. D. Essential role of Swp73p in the function of yeast SWI/SNF complex. *Genes Dev.* **10**, 2131–2144 (1996).

148. Peterson, C. L., Zhao, Y. & Chait, B. T. Subunits of the yeast SWI/SNF complex are members of the actin-related protein (ARP) family. *J. Biol. Chem.* **273**, 23641–23644 (1998).

149. Szerlong, H. *et al.* The HSA domain binds nuclear actin-related proteins to regulate chromatin-remodeling ATPases. *Nat. Struct. Mol. Biol.* **15**, 469–476 (2008).

150. Lee, K. *et al.* Proteomic analysis of chromatin-modifying complexes in Saccharomyces cerevisiae identifies

novel subunits. *Biochem. Soc. Trans.* **32**, 899–903 (2004).

151. Graumann, J. *et al.* Applicability of tandem affinity purification MudPIT to pathway proteomics in yeast. *Mol. Cell. Proteomics* **3**, 226–237 (2004).

152. Turegun, B., Baker, R. W., Leschziner, A. E. & Dominguez, R. Actin-related proteins regulate the RSC chromatin remodeler by weakening intramolecular interactions of the Sth1 ATPase. *Commun. Biol.* **1**, 1–11 (2018).

153. Cairns, B. R., Henry, N. L. & Kornberg, R. D. TFG/TAF30/ANC1, a component of the yeast SWI/SNF complex that is similar to the leukemogenic proteins ENL and AF-9. *Mol. Cell. Biol.* **16**, 3308–3316 (1996).

154. Treich, I., Cairns, B. R., de los Santos, T., Brewster, E. & Carlson, M. SNF11, a new component of the yeast SNF-SWI complex that interacts with a conserved region of SNF2. *Mol. Cell. Biol.* **15**, 4240–4248 (1995).

155. Sen, P. *et al.* Loss of Snf5 Induces Formation of an Aberrant SWI/SNF Complex. *Cell Rep.* **18**, 2135–2147 (2017).

156. Smith, C. L., Horowitz-Scherer, R., Flanagan, J. F., Woodcock, C. L. & Peterson, C. L. Structural analysis of the yeast SWI/SNF chromatin remodeling complex. *Nat. Struct. Biol.* **10**, 141–145 (2003).

157. Han, Y., Reyes, A. A., Malik, S. & He, Y. Cryo-EM structure of SWI/SNF complex bound to a nucleosome. *Nature* **579**, 452–455 (2020).

158. Cairns, B. R. *et al.* RSC, an essential, abundant chromatin-remodeling complex. *Cell* **87**, 1249–1260 (1996).

159. Ng, H. H., Robert, F., Young, R. A. & Struhl, K. Genome-wide location and regulated recruitment of the RSC nucleosome-remodeling complex. *Genes Dev.* **16**, 806–819 (2002).

160. Angus-Hill, M. L. *et al.* A Rsc3/Rsc30 zinc cluster dimer reveals novel roles for the chromatin remodeler RSC in gene expression and cell cycle control. *Mol. Cell* **7**, 741–751 (2001).

161. Du, J., Nasir, I., Benton, B. K., Kladde, M. P. & Laurent, B. C. Sth1p, a Saccharomyces cerevisiae Snf2p/Swi2p homolog, is an essential ATPase in RSC and differs from Snf/Swi in its interactions with histones and chromatin-associated proteins. *Genetics* **150**, 987–1005 (1998).

162. Cairns, B. R., Erdjument-Bromage, H., Tempst, P., Winston, F. & Kornberg, R. D. Two actin-related proteins are shared functional components of the chromatin-remodeling complexes RSC and SWI/SNF. *Mol. Cell* **2**, 639–651 (1998).

163. Turegun, B., Baker, R. W., Leschziner, A. E. & Dominguez, R. Actin-related proteins regulate the RSC chromatin remodeler by weakening intramolecular interactions of the Sth1 ATPase. *Commun. Biol.* **1**, 1–11 (2018).

164. Romeo, M. J. *et al.* HTL1 Encodes a Novel Factor That Interacts with the RSC Chromatin Remodeling Complex in Saccharomyces cerevisiae . *Mol. Cell. Biol.* **22**, 8165–8174 (2002).

165. Treich, I., Ho, L. & Carlson, M. Direct interaction between Rsc6 and Rsc8/Swh3, two proteins that are conserved in SWI/SNF-related complexes. *Nucleic Acids Res.* **26**, 3739–3745 (1998).

166. Cao, Y., Cairns, B. R., Kornberg, R. D. & Laurent, B. C. Sfh1p, a component of a novel chromatin-remodeling complex, is required for cell cycle progression. *Mol. Cell. Biol.* **17**, 3323–3334 (1997).

167. Lorch, Y., Cairns, B. R., Zhang, M. & Kornberg, R. D. Activated RSC-nucleosome complex and persistently altered form of the nucleosome. *Cell* **94**, 29–34 (1998).

168. Lorch, Y., Zhang, M. & Kornberg, R. D. Histone octamer transfer by a chromatin-remodeling complex. *Cell* **96**, 389–392 (1999).

169. Farrona, S., Hurtado, L., Bowman, J. L. & Reyes, J. C. The Arabidopsis thaliana SNF2 homolog AtBRM controls shoot development and flowering. *Development* **131**, 4965–4975 (2004).

170. Hurtado, L., Farrona, S. & Reyes, J. C. The putative SWI/SNF complex subunit BRAHMA activates flower homeotic genes in Arabidopsis thaliana. *Plant Mol. Biol.* **62**, 291–304 (2006).

171. Dingwall, A. K. *et al.* The Drosophila snr1 and brm proteins are related to yeast SWI/SNF proteins and are components of a large protein complex. *Mol. Biol. Cell* **6**, 777–791 (1995).

172. Tamkun, J. W. *et al.* brahma: A regulator of Drosophila homeotic genes structurally related to the yeast transcriptional activator SNF2 SWI2. *Cell* **68**, 561–572 (1992).

173. Gregg, R. G., Willer, G. B., Fadool, J. M., Dowling, J. E. & Link, B. A. Positional cloning of the young mutation identifies an essential role for the Brahma chromatin remodeling complex in mediating retinal cell differentiation. *Proc. Natl. Acad. Sci. U. S. A.* **100**, 6535–6540 (2003).

174. Goodwin, G. H. Isolation of cDNAs encoding chicken homologues of the yeast SNF2 and Drosophila Brahma proteins. *Gene* **184**, 27–32 (1997).

175. Schofield, J. *et al.* Expression of Drosophila trithorax-group homologues in chick embryos. *Mech. Dev.* **80**, 115–118 (1999).

176. Randazzo, F. M., Khavari, P., Crabtree, G., Tamkun, J. & Rossant, J. brg1: A putative murine homologue of the Drosophila brahma gene, a homeotic gene regulator. *Developmental Biology* vol. 161 229–242 (1994).

177. Khavari, P. A., Peterson, C. L., Tamkun, J. W., Mendel, D. B. & Crabtree, G. R. BRG1 contains a conserved domain of the SWI2/SNF2 family necessary for normal mitotic growth and transcription. *Nature* **366**, 170–174 (1993).

178. Duncan, I. The bithorax complex. *Annu. Rev. Genet.* **21**, 285–319 (1987).

179. Kaufman, T. C., Seeger, M. A. & Olsen, G. Molecular and genetic organization of the antennapedia gene complex of drosophila melanogaster. *Adv. Genet.* **27**, 309–362 (1990).

180. McKeon, J. & Brock, H. W. Interactions of the Polycomb group of genes with homeotic loci of Drosophila. *Roux's Arch. Dev. Biol.* **199**, 387–396 (1991).

181. Simon, J., Chiang, A. & Bender, W. Ten different Polycomb group genes are required for spatial control of the abdA and AbdB homeotic products. *Development* **505**, 493–505 (1992).

182. Kennison, J. A. Transcriptional activation of Drosphila homeotic genes form distant regulatory elements. *Trends Genet.* **9**, 75–79 (1993).

183. Kennison, J. A. & Tamkun, J. W. Dosage-dependent modifiers of Polycomb and Antennapedia mutations in Drosophila. *Proc. Natl. Acad. Sci. U. S. A.* **85**, 8136–8140 (1988).

184. Brizuela, B. J., Elfring, L., Ballard, J., Tamkun, J. W. & Kennison, J. A. Genetic analysis of the brahma gene of Drosophila melanogaster and polytene chromosome subdivisions 72AB. *Genetics* **137**, 803–813 (1994).

185. Elfring, L. K., Deuring, R., McCallum, C. M., Peterson, C. L. & Tamkun, J. W. Identification and characterization of Drosophila relatives of the yeast transcriptional activator SNF2/SWI2. *Mol. Cell. Biol.* **14**, 2225–2234 (1994).

186. Papoulas, O. *et al.* The Drosophila trithorax group proteins BRM, ASH1 and ASH2 are subunits of distinct protein complexes. *Development* **125**, 3955–3966 (1998).

187. Crosby, M. A. *et al.* The trithorax Group Gene moira Encodes a Brahma-Associated Putative Chromatin-Remodeling Factor in Drosophila melanogaster . *Mol. Cell. Biol.* **19**, 1159–1170 (1999).

188. Zraly, C. B. *et al.* SNR1 is an essential subunit in a subset of Drosophila brm complexes, targeting specific functions during development. *Dev. Biol.* **253**, 291–308 (2003).

189. Vázquez, M., Moore, L. & Kennison, J. A. The trithorax group gene osa encodes an ARID-domain protein that genetically interacts with the Brahma chromatin-remodeling factor to regulate transcription. *Development* **126**, 733–742 (1999).

190. Collins, R. T., Furukawa, T., Tanese, N. & Treisman, J. E. Osa associates with the Brahma chromatin remodeling complex and promotes the activation of some target genes. *EMBO J.* **18**, 7029–7040 (1999).

191. Papoulas, O. *et al.* The HMG-domain protein BAP111 is important for the function of the BRM chromatin-remodeling complex in vivo. *Proc. Natl. Acad. Sci. U. S. A.* **98**, 5728–5733 (2001).

192. Möller, A., Avila, F. W., Erickson, J. W. & Jäckle, H. Drosophila BAP60 is an essential component of the Brahma complex, required for gene activation and repression. *J. Mol. Biol.* **352**, 329–337 (2005).

193. Mohrmann, L. *et al.* Differential Targeting of Two Distinct SWI/SNF-Related Drosophila Chromatin-Remodeling Complexes. *Mol. Cell. Biol.* **24**, 3077–3088 (2004).

194. Arnoud J, K., Mahmoudi, T., Zak, N. B. & Verrijzer, C. P. The Drosophila Brahma complex is an essential coactivator for the trithorax group protein Zeste. *Genes Dev.* **14**, 1058–1071 (2000).

195. Armstrong, J. A. *et al.* The Drosophila BRM complex facilitates global transcription by RNA polymerase II. *EMBO J.* **21**, 5245–5254 (2002).

196. Zraly, C. B., Middleton, F. A. & Dingwall, A. K. Hormone-response genes are direct in vivo regulatory targets of Brahma (SWI/SNF) complex function. *J. Biol. Chem.* **281**, 35305–35315 (2006).

197. Elfring, L. K. *et al.* Genetic analysis of brahma: The drosophila homolog of the yeast chromatin remodeling factor SWI2/SNF2. *Genetics* **148**, 251–265 (1998).

198. Chiba, H., Muramatsu, M., Nomoto, A. & Kato, H. Two human homologues of saccharomyces cerevisiae SWI2/SNF2 and Drosophila brahma are transcriptional coactivators cooperating with the estrogen receptor and the retinoic acid receptor. *Nucleic Acids Res.* **22**, 1815–1820 (1994).

199. Kwon, H., Imbalzano, A. N., Khavari, P. A., Kingston, R. E. & Green, M. R. Nucleosome disruption and enhancement of activator binding by a human SW1/SNF complex. *Nature* **370**, 477–481 (1994).

200. Wang, W. *et al.* Purification and biochemical heterogeneity of the mammalian SWI-SNF complex. *EMBO J.* **15**, 5370–5382 (1996).

201. Xue, Y. *et al.* The human SWI/SNF-B chromatin-remodeling complex is related to yeast Rsc and localizes at kinetochores of mitotic chromosomes. *Proc. Natl. Acad. Sci. U. S. A.* **97**, 13015–13020 (2000).

202. Cairns, B. R. *et al.* Two functionally distinct forms of the RSC nucleosome-remodeling complex, containing essential AT hook, BAH, and bromodomains. *Mol. Cell* **4**, 715–723 (1999).

203. Damelin, M. *et al.* The genome-wide localization of Rsc9, a component of the RSC chromatin-remodeling complex, changes in response to stress. *Mol. Cell* **9**, 563–573 (2002).

204. Hatayama, M. & Aruga, J. Characterization of the tandem CWCH2 sequence motif: A hallmark of inter-zinc finger interactions. *BMC Evol. Biol.* **10**, 1–18 (2010).

205. Mani, U., S, A. S., Goutham R N, A. & Mohan S, S. SWI/SNF Infobase - An exclusive information portal for SWI/SNF remodeling complex subunits. *PLoS One* **12**, 1–11 (2017).

206. Lessard, J. *et al.* An Essential Switch in Subunit Composition of a Chromatin Remodeling Complex during Neural Development. *Neuron* **55**, 201–215 (2007).

207. Wu, J. I. *et al.* Regulation of Dendritic Development by Neuron-Specific Chromatin Remodeling Complexes. *Neuron* **56**, 94–108 (2007).

208. Staahl, B. T. *et al.* Kinetic analysis of npBAF to nBAF switching reveals exchange of SS18 with CREST and integration with neural developmental pathways. *J. Neurosci.* **33**, 10348–10361 (2013).

209. Braun, S. M. G. *et al.* BAF subunit switching regulates chromatin accessibility to control cell cycle exit in the developing mammalian cortex. *Genes Dev.* **35**, 335–353 (2021).

210. Ring, H. Z., Vameghi-Meyers, V., Wang, W., Crabtree, G. R. & Francke, U. Five SWI/SNF-related, matrix-associated, actin-dependent regulator of chromatin (SMARC) genes are dispersed in the human genome. *Genomics* **51**, 140–143 (1998).

211. Chestkov, A. V, Baka, I. D., Kost, M. V, Georgiev, G. P. & Buchman, V. L. The d4 gene family in the human genome. *Genomics* **36**, 174–177 (1996).

212. de Bruijn, D. R., Kater-Baats, E., Eleveld, M., Merkx, G. & Geurts Van Kessel, A. Mapping and characterization of the mouse and human SS18 genes, two human SS18-like genes and a mouse Ss18 pseudogene. *Cytogenet. Cell Genet.* **92**, 310–319 (2001).

213. Wang, X. *et al.* Two related ARID family proteins are alternative subunits of human SWI/SNF complexes. *Biochem. J.* **383**, 319–325 (2004).

214. Alpsoy, A. & Dykhuizen, E. C. Glioma tumor suppressor candidate region gene 1 (GLTSCR1) and its paralog GLTSCR1-like form SWI/SNF chromatin remodeling subcomplexes. *J. Biol. Chem.* **293**, 3892–3903 (2018).

215. Mashtalir, N. *et al.* Modular Organization and Assembly of SWI/SNF Family Chromatin Remodeling Complexes. *Cell* **175**, 1272-1288.e20 (2018).

216. Phelan, M. L., Sif, S., Narlikar, G. J. & Kingston, R. E. Reconstitution of a core chromatin remodeling complex from SWI/SNF subunits. *Mol. Cell* **3**, 247–253 (1999).

217. Wang, W. *et al.* Diversity and specialization of mammalian SWI/SNF complexes. *Genes Dev.* **10**, 2117–2130 (1996).

218. Ho, L. *et al.* An embryonic stem cell chromatin remodeling complex, esBAF, is essential for embryonic stem

cell self-renewal and pluripotency. *Proc. Natl. Acad. Sci. U. S. A.* **106**, 5181–5186 (2009).

219. Yan, L., Xie, S., Du, Y. & Qian, C. Structural Insights into BAF47 and BAF155 Complex Formation. *J. Mol. Biol.* **429**, 1650–1660 (2017).

220. Chen, G. *et al.* A heterotrimeric SMARCB1-SMARCC2 subcomplex is required for the assembly and tumor suppression function of the BAF chromatin-remodeling complex. *Cell Discov.* **6**, 66 (2020).

221. Kadam, S. *et al.* Functional selectivity of recombinant mammalian SWI/SNF subunits. *Genes Dev.* **14**, 2441–2451 (2000).

222. Koszewski, N. J., Henry, K. W., Lubert, E. J., Gravatte, H. & Noonan, D. J. Use of a modified yeast one-hybrid screen to identify BAF60a interactions with the Vitamin D receptor heterodimer. *J. Steroid Biochem. Mol. Biol.* **87**, 223–231 (2003).

223. Debril, M.-B. *et al.* Transcription factors and nuclear receptors interact with the SWI/SNF complex through the BAF60c subunit. *J. Biol. Chem.* **279**, 16677–16686 (2004).

224. Flajollet, S., Lefebvre, B., Cudejko, C., Staels, B. & Lefebvre, P. The core component of the mammalian SWI/SNF complex SMARCD3/BAF60c is a coactivator for the nuclear retinoic acid receptor. *Mol. Cell. Endocrinol.* **270**, 23–32 (2007).

225. Oh, J. *et al.* BAF60a interacts with p53 to recruit the SWI/SNF complex. *J. Biol. Chem.* **283**, 11924–11934 (2008).

226. Forcales, S. V *et al.* Signal-dependent incorporation of MyoD-BAF60c into Brg1-based SWI/SNF chromatin-remodelling complex. *EMBO J.* **31**, 301–316 (2012).

227. Kalpana, G. V, Marmon, S., Wang, W., Crabtree, G. R. & Goff, S. P. Binding and stimulation of HIV-1 integrase by a human homolog of yeast transcription factor SNF5. *Science* **266**, 2002–2006 (1994).

228. Nakayama, R. T. *et al.* SMARCB1 is required for widespread BAF complex-mediated activation of enhancers and bivalent promoters. *Nat. Genet.* **49**, 1613–1623 (2017).

229. Valencia, A. M. *et al.* Recurrent SMARCB1 Mutations Reveal a Nucleosome Acidic Patch Interaction Site That Potentiates mSWI/SNF Complex Chromatin Remodeling. *Cell* **179**, 1342-1356.e23 (2019).

230. Wattler, F., Wattler, S., Kelly, M., Skinner, H. B. & Nehls, M. Cloning, chromosomal location, and expression analysis of murine Smarce1-related, a new member of the high-mobility 365 group gene family. *Genomics* **60**, 172–178 (1999).

231. Heo, Y. *et al.* Crystal structure of the HMG domain of human BAF57 and its interaction with four-way junction DNA. *Biochem. Biophys. Res. Commun.* **533**, 919–924 (2020).

232. Kadoch, C. *et al.* Proteomic and bioinformatic analysis of mammalian SWI/SNF complexes identifies extensive roles in human malignancy. *Nat. Genet.* **45**, 592–601 (2013).

233. Schafer, D. A. & Schroer, T. A. Actin-related proteins. *Annu. Rev. Cell Dev. Biol.* **15**, 341–363 (1999).

234. Olave, I. A., Reck-Peterson, S. L. & Crabtree, G. R. Nuclear actin and actin-related proteins in chromatin remodeling. *Annu. Rev. Biochem.* **71**, 755–781 (2002).

235. Rando, O. J., Zhao, K., Janmey, P. & Crabtree, G. R. Phosphatidylinositol-dependent actin filament binding by the SWI/SNF-like BAF chromatin remodeling complex. *Proc. Natl. Acad. Sci. U. S. A.* **99**, 2824–2829 (2002).

236. Szerlong, H., Saha, A. & Cairns, B. R. The nuclear actin-related proteins Arp7 and Arp9: a dimeric module that cooperates with architectural proteins for chromatin remodeling. *EMBO J.* **22**, 3175–3187 (2003).

237. Nishimoto, N. *et al.* Heterocomplex formation by Arp4 and β-actin is involved in the integrity of the Brg1 chromatin remodeling complex. *J. Cell Sci.* **125**, 3870–3882 (2012).

238. Zhao, K. *et al.* Rapid and phosphoinositol-dependent binding of the SWI/SNF-like BAF complex to chromatin after T lymphocyte receptor signaling. *Cell* **95**, 625–636 (1998).

239. Choi, E. Y., Park, J. A., Sung, Y. H. & Kwon, H. Generation of the dominant-negative mutant of hArpNbeta: a component of human SWI/SNF chromatin remodeling complex. *Exp. Cell Res.* **271**, 180–188 (2001).

240. Sung, Y. H., Choi, E. Y. & Kwon, H. Identification of a nuclear protein ArpN as a component of human SWI/SNF complex and its selective association with a subset of active genes. *Mol. Cells* **11**, 75–81 (2001).

241. Clapier, C. R. *et al.* Regulation of DNA Translocation Efficiency within the Chromatin Remodeler RSC/Sth1

Potentiates Nucleosome Sliding and Ejection. *Mol. Cell* **62**, 453–461 (2016).

242. Bao, X. *et al.* ACTL6a enforces the epidermal progenitor state by suppressing SWI/SNF-dependent induction of KLF4. *Cell Stem Cell* **12**, 193–203 (2013).

243. Jeong, K. W., Lee, Y.-H. & Stallcup, M. R. Recruitment of the SWI/SNF chromatin remodeling complex to steroid hormone-regulated promoters by nuclear receptor coactivator flightless-I. *J. Biol. Chem.* **284**, 29298–29309 (2009).

244. Oma, Y., Nishimori, K. & Harata, M. The brain-specific actin-related protein ArpN alpha interacts with the transcriptional co-repressor CtBP. *Biochem. Biophys. Res. Commun.* **301**, 521–528 (2003).

245. Middeljans, E. *et al.* SS18 together with animal-specific factors defines human BAF-type SWI/SNF complexes. *PLoS One* **7**, e33834 (2012).

246. Baliñas-Gavira, C. *et al.* Frequent mutations in the amino-terminal domain of BCL7A impair its tumor suppressor role in DLBCL. *Leukemia* **34**, 2722–2735 (2020).

247. Raab, J. R., Resnick, S. & Magnuson, T. Genome-Wide Transcriptional Regulation Mediated by Biochemically Distinct SWI/SNF Complexes. *PLoS Genet.* **11**, e1005748 (2015).

248. Gatchalian, J. *et al.* A non-canonical BRD9-containing BAF chromatin remodeling complex regulates naive pluripotency in mouse embryonic stem cells. *Nat. Commun.* **9**, 5139 (2018).

249. Dallas, P. B. *et al.* The human SWI-SNF complex protein p270 is an ARID family member with non-sequence-specific DNA binding activity. *Mol. Cell. Biol.* **20**, 3137–3146 (2000).

250. Nie, Z. *et al.* A specificity and targeting subunit of a human SWI/SNF family-related chromatin-remodeling complex. *Mol. Cell. Biol.* **20**, 8879–8888 (2000).

251. Kozmik, Z. *et al.* Characterization of mammalian orthologues of the Drosophila osa gene: cDNA cloning, expression, chromosomal localization, and direct physical interaction with Brahma chromatin-remodeling complex. *Genomics* **73**, 140–148 (2001).

252. Hurlstone, A. F. L., Olave, I. A., Barker, N., van Noort, M. & Clevers, H. Cloning and characterization of hELD/OSA1, a novel BRG1 interacting protein. *Biochem. J.* **364**, 255–264 (2002).

253. Inoue, H. *et al.* Largest subunits of the human SWI/SNF chromatin-remodeling complex promote transcriptional activation by steroid hormone receptors. *J. Biol. Chem.* **277**, 41674–41685 (2002).

254. Wilsker, D. *et al.* The DNA-binding properties of the ARID-containing subunits of yeast and mammalian SWI/SNF complexes. *Nucleic Acids Res.* **32**, 1345–1353 (2004).

255. Kim, S., Zhang, Z., Upchurch, S., Isern, N. & Chen, Y. Structure and DNA-binding Sites of the SWI1 AT-rich Interaction Domain (ARID) Suggest Determinants for Sequence-specific DNA Recognition. *J. Biol. Chem.* **279**, 16670–16676 (2004).

256. Patsialou, A., Wilsker, D. & Moran, E. DNA-binding properties of ARID family proteins. *Nucleic Acids Res.* **33**, 66–80 (2005).

257. Sandhya, S., Maulik, A., Giri, M. & Singh, M. Domain architecture of BAF250a reveals the ARID and ARM-repeat domains with implication in function and assembly of the BAF remodeling complex. *PLoS One* **13**, e0205267 (2018).

258. He, S. *et al.* Structure of nucleosome-bound human BAF complex. *Science* **367**, 875–881 (2020).

259. Mashtalir, N. *et al.* A Structural Model of the Endogenous Human BAF Complex Informs Disease Mechanisms. *Cell* **183**, 802-817.e24 (2020).

260. Ninkina, N. N. *et al.* Cerd4, third member of the d4 gene family: expression and organization of genomic locus. *Mamm. Genome* **12**, 862–866 (2001).

261. Boamah, D. *et al.* Characteristics of a PHD Finger Subtype. *Biochemistry* **57**, 525–539 (2018).

262. Lange, M. *et al.* Regulation of muscle development by DPF3, a novel histone acetylation and methylation reader of the BAF chromatin remodeling complex. *Genes Dev.* **22**, 2370–2384 (2008).

263. Huber, F. M. *et al.* Histone-binding of DPF2 mediates its repressive role in myeloid differentiation. *Proc. Natl. Acad. Sci. U. S. A.* **114**, 6016–6021 (2017).

264. Local, A. *et al.* Identification of H3K4me1-associated proteins at mammalian enhancers. *Nat. Genet.* **50**, 73–

82 (2018).

265. Xiong, X. *et al.* Selective recognition of histone crotonylation by double PHD fingers of MOZ and DPF2. *Nat. Chem. Biol.* **12**, 1111–1118 (2016).

266. Liu, X. *et al.* MOF as an evolutionarily conserved histone crotonyltransferase and transcriptional activation by histone acetyltransferase-deficient and crotonyltransferase-competent CBP/p300. *Cell Discov.* **3**, 17016 (2017).

267. Kato, H. *et al.* SYT associates with human SNF/SWI complexes and the C-terminal region of its fusion partner SSX1 targets histones. *J. Biol. Chem.* **277**, 5498–5505 (2002).

268. Perani, M., Ingram, C. J. E., Cooper, C. S., Garrett, M. D. & Goodwin, G. H. Conserved SNH domain of the proto-oncoprotein SYT interacts with components of the human chromatin remodelling complexes, while the QPGY repeat domain forms homo-oligomers. *Oncogene* **22**, 8156–8167 (2003).

269. Kadoch, C. & Crabtree, G. R. Reversible disruption of mSWI/SNF (BAF) complexes by the SS18-SSX oncogenic fusion in synovial sarcoma. *Cell* **153**, 71–85 (2013).

270. McBride, M. J. *et al.* The SS18-SSX Fusion Oncoprotein Hijacks BAF Complex Targeting and Function to Drive Synovial Sarcoma. *Cancer Cell* **33**, 1128-1141.e7 (2018).

271. Lemon, B., Inouye, C., King, D. S. & Tjian, R. Selectivity of chromatin-remodelling cofactors for ligand-activated transcription. *Nature* **414**, 924–928 (2001).

272. Rafati, H. *et al.* Repressive LTR nucleosome positioning by the BAF complex is required for HIV latency. *PLoS Biol.* **9**, e1001206 (2011).

273. Xu, F., Flowers, S. & Moran, E. Essential role of ARID2 protein-containing SWI/SNF complex in tissue-specific gene expression. *J. Biol. Chem.* **287**, 5033–5041 (2012).

274. Kakarougkas, A. *et al.* Requirement for PBAF in transcriptional repression and repair at DNA breaks in actively transcribed regions of chromatin. *Mol. Cell* **55**, 723–732 (2014).

275. Brownlee, P. M., Chambers, A. L., Cloney, R., Bianchi, A. & Downs, J. A. BAF180 promotes cohesion and prevents genome instability and aneuploidy. *Cell Rep.* **6**, 973–981 (2014).

276. Kakarougkas, A., Downs, J. A. & Jeggo, P. A. The PBAF chromatin remodeling complex represses transcription and promotes rapid repair at DNA double-strand breaks. *Mol. Cell. Oncol.* **2**, e970072 (2015).

277. Yan, Z. *et al.* PBAF chromatin-remodeling complex requires a novel specificity subunit, BAF200, to regulate expression of selective interferon-responsive genes. *Genes Dev.* **19**, 1662–1667 (2005).

278. Kaeser, M. D., Aslanian, A., Dong, M. Q., Yates, J. R. & Emerson, B. M. BRD7, a novel PBAF-specific SWI/SNF subunit, is required for target gene activation and repression in embryonic stem cells. *J. Biol. Chem.* **283**, 32254–32263 (2008).

279. Bastiray, A., Giri, M. & Singh, M. Sequential backbone resonance assignment of AT-rich interaction domain of human BAF200. *Biomol. NMR Assign.* **13**, 115–119 (2019).

280. Cuppen, E., van Ham, M., Pepers, B., Wieringa, B. & Hendriks, W. Identification and molecular characterization of BP75, a novel bromodomain-containing protein. *FEBS Lett.* **459**, 291–298 (1999).

281. Zeng, L. & Zhou, M. M. Bromodomain: an acetyl-lysine binding domain. *FEBS Lett.* **513**, 124–128 (2002).

282. Sun, H. *et al.* Solution structure of BRD7 bromodomain and its interaction with acetylated peptides from histone H3 and H4. *Biochem. Biophys. Res. Commun.* **358**, 435–441 (2007).

283. Yu, Y. *et al.* Screening of BRD7 interacting proteins by yeast two-hybrid system. *Sci. China. Ser. C, Life Sci.* **45**, 546–552 (2002).

284. Zhou, M. *et al.* BRD2 is one of BRD7-interacting proteins and its over-expression could initiate apoptosis. *Mol. Cell. Biochem.* **292**, 205–212 (2006).

285. Peng, C. *et al.* The transcriptional regulation role of BRD7 by binding to acetylated histone through bromodomain. *J. Cell. Biochem.* **97**, 882–892 (2006).

286. Tae, S. *et al.* Bromodomain protein 7 interacts with PRMT5 and PRC2, and is involved in transcriptional repression of their target genes. *Nucleic Acids Res.* **39**, 5424–5438 (2011).

287. Harte, M. T. *et al.* BRD7, a subunit of SWI/SNF complexes, binds directly to BRCA1 and regulates BRCA1-

dependent transcription. *Cancer Res.* **70**, 2538–2547 (2010).

288. Brechalov, A. V, Georgieva, S. G. & Soshnikova, N. V. Mammalian cells contain two functionally distinct PBAF complexes incorporating different isoforms of PHF10 signature subunit. *Cell Cycle* **13**, 1970–1979 (2014).

289. Viryasova, G. M. *et al.* PBAF lacking PHD domains maintains transcription in human neutrophils. *Biochim. Biophys. acta. Mol. cell Res.* **1866**, 118525 (2019).

290. Nicolas, R. H. & Goodwin, G. H. Molecular cloning of polybromo, a nuclear protein containing multiple domains including five bromodomains, a truncated HMG-box, and two repeats of a novel domain. *Gene* **175**, 233–240 (1996).

291. Callebaut, I., Courvalin, J. C. & Mornon, J. P. The BAH (bromo-adjacent homology) domain: a link between DNA methylation, replication and transcriptional regulation. *FEBS Lett.* **446**, 189–193 (1999).

292. Oliver, A. W. *et al.* Crystal structure of the proximal BAH domain of the polybromo protein. *Biochem. J.* **389**, 657–664 (2005).

293. Chandrasekaran, R. & Thompson, M. Polybromo-1-bromodomains bind histone H3 at specific acetyl-lysine positions. *Biochem. Biophys. Res. Commun.* **355**, 661–666 (2007).

294. Park, D. E. *et al.* Merkel cell polyomavirus activates LSD1-mediated blockade of non-canonical BAF to regulate transformation and tumorigenesis. *Nat. Cell Biol.* **22**, 603–615 (2020).

295. Alpsoy, A. *et al.* BRD9 Is a Critical Regulator of Androgen Receptor Signaling and Prostate Cancer Progression. *Cancer Res.* **81**, 820–833 (2021).

296. Michel, B. C. *et al.* A non-canonical SWI/SNF complex is a synthetic lethal target in cancers driven by BAF complex perturbation. *Nat. Cell Biol.* **20**, 1410–1420 (2018).

297. Wang, X. *et al.* BRD9 defines a SWI/SNF sub-complex and constitutes a specific vulnerability in malignant rhabdoid tumors. *Nat. Commun.* **10**, 1881 (2019).

298. Smith, J. S. *et al.* A transcript map of the chromosome 19q-arm glioma tumor suppressor region. *Genomics* **64**, 44–50 (2000).

299. Han, F. *et al.* GLTSCR1 Negatively Regulates BRD4-Dependent Transcription Elongation and Inhibits CRC Metastasis. *Adv. Sci. (Weinheim, Baden-Wurttemberg, Ger.* **6**, 1901114 (2019).

300. Lloyd, J. T. & Glass, K. C. Biological function and histone recognition of family IV bromodomain-containing proteins. *J. Cell. Physiol.* **233**, 1877–1886 (2018).

301. Inoue, D. *et al.* Spliceosomal disruption of the non-canonical BAF complex in cancer. *Nature* **574**, 432–436 (2019).

302. Ho, L. *et al.* An embryonic stem cell chromatin remodeling complex, esBAF, is an essential component of the core pluripotency transcriptional network. *Proc. Natl. Acad. Sci. U. S. A.* **106**, 5187–5191 (2009).

303. Yan, L. & Chen, Z. A Unifying Mechanism of DNA Translocation Underlying Chromatin Remodeling. *Trends Biochem. Sci.* **45**, 217–227 (2020).

304. Quinn, J., Fyrberg, A. M., Ganster, R. W., Schmidt, M. C. & Peterson, C. L. DNA-binding properties of the yeast SWI/SNF complex. *Nature* **379**, 844–847 (1996).

305. Boyer, L. A., Shao, X., Ebright, R. H. & Peterson, C. L. Roles of the histone H2A-H2B dimers and the (H3-H4)2 tetramer in nucleosome remodeling by the SWI-SNF complex. *J. Biol. Chem.* **275**, 11545–11552 (2000).

306. Bazett-Jones, D. P., Côté, J., Landel, C. C., Peterson, C. L. & Workman, J. L. The SWI/SNF Complex Creates Loop Domains in DNA and Polynucleosome Arrays and Can Disrupt DNA-Histone Contacts within These Domains. *Mol. Cell. Biol.* **19**, 1470–1478 (1999).

307. Schnitzler, G., Sif, S. & Kingston, R. E. Human SWI/SNF interconverts a nucleosome between its base state and a stable remodeled state. *Cell* **94**, 17–27 (1998).

308. Côté, J., Peterson, C. L. & Workman, J. L. Perturbation of nucleosome core structure by the SWI/SNF complex persists after its detachment, enhancing subsequent transcription factor binding. *Proc. Natl. Acad. Sci. U. S. A.* **95**, 4947–4952 (1998).

309. Kassabov, S. R., Zhang, B., Persinger, J. & Bartholomew, B. SWI/SNF unwraps, slides, and rewraps the nucleosome. *Mol. Cell* **11**, 391–403 (2003).

310. Lorch, Y., Zhang, M. & Kornberg, R. D. RSC unravels the nucleosome. *Mol. Cell* **7**, 89–95 (2001).

311. Boeger, H., Griesenbeck, J., Strattan, J. S. & Kornberg, R. D. Nucleosomes unfold completely at a transcriptionally active promoter. *Mol. Cell* **11**, 1587–1598 (2003).

312. Boeger, H., Griesenbeck, J., Strattan, J. S. & Kornberg, R. D. Removal of promoter nucleosomes by disassembly rather than sliding in vivo. *Mol. Cell* **14**, 667–673 (2004).

313. Saha, A., Wittmeyer, J. & Cairns, B. R. Chromatin remodeling by RSC involves ATP-dependent DNA translocation. *Genes Dev.* **16**, 2120–2134 (2002).

314. Dürr, H., Flaus, A., Owen-Hughes, T. & Hopfner, K. P. Snf2 family ATPases and DExx box helicases: Differences and unifying concepts from high-resolution crystal structures. *Nucleic Acids Res.* **34**, 4160–4167 (2006).

315. Boyer, L. A. *et al.* Functional delineation of three groups of the ATP-dependent family of chromatin remodeling enzymes. *J. Biol. Chem.* **275**, 18864–18870 (2000).

316. Saha, A., Wittmeyer, J. & Cairns, B. R. Chromatin remodeling through directional DNA translocation from an internal nucleosomal site. *Nat. Struct. Mol. Biol.* **12**, 747–755 (2005).

317. Zofall, M., Persinger, J., Kassabov, S. R. & Bartholomew, B. Chromatin remodeling by ISW2 and SWI/SNF requires DNA translocation inside the nucleosome. *Nat. Struct. Mol. Biol.* **13**, 339–346 (2006).

318. Singleton, M. R., Dillingham, M. S. & Wigley, D. B. Structure and mechanism of helicases and nucleic acid translocases. *Annu. Rev. Biochem.* **76**, 23–50 (2007).

319. Sirinakis, G. *et al.* The RSC chromatin remodelling ATPase translocates DNA with high force and small step size. *EMBO J.* **30**, 2364–2372 (2011).

320. Harada, B. T. *et al.* Stepwise nucleosome translocation by RSC remodeling complexes. *Elife* **5**, 1–20 (2016).

321. Dechassa, M. L. *et al.* Architecture of the SWI/SNF-Nucleosome Complex. *Mol. Cell. Biol.* **28**, 6010–6021 (2008).

322. Baker, R. W. *et al.* Structural insights into assembly and function of the RSC chromatin remodeling complex. *Nat. Struct. Mol. Biol.* **28**, 71–80 (2021).

323. Winger, J., Nodelman, I. M., Levendosky, R. F. & Bowman, G. D. A twist defect mechanism for ATP-dependent translocation of nucleosomal DNA. *Elife* **7**, 1–23 (2018).

324. Leschziner, A. E., Lemon, B., Tjian, R. & Nogales, E. Structural studies of the human PBAF chromatin-remodeling complex. *Structure* **13**, 267–275 (2005).

325. Wagner, F. R. *et al.* Structure of SWI/SNF chromatin remodeller RSC bound to a nucleosome. *Nature* **579**, 448–451 (2020).

326. Sen, P., Ghosh, S., Pugh, B. F. & Bartholomew, B. A new, highly conserved domain in Swi2/Snf2 is required for SWI/SNF remodeling. *Nucleic Acids Res.* **39**, 9155–9166 (2011).

327. Liu, X., Li, M., Xia, X., Li, X. & Chen, Z. Mechanism of chromatin remodelling revealed by the Snf2-nucleosome structure. *Nature* **544**, 440–445 (2017).

328. Li, M. *et al.* Mechanism of DNA translocation underlying chromatin remodelling by Snf2. *Nature* **567**, 409–413 (2019).

329. Gavin, I., Horn, P. J. & Peterson, C. L. SWI/SNF chromatin remodeling requires changes in DNA topology. *Mol. Cell* **7**, 97–104 (2001).

330. Engeholm, M. *et al.* Nucleosomes can invade DNA territories occupied by their neighbors. *Nat. Struct. Mol. Biol.* **16**, 151–158 (2009).

331. Gresh, L. *et al.* The SWI/SNF chromatin-remodeling complex subunit SNF5 is essential for hepatocyte differentiation. *EMBO J.* **24**, 3313–3324 (2005).

332. Singhal, N. *et al.* Chromatin-remodeling components of the baf complex facilitate reprogramming. *Cell* **141**, 943–955 (2010).

333. Euskirchen, G. M. *et al.* Diverse roles and interactions of the SWI/SNF chromatin remodeling complex revealed using global approaches. *PLoS Genet.* **7**, e1002008 (2011).

334. Rada-Iglesias, A. *et al.* A unique chromatin signature uncovers early developmental enhancers in humans.

Nature **470**, 279–283 (2011).

335. Albert, I. *et al.* Translational and rotational settings of H2A.Z nucleosomes across the Saccharomyces cerevisiae genome. *Nature* **446**, 572–576 (2007).

336. Shivaswamy, S. *et al.* Dynamic remodeling of individual nucleosomes across a eukaryotic genome in response to transcriptional perturbation. *PLoS Biol.* **6**, e65 (2008).

337. Buenrostro, J. D., Giresi, P. G., Zaba, L. C., Chang, H. Y. & Greenleaf, W. J. Transposition of native chromatin for fast and sensitive epigenomic profiling of open chromatin, DNA-binding proteins and nucleosome position. *Nat. Methods* **10**, 1213–1218 (2013).

338. Morris, S. A. *et al.* Overlapping chromatin-remodeling systems collaborate genome wide at dynamic chromatin transitions. *Nat. Struct. Mol. Biol.* **21**, 73–81 (2014).

339. Bao, X. *et al.* A novel ATAC-seq approach reveals lineage-specific reinforcement of the open chromatin landscape via cooperation between BAF and p63. *Genome Biol.* **16**, 284 (2015).

340. Nocetti, N. & Whitehouse, I. Nucleosome repositioning underlies dynamic gene expression. *Genes Dev.* **30**, 660–672 (2016).

341. Hota, S. K. & Bruneau, B. G. ATP-dependent chromatin remodeling during mammalian development. *Development* **143**, 2882–2897 (2016).

342. Lickert, H. *et al.* Baf60c is essential for function of BAF chromatin remodelling complexes in heart development. *Nature* **432**, 107–112 (2004).

343. Chi, T. H. *et al.* Sequential roles of Brg, the ATPase subunit of BAF chromatin remodeling complexes, in thymocyte development. *Immunity* **19**, 169–182 (2003).

344. de la Serna, I. L., Carlson, K. A. & Imbalzano, A. N. Mammalian SWI/SNF complexes promote MyoD-mediated muscle differentiation. *Nat. Genet.* **27**, 187–190 (2001).

345. Hohmann, A. F. & Vakoc, C. R. A rationale to target the SWI/SNF complex for cancer therapy. *Trends Genet.* **30**, 356–363 (2014).

346. Zhang, X. *et al.* Transcriptional repression by the BRG1-SWI/SNF complex affects the pluripotency of human embryonic stem cells. *Stem Cell Reports* **3**, 460–474 (2014).

347. Novershtern, N. & Hanna, J. H. esBAF safeguards Stat3 binding to maintain pluripotency. *Nature cell biology* vol. 13 886–888 (2011).

348. Ho, L. *et al.* esBAF facilitates pluripotency by conditioning the genome for LIF/STAT3 signalling and by regulating polycomb function. *Nat. Cell Biol.* **13**, 903–913 (2011).

349. Bi-Lin, K. W. *et al.* Critical role of the BAF chromatin remodeling complex during murine neural crest development. *PLoS Genet.* **17**, e1009446 (2021).

350. Bajpai, R. *et al.* CHD7 cooperates with PBAF to control multipotent neural crest formation. *Nature* **463**, 958–962 (2010).

351. Vicent, G. P. *et al.* Two chromatin remodeling activities cooperate during activation of hormone responsive promoters. *PLoS Genet.* **5**, e1000567 (2009).

352. Alver, B. H. *et al.* The SWI/SNF chromatin remodelling complex is required for maintenance of lineage specific enhancers. *Nat. Commun.* **8**, 14648 (2017).

353. Pan, J. *et al.* The ATPase module of mammalian SWI/SNF family complexes mediates subcomplex identity and catalytic activity–independent genomic targeting. *Nat. Genet.* **51**, 618–626 (2019).

354. Pennacchio, L. A., Bickmore, W., Dean, A., Nobrega, M. A. & Bejerano, G. Enhancers: five essential questions. *Nature reviews. Genetics* vol. 14 288–295 (2013).

355. Heintzman, N. D. *et al.* Distinct and predictive chromatin signatures of transcriptional promoters and enhancers in the human genome. *Nat. Genet.* **39**, 311–318 (2007).

356. Easley, R. *et al.* Transcription through the HIV-1 nucleosomes: Effects of the PBAF complex in Tat activated transcription. *Virology* **405**, 322–333 (2010).

357. Dixon, J. R. *et al.* Topological domains in mammalian genomes identified by analysis of chromatin interactions. *Nature* **485**, 376–380 (2012).

358. Bell, A. C., West, A. G. & Felsenfeld, G. The protein CTCF is required for the enhancer blocking activity of vertebrate insulators. *Cell* **98**, 387–396 (1999).

359. Hark, A. T. *et al.* CTCF mediates methylation-sensitive enhancer-blocking activity at the H19/Igf2 locus. *Nature* **405**, 486–489 (2000).

360. Zhang, W. *et al.* Zscan4c activates endogenous retrovirus MERVL and cleavage embryo genes. *Nucleic Acids Res.* **47**, 8485–8501 (2019).

361. Wilson, B. G. & Roberts, C. W. M. SWI/SNF nucleosome remodellers and cancer. *Nat. Rev. Cancer* **11**, 481–492 (2011).

362. Moreira, J. M. & Holmberg, S. Transcriptional repression of the yeast CHA1 gene requires the chromatin-remodeling complex RSC. *EMBO J.* **18**, 2836–2844 (1999).

363. Dror, V. & Winston, F. The Swi/Snf chromatin remodeling complex is required for ribosomal DNA and telomeric silencing in Saccharomyces cerevisiae. *Mol. Cell. Biol.* **24**, 8227–8235 (2004).

364. Shivaswamy, S. & Iyer, V. R. Stress-dependent dynamics of global chromatin remodeling in yeast: dual role for SWI/SNF in the heat shock stress response. *Mol. Cell. Biol.* **28**, 2221–2234 (2008).

365. Martens, J. A. & Winston, F. Evidence that Swi/Snf directly represses transcription in S. cerevisiae. *Genes Dev.* **16**, 2231–2236 (2002).

366. Dimova, D., Nackerdien, Z., Furgeson, S., Eguchi, S. & Osley, M. A. A role for transcriptional repressors in targeting the yeast Swi/Snf complex. *Mol. Cell* **4**, 75–83 (1999).

367. Murphy, D. J., Hardy, S. & Engel, D. A. Human SWI-SNF component BRG1 represses transcription of the c-fos gene. *Mol. Cell. Biol.* **19**, 2724–2733 (1999).

368. Menon, D. U., Shibata, Y., Mu, W. & Magnuson, T. Mammalian SWI/SNF collaborates with a polycomb-associated protein to regulate male germline transcription in the mouse. *Development* **146**, (2019).

369. Jayaprakash, S., Drakulic, S., Zhao, Z., Sander, B. & Golas, M. M. The ATPase BRG1/SMARCA4 is a protein interaction platform that recruits BAF subunits and the transcriptional repressor REST/NRSF in neural progenitor cells. *Mol. Cell. Biochem.* **461**, 171–182 (2019).

370. Sif, S., Saurin, A. J., Imbalzano, A. N. & Kingston, R. E. Purification and characterization of mSin3A-containing Brg1 and hBrm chromatin remodeling complexes. *Genes Dev.* **15**, 603–618 (2001).

371. Wu, S. *et al.* BRG1, the ATPase subunit of SWI/SNF chromatin remodeling complex, interacts with HDAC2 to modulate telomerase expression in human cancer cells. *Cell cycle* **13**, 2869–2878 (2014).

372. Leung, J. Y. & Nevins, J. R. E2F6 associates with BRG1 in transcriptional regulation. *PLoS One* **7**, e47967 (2012).

373. Wan, M. *et al.* Molecular basis of CD4 repression by the Swi/Snf-like BAF chromatin remodeling complex. *Eur. J. Immunol.* **39**, 580–588 (2009).

374. Zhang, B., Chambers, K. J., Faller, D. V & Wang, S. Reprogramming of the SWI/SNF complex for co-activation or co-repression in prohibitin-mediated estrogen receptor regulation. *Oncogene* **26**, 7153–7157 (2007).

375. Gunawardena, R. W., Fox, S. R., Siddiqui, H. & Knudsen, E. S. SWI/SNF activity is required for the repression of deoxyribonucleotide triphosphate metabolic enzymes via the recruitment of mSin3B. *J. Biol. Chem.* **282**, 20116–20123 (2007).

376. Rao, M. *et al.* Inhibition of cyclin D1 gene transcription by Brg-1. *Cell cycle* **7**, 647–655 (2008).

377. Bilodeau, S. *et al.* Role of Brg1 and HDAC2 in GR trans-repression of the pituitary POMC gene and misexpression in Cushing disease. *Genes Dev.* **20**, 2871–2886 (2006).

378. Langer, L. F., Ward, J. M. & Archer, T. K. Tumor suppressor SMARCB1 suppresses super-enhancers to govern hESC lineage determination. *Elife* **8**, (2019).

379. Choi, J., Jeon, S., Choi, S., Park, K. & Seong, R. H. The SWI/SNF chromatin remodeling complex regulates germinal center formation by repressing Blimp-1 expression. *Proc. Natl. Acad. Sci. U. S. A.* **112**, E718-27 (2015).

380. Hainer, S. J. *et al.* Suppression of pervasive noncoding transcription in embryonic stem cells by esBAF. *Genes Dev.* **29**, 362–378 (2015).

381. Li, M. *et al.* Dynamic regulation of transcription factors by nucleosome remodeling. *Elife* **4**, (2015).

382. Weber, C. M. *et al.* mSWI/SNF promotes Polycomb repression both directly and through genome-wide redistribution. *Nat. Struct. Mol. Biol.* **28**, 501–511 (2021).

383. Harrod, A., Lane, K. A. & Downs, J. A. The role of the SWI/SNF chromatin remodelling complex in the response to DNA double strand breaks. *DNA Repair (Amst).* **93**, 102919 (2020).

384. Lee, H.-S., Park, J.-H., Kim, S.-J., Kwon, S.-J. & Kwon, J. A cooperative activation loop among SWI/SNF, gamma-H2AX and H3 acetylation for DNA double-strand break repair. *EMBO J.* **29**, 1434–1445 (2010).

385. Brownlee, P. M., Meisenberg, C. & Downs, J. A. The SWI/SNF chromatin remodelling complex: Its role in maintaining genome stability and preventing tumourigenesis. *DNA Repair (Amst).* **32**, 127–133 (2015).

386. Qi, W. *et al.* BRG1 promotes the repair of DNA double-strand breaks by facilitating the replacement of RPA with RAD51. *J. Cell Sci.* **128**, 317–330 (2015).

387. Karki, M. *et al.* A cytoskeletal function for PBRM1 reading methylated microtubules. *Sci. Adv.* **7**, (2021).

388. Niimi, A., Hopkins, S. R., Downs, J. A. & Masutani, C. The BAH domain of BAF180 is required for PCNA ubiquitination. *Mutat. Res.* **779**, 16–23 (2015).

389. de Castro, R. O. *et al.* The chromatin-remodeling subunit Baf200 promotes homology-directed DNA repair and regulates distinct chromatin-remodeling complexes. *J. Biol. Chem.* **292**, 8459–8471 (2017).

390. Chabanon, R. M. *et al.* PBRM1 Deficiency Confers Synthetic Lethality to DNA Repair Inhibitors in Cancer. *Cancer Res.* **81**, 2888–2902 (2021).

391. Ichinose, H., Garnier, J. M., Chambon, P. & Losson, R. Ligand-dependent interaction between the estrogen receptor and the human homologues of SWI2/SNF2. *Gene* **188**, 95–100 (1997).

392. Ostlund Farrants, A. K., Blomquist, P., Kwon, H. & Wrange, O. Glucocorticoid receptor-glucocorticoid response element binding stimulates nucleosome disruption by the SWI/SNF complex. *Mol. Cell. Biol.* **17**, 895–905 (1997).

393. Ryan, M. P., Jones, R. & Morse, R. H. SWI-SNF complex participation in transcriptional activation at a step subsequent to activator binding. *Mol. Cell. Biol.* **18**, 1774–1782 (1998).

394. Yudkovsky, N., Logie, C., Hahn, S. & Peterson, C. L. Recruitment of the SWI/SNF chromatin remodeling complex by transcriptional activators. *Genes Dev.* **13**, 2369–2374 (1999).

395. Gutiérrez, J. L., Chandy, M., Carrozza, M. J. & Workman, J. L. Activation domains drive nucleosome eviction by SWI/SNF. *EMBO J.* **26**, 730–740 (2007).

396. Xi, Q., He, W., Zhang, X. H.-F., Le, H.-V. & Massagué, J. Genome-wide impact of the BRG1 SWI/SNF chromatin remodeler on the transforming growth factor beta transcriptional program. *J. Biol. Chem.* **283**, 1146–1155 (2008).

397. Ho, P. J., Lloyd, S. M. & Bao, X. Unwinding chromatin at the right places: how BAF is targeted to specific genomic locations during development. *Development* **146**, (2019).

398. Boyer, L. A., Latek, R. R. & Peterson, C. L. The SANT domain: a unique histone-tail-binding module? *Nat. Rev. Mol. Cell Biol.* **5**, 158–163 (2004).

399. Allen, M. D., Freund, S. M. V, Bycroft, M. & Zinzalla, G. SWI/SNF subunit BAF155 N-terminus structure informs the impact of cancer-associated mutations and reveals a potential drug binding site. *Commun. Biol.* **4**, 528 (2021).

400. Skiniotis, G., Moazed, D. & Walz, T. Acetylated histone tail peptides induce structural rearrangements in the RSC chromatin remodeling complex. *J. Biol. Chem.* **282**, 20804–20808 (2007).

401. Shen, W. *et al.* Solution structure of human Brg1 bromodomain and its specific binding to acetylated histone tails. *Biochemistry* **46**, 2100–2110 (2007).

402. Hassan, A. H. *et al.* Function and selectivity of bromodomains in anchoring chromatin-modifying complexes to promoter nucleosomes. *Cell* **111**, 369–379 (2002).

403. Ferreira, H., Flaus, A. & Owen-Hughes, T. Histone modifications influence the action of Snf2 family remodelling enzymes by different mechanisms. *J. Mol. Biol.* **374**, 563–579 (2007).

404. Awad, S. & Hassan, A. H. The Swi2/Snf2 bromodomain is important for the full binding and remodeling

activity of the SWI/SNF complex on H3- and H4-acetylated nucleosomes. *Ann. N. Y. Acad. Sci.* **1138**, 366–375 (2008).

405. Pulice, J. L. & Kadoch, C. Composition and Function of Mammalian SWI/SNF Chromatin Remodeling Complexes in Human Disease. *Cold Spring Harb. Symp. Quant. Biol.* **81**, 53–60 (2016).

406. Porter, E. G. & Dykhuizen, E. C. Individual Bromodomains of Polybromo-1 Contribute to Chromatin Association and Tumor Suppression in Clear Cell Renal Carcinoma. *J. Biol. Chem.* **292**, 2601–2610 (2017).

407. Kebede, A. F. *et al.* Histone propionylation is a mark of active chromatin. *Nat. Struct. Mol. Biol.* **24**, 1048–1056 (2017).

408. Slaughter, M. J. *et al.* PBRM1 bromodomains variably influence nucleosome interactions and cellular function. *J. Biol. Chem.* **293**, 13592–13603 (2018).

409. Mitra, D., Parnell, E. J., Landon, J. W., Yu, Y. & Stillman, D. J. SWI/SNF binding to the HO promoter requires histone acetylation and stimulates TATA-binding protein recruitment. *Mol. Cell. Biol.* **26**, 4095–4110 (2006).

410. Chatterjee, N. *et al.* Histone H3 tail acetylation modulates ATP-dependent remodeling through multiple mechanisms. *Nucleic Acids Res.* **39**, 8378–8391 (2011).

411. Hassan, A. H., Neely, K. E. & Workman, J. L. Histone acetyltransferase complexes stabilize swi/snf binding to promoter nucleosomes. *Cell* **104**, 817–827 (2001).

412. Hassan, A. H., Awad, S. & Prochasson, P. The Swi2/Snf2 bromodomain is required for the displacement of SAGA and the octamer transfer of SAGA-acetylated nucleosomes. *J. Biol. Chem.* **281**, 18126–18134 (2006).

413. Suganuma, T. & Workman, J. L. Signals and combinatorial functions of histone modifications. *Annu. Rev. Biochem.* **80**, 473–499 (2011).

414. Soshnikova, N. V, Sheynov, A. A., Tatarskiy, E. V & Georgieva, S. G. The DPF Domain As a Unique Structural Unit Participating in Transcriptional Activation, Cell Differentiation, and Malignant Transformation. *Acta Naturae* **12**, 57–65 (2020).

415. Mashtalir, N. *et al.* Chromatin landscape signals differentially dictate the activities of mSWI/SNF family complexes. *Science* **373**, 306–315 (2021).

416. Peterson, C. L. Chromatin remodeling enzymes: taming the machines. Third in review series on chromatin dynamics. *EMBO Rep.* **3**, 319–322 (2002).

417. Skvortsova, K., Iovino, N. & Bogdanović, O. Functions and mechanisms of epigenetic inheritance in animals. *Nat. Rev. Mol. Cell Biol.* **19**, 774–790 (2018).

418. Tang, Y. *et al.* Linking long non-coding RNAs and SWI/SNF complexes to chromatin remodeling in cancer. *Mol. Cancer* **16**, 42 (2017).

419. Singh, M., D'Silva, L. & Holak, T. A. DNA-binding properties of the recombinant high-mobility-group-like AT-hook-containing region from human BRG1 protein. *Biol. Chem.* **387**, 1469–1478 (2006).

420. Filarsky, M. *et al.* The extended AT-hook is a novel RNA binding motif. *RNA Biol.* **12**, 864–876 (2015).

421. Wang, Y. *et al.* The long noncoding RNA lncTCF7 promotes self-renewal of human liver cancer stem cells through activation of Wnt signaling. *Cell Stem Cell* **16**, 413–425 (2015).

422. Chen, Z. *et al.* LncFZD6 initiates Wnt/β-catenin and liver TIC self-renewal through BRG1-mediated FZD6 transcriptional activation. *Oncogene* **37**, 3098–3112 (2018).

423. Chen, Z. *et al.* The long noncoding RNA lncZic2 drives the self-renewal of liver tumor-initiating cells via the protein kinase C substrates MARCKS and MARCKSL1. *J. Biol. Chem.* **293**, 7982–7992 (2018).

424. Liu, X. *et al.* A Long Noncoding RNA, Antisense IL-7, Promotes Inflammatory Gene Transcription through Facilitating Histone Acetylation and Switch/Sucrose Nonfermentable Chromatin Remodeling. *J. Immunol.* **203**, 1548–1559 (2019).

425. Han, P. *et al.* A long noncoding RNA protects the heart from pathological hypertrophy. *Nature* **514**, 102–106 (2014).

426. Zhu, P. *et al.* LncBRM initiates YAP1 signalling activation to drive self-renewal of liver cancer stem cells. *Nat. Commun.* **7**, 13608 (2016).

427. Kawaguchi, T. *et al.* SWI/SNF chromatin-remodeling complexes function in noncoding RNA-dependent

assembly of nuclear bodies. *Proc. Natl. Acad. Sci. U. S. A.* **112**, 4304–4309 (2015).

428. Fang, C. *et al.* Upregulation of lncRNA DGCR5 correlates with better prognosis and inhibits bladder cancer progression via transcriptionally facilitating P21 expression. *J. Cell. Physiol.* **234**, 6254–6262 (2019).

429. Cajigas, I. *et al.* Evf2 lncRNA/BRG1/DLX1 interactions reveal RNA-dependent inhibition of chromatin remodeling. *Development* **142**, 2641–2652 (2015).

430. Guo, X. *et al.* LncRNA LINC00163 upregulation suppresses lung cancer development though transcriptionally increasing TCF21 expression. *Am. J. Cancer Res.* **8**, 2494–2506 (2018).

431. Hu, G. *et al.* LincRNA-Cox2 Promotes Late Inflammatory Gene Transcription in Macrophages through Modulating SWI/SNF-Mediated Chromatin Remodeling. *J. Immunol.* **196**, 2799–2808 (2016).

432. Leisegang, M. S. *et al.* Long Noncoding RNA MANTIS Facilitates Endothelial Angiogenic Function. *Circulation* **136**, 65–79 (2017).

433. Yu, X. *et al.* Long non-coding RNA Linc-RAM enhances myogenic differentiation by interacting with MyoD. *Nat. Commun.* **8**, 14016 (2017).

434. Grossi, E. *et al.* A lncRNA-SWI/SNF complex crosstalk controls transcriptional activation at specific promoter regions. *Nat. Commun.* **11**, 936 (2020).

435. Zhou, X. *et al.* Long noncoding RNA CPS1-IT1 suppresses melanoma cell metastasis through inhibiting Cyr61 via competitively binding to BRG1. *J. Cell. Physiol.* **234**, 22017–22027 (2019).

436. Prensner, J. R. *et al.* The long noncoding RNA SChLAP1 promotes aggressive prostate cancer and antagonizes the SWI/SNF complex. *Nat. Genet.* **45**, 1392–1398 (2013).

437. Wang, X. *et al.* Long non-coding RNA urothelial carcinoma associated 1 induces cell replication by inhibiting BRG1 in 5637 cells. *Oncol. Rep.* **32**, 1281–1290 (2014).

438. Jégu, T. *et al.* Xist RNA antagonizes the SWI/SNF chromatin remodeler BRG1 on the inactive X chromosome. *Nat. Struct. Mol. Biol.* **26**, 96–109 (2019).

439. Lino Cardenas, C. L. *et al.* An HDAC9-MALAT1-BRG1 complex mediates smooth muscle dysfunction in thoracic aortic aneurysm. *Nat. Commun.* **9**, 1009 (2018).

440. Panatta, E. *et al.* Long non-coding RNA uc.291 controls epithelial differentiation by interfering with the ACTL6A/BAF complex. *EMBO Rep.* **21**, e46734 (2020).

441. Ming, N., Na, H. S. T., He, J.-L., Meng, Q.-T. & Xia, Z.-Y. Propofol alleviates oxidative stress via upregulating lncRNA-TUG1/Brg1 pathway in hypoxia/reoxygenation hepatic cells. *J. Biochem.* **166**, 415–421 (2019).

442. Cheng, S., Wang, L., Deng, C.-H., Du, S.-C. & Han, Z.-G. ARID1A represses hepatocellular carcinoma cell proliferation and migration through lncRNA MVIH. *Biochem. Biophys. Res. Commun.* **491**, 178–182 (2017).

443. Imai-Sumida, M. *et al.* Genistein Represses HOTAIR/Chromatin Remodeling Pathways to Suppress Kidney Cancer. *Cell. Physiol. Biochem. Int. J. Exp. Cell. Physiol. Biochem. Pharmacol.* **54**, 53–70 (2020).

444. Raab, J. R. *et al.* SWI/SNF remains localized to chromatin in the presence of SCHLAP1. *Nat. Genet.* **51**, 26–29 (2019).

445. G Hendrickson, D., Kelley, D. R., Tenen, D., Bernstein, B. & Rinn, J. L. Widespread RNA binding by chromatin-associated proteins. *Genome Biol.* **17**, 28 (2016).

446. Wei, Z. *et al.* Vitamin D Switches BAF Complexes to Protect β Cells. *Cell* **173**, 1135–1149 (2018).

447. Zhang, W. *et al.* PRMT5 restricts hepatitis B virus replication through epigenetic repression of covalently closed circular DNA transcription and interference with pregenomic RNA encapsidation. *Hepatology* **66**, 398–415 (2017).

448. Shu, X.-S. *et al.* The epigenetic modifier PBRM1 restricts the basal activity of the innate immune system by repressing retinoic acid-inducible gene-I-like receptor signalling and is a potential prognostic biomarker for colon cancer. *J. Pathol.* **244**, 36–48 (2018).

449. Agaimy, A. & Foulkes, W. D. Hereditary SWI/SNF complex deficiency syndromes. *Semin. Diagn. Pathol.* **35**, 193–198 (2018).

450. Kosho, T. & Okamoto, N. Genotype-phenotype correlation of Coffin-Siris syndrome caused by mutations in SMARCB1, SMARCA4, SMARCE1, and ARID1A. *Am. J. Med. Genet. C. Semin. Med. Genet.* **166C**, 262–275

(2014).

451. Vasileiou, G. *et al.* Mutations in the BAF-Complex Subunit DPF2 Are Associated with Coffin-Siris Syndrome. *Am. J. Hum. Genet.* **102**, 468–479 (2018).

452. van der Sluijs, P. J. *et al.* The ARID1B spectrum in 143 patients: from nonsyndromic intellectual disability to Coffin-Siris syndrome. *Genet. Med.* **21**, 1295–1307 (2019).

453. Machol, K. *et al.* Expanding the Spectrum of BAF-Related Disorders: De Novo Variants in SMARCC2 Cause a Syndrome with Intellectual Disability and Developmental Delay. *Am. J. Hum. Genet.* **104**, 164–178 (2019).

454. Vasko, A., Drivas, T. G. & Schrier Vergano, S. A. Genotype-Phenotype Correlations in 208 Individuals with Coffin-Siris Syndrome. *Genes (Basel).* **12**, (2021).

455. Moffat, J. J., Smith, A. L., Jung, E.-M., Ka, M. & Kim, W.-Y. Neurobiology of ARID1B haploinsufficiency related to neurodevelopmental and psychiatric disorders. *Mol. Psychiatry* (2021) doi:10.1038/s41380-021-01060-x.

456. Muchardt, C. & Yaniv, M. A human homologue of Saccharomyces cerevisiae SNF2/SWI2 and Drosophila brm genes potentiates transcriptional activation by the glucocorticoid receptor. *EMBO J.* **12**, 4279–4290 (1993).

457. Dunaief, J. L. *et al.* The retinoblastoma protein and BRG1 form a complex and cooperate to induce cell cycle arrest. *Cell* **79**, 119–130 (1994).

458. Strobeck, M. W. *et al.* BRG-1 is required for RB-mediated cell cycle arrest. *Proc. Natl. Acad. Sci. U. S. A.* **97**, 7748–7753 (2000).

459. Reisman, D. N. *et al.* Concomitant down-regulation of BRM and BRG1 in human tumor cell lines: differential effects on RB-mediated growth arrest vs CD44 expression. *Oncogene* **21**, 1196–1207 (2002).

460. Wong, A. K. *et al.* BRG1, a component of the SWI-SNF complex, is mutated in multiple human tumor cell lines. *Cancer Res.* **60**, 6171–6177 (2000).

461. Rosson, G. B., Bartlett, C., Reed, W. & Weissman, B. E. BRG1 loss in MiaPaCa2 cells induces an altered cellular morphology and disruption in the organization of the actin cytoskeleton. *J. Cell. Physiol.* **205**, 286–294 (2005).

462. Medina, P. P. *et al.* Frequent BRG1/SMARCA4-inactivating mutations in human lung cancer cell lines. *Hum. Mutat.* **29**, 617–622 (2008).

463. Shain, A. H. *et al.* Convergent structural alterations define SWItch/Sucrose NonFermentable (SWI/SNF) chromatin remodeler as a central tumor suppressive complex in pancreatic cancer. *Proc. Natl. Acad. Sci. U. S. A.* **109**, E252-9 (2012).

464. Reisman, D. N., Sciarrotta, J., Wang, W., Funkhouser, W. K. & Weissman, B. E. Loss of BRG1/BRM in human lung cancer cell lines and primary lung cancers: correlation with poor prognosis. *Cancer Res.* **63**, 560–566 (2003).

465. Medina, P. P. *et al.* Genetic and epigenetic screening for gene alterations of the chromatin-remodeling factor, SMARCA4/BRG1, in lung tumors. *Genes. Chromosomes Cancer* **41**, 170–177 (2004).

466. Yamamichi, N. *et al.* Frequent loss of Brm expression in gastric cancer correlates with histologic features and differentiation state. *Cancer Res.* **67**, 10727–10735 (2007).

467. Gunduz, E. *et al.* Genetic and epigenetic alterations of BRG1 promote oral cancer development. *Int. J. Oncol.* **26**, 201–210 (2005).

468. Bock, V. L. *et al.* BRM and BRG1 subunits of the SWI/SNF chromatin remodelling complex are downregulated upon progression of benign skin lesions into invasive tumours. *Br. J. Dermatol.* **164**, 1221–1227 (2011).

469. Decristofaro, M. F. *et al.* Characterization of SWI/SNF protein expression in human breast cancer cell lines and other malignancies. *J. Cell. Physiol.* **186**, 136–145 (2001).

470. Versteege, I. *et al.* Truncating mutations of hSNF5/INI1 in aggressive paediatric cancer. *Nature* **394**, 203–206 (1998).

471. Wang, X. *et al.* Expression of p270 (ARID1A), a component of human SWI/SNF complexes, in human tumors. *Int. J. cancer* **112**, 636 (2004).

472. Bailey, P. *et al.* Genomic analyses identify molecular subtypes of pancreatic cancer. *Nature* **531**, 47–52 (2016).

473. Dal Molin, M. *et al.* Loss of expression of the SWI/SNF chromatin remodeling subunit BRG1/SMARCA4 is

frequently observed in intraductal papillary mucinous neoplasms of the pancreas. *Hum. Pathol.* **43**, 585–591 (2012).

474. Tessier-Cloutier, B. *et al.* Loss of switch/sucrose non-fermenting complex protein expression in undifferentiated gastrointestinal and pancreatic carcinomas. *Histopathology* **77**, 46–54 (2020).

475. von Figura, G. *et al.* The chromatin regulator Brg1 suppresses formation of intraductal papillary mucinous neoplasm and pancreatic ductal adenocarcinoma. *Nat. Cell Biol.* **16**, 255–267 (2014).

476. Orvis, T. *et al.* BRG1/SMARCA4 inactivation promotes non-small cell lung cancer aggressiveness by altering chromatin organization. *Cancer Res.* **74**, 6486–6498 (2014).

477. Romero, O. A. *et al.* The tumour suppressor and chromatin-remodelling factor BRG1 antagonizes Myc activity and promotes cell differentiation in human cancer. *EMBO Mol. Med.* **4**, 603–616 (2012).

478. Jelinic, P. *et al.* Recurrent SMARCA4 mutations in small cell carcinoma of the ovary. *Nat. Genet.* **46**, 424–426 (2014).

479. Ramos, P. *et al.* Loss of the tumor suppressor SMARCA4 in small cell carcinoma of the ovary, hypercalcemic type (SCCOHT). *Rare Dis. (Austin, Tex.)* **2**, e967148 (2014).

480. Jelinic, P. *et al.* Concomitant loss of SMARCA2 and SMARCA4 expression in small cell carcinoma of the ovary, hypercalcemic type. *Mod. Pathol. an Off. J. United States Can. Acad. Pathol. Inc* **29**, 60–66 (2016).

481. Karnezis, A. N. *et al.* Dual loss of the SWI/SNF complex ATPases SMARCA4/BRG1 and SMARCA2/BRM is highly sensitive and specific for small cell carcinoma of the ovary, hypercalcaemic type. *J. Pathol.* **238**, 389–400 (2016).

482. Orlando, K. A. *et al.* Re-expression of SMARCA4/BRG1 in small cell carcinoma of ovary, hypercalcemic type (SCCOHT) promotes an epithelial-like gene signature through an AP-1-dependent mechanism. *Elife* **9**, (2020).

483. Parsons, D. W. *et al.* The genetic landscape of the childhood cancer medulloblastoma. *Science* **331**, 435–439 (2011).

484. Pugh, T. J. *et al.* Medulloblastoma exome sequencing uncovers subtype-specific somatic mutations. *Nature* **488**, 106–110 (2012).

485. Robinson, G. *et al.* Novel mutations target distinct subgroups of medulloblastoma. *Nature* **488**, 43–48 (2012).

486. Yoshikawa, Y. *et al.* Biallelic germline and somatic mutations in malignant mesothelioma: multiple mutations in transcription regulators including mSWI/SNF genes. *Int. J. cancer* **136**, 560–571 (2015).

487. Bellini, A. *et al.* Study of chromatin remodeling genes implicates SMARCA4 as a putative player in oncogenesis in neuroblastoma. *Int. J. cancer* **145**, 2781–2791 (2019).

488. Agaimy, A. *et al.* Loss of expression of the SWI/SNF complex is a frequent event in undifferentiated/dedifferentiated urothelial carcinoma of the urinary tract. *Virchows Arch.* **469**, 321–330 (2016).

489. Horton, R. K. *et al.* SMARCA4/SMARCA2-deficient Carcinoma of the Esophagus and Gastroesophageal Junction. *Am. J. Surg. Pathol.* **45**, 414–420 (2021).

490. Bultman, S. J. *et al.* Characterization of mammary tumors from Brg1 heterozygous mice. *Oncogene* **27**, 460–468 (2008).

491. Serber, D. W. *et al.* The BRG1 chromatin remodeler protects against ovarian cysts, uterine tumors, and mammary tumors in a lineage-specific manner. *PLoS One* **7**, e31346 (2012).

492. Aldiri, I. *et al.* Brg1 coordinates multiple processes during retinogenesis and is a tumor suppressor in retinoblastoma. *Development* **142**, 4092–4106 (2015).

493. Metovic, J., Bianchi, F., Barella, M., Papotti, M. & Pelosi, G. SMARCA2 Deficiency While Preserving SMARCA4 and SMARCB1 in Lung Neuroendocrine Carcinomas. *Journal of thoracic oncology : official publication of the International Association for the Study of Lung Cancer* vol. 16 e32–e35 (2021).

494. Wu, J. *et al.* Inactivation of SMARCA2 by promoter hypermethylation drives lung cancer development. *Gene* **687**, 193–199 (2019).

495. Ehrenhöfer-Wölfer, K. *et al.* SMARCA2-deficiency confers sensitivity to targeted inhibition of SMARCA4 in

esophageal squamous cell carcinoma cell lines. *Sci. Rep.* **9**, 11661 (2019).

496. Wiegand, K. C. *et al.* ARID1A mutations in endometriosis-associated ovarian carcinomas. *N. Engl. J. Med.* **363**, 1532–1543 (2010).

497. Jones, S. *et al.* Frequent mutations of chromatin remodeling gene ARID1A in ovarian clear cell carcinoma. *Science* **330**, 228–231 (2010).

498. Network, C. G. A. R. Integrated genomic analyses of ovarian carcinoma. *Nature* **474**, 609–615 (2011).

499. Huang, H.-N., Lin, M.-C., Huang, W.-C., Chiang, Y.-C. & Kuo, K.-T. Loss of ARID1A expression and its relationship with PI3K-Akt pathway alterations and ZNF217 amplification in ovarian clear cell carcinoma. *Mod. Pathol. an Off. J. United States Can. Acad. Pathol. Inc* **27**, 983–990 (2014).

500. Coatham, M. *et al.* Concurrent ARID1A and ARID1B inactivation in endometrial and ovarian dedifferentiated carcinomas. *Mod. Pathol. an Off. J. United States Can. Acad. Pathol. Inc* **29**, 1586–1593 (2016).

501. Guan, B., Wang, T.-L. & Shih, I.-M. ARID1A, a factor that promotes formation of SWI/SNF-mediated chromatin remodeling, is a tumor suppressor in gynecologic cancers. *Cancer Res.* **71**, 6718–6727 (2011).

502. Guan, B. *et al.* Mutation and loss of expression of ARID1A in uterine low-grade endometrioid carcinoma. *Am. J. Surg. Pathol.* **35**, 625–632 (2011).

503. Wiegand, K. C. *et al.* Loss of BAF250a (ARID1A) is frequent in high-grade endometrial carcinomas. *J. Pathol.* **224**, 328–333 (2011).

504. Biankin, A. V *et al.* Pancreatic cancer genomes reveal aberrations in axon guidance pathway genes. *Nature* **491**, 399–405 (2012).

505. Wang, W. *et al.* ARID1A, a SWI/SNF subunit, is critical to acinar cell homeostasis and regeneration and is a barrier to transformation and epithelial-mesenchymal transition in the pancreas. *Gut* **68**, 1245–1258 (2019).

506. Kimura, Y. *et al.* ARID1A Maintains Differentiation of Pancreatic Ductal Cells and Inhibits Development of Pancreatic Ductal Adenocarcinoma in Mice. *Gastroenterology* **155**, 194-209.e2 (2018).

507. Wang, K. *et al.* Exome sequencing identifies frequent mutation of ARID1A in molecular subtypes of gastric cancer. *Nat. Genet.* **43**, 1219–1223 (2011).

508. Zang, Z. J. *et al.* Exome sequencing of gastric adenocarcinoma identifies recurrent somatic mutations in cell adhesion and chromatin remodeling genes. *Nat. Genet.* **44**, 570–574 (2012).

509. Wiegand, K. C. *et al.* ARID1A/BAF250a as a prognostic marker for gastric carcinoma: a study of 2 cohorts. *Hum. Pathol.* **45**, 1258–1268 (2014).

510. Yan, H.-B. *et al.* Reduced expression of the chromatin remodeling gene ARID1A enhances gastric cancer cell migration and invasion via downregulation of E-cadherin transcription. *Carcinogenesis* **35**, 867–876 (2014).

511. Zhang, Q. *et al.* Chromatin remodeling gene AT-rich interactive domain-containing protein 1A suppresses gastric cancer cell proliferation by targeting PIK3CA and PDK1. *Oncotarget* **7**, 46127–46141 (2016).

512. Imielinski, M. *et al.* Mapping the hallmarks of lung adenocarcinoma with massively parallel sequencing. *Cell* **150**, 1107–1120 (2012).

513. Govindan, R. *et al.* Genomic landscape of non-small cell lung cancer in smokers and never-smokers. *Cell* **150**, 1121–1134 (2012).

514. Sun, D. *et al.* Loss of ARID1A expression promotes lung adenocarcinoma metastasis and predicts a poor prognosis. *Cell. Oncol. (Dordr).* (2021) doi:10.1007/s13402-021-00616-x.

515. Jang, S.-H. *et al.* Loss of ARID1A expression is associated with poor prognosis in non-small cell lung cancer. *Pathol. Res. Pract.* **216**, 153156 (2020).

516. Zhang, Y. *et al.* ARID1A is downregulated in non-small cell lung cancer and regulates cell proliferation and apoptosis. *Tumour Biol. J. Int. Soc. Oncodevelopmental Biol. Med.* **35**, 5701–5707 (2014).

517. Yoshimoto, Y. *et al.* Mutation profiling of uterine cervical cancer patients treated with definitive radiotherapy. *Gynecol. Oncol.* **159**, 546–553 (2020).

518. Cho, H. *et al.* Loss of ARID1A/BAF250a expression is linked to tumor progression and adverse prognosis in cervical cancer. *Hum. Pathol.* **44**, 1365–1374 (2013).

519. Yang, Y., Zhao, X. & Li, H.-X. MiR-221 and miR-222 simultaneously target ARID1A and enhance proliferation

and invasion of cervical cancer cells. *Eur. Rev. Med. Pharmacol. Sci.* **20**, 1509–1515 (2016).

520. Lichner, Z. *et al.* The chromatin remodeling gene ARID1A is a new prognostic marker in clear cell renal cell carcinoma. *Am. J. Pathol.* **182**, 1163–1170 (2013).

521. Cancer Genome Atlas Research Network. Comprehensive molecular characterization of clear cell renal cell carcinoma. *Nature* **499**, 43–49 (2013).

522. Park, J. H. *et al.* Decreased ARID1A expression correlates with poor prognosis of clear cell renal cell carcinoma. *Hum. Pathol.* **46**, 454–460 (2015).

523. Somsuan, K. *et al.* ARID1A knockdown triggers epithelial-mesenchymal transition and carcinogenesis features of renal cells: role in renal cell carcinoma. *FASEB J. Off. Publ. Fed. Am. Soc. Exp. Biol.* **33**, 12226–12239 (2019).

524. Lee, J.-H., Ahn, B. K., Baik, S. S. & Lee, K. H. Comprehensive Analysis of Somatic Mutations in Colorectal Cancer With Peritoneal Metastasis. *In Vivo* **33**, 447–452 (2019).

525. Cajuso, T. *et al.* Exome sequencing reveals frequent inactivating mutations in ARID1A, ARID1B, ARID2 and ARID4A in microsatellite unstable colorectal cancer. *Int. J. cancer* **135**, 611–623 (2014).

526. Xie, C., Fu, L., Han, Y., Li, Q. & Wang, E. Decreased ARID1A expression facilitates cell proliferation and inhibits 5-fluorouracil-induced apoptosis in colorectal carcinoma. *Tumour Biol. J. Int. Soc. Oncodevelopmental Biol. Med.* **35**, 7921–7927 (2014).

527. Wei, X.-L. *et al.* Clinicopathologic and prognostic relevance of ARID1A protein loss in colorectal cancer. *World J. Gastroenterol.* **20**, 18404–18412 (2014).

528. Erfani, M. *et al.* ARID1A regulates E-cadherin expression in colorectal cancer cells: a promising candidate therapeutic target. *Mol. Biol. Rep.* **48**, 6749–6756 (2021).

529. Kaseb, A. O. *et al.* Molecular Profiling of Hepatocellular Carcinoma Using Circulating Cell-Free DNA. *Clin. cancer Res. an Off. J. Am. Assoc. Cancer Res.* **25**, 6107–6118 (2019).

530. Howell, J. *et al.* Identification of mutations in circulating cell-free tumour DNA as a biomarker in hepatocellular carcinoma. *Eur. J. Cancer* **116**, 56–66 (2019).

531. Fujimoto, A. *et al.* Whole-genome sequencing of liver cancers identifies etiological influences on mutation patterns and recurrent mutations in chromatin regulators. *Nat. Genet.* **44**, 760–764 (2012).

532. Xiao, Y. *et al.* Loss of ARID1A Promotes Hepatocellular Carcinoma Progression via Up-regulation of MYC Transcription. *J. Clin. Transl. Hepatol.* **9**, 528–536 (2021).

533. Yim, S. Y. *et al.* Low ARID1A Expression is Associated with Poor Prognosis in Hepatocellular Carcinoma. *Cells* **9**, (2020).

534. Sun, X. *et al.* Arid1a Has Context-Dependent Oncogenic and Tumor Suppressor Functions in Liver Cancer. *Cancer Cell* **32**, 574-589.e6 (2017).

535. Hoppe, S. *et al.* Genomic and Transcriptomic Characteristics of Esophageal Adenocarcinoma. *Cancers (Basel).* **13**, (2021).

536. Ozawa, Y. *et al.* Decreased expression of ARID1A contributes to infiltrative growth of esophageal squamous cell carcinoma. *Tohoku J. Exp. Med.* **235**, 185–191 (2015).

537. Lee, S. H. *et al.* ARID1B alterations identify aggressive tumors in neuroblastoma. *Oncotarget* **8**, 45943–45950 (2017).

538. Sausen, M. *et al.* Integrated genomic analyses identify ARID1A and ARID1B alterations in the childhood cancer neuroblastoma. *Nat. Genet.* **45**, 12–17 (2013).

539. Cimmino, F., Lasorsa, V. A., Vetrella, S., Iolascon, A. & Capasso, M. A Targeted Gene Panel for Circulating Tumor DNA Sequencing in Neuroblastoma. *Front. Oncol.* **10**, 596191 (2020).

540. Shi, H. *et al.* ARID1A loss in neuroblastoma promotes the adrenergic-to-mesenchymal transition by regulating enhancer-mediated gene expression. *Sci. Adv.* **6**, 1–12 (2020).

541. García-López, J. *et al.* Large 1p36 Deletions Affecting Arid1a Locus Facilitate Mycn-Driven Oncogenesis in Neuroblastoma. *Cell Rep.* **30**, 454-464.e5 (2020).

542. Li, C. *et al.* ARID1A gene knockdown promotes neuroblastoma migration and invasion. *Neoplasma* **64**, 367–

376 (2017).

543. Giulino-Roth, L. *et al.* Targeted genomic sequencing of pediatric Burkitt lymphoma identifies recurrent alterations in antiapoptotic and chromatin-remodeling genes. *Blood* **120**, 5181–5184 (2012).

544. Saqcena, M. *et al.* SWI/SNF Complex Mutations Promote Thyroid Tumor Progression and Insensitivity to Redifferentiation Therapies. *Cancer Discov.* **11**, 1158–1175 (2021).

545. Padul, V., Epari, S., Moiyadi, A., Shetty, P. & Shirsat, N. V. ETV/Pea3 family transcription factor-encoding genes are overexpressed in CIC-mutant oligodendrogliomas. *Genes. Chromosomes Cancer* **54**, 725–733 (2015).

546. Zhang, X. *et al.* Frequent low expression of chromatin remodeling gene ARID1A in breast cancer and its clinical significance. *Cancer Epidemiol.* **36**, 288–293 (2012).

547. Mao, Q. *et al.* Whole-exon sequencing insights into pancreatic synovial sarcoma: a case report. *Gland surgery* vol. 10 1812–1818 (2021).

548. Botta, G. P. *et al.* SWI/SNF complex alterations as a biomarker of immunotherapy efficacy in pancreatic cancer. *JCI insight* **6**, (2021).

549. Khursheed, M. *et al.* ARID1B, a member of the human SWI/SNF chromatin remodeling complex, exhibits tumour-suppressor activities in pancreatic cancer cell lines. *Br. J. Cancer* **108**, 2056–2062 (2013).

550. Kang, E.-Y. *et al.* Loss of ARID1B and SMARCB1 expression are specific for the diagnosis of dedifferentiated/undifferentiated carcinoma in tumours of the upper gynaecological tract and cervix. *Histopathology* **79**, 160–167 (2021).

551. Tordella, L. *et al.* SWI/SNF regulates a transcriptional program that induces senescence to prevent liver cancer. *Genes Dev.* **30**, 2187–2198 (2016).

552. Deogharkar, A. *et al.* Downregulation of ARID1B, a tumor suppressor in the WNT subgroup medulloblastoma, activates multiple oncogenic signaling pathways. *Hum. Mol. Genet.* **30**, 1721–1733 (2021).

553. Li, M. *et al.* Inactivating mutations of the chromatin remodeling gene ARID2 in hepatocellular carcinoma. *Nat. Genet.* **43**, 828–829 (2011).

554. You, J. *et al.* ARID2, p110α, p53, and β-catenin protein expression in hepatocellular carcinoma and clinicopathologic implications. *Human pathology* vol. 46 1068–1077 (2015).

555. Jiang, H. *et al.* Chromatin remodeling factor ARID2 suppresses hepatocellular carcinoma metastasis via DNMT1-Snail axis. *Proc. Natl. Acad. Sci. U. S. A.* **117**, 4770–4780 (2020).

556. Duan, Y. *et al.* Chromatin remodeling gene ARID2 targets cyclin D1 and cyclin E1 to suppress hepatoma cell progression. *Oncotarget* **7**, 45863–45875 (2016).

557. Manceau, G. *et al.* Recurrent inactivating mutations of ARID2 in non-small cell lung carcinoma. *Int. J. cancer* **132**, 2217–2221 (2013).

558. Moreno, T. *et al.* ARID2 deficiency promotes tumor progression and is associated with higher sensitivity to chemotherapy in lung cancer. *Oncogene* **40**, 2923–2935 (2021).

559. Bala, P. *et al.* Exome sequencing identifies ARID2 as a novel tumor suppressor in early-onset sporadic rectal cancer. *Oncogene* **40**, 863–874 (2021).

560. Varela, I. *et al.* Exome sequencing identifies frequent mutation of the SWI/SNF complex gene PBRM1 in renal carcinoma. *Nature* **469**, 539–542 (2011).

561. da Costa, W. H. *et al.* Polybromo-1 (PBRM1), a SWI/SNF complex subunit is a prognostic marker in clear cell renal cell carcinoma. *BJU Int.* **113**, E157-63 (2014).

562. Cai, W. *et al.* PBRM1 acts as a p53 lysine-acetylation reader to suppress renal tumor growth. *Nat. Commun.* **10**, 5800 (2019).

563. Kim, K. H. & Roberts, C. W. M. Mechanisms by which SMARCB1 loss drives rhabdoid tumor growth. *Cancer Genet.* **207**, 365–372 (2014).

564. Roberts, C. W., Galusha, S. A., McMenamin, M. E., Fletcher, C. D. & Orkin, S. H. Haploinsufficiency of Snf5 (integrase interactor 1) predisposes to malignant rhabdoid tumors in mice. *Proc. Natl. Acad. Sci. U. S. A.* **97**, 13796–13800 (2000).

565. Betz, B. L., Strobeck, M. W., Reisman, D. N., Knudsen, E. S. & Weissman, B. E. Re-expression of hSNF5/INI1/BAF47 in pediatric tumor cells leads to G1 arrest associated with induction of p16ink4a and activation of RB. *Oncogene* **21**, 5193–5203 (2002).

566. Uno, K. *et al.* Aberrations of the hSNF5/INI1 gene are restricted to malignant rhabdoid tumors or atypical teratoid/rhabdoid tumors in pediatric solid tumors. *Genes. Chromosomes Cancer* **34**, 33–41 (2002).

567. Sápi, Z. *et al.* Epigenetic regulation of SMARCB1 By miR-206, -381 and -671-5p is evident in a variety of SMARCB1 immunonegative soft tissue sarcomas, while miR-765 appears specific for epithelioid sarcoma. A miRNA study of 223 soft tissue sarcomas. *Genes. Chromosomes Cancer* **55**, 786–802 (2016).

568. Li, L. *et al.* Concurrent loss of INI1, PBRM1, and BRM expression in epithelioid sarcoma: implications for the cocontributions of multiple SWI/SNF complex members to pathogenesis. *Hum. Pathol.* **45**, 2247–2254 (2014).

569. Eelloo, J. A. *et al.* Multiple primary malignancies associated with a germline SMARCB1 pathogenic variant. *Fam. Cancer* **18**, 445–449 (2019).

570. Grand, F. *et al.* Frequent deletion of hSNF5/INI1, a component of the SWI/SNF complex, in chronic myeloid leukemia. *Cancer Res.* **59**, 3870–3874 (1999).

571. Chatterjee, S. S., Biswas, M., Boila, L. D., Banerjee, D. & Sengupta, A. SMARCB1 Deficiency Integrates Epigenetic Signals to Oncogenic Gene Expression Program Maintenance in Human Acute Myeloid Leukemia. *Mol. Cancer Res.* **16**, 791–804 (2018).

572. Kohashi, K. *et al.* Reduced expression of SMARCB1/INI1 protein in synovial sarcoma. *Mod. Pathol. an Off. J. United States Can. Acad. Pathol. Inc* **23**, 981–990 (2010).

573. Li, J. *et al.* A Role for SMARCB1 in Synovial Sarcomagenesis Reveals That SS18-SSX Induces Canonical BAF Destruction. *Cancer Discov.* **11**, 2620–2637 (2021).

574. Morin, R. D. *et al.* Frequent mutation of histone-modifying genes in non-Hodgkin lymphoma. *Nature* **476**, 298–303 (2011).

575. Chapman, M. A. *et al.* Initial genome sequencing and analysis of multiple myeloma. *Nature* **471**, 467–472 (2011).

576. DelBove, J. *et al.* Identification of a core member of the SWI/SNF complex, BAF155/SMARCC1, as a human tumor suppressor gene. *Epigenetics* **6**, 1444–1453 (2011).

577. Xiao, Z.-M. *et al.* SMARCC1 Suppresses Tumor Progression by Inhibiting the PI3K/AKT Signaling Pathway in Prostate Cancer. *Front. cell Dev. Biol.* **9**, 678967 (2021).

578. Park, Y.-A. *et al.* Tumor suppressive effects of bromodomain-containing protein 7 (BRD7) in epithelial ovarian carcinoma. *Clin. cancer Res. an Off. J. Am. Assoc. Cancer Res.* **20**, 565–575 (2014).

579. Gao, Y., Wang, B. & Gao, S. BRD7 Acts as a Tumor Suppressor Gene in Lung Adenocarcinoma. *PLoS One* **11**, e0156701 (2016).

580. Wu, W.-J. *et al.* Prognostic relevance of BRD7 expression in colorectal carcinoma. *Eur. J. Clin. Invest.* **43**, 131–140 (2013).

581. Yu, X., Li, Z. & Shen, J. BRD7: a novel tumor suppressor gene in different cancers. *Am. J. Transl. Res.* **8**, 742–748 (2016).

582. Wang, L. *et al.* The BRG1- and hBRM-associated factor BAF57 induces apoptosis by stimulating expression of the cylindromatosis tumor suppressor gene. *Mol. Cell. Biol.* **25**, 7953–7965 (2005).

583. Tropée, R. *et al.* The SWI/SNF subunit SMARCD3 regulates cell cycle progression and predicts survival outcome in ER+ breast cancer. *Breast Cancer Res. Treat.* **185**, 601–614 (2021).

584. Chandler, R. L. *et al.* Coexistent ARID1A-PIK3CA mutations promote ovarian clear-cell tumorigenesis through pro-tumorigenic inflammatory cytokine signalling. *Nat. Commun.* **6**, 6118 (2015).

585. Reyes, J. C. *et al.* Altered control of cellular proliferation in the absence of mammalian brahma (SNF2alpha). *EMBO J.* **17**, 6979–6991 (1998).

586. Bultman, S. *et al.* A Brg1 null mutation in the mouse reveals functional differences among mammalian SWI/SNF complexes. *Mol. Cell* **6**, 1287–1295 (2000).

587. Young, R. H., Oliva, E. & Scully, R. E. Small cell carcinoma of the ovary, hypercalcemic type. A clinicopathological analysis of 150 cases. *Am. J. Surg. Pathol.* **18**, 1102–1116 (1994).

588. Ogino, S., Ro, T. Y. & Redline, R. W. Malignant rhabdoid tumor: A phenotype? An entity?--A controversy revisited. *Adv. Anat. Pathol.* **7**, 181–190 (2000).

589. Oda, Y. & Tsuneyoshi, M. Extrarenal rhabdoid tumors of soft tissue: clinicopathological and molecular genetic review and distinction from other soft-tissue sarcomas with rhabdoid features. *Pathol. Int.* **56**, 287–295 (2006).

590. Parham, D. M., Weeks, D. A. & Beckwith, J. B. The clinicopathologic spectrum of putative extrarenal rhabdoid tumors. An analysis of 42 cases studied with immunohistochemistry or electron microscopy. *Am. J. Surg. Pathol.* **18**, 1010–1029 (1994).

591. Bhattacharjee, M. *et al.* Central nervous system atypical teratoid/rhabdoid tumors of infancy and childhood. *Ultrastruct. Pathol.* **21**, 369–378 (1997).

592. Romagosa, C. *et al.* p16(Ink4a) overexpression in cancer: a tumor suppressor gene associated with senescence and high-grade tumors. *Oncogene* **30**, 2087–2097 (2011).

593. Versteege, I., Medjkane, S., Rouillard, D. & Delattre, O. A key role of the hSNF5/INI1 tumour suppressor in the control of the G1-S transition of the cell cycle. *Oncogene* **21**, 6403–6412 (2002).

594. Tsikitis, M., Zhang, Z., Edelman, W., Zagzag, D. & Kalpana, G. V. Genetic ablation of Cyclin D1 abrogates genesis of rhabdoid tumors resulting from Ini1 loss. *Proc. Natl. Acad. Sci. U. S. A.* **102**, 12129–12134 (2005).

595. Jagani, Z. *et al.* Loss of the tumor suppressor Snf5 leads to aberrant activation of the Hedgehog-Gli pathway. *Nat. Med.* **16**, 1429–1433 (2010).

596. Mora-Blanco, E. L. *et al.* Activation of β-catenin/TCF targets following loss of the tumor suppressor SNF5. *Oncogene* **33**, 933–938 (2014).

597. Doan, D. N. *et al.* Loss of the INI1 tumor suppressor does not impair the expression of multiple BRG1-dependent genes or the assembly of SWI/SNF enzymes. *Oncogene* **23**, 3462–3473 (2004).

598. Wilson, B. G. *et al.* Epigenetic antagonism between polycomb and SWI/SNF complexes during oncogenic transformation. *Cancer Cell* **18**, 316–328 (2010).

599. Lualdi, E. *et al.* Molecular cytogenetic characterization of proximal-type epithelioid sarcoma. *Genes. Chromosomes Cancer* **41**, 283–290 (2004).

600. Papp, G. *et al.* SMARCB1 protein and mRNA loss is not caused by promoter and histone hypermethylation in epithelioid sarcoma. *Mod. Pathol. an Off. J. United States Can. Acad. Pathol. Inc* **26**, 393–403 (2013).

601. Holdhof, D. *et al.* Atypical teratoid/rhabdoid tumors (ATRTs) with SMARCA4 mutation are molecularly distinct from SMARCB1-deficient cases. *Acta Neuropathol.* **141**, 291–301 (2021).

602. Andrianteranagna, M. *et al.* SMARCA4-deficient rhabdoid tumours show intermediate molecular features between SMARCB1-deficient rhabdoid tumours and small cell carcinomas of the ovary, hypercalcaemic type. *J. Pathol.* **255**, 1–15 (2021).

603. Fahiminiya, S. *et al.* Molecular analyses reveal close similarities between small cell carcinoma of the ovary, hypercalcemic type and atypical teratoid/rhabdoid tumor. *Oncotarget* **7**, 1732–1740 (2016).

604. Foulkes, W. D. *et al.* No small surprise - small cell carcinoma of the ovary, hypercalcaemic type, is a malignant rhabdoid tumour. *J. Pathol.* **233**, 209–214 (2014).

605. Gazendam, A. M. *et al.* Synovial Sarcoma: A Clinical Review. *Curr. Oncol.* **28**, 1909–1920 (2021).

606. Clark, J. *et al.* Identification of novel genes, SYT and SSX, involved in the t(X;18)(p11.2;q11.2) translocation found in human synovial sarcoma. *Nat. Genet.* **7**, 502–508 (1994).

607. de Leeuw, B., Balemans, M., Olde Weghuis, D. & Geurts van Kessel, A. Identification of two alternative fusion genes, SYT-SSX1 and SYT-SSX2, in t(X;18)(p11.2;q11.2)-positive synovial sarcomas. *Hum. Mol. Genet.* **4**, 1097–1099 (1995).

608. Crew, A. J. *et al.* Fusion of SYT to two genes, SSX1 and SSX2, encoding proteins with homology to the Kruppel-associated box in human synovial sarcoma. *EMBO J.* **14**, 2333–2340 (1995).

609. Lin, H., Wong, R. P. C., Martinka, M. & Li, G. BRG1 expression is increased in human cutaneous melanoma. *Br.*

J. Dermatol. **163**, 502–510 (2010).

610. Keenen, B., Qi, H., Saladi, S. V, Yeung, M. & de la Serna, I. L. Heterogeneous SWI/SNF chromatin remodeling complexes promote expression of microphthalmia-associated transcription factor target genes in melanoma. *Oncogene* **29**, 81–92 (2010).

611. Vachtenheim, J., Ondrusová, L. & Borovanský, J. SWI/SNF chromatin remodeling complex is critical for the expression of microphthalmia-associated transcription factor in melanoma cells. *Biochem. Biophys. Res. Commun.* **392**, 454–459 (2010).

612. Ondrušová, L., Vachtenheim, J., Réda, J., Záková, P. & Benková, K. MITF-independent pro-survival role of BRG1-containing SWI/SNF complex in melanoma cells. *PLoS One* **8**, e54110 (2013).

613. Saladi, S. V. *et al.* Modulation of extracellular matrix/adhesion molecule expression by BRG1 is associated with increased melanoma invasiveness. *Mol. Cancer* **9**, 280 (2010).

614. Saladi, S. V *et al.* BRG1 promotes survival of UV-irradiated melanoma cells by cooperating with MITF to activate the melanoma inhibitor of apoptosis gene. *Pigment Cell Melanoma Res.* **26**, 377–391 (2013).

615. Zhang, L., Nemzow, L., Chen, H., Hu, J. J. & Gong, F. Whole genome expression profiling shows that BRG1 transcriptionally regulates UV inducible genes and other novel targets in human cells. *PLoS One* **9**, e105764 (2014).

616. Shi, J. *et al.* Role of SWI/SNF in acute leukemia maintenance and enhancer-mediated Myc regulation. *Genes Dev.* **27**, 2648–2662 (2013).

617. Buscarlet, M. *et al.* Essential role of BRG, the ATPase subunit of BAF chromatin remodeling complexes, in leukemia maintenance. *Blood* **123**, 1720–1728 (2014).

618. Cruickshank, V. A. *et al.* SWI/SNF Subunits SMARCA4, SMARCD2 and DPF2 Collaborate in MLL-Rearranged Leukaemia Maintenance. *PLoS One* **10**, e0142806 (2015).

619. Watanabe, T., Semba, S. & Yokozaki, H. Regulation of PTEN expression by the SWI/SNF chromatin-remodelling protein BRG1 in human colorectal carcinoma cells. *Br. J. Cancer* **104**, 146–154 (2011).

620. Barker, N. *et al.* The chromatin remodelling factor Brg-1 interacts with beta-catenin to promote target gene activation. *EMBO J.* **20**, 4935–4943 (2001).

621. Sun, A. *et al.* Aberrant expression of SWI/SNF catalytic subunits BRG1/BRM is associated with tumor development and increased invasiveness in prostate cancers. *Prostate* **67**, 203–213 (2007).

622. Shen, H. *et al.* The SWI/SNF ATPase Brm is a gatekeeper of proliferative control in prostate cancer. *Cancer Res.* **68**, 10154–10162 (2008).

623. Giles, K. A. *et al.* BRG1 knockdown inhibits proliferation through multiple cellular pathways in prostate cancer. *Clin. Epigenetics* **13**, 37 (2021).

624. Bai, J. *et al.* BRG1 is a prognostic marker and potential therapeutic target in human breast cancer. *PLoS One* **8**, e59772 (2013).

625. Wu, Q. *et al.* The SWI/SNF ATPases Are Required for Triple Negative Breast Cancer Cell Proliferation. *J. Cell. Physiol.* **230**, 2683–2694 (2015).

626. Wu, Q. *et al.* Targeting the chromatin remodeling enzyme BRG1 increases the efficacy of chemotherapy drugs in breast cancer cells. *Oncotarget* **7**, 27158–27175 (2016).

627. Kaufmann, B. *et al.* BRG1 promotes hepatocarcinogenesis by regulating proliferation and invasiveness. *PLoS One* **12**, e0180225 (2017).

628. Sentani, K. *et al.* Increased expression but not genetic alteration of BRG1, a component of the SWI/SNF complex, is associated with the advanced stage of human gastric carcinomas. *Pathobiology* **69**, 315–320 (2001).

629. Shi, X., Wang, Q., Gu, J., Xuan, Z. & Wu, J. I. SMARCA4/Brg1 coordinates genetic and epigenetic networks underlying Shh-type medulloblastoma development. *Oncogene* **35**, 5746–5758 (2016).

630. Jubierre, L. *et al.* BRG1/SMARCA4 is essential for neuroblastoma cell viability through modulation of cell death and survival pathways. *Oncogene* **35**, 5179–5190 (2016).

631. Wang, Y. *et al.* Brahma-Related Gene-1 (BRG1) promotes the malignant phenotype of glioblastoma cells. *J.*

Cell. Mol. Med. **25**, 2956–2966 (2021).

632. Sethuraman, A. *et al.* SMARCE1 regulates metastatic potential of breast cancer cells through the HIF1A/PTK2 pathway. *Breast Cancer Res.* **18**, 81 (2016).

633. García-Pedrero, J. M., Kiskinis, E., Parker, M. G. & Belandia, B. The SWI/SNF chromatin remodeling subunit BAF57 is a critical regulator of estrogen receptor function in breast cancer cells. *J. Biol. Chem.* **281**, 22656–22664 (2006).

634. Sokol, E. S. *et al.* SMARCE1 is required for the invasive progression of in situ cancers. *Proc. Natl. Acad. Sci. U. S. A.* **114**, 4153–4158 (2017).

635. Link, K. A. *et al.* Targeting the BAF57 SWI/SNF subunit in prostate cancer: a novel platform to control androgen receptor activity. *Cancer Res.* **68**, 4551–4558 (2008).

636. Balasubramaniam, S. *et al.* Aberrant BAF57 signaling facilitates prometastatic phenotypes. *Clin. cancer Res. an Off. J. Am. Assoc. Cancer Res.* **19**, 2657–2667 (2013).

637. Yamaguchi, T. *et al.* Expression of BAF57 in ovarian cancer cells and drug sensitivity. *Cancer Sci.* **106**, 359–366 (2015).

638. Liu, H., Zhao, Y.-R., Chen, B., Ge, Z. & Huang, J.-S. High expression of SMARCE1 predicts poor prognosis and promotes cell growth and metastasis in gastric cancer. *Cancer Manag. Res.* **11**, 3493–3509 (2019).

639. Saladi, S. V. *et al.* ACTL6A Is Co-Amplified with p63 in Squamous Cell Carcinoma to Drive YAP Activation, Regenerative Proliferation, and Poor Prognosis. *Cancer Cell* **31**, 35–49 (2017).

640. Li, R.-Z., Li, Y.-Y., Qin, H. & Li, S.-S. ACTL6A Promotes the Proliferation of Esophageal Squamous Cell Carcinoma Cells and Correlates with Poor Clinical Outcomes. *Onco. Targets. Ther.* **14**, 199–211 (2021).

641. Taulli, R. *et al.* Failure to downregulate the BAF53a subunit of the SWI/SNF chromatin remodeling complex contributes to the differentiation block in rhabdomyosarcoma. *Oncogene* **33**, 2354–2362 (2014).

642. Faraj, S. F. *et al.* ARID1A immunohistochemistry improves outcome prediction in invasive urothelial carcinoma of urinary bladder. *Hum. Pathol.* **45**, 2233–2239 (2014).

643. Wang, B. *et al.* Expression of ARID1B Is Associated With Poor Outcomes and Predicts the Benefit from Adjuvant Chemotherapy in Bladder Urothelial Carcinoma. *J. Cancer* **8**, 3490–3497 (2017).

644. Heebøll, S. *et al.* SMARCC1 expression is upregulated in prostate cancer and positively correlated with tumour recurrence and dedifferentiation. *Histol. Histopathol.* **23**, 1069–1076 (2008).

645. Hiramatsu, H. *et al.* The role of the SWI/SNF chromatin remodeling complex in maintaining the stemness of glioma initiating cells. *Sci. Rep.* **7**, 889 (2017).

646. Zhou, Y. *et al.* Enhanced SMARCD1, a subunit of the SWI/SNF complex, promotes liver cancer growth through the mTOR pathway. *Clin. Sci. (Lond).* **134**, 1457–1472 (2020).

647. Wessely, A., Steeb, T., Berking, C. & Heppt, M. V. How Neural Crest Transcription Factors Contribute to Melanoma Heterogeneity, Cellular Plasticity, and Treatment Resistance. *Int. J. Mol. Sci.* **22**, (2021).

648. Park, J., Wood, M. A. & Cole, M. D. BAF53 forms distinct nuclear complexes and functions as a critical c-Myc-interacting nuclear cofactor for oncogenic transformation. *Mol. Cell. Biol.* **22**, 1307–1316 (2002).

649. Helming, K. C., Wang, X. & Roberts, C. W. M. Vulnerabilities of mutant SWI/SNF complexes in cancer. *Cancer Cell* **26**, 309–317 (2014).

650. Wanior, M., Krämer, A., Knapp, S. & Joerger, A. C. Exploiting vulnerabilities of SWI/SNF chromatin remodelling complexes for cancer therapy. *Oncogene* **40**, 3637–3654 (2021).

651. Oike, T. *et al.* A synthetic lethality-based strategy to treat cancers harboring a genetic deficiency in the chromatin remodeling factor BRG1. *Cancer Res.* **73**, 5508–5518 (2013).

652. Hoffman, G. R. *et al.* Functional epigenetics approach identifies BRM/SMARCA2 as a critical synthetic lethal target in BRG1-deficient cancers. *Proc. Natl. Acad. Sci. U. S. A.* **111**, 3128–3133 (2014).

653. Wilson, B. G. *et al.* Residual complexes containing SMARCA2 (BRM) underlie the oncogenic drive of SMARCA4 (BRG1) mutation. *Mol. Cell. Biol.* **34**, 1136–1144 (2014).

654. Zernickel, E. *et al.* Targeting of BRM Sensitizes BRG1-Mutant Lung Cancer Cell Lines to Radiotherapy. *Mol. Cancer Ther.* **18**, 656–666 (2019).

655. Vangamudi, B. *et al.* The SMARCA2/4 ATPase Domain Surpasses the Bromodomain as a Drug Target in SWI/SNF-Mutant Cancers: Insights from cDNA Rescue and PFI-3 Inhibitor Studies. *Cancer Res.* **75**, 3865–3878 (2015).

656. Helming, K. C. *et al.* ARID1B is a specific vulnerability in ARID1A-mutant cancers. *Nat. Med.* **20**, 251–254 (2014).

657. Sato, E. *et al.* ARID1B as a Potential Therapeutic Target for ARID1A-Mutant Ovarian Clear Cell Carcinoma. *Int. J. Mol. Sci.* **19**, (2018).

658. Mathur, R. *et al.* ARID1A loss impairs enhancer-mediated gene regulation and drives colon cancer in mice. *Nat. Genet.* **49**, 296–302 (2017).

659. Niedermaier, B. *et al.* Targeting ARID1A-mutant colorectal cancer: depletion of ARID1B increases radiosensitivity and modulates DNA damage response. *Sci. Rep.* **9**, 18207 (2019).

660. Kelso, T. W. R. *et al.* Chromatin accessibility underlies synthetic lethality of SWI/SNF subunits in ARID1A-mutant cancers. *Elife* **6**, e30506 (2017).

661. Krämer, K. F., Moreno, N., Frühwald, M. C. & Kerl, K. BRD9 Inhibition, Alone or in Combination with Cytostatic Compounds as a Therapeutic Approach in Rhabdoid Tumors. *Int. J. Mol. Sci.* **18**, (2017).

662. Brien, G. L. *et al.* Targeted degradation of BRD9 reverses oncogenic gene expression in synovial sarcoma. *Elife* **7**, (2018).

663. Schick, S. *et al.* Systematic characterization of BAF mutations provides insights into intracomplex synthetic lethalities in human cancers. *Nat. Genet.* **51**, 1399–1410 (2019).

664. Kim, K. H. *et al.* SWI/SNF-mutant cancers depend on catalytic and non-catalytic activity of EZH2. *Nat. Med.* **21**, 1491–1496 (2015).

665. Januario, T. *et al.* PRC2-mediated repression of SMARCA2 predicts EZH2 inhibitor activity in SWI/SNF mutant tumors. *Proc. Natl. Acad. Sci. U. S. A.* **114**, 12249–12254 (2017).

666. Chan-Penebre, E. *et al.* Selective Killing of SMARCA2- and SMARCA4-deficient Small Cell Carcinoma of the Ovary, Hypercalcemic Type Cells by Inhibition of EZH2: In Vitro and In Vivo Preclinical Models. *Mol. Cancer Ther.* **16**, 850–860 (2017).

667. Bitler, B. G., Aird, K. M. & Zhang, R. Epigenetic synthetic lethality in ovarian clear cell carcinoma: EZH2 and ARID1A mutations. *Mol. Cell. Oncol.* **3**, e1032476 (2016).

668. Knutson, S. K. *et al.* Durable tumor regression in genetically altered malignant rhabdoid tumors by inhibition of methyltransferase EZH2. *Proc. Natl. Acad. Sci. U. S. A.* **110**, 7922–7927 (2013).

669. Wu, S. *et al.* SWI/SNF catalytic subunits' switch drives resistance to EZH2 inhibitors in ARID1A-mutated cells. *Nat. Commun.* **9**, 4116 (2018).

670. Berns, K. *et al.* ARID1A mutation sensitizes most ovarian clear cell carcinomas to BET inhibitors. *Oncogene* **37**, 4611–4625 (2018).

671. Bitler, B. G. *et al.* ARID1A-mutated ovarian cancers depend on HDAC6 activity. *Nat. Cell Biol.* **19**, 962–973 (2017).

672. Fukumoto, T. *et al.* Repurposing Pan-HDAC Inhibitors for ARID1A-Mutated Ovarian Cancer. *Cell Rep.* **22**, 3393–3400 (2018).

673. Fukumoto, T. *et al.* HDAC6 Inhibition Synergizes with Anti-PD-L1 Therapy in ARID1A-Inactivated Ovarian Cancer. *Cancer Res.* **79**, 5482–5489 (2019).

674. Romero, O. A. *et al.* SMARCA4 deficient tumours are vulnerable to KDM6A/UTX and KDM6B/JMJD3 blockade. *Nat. Commun.* **12**, 4319 (2021).

675. Davidson, J., Shen, Z., Gong, X. & Pollack, J. R. SWI/SNF aberrations sensitize pancreatic cancer cells to DNA crosslinking agents. *Oncotarget* **9**, 9608–9617 (2018).

676. Lee, D. *et al.* The Bromodomain Inhibitor PFI-3 Sensitizes Cancer Cells to DNA Damage by Targeting SWI/SNF. *Mol. Cancer Res.* **19**, 900–912 (2021).

677. Oba, A. *et al.* ARID2 modulates DNA damage response in human hepatocellular carcinoma cells. *J. Hepatol.* **66**, 942–951 (2017).

678. Ogiwara, H. *et al.* Targeting the Vulnerability of Glutathione Metabolism in ARID1A-Deficient Cancers. *Cancer Cell* **35**, 177-190.e8 (2019).

679. Sasaki, M. *et al.* Efficacy of glutathione inhibitors for the treatment of ARID1A-deficient diffuse-type gastric cancers. *Biochem. Biophys. Res. Commun.* **522**, 342–347 (2020).

680. Shen, J. *et al.* ARID1A Deficiency Impairs the DNA Damage Checkpoint and Sensitizes Cells to PARP Inhibitors. *Cancer Discov.* **5**, 752–767 (2015).

681. Park, Y. *et al.* Loss of ARID1A in Tumor Cells Renders Selective Vulnerability to Combined Ionizing Radiation and PARP Inhibitor Therapy. *Clin. cancer Res. an Off. J. Am. Assoc. Cancer Res.* **25**, 5584–5594 (2019).

682. Gupta, M. *et al.* BRG1 Loss Predisposes Lung Cancers to Replicative Stress and ATR Dependency. *Cancer Res.* **80**, 3841–3854 (2020).

683. Chory, E. J. *et al.* Chemical Inhibitors of a Selective SWI/SNF Function Synergize with ATR Inhibition in Cancer Cell Killing. *ACS Chem. Biol.* **15**, 1685–1696 (2020).

684. Wu, C. *et al.* Targeting AURKA-CDC25C axis to induce synthetic lethality in ARID1A-deficient colorectal cancer cells. *Nat. Commun.* **9**, 3212 (2018).

685. Xue, Y. *et al.* SMARCA4 loss is synthetic lethal with CDK4/6 inhibition in non-small cell lung cancer. *Nat. Commun.* **10**, 557 (2019).

686. Xue, Y. *et al.* CDK4/6 inhibitors target SMARCA4-determined cyclin D1 deficiency in hypercalcemic small cell carcinoma of the ovary. *Nat. Commun.* **10**, 558 (2019).

687. Lissanu Deribe, Y. *et al.* Mutations in the SWI/SNF complex induce a targetable dependence on oxidative phosphorylation in lung cancer. *Nat. Med.* **24**, 1047–1057 (2018).

688. Chabanon, R. M., Morel, D. & Postel-Vinay, S. Exploiting epigenetic vulnerabilities in solid tumors: Novel therapeutic opportunities in the treatment of SWI/SNF-defective cancers. *Semin. Cancer Biol.* **61**, 180–198 (2020).

689. Fedorov, O. *et al.* Selective targeting of the BRG/PB1 bromodomains impairs embryonic and trophoblast stem cell maintenance. *Sci. Adv.* **1**, e1500723 (2015).

690. Clark, P. G. K. *et al.* LP99: Discovery and Synthesis of the First Selective BRD7/9 Bromodomain Inhibitor. *Angew. Chem. Weinheim. Bergstr. Ger.* **127**, 6315–6319 (2015).

691. Myrianthopoulos, V. *et al.* Discovery and Optimization of a Selective Ligand for the Switch/Sucrose Nonfermenting-Related Bromodomains of Polybromo Protein-1 by the Use of Virtual Screening and Hydration Analysis. *J. Med. Chem.* **59**, 8787–8803 (2016).

692. Mélin, L. *et al.* Design and Synthesis of LM146, a Potent Inhibitor of PB1 with an Improved Selectivity Profile over SMARCA2. *ACS omega* **6**, 21327–21338 (2021).

693. Lu, T. *et al.* Identification of small molecule inhibitors targeting the SMARCA2 bromodomain from a high-throughput screening assay. *Acta Pharmacol. Sin.* **39**, 1544–1552 (2018).

694. Zheng, P. *et al.* Design, synthesis and biological evaluation of imidazo[1,5-a]pyrazin-8(7H)-one derivatives as BRD9 inhibitors. *Bioorg. Med. Chem.* **27**, 1391–1404 (2019).

695. Theodoulou, N. H. *et al.* Discovery of I-BRD9, a Selective Cell Active Chemical Probe for Bromodomain Containing Protein 9 Inhibition. *J. Med. Chem.* **59**, 1425–1439 (2016).

696. Martin, L. J. *et al.* Structure-Based Design of an in Vivo Active Selective BRD9 Inhibitor. *J. Med. Chem.* **59**, 4462–4475 (2016).

697. Sutherell, C. L. *et al.* Identification and Development of 2,3-Dihydropyrrolo[1,2-a]quinazolin-5(1H)-one Inhibitors Targeting Bromodomains within the Switch/Sucrose Nonfermenting Complex. *J. Med. Chem.* **59**, 5095–5101 (2016).

698. Wanior, M. *et al.* Pan-SMARCA/PB1 Bromodomain Inhibitors and Their Role in Regulating Adipogenesis. *J. Med. Chem.* **63**, 14680–14699 (2020).

699. Hohmann, A. F. *et al.* Sensitivity and engineered resistance of myeloid leukemia cells to BRD9 inhibition. *Nat. Chem. Biol.* **12**, 672–679 (2016).

700. Farnaby, W. *et al.* BAF complex vulnerabilities in cancer demonstrated via structure-based PROTAC design.

Nat. Chem. Biol. **15**, 672–680 (2019).

701. Remillard, D. *et al.* Degradation of the BAF Complex Factor BRD9 by Heterobifunctional Ligands. *Angew. Chem. Int. Ed.* **56**, 5738–5743 (2017).

702. Zoppi, V. *et al.* Iterative Design and Optimization of Initially Inactive Proteolysis Targeting Chimeras (PROTACs) Identify VZ185 as a Potent, Fast, and Selective von Hippel-Lindau (VHL) Based Dual Degrader Probe of BRD9 and BRD7. *J. Med. Chem.* **62**, 699–726 (2019).

703. Papillon, J. P. N. *et al.* Discovery of Orally Active Inhibitors of Brahma Homolog (BRM)/SMARCA2 ATPase Activity for the Treatment of Brahma Related Gene 1 (BRG1)/SMARCA4-Mutant Cancers. *J. Med. Chem.* **61**, 10155–10172 (2018).

704. Marian, C. A. *et al.* Small Molecule Targeting of Specific BAF (mSWI/SNF) Complexes for HIV Latency Reversal. *Cell Chem. Biol.* **25**, 1443-1455.e14 (2018).

705. Toure, M. & Crews, C. M. Small-Molecule PROTACS: New Approaches to Protein Degradation. *Angew. Chem. Int. Ed. Engl.* **55**, 1966–1973 (2016).

706. Siegel, R. L., Miller, K. D., Fuchs, H. E. & Jemal, A. Cancer Statistics, 2021. *CA. Cancer J. Clin.* **71**, 7–33 (2021).

707. Ward, E., DeSantis, C., Robbins, A., Kohler, B. & Jemal, A. Childhood and adolescent cancer statistics, 2014. *CA. Cancer J. Clin.* **64**, 83–103 (2014).

708. Downing, J. R. *et al.* The Pediatric Cancer Genome Project. *Nat. Genet.* **44**, 619–622 (2012).

709. Maris, J. M. Recent Advances in Neuroblastoma. *N Engl J Med* **362**, 2202–2211 (2010).

710. Irwin, M. S. & Park, J. R. Neuroblastoma: Paradigm for precision medicine. *Pediatr. Clin. North Am.* **62**, 225–256 (2015).

711. Tomolonis, J. A., Agarwal, S. & Shohet, J. M. Neuroblastoma pathogenesis: deregulation of embryonic neural crest development. *Cell Tissue Res.* **372**, 245–262 (2018).

712. Marshall, G. M. *et al.* The prenatal origins of cancer. *Nature reviews. Cancer* vol. 14 277–289 (2014).

713. Matthay, K. K. *et al.* Neuroblastoma. *Nat. Rev. Dis. Prim.* **2**, 16078 (2016).

714. Reiff, T. *et al.* Neuroblastoma phox2b variants stimulate proliferation and dedifferentiation of immature sympathetic neurons. *J. Neurosci.* **30**, 905–915 (2010).

715. Krona, C. *et al.* Analysis of neuroblastoma tumour progression; loss of PHOX2B on 4p13 and 17q gain are early events in neuroblastoma tumourigenesis. *Int. J. Oncol.* **32**, 575–583 (2008).

716. Bourdeaut, F. *et al.* Germline mutations of the paired-like homeobox 2B (PHOX2B) gene in neuroblastoma. *Cancer Lett.* **228**, 51–58 (2005).

717. Caron, H. *et al.* Allelic loss of chromosome 1p as a predictor of unfavorable outcome in patients with neuroblastoma. *N. Engl. J. Med.* **334**, 225–230 (1996).

718. Attiyeh, E. F. *et al.* Chromosome 1p and 11q Deletions and Outcome in Neuroblastoma. *N Engl J Med* **353**, 2243–53 (2005).

719. Carén, H. *et al.* High-risk neuroblastoma tumors with 11q-deletion display a poor prognostic, chromosome instability phenotype with later onset. *Proc. Natl. Acad. Sci. U. S. A.* **107**, 4323–4328 (2010).

720. Theissen, J. *et al.* Chromosome 17/17q gain and unaltered profiles in high resolution array-CGH are prognostically informative in neuroblastoma. *Genes. Chromosomes Cancer* **53**, 639–649 (2014).

721. Bown, N. *et al.* 17q gain in neuroblastoma predicts adverse clinical outcome. U.K. Cancer Cytogenetics Group and the U.K. Children's Cancer Study Group. *Med. Pediatr. Oncol.* **36**, 14–19 (2001).

722. Schleiermacher, G. *et al.* Segmental chromosomal alterations lead to a higher risk of relapse in infants with MYCN-non-amplified localised unresectable/disseminated neuroblastoma (a SIOPEN collaborative study). *Br. J. Cancer* **105**, 1940–1948 (2011).

723. George, R. E. *et al.* Hyperdiploidy plus nonamplified MYCN confers a favorable prognosis in children 12 to 18 months old with disseminated neuroblastoma: a Pediatric Oncology Group study. *J. Clin. Oncol. Off. J. Am. Soc. Clin. Oncol.* **23**, 6466–6473 (2005).

724. Schwab, M. *et al.* Amplified DNA with limited homology to myc cellular oncogene is shared by human neuroblastoma cell lines and a neuroblastoma tumour. *Nature* **305**, 245–248 (1983).

725. Adhikary, S. & Eilers, M. Transcriptional regulation and transformation by Myc proteins. *Nat. Rev. Mol. Cell Biol.* **6**, 635–645 (2005).

726. Look, A. T. *et al.* Clinical relevance of tumor cell ploidy and N-myc gene amplification in childhood neuroblastoma: a Pediatric Oncology Group study. *J. Clin. Oncol. Off. J. Am. Soc. Clin. Oncol.* **9**, 581–591 (1991).

727. Weiss, W. A., Aldape, K., Mohapatra, G., Feuerstein, B. G. & Bishop, J. M. Targeted expression of MYCN causes neuroblastoma in transgenic mice. *EMBO J.* **16**, 2985–2995 (1997).

728. Huang, M. & Weiss, W. A. Neuroblastoma and MYCN. *Cold Spring Harb. Perspect. Med.* **3**, a014415 (2013).

729. Wang, C. *et al.* Alternative approaches to target Myc for cancer treatment. *Signal Transduct. Target. Ther.* **6**, 117 (2021).

730. Chen, Y. *et al.* Oncogenic mutations of ALK kinase in neuroblastoma. *Nature* **455**, 971–974 (2008).

731. Janoueix-Lerosey, I. *et al.* Somatic and germline activating mutations of the ALK kinase receptor in neuroblastoma. *Nature* **455**, 967–970 (2008).

732. Heukamp, L. C. *et al.* Targeted expression of mutated ALK induces neuroblastoma in transgenic mice. *Sci. Transl. Med.* **4**, (2012).

733. Berry, T. *et al.* The ALK(F1174L) mutation potentiates the oncogenic activity of MYCN in neuroblastoma. *Cancer Cell* **22**, 117–130 (2012).

734. Mossé, Y. P. *et al.* Identification of ALK as a major familial neuroblastoma predisposition gene. *Nature* **455**, 930–935 (2008).

735. De La Fuente, R., Baumann, C. & Viveiros, M. M. Role of ATRX in chromatin structure and function: implications for chromosome instability and human disease. *Reproduction* **142**, 221–234 (2011).

736. Cheung, N.-K. V *et al.* Association of age at diagnosis and genetic mutations in patients with neuroblastoma. *JAMA* **307**, 1062–1071 (2012).

737. Peifer, M. *et al.* Telomerase activation by genomic rearrangements in high-risk neuroblastoma. *Nature* **526**, 700–704 (2015).

738. Kaatsch, P. Epidemiology of childhood cancer. *Cancer Treat. Rev.* **36**, 277–285 (2010).

739. Vo, K. T. *et al.* Clinical, biologic, and prognostic differences on the basis of primary tumor site in neuroblastoma: a report from the international neuroblastoma risk group project. *J. Clin. Oncol. Off. J. Am. Soc. Clin. Oncol.* **32**, 3169–3176 (2014).

740. Maris, J. M., Hogarty, M. D., Bagatell, R. & Cohn, S. L. Neuroblastoma. *Lancet* **369**, 2106–2120 (2007).

741. Brodeur, G. M. *et al.* Revisions of the international criteria for neuroblastoma diagnosis, staging, and response to treatment. *J. Clin. Oncol. Off. J. Am. Soc. Clin. Oncol.* **11**, 1466–1477 (1993).

742. Monclair, T. *et al.* The International Neuroblastoma Risk Group (INRG) staging system: an INRG Task Force report. *J. Clin. Oncol. Off. J. Am. Soc. Clin. Oncol.* **27**, 298–303 (2009).

743. Du, W., Hozumi, N., Sakamoto, M., Hata, J. & Yamada, T. Reconstitution of Schwannian stroma in neuroblastomas using human bone marrow stromal cells. *Am. J. Pathol.* **173**, 1153–1164 (2008).

744. Mora, J. *et al.* Neuroblastic and Schwannian stromal cells of neuroblastoma are derived from a tumoral progenitor cell. *Cancer Res.* **61**, 6892–6898 (2001).

745. Pudela, C., Balyasny, S. & Applebaum, M. A. Nervous system: Embryonal tumors: Neuroblastoma. *Atlas Genet. Cytogenet. Oncol. Haematol.* **24**, 284–290 (2020).

746. Shimada, H. *et al.* International Neuroblastoma Pathology Classification for prognostic evaluation of patients with peripheral neuroblastic tumors: A report from the Children's Cancer Group. *Cancer* **92**, 2451–2461 (2001).

747. Brodeur, G. M. Spontaneous regression of neuroblastoma. *Cell Tissue Res.* **372**, 277–286 (2018).

748. Carlsen, N. L. How frequent is spontaneous remission of neuroblastomas? Implications for screening. *Br. J. Cancer* **61**, 441–446 (1990).

749. Brodeur, G. M. & Bagatell, R. Mechanisms of neuroblastoma regression. *Nat. Rev. Clin. Oncol.* **11**, 704–713 (2014).

750. Pinto, N. R. *et al.* Advances in Risk Classification and Treatment Strategies for Neuroblastoma. *J. Clin. Oncol. Off. J. Am. Soc. Clin. Oncol.* **33**, 3008–3017 (2015).

751. Strother, D. R. *et al.* Outcome after surgery alone or with restricted use of chemotherapy for patients with low-risk neuroblastoma: results of Children's Oncology Group study P9641. *J. Clin. Oncol. Off. J. Am. Soc. Clin. Oncol.* **30**, 1842–1848 (2012).

752. Rubie, H. *et al.* Excellent outcome with reduced treatment in infants with nonmetastatic and unresectable neuroblastoma without MYCN amplification: results of the prospective INES 99.1. *J. Clin. Oncol. Off. J. Am. Soc. Clin. Oncol.* **29**, 449–455 (2011).

753. Nuchtern, J. G. *et al.* A prospective study of expectant observation as primary therapy for neuroblastoma in young infants: a Children's Oncology Group study. *Ann. Surg.* **256**, 573–580 (2012).

754. Baker, D. L. *et al.* Outcome after reduced chemotherapy for intermediate-risk neuroblastoma. *N. Engl. J. Med.* **363**, 1313–1323 (2010).

755. Kohler, J. A. *et al.* Treatment of children over the age of one year with unresectable localised neuroblastoma without MYCN amplification: results of the SIOPEN study. *Eur. J. Cancer* **49**, 3671–3679 (2013).

756. Ladenstein, R. *et al.* Randomized Trial of prophylactic granulocyte colony-stimulating factor during rapid COJEC induction in pediatric patients with high-risk neuroblastoma: the European HR-NBL1/SIOPEN study. *J. Clin. Oncol. Off. J. Am. Soc. Clin. Oncol.* **28**, 3516–3524 (2010).

757. Matthay, K. K. *et al.* Treatment of high-risk neuroblastoma with intensive chemotherapy, radiotherapy, autologous bone marrow transplantation, and 13-cis-retinoic acid. Children's Cancer Group. *N. Engl. J. Med.* **341**, 1165–1173 (1999).

758. Ladenstein, R. *et al.* Busulfan and melphalan versus carboplatin, etoposide, and melphalan as high-dose chemotherapy for high-risk neuroblastoma (HR-NBL1/SIOPEN): an international, randomised, multi-arm, open-label, phase 3 trial. *Lancet. Oncol.* **18**, 500–514 (2017).

759. Cheung, N.-K. V *et al.* Murine anti-GD2 monoclonal antibody 3F8 combined with granulocyte-macrophage colony-stimulating factor and 13-cis-retinoic acid in high-risk patients with stage 4 neuroblastoma in first remission. *J. Clin. Oncol. Off. J. Am. Soc. Clin. Oncol.* **30**, 3264–3270 (2012).

760. Simon, T. *et al.* Treatment and outcomes of patients with relapsed, high-risk neuroblastoma: results of German trials. *Pediatr. Blood Cancer* **56**, 578–583 (2011).

761. London, W. B. *et al.* Clinical and biologic features predictive of survival after relapse of neuroblastoma: a report from the International Neuroblastoma Risk Group project. *J. Clin. Oncol. Off. J. Am. Soc. Clin. Oncol.* **29**, 3286–3292 (2011).

762. Moreno, L. *et al.* Accelerating drug development for neuroblastoma: Summary of the Second Neuroblastoma Drug Development Strategy forum from Innovative Therapies for Children with Cancer and International Society of Paediatric Oncology Europe Neuroblastoma. *Eur. J. Cancer* **136**, 52–68 (2020).

763. Durinck, K. & Speleman, F. Epigenetic regulation of neuroblastoma development. *Cell Tissue Res.* **372**, 309–324 (2018).

764. Teitz, T. *et al.* Caspase 8 is deleted or silenced preferentially in childhood neuroblastomas with amplification of MYCN. *Nat. Med.* **6**, 529–535 (2000).

765. Alaminos, M., Davalos, V., Cheung, N.-K. V, Gerald, W. L. & Esteller, M. Clustering of gene hypermethylation associated with clinical risk groups in neuroblastoma. *J. Natl. Cancer Inst.* **96**, 1208–1219 (2004).

766. Grau, E. *et al.* Hypermethylation of apoptotic genes as independent prognostic factor in neuroblastoma disease. *Mol. Carcinog.* **50**, 153–162 (2011).

767. Henrich, K.-O., Schwab, M. & Westermann, F. 1p36 tumor suppression--a matter of dosage? *Cancer Res.* **72**, 6079–6088 (2012).

768. Gómez, S. *et al.* DNA methylation fingerprint of neuroblastoma reveals new biological and clinical insights. *Epigenomics* **7**, 1137–1153 (2015).

769. Decock, A. *et al.* Stage 4S neuroblastoma tumors show a characteristic DNA methylation portrait. *Epigenetics* **11**, 761–771 (2016).

770. Olsson, M., Beck, S., Kogner, P., Martinsson, T. & Carén, H. Genome-wide methylation profiling identifies

novel methylated genes in neuroblastoma tumors. *Epigenetics* **11**, 74–84 (2016).

771. Henrich, K.-O. *et al.* Integrative Genome-Scale Analysis Identifies Epigenetic Mechanisms of Transcriptional Deregulation in Unfavorable Neuroblastomas. *Cancer Res.* **76**, 5523–5537 (2016).

772. Gartlgruber, M. *et al.* Super enhancers define regulatory subtypes and cell identity in neuroblastoma. *Nat. Cancer* **2**, 114–128 (2021).

773. Oldridge, D. A. *et al.* Genetic predisposition to neuroblastoma mediated by a LMO1 super-enhancer polymorphism. *Nature* **528**, 418–421 (2015).

774. Saint-André, V. *et al.* Models of human core transcriptional regulatory circuitries. *Genome Res.* **26**, 385–396 (2016).

775. Boeva, V. *et al.* Heterogeneity of neuroblastoma cell identity defined by transcriptional circuitries. *Nat. Genet.* **49**, 1408–1413 (2017).

776. Sahu, D. *et al.* Co-expression analysis identifies long noncoding RNA SNHG1 as a novel predictor for event-free survival in neuroblastoma. *Oncotarget* **7**, 58022–58037 (2016).

777. Pandey, G. K. *et al.* The risk-associated long noncoding RNA NBAT-1 controls neuroblastoma progression by regulating cell proliferation and neuronal differentiation. *Cancer Cell* **26**, 722–737 (2014).

778. Bi, S. *et al.* LncRNA-MALAT1-mediated Axl promotes cell invasion and migration in human neuroblastoma. *Tumour Biol. J. Int. Soc. Oncodevelopmental Biol. Med.* **39**, 1010428317699796 (2017).

779. Bartolucci, S. *et al.* Effect of cytidine analogs on cell growth and differentiation on a human neuroblastoma line. *Cell Biophys.* **15**, 67–77 (1989).

780. Carpinelli, P., Granata, F., Augusti-Tocco, G., Rossi, M. & Bartolucci, S. Antiproliferative effects and DNA hypomethylation by 5-aza-2′-deoxycytidine in human neuroblastoma cell lines. *Anticancer. Drugs* **4**, 629–635 (1993).

781. Qiu, Y.-Y., Mirkin, B. L. & Dwivedi, R. S. Inhibition of DNA methyltransferase reverses cisplatin induced drug resistance in murine neuroblastoma cells. *Cancer Detect. Prev.* **29**, 456–463 (2005).

782. Charlet, J., Schnekenburger, M., Brown, K. W. & Diederich, M. DNA demethylation increases sensitivity of neuroblastoma cells to chemotherapeutic drugs. *Biochem. Pharmacol.* **83**, 858–865 (2012).

783. Puissant, A. *et al.* Targeting MYCN in neuroblastoma by BET bromodomain inhibition. *Cancer Discov.* **3**, 308–323 (2013).

784. Henssen, A. *et al.* Targeting MYCN-Driven Transcription By BET-Bromodomain Inhibition. *Clin. cancer Res. an Off. J. Am. Assoc. Cancer Res.* **22**, 2470–2481 (2016).

785. Potts, R. C. *et al.* CHD5, a brain-specific paralog of Mi2 chromatin remodeling enzymes, regulates expression of neuronal genes. *PLoS One* **6**, e24515 (2011).

786. Higashi, M. *et al.* Retinoic acid-induced CHD5 upregulation and neuronal differentiation of neuroblastoma. *Mol. Cancer* **14**, 150 (2015).

787. Bagchi, A. *et al.* CHD5 is a tumor suppressor at human 1p36. *Cell* **128**, 459–475 (2007).

788. Quan, J., Adelmant, G., Marto, J. A., Look, A. T. & Yusufzai, T. The chromatin remodeling factor CHD5 is a transcriptional repressor of WEE1. *PLoS One* **9**, e108066 (2014).

789. Takeuchi, T. *et al.* Expression of SMARCF1, a truncated form of SWI1, in neuroblastoma. *Am. J. Pathol.* **158**, 663–672 (2001).

790. Suryo Rahmanto, Y. *et al.* Inactivating ARID1A Tumor Suppressor Enhances TERT Transcription and Maintains Telomere Length in Cancer Cells. *J. Biol. Chem.* **291**, 9690–9699 (2016).

791. Vasileiou, G. *et al.* Chromatin-Remodeling-Factor ARID1B Represses Wnt/β-Catenin Signaling. *Am. J. Hum. Genet.* **97**, 445–456 (2015).

792. Esposito, M. R. *et al.* Somatic mutations in specific and connected subpathways are associated with short neuroblastoma patients' survival and indicate proteins targetable at onset of disease. *Int. J. cancer* **143**, 2525–2536 (2018).

793. Bairoch, A. The Cellosaurus, a Cell-Line Knowledge Resource. *J. Biomol. Tech.* **29**, 25–38 (2018).

794. Naldini, L. *et al.* In Vivo Gene Delivery and Stable Transduction of Nondividing Cells by a Lentiviral Vector.

Science **272**, 263–267 (1996).

795. Zufferey, R. *et al.* Self-Inactivating Lentivirus Vector for Safe and Efficient In Vivo Gene Delivery. *J. Virol.* **72**, 9873–9880 (1998).

796. Perkins, D. N., Pappin, D. J., Creasy, D. M. & Cottrell, J. S. Probability-based protein identification by searching sequence databases using mass spectrometry data. *Electrophoresis* **20**, 3551–3567 (1999).

797. Choi, H. *et al.* SAINT: probabilistic scoring of affinity purification-mass spectrometry data. *Nat. Methods* **8**, 70–73 (2011).

798. Trizzino, M. *et al.* The Tumor Suppressor ARID1A Controls Global Transcription via Pausing of RNA Polymerase II. *Cell Rep.* **23**, 3933–3945 (2018).

799. Dobin, A. *et al.* STAR: ultrafast universal RNA-seq aligner. *Bioinformatics* **29**, 15–21 (2013).

800. Li, B. & Dewey, C. N. RSEM: accurate transcript quantification from RNA-Seq data with or without a reference genome. *BMC Bioinformatics* **12**, 323 (2011).

801. Love, M. I., Huber, W. & Anders, S. Moderated estimation of fold change and dispersion for RNA-seq data with DESeq2. *Genome Biol.* **15**, 550 (2014).

802. Subramanian, A. *et al.* Gene set enrichment analysis: A knowledge-based approach for interpreting genome-wide expression profiles. *Proc. Natl. Acad. Sci. U. S. A.* **102**, 15545–50 (2005).

803. Mootha, V. K. *et al.* PGC-1α-responsive genes involved in oxidative phosphorylation are coordinately downregulated in human diabetes. *Nat. Genet.* **34**, 267–273 (2003).

804. Saeed, A. I. *et al.* TM4: a free, open-source system for microarray data management and analysis. *Biotechniques* **34**, 374–378 (2003).

805. Masanas, M. *et al.* The oral KIF11 inhibitor 4SC-205 exhibits antitumor activity and potentiates standard and targeted therapies in primary and metastatic neuroblastoma models. *Clinical and translational medicine* vol. 11 e533 (2021).

806. Halgren, T. A. Identifying and characterizing binding sites and assessing druggability. *J. Chem. Inf. Model.* **49**, 377–389 (2009).

807. Schmidtke, P., Bidon-Chanal, A., Luque, F. J. & Barril, X. MDpocket: open-source cavity detection and characterization on molecular dynamics trajectories. *Bioinformatics* **27**, 3276–3285 (2011).

808. Larkin, M. A. *et al.* Clustal W and Clustal X version 2.0. *Bioinformatics* **23**, 2947–2948 (2007).

809. Irwin, J. J., Sterling, T., Mysinger, M. M., Bolstad, E. S. & Coleman, R. G. ZINC: a free tool to discover chemistry for biology. *J. Chem. Inf. Model.* **52**, 1757–1768 (2012).

810. Friesner, R. A. *et al.* Extra precision glide: docking and scoring incorporating a model of hydrophobic enclosure for protein-ligand complexes. *J. Med. Chem.* **49**, 6177–6196 (2006).

811. Hodges, H. C. *et al.* Dominant-negative SMARCA4 mutants alter the accessibility landscape of tissue-unrestricted enhancers. *Nat. Struct. Mol. Biol.* **25**, 61–72 (2018).

812. Tilly, B. C. *et al.* In vivo analysis reveals that ATP-hydrolysis couples remodeling to SWI/SNF release from chromatin. *Elife* **10**, 1–27 (2021).

813. Schick, S. *et al.* Acute BAF perturbation causes immediate changes in chromatin accessibility. *Nat. Genet.* **53**, 269–278 (2021).

814. Thiele, C. J. Neuroblastoma Cell Lines. in *Neuroblastoma* (ed. Masters, J.) vol. 1 21–53 (Kluwer Academic Publishers, 1998).

815. Tweddle, D. A., Malcolm, A. J., Bown, N., Pearson, A. D. J. & Lunec, J. Evidence for the Development of p53 Mutations after Cytotoxic Therapy in a Neuroblastoma Cell Line. *Cancer Res.* **61**, 8–13 (2001).

816. Van Maerken, T. *et al.* Functional Analysis of the p53 Pathway in Neuroblastoma Cells Using the Small-Molecule MDM2 Antagonist Nutlin-3. *Mol. Cancer Ther.* **10**, 983–994 (2011).

817. Chen, J. & Archer, T. K. Regulating SWI/SNF subunit levels via protein-protein interactions and proteasomal degradation: BAF155 and BAF170 limit expression of BAF57. *Mol. Cell. Biol.* **25**, 9016–9027 (2005).

818. Perrin, B. J. & Ervasti, J. M. The Actin Gene Family: Function Follows Isoform. *Cytoskelet.* **67**, 630–634 (2010).

819. Ng, D. T. W., Watowich, S. S. & Lamb, R. A. Analysis In Vivo of GRP78-BiP/Substrate Interactions and Their

Role in Induction of the GRP78-BiP Gene. *Mol. Biol. Cell* **3**, 143–155 (1992).

820. Weis, K., Mattaj, I. W. & Lamond, A. I. Identification of hSRP1α as a Functional Receptor for Nuclear Localization Sequences. *Science* **268**, 1049–1053 (1995).

821. Leffers, H., Dejgaard, K. & Celis, J. E. Characterisation of two major cellular poly(rC)-binding human proteins, each containing three K-homologous (KH) domains. *Eur. J. Biochem.* **230**, 447–453 (1995).

822. Yoshihama, M. *et al.* The Human Ribosomal Protein Genes: Sequencing and Comparative Analysis of 73 Genes. *Genome Res.* **12**, 379–390 (2002).

823. Large, E. E. & Mathies, L. D. Caenorhabditis elegans SWI/SNF subunits control sequential developmental stages in the somatic gonad. *G3 Genes, Genomes, Genet.* **4**, 471–483 (2014).

824. Nagl, N. G., Wang, X., Patsialou, A., Scoy, M. Van & Moran, E. Distinct mammalian SWI / SNF chromatin remodeling complexes with opposing roles in cell-cycle control. *EMBO J.* **26**, 752–763 (2007).

825. Flores-Alcantar, A., Gonzalez-Sandoval, A., Escalante-Alcalde, D. & Lomelí, H. Dynamics of expression of ARID1A and ARID1B subunits in mouse embryos and in cells during the cell cycle. *Cell Tissue Res.* **345**, 137–148 (2011).

826. Wang, Z. *et al.* Dual ARID1A/ARID1B loss leads to rapid carcinogenesis and disruptive redistribution of BAF complexes. *Nat. Cancer* **1**, 909–922 (2020).

827. Du, J. *et al.* Arid1a-Plagl1-Hh signaling is indispensable for differentiation-associated cell cycle arrest of tooth root progenitors. *Cell Rep.* **35**, 108964 (2021).

828. Watanabe, R. *et al.* SWI/SNF Factors Required for Cellular Resistance to DNA Damage Include ARID1A and ARID1B and Show Interdependent Protein Stability. *Cancer Res.* **74**, 2465–2475 (2014).

829. Liberzon, A. *et al.* Molecular signatures database (MSigDB) 3.0. *Bioinformatics* **27**, 1739–1740 (2011).

830. Liberzon, A. *et al.* The Molecular Signatures Database Hallmark Gene Set Collection. *Cell Syst.* **1**, 417–425 (2015).

831. Hanahan, D. & Weinberg, R. A. Hallmarks of cancer: The next generation. *Cell* **144**, 646–674 (2011).

832. Dimova, D. K. & Dyson, N. J. The E2F transcriptional network: Old acquaintances with new faces. *Oncogene* **24**, 2810–2826 (2005).

833. Kent, L. N. & Leone, G. The broken cycle: E2F dysfunction in cancer. *Nat. Rev. Cancer* **19**, 326–338 (2019).

834. Rubin, S. M., Sage, J. & Skotheim, J. M. Integrating Old and New Paradigms of G1/S Control. *Mol. Cell* **80**, 183–192 (2020).

835. Kastan, M. B. & Bartek, J. Cell-cycle checkpoints and cancer. *Nature* **432**, 316–323 (2004).

836. Stark, G. R. & Taylor, W. R. Analyzing the G2 / M Checkpoint. *Methods Mol. Biol.* **280**, 51–82 (2004).

837. Prosser, S. L. & Pelletier, L. Mitotic spindle assembly in animal cells: A fine balancing act. *Nat. Rev. Mol. Cell Biol.* **18**, 187–201 (2017).

838. Thiery, J. P. & Sleeman, J. P. Complex networks orchestrate epithelial-mesenchymal transitions. *Nat. Rev. Mol. Cell Biol.* **7**, 131–142 (2006).

839. Kalluri, R. & Weinberg, R. A. The basics of epithelial-mesenchymal transition. *J. Clin. Invest.* **119**, 1420–1428 (2009).

840. Lavin, D. P. & Tiwari, V. K. Unresolved Complexity in the Gene Regulatory Network Underlying EMT. *Front. Oncol.* **10**, 1–19 (2020).

841. Cook, D. P. & Vanderhyden, B. C. Context specificity of the EMT transcriptional response. *Nat. Commun.* **11**, 1–9 (2020).

842. Yang, J. & Weinberg, R. A. Epithelial-Mesenchymal Transition: At the Crossroads of Development and Tumor Metastasis. *Dev. Cell* **14**, 818–829 (2008).

843. Thiery, J. P., Acloque, H., Huang, R. Y. J. & Nieto, M. A. Epithelial-Mesenchymal Transitions in Development and Disease. *Cell* **139**, 871–890 (2009).

844. Nieto, M. A. The ins and outs of the epithelial to mesenchymal transition in health and disease. *Annu. Rev. Cell Dev. Biol.* **27**, 347–376 (2011).

845. van Groningen, T. *et al.* A NOTCH feed-forward loop drives reprogramming from adrenergic to mesenchymal state in neuroblastoma. *Nat. Commun.* **10**, 1–11 (2019).

846. Szemes, M., Greenhough, A. & Malik, K. Wnt signaling is a major determinant of neuroblastoma cell lineages. *Front. Mol. Neurosci.* **12**, 1–12 (2019).

847. Peinado, H. *et al.* A molecular role for lysyl oxidase-like 2 enzyme in Snail regulation and tumor progression. *EMBO J.* **24**, 3446–3458 (2005).

848. Millanes-Romero, A. *et al.* Regulation of heterochromatin transcription by snail1/LOXL2 during epithelial-to-mesenchymal transition. *Mol. Cell* **52**, 746–757 (2013).

849. Herranz, N. *et al.* Lysyl oxidase-like 2 (LOXL2) oxidizes trimethylated lysine 4 in histone H3. *FEBS J.* **283**, 4263–4273 (2016).

850. Peinado, H., Olmeda, D. & Cano, A. Snail, ZEB and bHLH factors in tumour progression: An alliance against the epithelial phenotype? *Nat. Rev. Cancer* **7**, 415–428 (2007).

851. Hazan, R. B., Qiao, R., Keren, R., Badano, I. & Suyama, K. Cadherin switch in tumor progression. *Ann. N. Y. Acad. Sci.* **1014**, 155–163 (2004).

852. Wheelock, M. J., Shintani, Y., Maeda, M., Fukumoto, Y. & Johnson, K. R. Cadherin switching. *J. Cell Sci.* **121**, 727–735 (2008).

853. Okazaki, M. *et al.* Molecular cloning and characterization of OB-cadherin, a new member of cadherin family expressed in osteoblasts. *J. Biol. Chem.* **269**, 12092–12098 (1994).

854. Chu, Y. S. *et al.* Prototypical type I E-cadherin and type II cadherin-7 mediate very distinct adhesiveness through their extracellular domains. *J. Biol. Chem.* **281**, 2901–2910 (2006).

855. Blaue, C., Kashef, J. & Franz, C. M. Cadherin-11 promotes neural crest cell spreading by reducing intracellular tension—Mapping adhesion and mechanics in neural crest explants by atomic force microscopy. *Semin. Cell Dev. Biol.* **73**, 95–106 (2018).

856. Manohar, S., Camacho-Magallanes, A., Echeverria, C. & Rogers, C. D. Cadherin-11 Is Required for Neural Crest Specification and Survival. *Front. Physiol.* **11**, (2020).

857. Huang, C. F. *et al.* Cadherin-11 increases migration and invasion of prostate cancer cells and enhances their interaction with osteoblasts. *Cancer Res.* **70**, 4580–4589 (2010).

858. Kaur, H. *et al.* Cadherin-11, a marker of the mesenchymal phenotype, regulates glioblastoma cell migration and survival in vivo. *Mol. Cancer Res.* **10**, 293–304 (2012).

859. Satcher, R. L. *et al.* Cadherin-11 in renal cell carcinoma bone metastasis. *PLoS One* **9**, 1–10 (2014).

860. Pohlodek, K., Tan, Y. Y., Singer, C. F. & Gschwantler-Kaulich, D. Cadherin-11 expression is upregulated in invasive human breast cancer. *Oncol. Lett.* **12**, 4393–4398 (2016).

861. Hamidi, H. & Ivaska, J. Every step of the way: Integrins in cancer progression and metastasis. *Nat. Rev. Cancer* **18**, 533–548 (2018).

862. Buck, C. A., Shea, E., Duggan, K. & Horwitz, A. F. Integrin (The C SAT Antigen): Functionality Requires Oligomeric Integrity. *J. Cell Biol.* **103**, 2421–2428 (1986).

863. Fuentes, P. *et al.* ITGB3-mediated uptake of small extracellular vesicles facilitates intercellular communication in breast cancer cells. *Nat. Commun.* **11**, 1–15 (2020).

864. Molist, C. *et al.* miRNA-7 and miRNA-324-5p regulate alpha9-Integrin expression and exert anti-oncogenic effects in rhabdomyosarcoma. *Cancer Lett.* **477**, 49–59 (2020).

865. Humphries, J. D., Byron, A. & Humphries, M. J. Integrin ligands at a glance. *J. Cell Sci.* **119**, 3901–3903 (2006).

866. Livne, A. & Geiger, B. The inner workings of stress fibers - From contractile machinery to focal adhesions and back. *J. Cell Sci.* **129**, 1293–1304 (2016).

867. Soriano, A. *et al.* microRNAs as pharmacological targets in cancer. *Pharmacol. Res.* **75**, 3–14 (2013).

868. Lu, H. *et al.* Recent advances in the development of protein-protein interactions modulators: mechanisms and clinical trials. *Signal Transduct. Target. Ther.* **5**, 213 (2020).

869. Trinkle-Mulcahy, L. *et al.* Identifying specific protein interaction partners using quantitative mass spectrometry and bead proteomes. *J. Cell Biol.* **183**, 223–239 (2008).

870. Lee, J. H. *et al.* Cytoplasmic localization and nucleo-cytoplasmic shuttling of BAF53, a component of chromatin-modifying complexes. *Mol. Cells* **16**, 78–83 (2003).

871. Gunduz, E. *et al.* Epigenetic alterations of BRG1 leads to cancer development through its nuclear-cytoplasmic shuttling abnormalities. *Med. Hypotheses* **67**, 1313–1316 (2006).

872. Craig, E., Zhang, Z.-K., Davies, K. P. & Kalpana, G. V. A masked NES in INI1/hSNF5 mediates hCRM1-dependent nuclear export: implications for tumorigenesis. *EMBO J.* **21**, 31–42 (2002).

873. Crodian, J. S., Weldon, B. M., Tseng, Y.-C., Cabot, B. & Cabot, R. Nuclear trafficking dynamics of Bromodomain-containing protein 7 (BRD7), a switch/sucrose non-fermentable (SWI/SNF) chromatin remodelling complex subunit, in porcine oocytes and cleavage-stage embryos. *Reprod. Fertil. Dev.* **31**, 1497–1506 (2019).

874. Sena, J. A., Wang, L. & Hu, C.-J. BRG1 and BRM chromatin-remodeling complexes regulate the hypoxia response by acting as coactivators for a subset of hypoxia-inducible transcription factor target genes. *Mol. Cell. Biol.* **33**, 3849–3863 (2013).

875. Bultman, S. J., Gebuhr, T. C. & Magnuson, T. A Brg1 mutation that uncouples ATPase activity from chromatin remodeling reveals an essential role for SWI/SNF-related complexes in beta-globin expression and erythroid development. *Genes Dev.* **19**, 2849–2861 (2005).

876. Kim, J. M. *et al.* Single-molecule imaging of chromatin remodelers reveals role of ATPase in promoting fast kinetics of target search and dissociation from chromatin. *Elife* **10**, e69387 (2021).

877. Imbalzano, A. N., Schnitzler, G. R. & Kingston, R. E. Nucleosome disruption by human SWI/SNF is maintained in the absence of continued ATP hydrolysis. *J. Biol. Chem.* **271**, 20726–20733 (1996).

878. Jordán-Pla, A. *et al.* SWI/SNF regulates half of its targets without the need of ATP-driven nucleosome remodeling by Brahma. *BMC Genomics* **19**, 367 (2018).

879. Kwok, R. S., Li, Y. H., Lei, A. J., Edery, I. & Chiu, J. C. The Catalytic and Non-catalytic Functions of the Brahma Chromatin-Remodeling Protein Collaborate to Fine-Tune Circadian Transcription in Drosophila. *PLoS Genet.* **11**, e1005307 (2015).

880. Kia, S. K., Gorski, M. M., Giannakopoulos, S. & Verrijzer, C. P. SWI/SNF mediates polycomb eviction and epigenetic reprogramming of the INK4b-ARF-INK4a locus. *Mol. Cell. Biol.* **28**, 3457–3464 (2008).

881. Iurlaro, M. *et al.* Mammalian SWI/SNF continuously restores local accessibility to chromatin. *Nat. Genet.* **53**, 279–287 (2021).

882. Kadoch, C., Copeland, R. A. & Keilhack, H. PRC2 and SWI/SNF Chromatin Remodeling Complexes in Health and Disease. *Biochemistry* **55**, 1600–1614 (2016).

883. Kadoch, C. *et al.* Dynamics of BAF-Polycomb complex opposition on heterochromatin in normal and oncogenic states. *Nat. Genet.* **49**, 213–222 (2017).

884. van der Vaart, A., Godfrey, M., Portegijs, V. & van den Heuvel, S. Dose-dependent functions of SWI/SNF BAF in permitting and inhibiting cell proliferation in vivo. *Sci. Adv.* **6**, eaay3823 (2020).

885. Erkek, S. *et al.* Comprehensive Analysis of Chromatin States in Atypical Teratoid/Rhabdoid Tumor Identifies Diverging Roles for SWI/SNF and Polycomb in Gene Regulation. *Cancer Cell* **35**, 95-110.e8 (2019).

886. Lukas, J. *et al.* DNA tumor virus oncoproteins and retinoblastoma gene mutations share the ability to relieve the cell's requirement for cyclin D1 function in G1. *J. Cell Biol.* **125**, 625–638 (1994).

887. Molenaar, J. J. *et al.* Cyclin D1 and CDK4 activity contribute to the undifferentiated phenotype in neuroblastoma. *Cancer Res.* **68**, 2599–2609 (2008).

888. Wainwright, L. J., Lasorella, A. & Iavarone, A. Distinct mechanisms of cell cycle arrest control the decision between differentiation and senescence in human neuroblastoma cells. *Proc. Natl. Acad. Sci. U. S. A.* **98**, 9396–9400 (2001).

889. Segerström, L. *et al.* Effects of small molecule inhibitors of PI3K/Akt/mTOR signaling on neuroblastoma growth in vitro and in vivo. *Int. J. cancer* **129**, 2958–2965 (2011).

890. Dodurga, Y. *et al.* Valproic acid inhibits the proliferation of SHSY5Y neuroblastoma cancer cells by downregulating URG4/URGCP and CCND1 gene expression. *Mol. Biol. Rep.* **41**, 4595–4599 (2014).

891. Soriano, A. *et al.* Functional high-throughput screening reveals miR-323a-5p and miR-342-5p as new

tumor-suppressive microRNA for neuroblastoma. *Cell. Mol. Life Sci.* **76**, 2231–2243 (2019).

892. Roth, S. A. *et al.* MicroRNA-193b-3p represses neuroblastoma cell growth via downregulation of Cyclin D1, MCL-1 and MYCN. *Oncotarget* **9**, 18160–18179 (2018).

893. Molenaar, J. J., van Sluis, P., Boon, K., Versteeg, R. & Caron, H. N. Rearrangements and increased expression of cyclin D1 (CCND1) in neuroblastoma. *Genes. Chromosomes Cancer* **36**, 242–249 (2003).

894. Molenaar, J. J. *et al.* Copy number defects of G1-cell cycle genes in neuroblastoma are frequent and correlate with high expression of E2F target genes and a poor prognosis. *Genes. Chromosomes Cancer* **51**, 10–19 (2012).

895. Molenaar, J. J. *et al.* Cyclin D1 is a direct transcriptional target of GATA3 in neuroblastoma tumor cells. *Oncogene* **29**, 2739–2745 (2010).

896. Lim, K. C. *et al.* Gata3 loss leads to embryonic lethality due to noradrenaline deficiency of the sympathetic nervous system. *Nat. Genet.* **25**, 209–212 (2000).

897. Tsarovina, K. *et al.* The Gata3 transcription factor is required for the survival of embryonic and adult sympathetic neurons. *J. Neurosci.* **30**, 10833–10843 (2010).

898. Burstyn-Cohen, T. & Kalcheim, C. Association between the cell cycle and neural crest delamination through specific regulation of G1/S transition. *Dev. Cell* **3**, 383–395 (2002).

899. Fujisawa, H., Misaki, K., Takabatake, Y., Hasegawa, M. & Yamashita, J. Cyclin D1 is overexpressed in atypical teratoid/rhabdoid tumor with hSNF5/INI1 gene inactivation. *J. Neurooncol.* **73**, 117–124 (2005).

900. Xue, Y. *et al.* SMARCB1 loss induces druggable cyclin D1 deficiency via upregulation of MIR17HG in atypical teratoid rhabdoid tumors. *J. Pathol.* **252**, 77–87 (2020).

901. McDonald, O. G., Wu, H., Timp, W., Doi, A. & Feinberg, A. P. Genome-scale epigenetic reprogramming during epithelial-to-mesenchymal transition. *Nat. Struct. Mol. Biol.* **18**, 867–874 (2011).

902. Sun, L. & Fang, J. Epigenetic regulation of epithelial–mesenchymal transition. *Cell. Mol. Life Sci.* **73**, 4493–4515 (2016).

903. Carl, T. F., Dufton, C., Hanken, J. & Klymkowsky, M. W. Inhibition of neural crest migration in Xenopus using antisense slug RNA. *Dev. Biol.* **213**, 101–115 (1999).

904. Li, J. *et al.* A new transgenic reporter line reveals Wnt-dependent Snai2 re-expression and cranial neural crest differentiation in Xenopus. *Sci. Rep.* **9**, 11191 (2019).

905. Nieto, M. A., Sargent, M. G., Wilkinson, D. G. & Cooke, J. Control of cell behavior during vertebrate development by Slug, a zinc finger gene. *Science* **264**, 835–839 (1994).

906. Huang, C., Kratzer, M.-C., Wedlich, D. & Kashef, J. E-cadherin is required for cranial neural crest migration in Xenopus laevis. *Dev. Biol.* **411**, 159–171 (2016).

907. Jiang, R., Lan, Y., Norton, C. R., Sundberg, J. P. & Gridley, T. The Slug gene is not essential for mesoderm or neural crest development in mice. *Dev. Biol.* **198**, 277–285 (1998).

908. Oram, K. F., Carver, E. A. & Gridley, T. Slug expression during organogenesis in mice. *Anat. Rec. Part A, Discov. Mol. Cell. Evol. Biol.* **271**, 189–191 (2003).

909. Vrenken, K. S. *et al.* The transcriptional repressor SNAI2 impairs neuroblastoma differentiation and inhibits response to retinoic acid therapy. *Biochim. Biophys. acta. Mol. basis Dis.* **1866**, 165644 (2020).

910. Manohar, S., Camacho-Magallanes, A., Echeverria, C. J. & Rogers, C. D. Cadherin-11 Is Required for Neural Crest Specification and Survival. *Front. Physiol.* **11**, 563372 (2020).

911. Becker, S. F. S., Mayor, R. & Kashef, J. Cadherin-11 mediates contact inhibition of locomotion during Xenopus neural crest cell migration. *PLoS One* **8**, e85717 (2013).

912. Langhe, R. P. *et al.* Cadherin-11 localizes to focal adhesions and promotes cell-substrate adhesion. *Nat. Commun.* **7**, 10909 (2016).

913. Wang, Q., Jia, Y., Peng, X. & Li, C. Clinical and prognostic association of oncogene cadherin 11 in gastric cancer. *Oncol. Lett.* **19**, 4011–4023 (2020).

914. Peran, I. *et al.* Cadherin 11 Promotes Immunosuppression and Extracellular Matrix Deposition to Support Growth of Pancreatic Tumors and Resistance to Gemcitabine in Mice. *Gastroenterology* **160**, 1359-1372.e13

(2021).

915. Zheng, B.-T. *et al.* CDH11 Regulates Adhesion and Transcellular Migration of Tongue Squamous Cell Carcinoma. *Onco. Targets. Ther.* **14**, 4211–4222 (2021).

916. Shimono, R., Matsubara, S., Takamatsu, H., Fukushige, T. & Ozawa, M. The expression of cadherins in human neuroblastoma cell lines and clinical tumors. *Anticancer Res.* **20**, 917–923 (2000).

917. Cuevas, E. P. *et al.* LOXL2 drives epithelial-mesenchymal transition via activation of IRE1-XBP1 signalling pathway. *Sci. Rep.* **7**, 44988 (2017).

918. Salvador, F. *et al.* Lysyl Oxidase-like Protein LOXL2 Promotes Lung Metastasis of Breast Cancer. *Cancer Res.* **77**, 5846–5859 (2017).

919. Ferreira, S., Saraiva, N., Rijo, P. & Fernandes, A. S. LOXL2 Inhibitors and Breast Cancer Progression. *Antioxidants (Basel, Switzerland)* **10**, (2021).

920. Cebrià-Costa, J. P. *et al.* LOXL2-mediated H3K4 oxidation reduces chromatin accessibility in triple-negative breast cancer cells. *Oncogene* **39**, 79–121 (2020).

921. Cohn, S. L. *et al.* The International Neuroblastoma Risk Group (INRG) classification system: an INRG Task Force report. *J. Clin. Oncol. Off. J. Am. Soc. Clin. Oncol.* **27**, 289–297 (2009).

922. Villanueva, A. A. *et al.* The Netrin-1-Neogenin-1 signaling axis controls neuroblastoma cell migration via integrin-β1 and focal adhesion kinase activation. *Cell Adh. Migr.* **15**, 58–73 (2021).

923. Ishizuka, Y. *et al.* NRP1 knockdown promotes the migration and invasion of human neuroblastoma-derived SK-N-AS cells via the activation of β1 integrin expression. *Int. J. Oncol.* **53**, 159–166 (2018).

924. Young, S. A. *et al.* Integrin α4 Enhances Metastasis and May Be Associated with Poor Prognosis in MYCN-low Neuroblastoma. *PLoS One* **10**, e0120815 (2015).

925. Lee, S. *et al.* FAK is a critical regulator of neuroblastoma liver metastasis. *Oncotarget* **3**, 1576–1587 (2012).

926. Petridis, A. K., Nikolopoulos, S. N. & El-Maarouf, A. Physical and functional cooperation of neural cell adhesion molecule and β1-integrin in neurite outgrowth induction. *J. Clin. Neurosci. Off. J. Neurosurg. Soc. Australas.* **18**, 1109–1113 (2011).

927. Tanaka, N. & Fukuzawa, M. MYCN downregulates integrin alpha1 to promote invasion of human neuroblastoma cells. *Int. J. Oncol.* **33**, 815–821 (2008).

928. Tzinia, A. K., Kitsiou, P. V, Talamagas, A. A., Georgopoulos, A. & Tsilibary, E. C. Effects of collagen IV on neuroblastoma cell matrix-related functions. *Exp. Cell Res.* **274**, 169–177 (2002).

929. Bozzo, C., Bellomo, G., Silengo, L., Tarone, G. & Altruda, F. Soluble integrin ligands and growth factors independently rescue neuroblastoma cells from apoptosis under nonadherent conditions. *Exp. Cell Res.* **237**, 326–337 (1997).

930. Yoshihara, T., Hibi, S., Tsunamoto, K., Todo, S. & Imashuku, S. Increased levels of alpha V-associated integrins in association with growth inhibition of cultured tumor cells by bromodeoxyuridine. *Anticancer Res.* **17**, 833–838 (1997).

931. Sugahara, M., Nakaoki, Y., Yamaguchi, A., Hashimoto, K. & Miyamoto, Y. Vitronectin is Involved in the Morphological Transition of Neurites in Retinoic Acid-Induced Neurogenesis of Neuroblastoma Cell Line Neuro2a. *Neurochem. Res.* **44**, 1621–1635 (2019).

932. Karakus, O. O., Godugu, K., Fujioka, K. & Mousa, S. A. Design, synthesis, and biological evaluation of novel bifunctional thyrointegrin antagonists for neuroblastoma. *Bioorg. Med. Chem.* **42**, 116250 (2021).

933. Karakus, O. O., Godugu, K., Rajabi, M. & Mousa, S. A. Dual Targeting of Norepinephrine Transporter (NET) Function and Thyrointegrin αvβ3 Receptors in the Treatment of Neuroblastoma. *J. Med. Chem.* **63**, 7653–7662 (2020).

934. Wei, Z.-H., Chen, H., Zhang, C. & Ye, B.-C. FRET-based system for probing protein-protein interactions between σR and RsrA from Streptomyces coelicolor in response to the redox environment. *PLoS One* **9**, e92330 (2014).

935. Ems-McClung, S. C. & Walczak, C. E. In Vitro FRET- and Fluorescence-Based Assays to Study Protein Conformation and Protein-Protein Interactions in Mitosis. *Methods Mol. Biol.* **2101**, 93–122 (2020).

936. Margineanu, A. *et al.* Screening for protein-protein interactions using Förster resonance energy transfer (FRET) and fluorescence lifetime imaging microscopy (FLIM). *Sci. Rep.* **6**, 28186 (2016).

937. Melero, I., Castanon, E., Alvarez, M., Champiat, S. & Marabelle, A. Intratumoural administration and tumour tissue targeting of cancer immunotherapies. *Nat. Rev. Clin. Oncol.* **18**, 558–576 (2021).

938. Rihani, A., Vandesompele, J., Speleman, F. & Van Maerken, T. Inhibition of CDK4/6 as a novel therapeutic option for neuroblastoma. *Cancer Cell Int.* **15**, 76 (2015).

8. **ANNEXES**

No sonamos mal
Sonamos mejor que ayer

Las Canciones De Juanita
Carolina Durante
Las Canciones De Juanita
2019

8.1. **Annex I**: List of publications

During my PhD stage I had the chance to participate in other research projects of the Neural Tumors laboratory, as well as in collaborations with other research groups, resulting in the following publications:

1. Segura MF, Soriano A, Roma J, Piskareva O, **Jiménez C**, Boloix A, Fletcher JI, Haber M, Gray JC, Cerdá-Alberich L, Martínez de Las Heras B, Cañete A, Gallego S, Moreno L. Methodological advances in the discovery of novel neuroblastoma therapeutics. Expert Opin Drug Discov. 2021. Online ahead of print. doi: 10.1080/17460441.2022.2002297

2. Masanas M, Masiá N, Suárez-Cabrera L, Olivan M, Soriano A, Majem B, Devis-Jauregui D, Burgos-Panadero R, **Jiménez C**, Rodriguez-Sodupe P, Boloix A, Toledano I, Guillén G, Navarro A, Llobet-Navas D, Villanueva A, Sánchez de Toledo J, Roma J, Noguera R, Moreno L, Krauss R, Gallego S, Santamaria A, Segura MF. The oral KIF11 inhibitor 4SC-205 exhibits antitumor activity and potentiates standard and targeted therapies in primary and metastatic neuroblastoma models. Clin Transl Med. 2021; 11(10):e533.

3. **Jiménez C**, Antonelli R, Masanas M, Soriano A, Devis-Jauregui L, Camacho J, Magdaleno A, Guillén G, Hladun R, Jubierre L, Roma J, Llobet-Navas D, Sánchez de Toledo J, Moreno L, Gallego S, Segura MF. Neuronal Differentiation-Related Epigenetic Regulator *ZRF1* Has Independent Prognostic Value in Neuroblastoma but Is Functionally Dispensable In Vitro. Cancers (Basel). 2021; 13(19):4845.

4. París-Coderch L, Soriano A, **Jiménez C**, Erazo T, Muñoz-Guardiola P, Masanas M, Antonelli R, Boloix A, Alfón J, Pérez-Montoyo H, Yeste-Velasco M, Domènech C, Roma J, Sánchez de Toledo J, Moreno L, Lizcano JM, Gallego S, Segura MF. The antitumour drug ABTL0812 impairs neuroblastoma growth through endoplasmic reticulum stress-mediated autophagy and apoptosis. Cell Death Dis. 2020; 11(9):773.

5. Antonelli R, **Jiménez C**, Riley M, Servidei T, Riccardi R, Soriano A, Roma J, Martínez-Saez E, Martini M, Ruggiero A, Moreno L, Sánchez de Toledo J, Gallego S, Bové J, Hooker JM, Segura MF. CN133, a Novel Brain-Penetrating Histone Deacetylase Inhibitor, Hampers Tumor Growth in Patient-Derived Pediatric Posterior Fossa Ependymoma Models. Cancers (Basel). 2020; 12(7):1922.

6. Boloix A, Masanas M, **Jiménez C**, Antonelli R, Soriano A, Roma J, Sánchez de Toledo J, Gallego S, Segura MF. Long Non-coding RNA PVT1 as a Prognostic and Therapeutic Target in Pediatric Cancer. Front Oncol. 2019; 9:1173.

7. Majem B, Parrilla A, **Jiménez C**, Suárez-Cabrera L, Barber M, Marín A, Castellví J, Tamayo G, Moreno-Bueno G, Ponce J, Matias-Guiu X, Alameda F, Romero I, Sánchez JL, Pérez-Benavente A, Moran S, Esteller M, Reventós J, Rigau M, Gil-Moreno A, Segura MF, Santamaría A. MicroRNA-654-5p suppresses ovarian cancer development impacting on MYC, WNT and AKT pathways. Oncogene. 2019; 38(32):6035-6050.

8. Soriano A, Masanas M, Boloix A, Masiá N, París-Coderch L, Piskareva O, **Jiménez C**, Henrich KO, Roma J, Westermann F, Stallings RL, Sábado C, de Toledo JS, Santamaria A, Gallego S, Segura MF. Functional high-throughput screening reveals miR-323a-5p and miR-342-5p as new tumor-suppressive microRNA for neuroblastoma. Cell Mol Life Sci. 2019; 76(11):2231-2243.

9. Jubierre L, **Jiménez C**, Rovira E, Soriano A, Sábado C, Gros L, Llort A, Hladun R, Roma J, Toledo JS, Gallego S, Segura MF. Targeting of epigenetic regulators in neuroblastoma. Exp Mol Med. 2018; 50(4):1-12.

8.2. **Annex II:** Research article published as first author

"Neuronal Differentiation-Related Epigenetic Regulator *ZRF1* Has Independent Prognostic Value in Neuroblastoma but Is Functionally Dispensable In Vitro"

Carlos Jiménez, Roberta Antonelli, Marc Masanas, Aroa Soriano, Laura Devis-Jauregui, Jessica Camacho, Ainara Magdaleno, Gabriela Guillén, Raquel Hladun, Luz Jubierre, Josep Roma, David Llobet-Navas, Josep Sánchez de Toledo, Lucas Moreno, Soledad Gallego and Miguel F. Segura.

Cancers (Basel). **2021**, 13(19), 4845.

cancers

MDPI

Article

Neuronal Differentiation-Related Epigenetic Regulator *ZRF1* Has Independent Prognostic Value in Neuroblastoma but Is Functionally Dispensable In Vitro

Carlos Jiménez [1], Roberta Antonelli [1], Marc Masanas [1], Aroa Soriano [1], Laura Devis-Jauregui [2,3], Jessica Camacho [4], Ainara Magdaleno [1], Gabriela Guillén [1,5], Raquel Hladun [1,6], Luz Jubierre [1], Josep Roma [1], David Llobet-Navas [2,3], Josep Sánchez de Toledo [1,7], Lucas Moreno [1,6], Soledad Gallego [1,6] and Miguel F. Segura [1,*]

1 Group of Translational Research in Child and Adolescent Cancer, Vall d'Hebron Research Institute (VHIR), Universitat Autònoma de Barcelona (UAB), 08035 Barcelona, Spain; carlos.jimenez@vhir.org (C.J.); roberta.antonelli@vhir.org (R.A.); marc.masanas@vhir.org (M.M.); aroa.soriano@vhir.org (A.S.); ainara.magdaleno@vhir.org (A.M.); gguillen@vhebron.net (G.G.); rhladun@vhebron.net (R.H.); jubierrl@mskcc.org (L.J.); josep.roma@vhir.org (J.R.); jsanchezdetoledo@iconcologia.net (J.S.d.T.); lucas.moreno@vhebron.net (L.M.); sgallego@vhebron.net (S.G.)
2 Molecular Mechanisms and Experimental Therapy in Oncology-Oncobell Program, Bellvitge Biomedical Research Institute (IDIBELL), 08908 L'Hospitalet de Llobregat, Spain; ldevis@idibell.cat (L.D.-J.); dllobet@idibell.cat (D.L.-N.)
3 Centro de Investigación Biomédica en Red de Cáncer (CIBERONC), Instituto de Salud Carlos III, 28029 Madrid, Spain
4 Pathology Department, Vall d'Hebron University Hospital—UAB, 08035 Barcelona, Spain; jcamacho@vhebron.net
5 Surgery Department, Vall d'Hebron University Hospital—UAB, 08035 Barcelona, Spain
6 Pediatric Oncology and Hematology Department, Vall d'Hebron University Hospital—UAB, 08035 Barcelona, Spain
7 Catalan Institute of Oncology (ICO), 08908 L'Hospitalet de Llobregat, Spain
* Correspondence: miguel.segura@vhir.org

check for updates

Citation: Jiménez, C.; Antonelli, R.; Masanas, M.; Soriano, A.; Devis-Jauregui, L.; Camacho, J.; Magdaleno, A.; Guillén, G.; Hladun, R.; Jubierre, L.; et al. Neuronal Differentiation-Related Epigenetic Regulator *ZRF1* Has Independent Prognostic Value in Neuroblastoma but Is Functionally Dispensable In Vitro. *Cancers* **2021**, *13*, 4845. https://doi.org/10.3390/cancers13194845

Academic Editors: Luis Franco and Rakesh K. Singh

Received: 26 August 2021
Accepted: 25 September 2021
Published: 28 September 2021

Simple Summary: Neuroblastoma is the most common pediatric solid tumor occurring outside the brain, and it is thought to arise from cells that acquire errors during the normal process of embryonal development. Today, we know that embryonal development is regulated by epigenetics, a mechanism that determines which genes need to be expressed in each cell type and developmental step. Epigenetic errors, therefore, are considered contributory to the appearance and progression of tumors such as neuroblastoma. Here, we aimed at finding whether *ZRF1*, a known epigenetic regulator, could play a significant role in the aggressiveness of neuroblastoma. Our results suggest that *ZRF1* does not seem to have any relevant function in neuroblastoma cells; however, the levels of this epigenetic regulator are related to the prognostic of neuroblastoma patients and could be used to predict their progression and improve the diagnosis.

Abstract: Neuroblastoma is a pediatric tumor of the peripheral nervous system that accounts for up to ~15% of all cancer-related deaths in children. Recently, it has become evident that epigenetic deregulation is a relevant event in pediatric tumors such as high-risk neuroblastomas, and a determinant for processes, such as cell differentiation blockade and sustained proliferation, which promote tumor progression and resistance to current therapies. Thus, a better understanding of epigenetic factors implicated in the aggressive behavior of neuroblastoma cells is crucial for the development of better treatments. In this study, we characterized the role of *ZRF1*, an epigenetic activator recruited to genes involved in the maintenance of the identity of neural progenitors. We combined analysis of patient sample expression datasets with loss- and gain-of-function studies on neuroblastoma cell lines. Functional analyses revealed that *ZRF1* is functionally dispensable for those cellular functions related to cell differentiation, proliferation, migration, and invasion, and does not affect the cellular response to chemotherapeutic agents. However, we found that high levels of *ZRF1* mRNA expression are associated to shorter overall survival of neuroblastoma patients, even when those patients with

the most common molecular alterations used as prognostic factors are removed from the analyses, thereby suggesting that *ZRF1* expression could be used as an independent prognostic factor in neuroblastoma.

Keywords: *ZRF1*; neuronal differentiation; epigenetics; pediatric cancer; neuroblastoma

1. Introduction

Neuroblastoma, a pediatric cancer of the peripheral nervous system, is one of the most common embryonal tumors outside the brain [1]. It is thought to arise from tissues of the sympathoadrenergic system at early stages of embryonic development, specifically from neural crest progenitors that fail to differentiate during dorsolateral migration [2]. From a histopathological perspective, neuroblastoma can be classified based on the grade of morphological differentiation into distinct categories, namely neuroblastoma, ganglioneuroblastoma, and ganglioneuroma, from less to more differentiated tumors. The last two categories are considered to be benign forms of neuroblastoma [3]. The pathological category can be further classified according to the degree of cellular differentiation. For example, neuroblastoma can be further classified into undifferentiated, poorly differentiated, and differentiating tumors (reviewed in [4]). The degree of differentiation is part of routine prognostic risk assessment. In fact, high-risk neuroblastomas, which represent up to ~60% of all diagnosed neuroblastomas, are usually undifferentiated or poorly differentiated tumors that present very aggressive behavior and have a five-year overall survival rate below 40% [5]. Pro-differentiation therapies (i.e., with retinoic acid derivatives) are part of the standard of care in neuroblastoma, although they are restricted to the treatment of neuroblastoma minimal residual disease [6]. However, not all patients respond to this treatment. Therefore, a better understanding of the molecular mechanisms that maintain these types of tumors in an undifferentiated state may reveal new opportunities for therapeutic intervention.

Epigenetic regulation (e.g., DNA methylation, histone post-translational modifications, non-coding RNA expression, etc.) is one of the mechanisms that controls the differentiation of neuroblasts (i.e., neuroblastoma precursors). The disruption of the homeostatic epigenetic balance contributes to the developmental arrest of sympathetic progenitors, thereby contributing to neuroblastoma oncogenesis [7]. One of the genes that is determinant in the maintenance of neuronal progenitor identity is zuotin-related factor 1 (*ZRF1*; also known as MPP11), which is encoded by the *DNAJC2* gene [8,9]. *ZRF1* belongs to the M-phase phosphoprotein (MPP) family and was first discovered as a chaperone in the cytosol [10–12]. However, later evidence has shown that it also acts as a chromatin regulator in the nucleus, where it is recruited to ubiquitinated histone H2A at 'Lys-119' (H2AK119ub), displacing the polycomb repressor complex 1 (PRC1) from chromatin and facilitating the transcription of neural progenitor-associated genes [13].

In addition to its physiological role in the maintenance of the pluripotency of neural progenitor cells, *ZRF1* has already been functionally implicated in cancer. *ZRF1* was shown to be oncogenic in solid tumors such as breast [14] and gastric [15] cancers. Furthermore, *ZRF1* was shown to be overexpressed in acute myeloid leukemia (AML) acting as a negative regulator of differentiation. In the same study, Demajo and collaborators showed that *ZRF1* depletion cooperated with differentiating agents (i.e., retinoic acid) to suppress leukemia in vivo [16].

Thus, owing to the role of *ZRF1* of maintaining the undifferentiated state of neural progenitor cells and its functional relevance in the differentiation of some tumors, we sought to determine whether *ZRF1* plays a major role in neuroblastoma. Here, we found that the expression of *ZRF1* mRNA is increased in advanced disease stages and in tumors, with the most common genetic alterations associated with poor prognosis in neuroblastoma, such as MYCN amplification, gain of chromosome 17q, and loss of 1p36. Moreover, the

ZRF1 mRNA level was clearly associated with poor neuroblastoma survival in the absence of other poor-prognosis molecular alterations. However, our gain- and loss-of-function experiments suggest that *ZRF1* is neither sufficient nor necessary to sustain the oncogenic properties of neuroblastoma cells, such as cell differentiation, proliferation, or migration. Our results validate *ZRF1* as a potential prognostic marker, but discard it as a target for differentiation therapy.

2. Materials and Methods

2.1. Analysis of Neuroblastoma Gene Expression Datasets

ZRF1 mRNA expression levels were analyzed from neuroblastoma patient data from the GSE62564, GSE45547 and GSE3960 publicly available datasets. The GSE62564 dataset was used to construct receiver operating characteristic (ROC) curves to determine the prognostic value of *ZRF1* expression. The optimal cutoff value was defined according to the Youden index. Overall survival (OS) and the cumulative survival rate were estimated using the Kaplan–Meier method, and the log-rank test was performed to assess differences between groups. Univariate and multivariate Cox proportional hazard regression analyses were used to assess the prognostic significance of *ZRF1* on OS. These statistical analyses were performed using the IBM SPSS 21 software. For GSE45547 and GSE3960 datasets, gene expression data was extracted and Kaplan–Meier survival plots were generated using the R2 Genomics Analysis and Visualization Platform (http://r2.amc.nl; accessed date: 21 January 2021). *ZRF1* mRNA expression levels between different patient groups were analyzed using GraphPad Prism Software (La Jolla, CA, USA), and statistical significance was assessed by Kruskal–Wallis test as a non-parametric ANOVA, and Dunn's test for multiple comparisons.

2.2. Cell Lines

Neuroblastoma cell lines (SK-N-AS, SH-SY5Y, and IMR-32) and embryonic kidney cells (HEK293T) were purchased from American Type Culture Collection (ATCC, Manassas, VA, USA), the CHLA-90 cell line was purchased from the Children's Oncology Group Cell Culture and Xenograft Repository (Lubbock, TX, USA), and SK-N-BE(2), and LA1-5s were procured from the Public Health England Culture Collection (Salisbury, UK). Neuroblastoma cells were cultured and maintained in Iscove's modified Dulbecco's medium (Life Technologies, Waltham, MA, USA), supplemented with 20% heat-inactivated fetal bovine serum (South America Premium, Biowest, Nuaillé, France) and 1% insulin-transferrin-selenium supplement (Life Technologies). HEK293T cells were grown in Dulbecco's modified Eagle's medium (Life Technologies), supplemented with 10% heat-inactivated fetal bovine serum. Media were supplemented with 100 U/mL penicillin, 100 μg/mL streptomycin (Life Technologies), and 5 μg/mL plasmocin (InvivoGen, San Diego, CA, USA). Cultures were maintained at 37 °C in a 5% CO_2 saturated atmosphere, and periodically tested for mycoplasma contamination.

2.3. Western Blot Analysis

Cells were lysed in RIPA buffer (Thermo Fisher Scientific, Waltham, MA, USA), supplemented with EDTA-free protease inhibitor cocktail (Roche, Basel, Switzerland). Cell lysates were quantified using a DC protein assay (Bio-Rad, Hercules, CA, USA) and 30 μg of protein was resolved on a 4–12% Tris-glycine sodium dodecyl sulfate polyacrylamide electrophoresis gel (Invitrogen, Carlsbad, CA, USA), then transferred onto polyvinylidene difluoride (PVDF) membranes. Membranes were blocked for 1 h with 5% non-fat milk or 5% bovine serum albumin (BSA) in Tris-buffered saline with 0.1% Tween and probed with primary antibodies overnight at 4 °C. Membranes were incubated with secondary antibodies for 1 h before developing with a chemiluminescent horseradish peroxidase substrate EZ-ECL Chemoluminiscence Detection Kit (Biological Industries, Kibbutz Beit-Haemek, Israel). Protein levels were quantified by densitometry using ImageJ software

(National Institutes of Health, Bethesda, MD, USA). Antibodies used for Western blot are listed in Table S1. Original western blot images can be found in Figure S7.

2.4. Proliferation and Colony Formation Assays

For the proliferation experiments, transduced or transfected cells were plated at a density of 2–8 $\times$ 10^4 cells /well in 6-well plates and allowed to grow for 7 days with a medium change on day 4. Cells were fixed with 1% glutaraldehyde and stained with 0.5% crystal violet. Stained cells were treated in 15% acetic acid, and the absorbance was read at 590 nm. For the colony formation experiments, cells were plated at a very low density (5–10 $\times$ 10^2 cells/well in 6-well plates) and the medium was changed every 3–4 days. The plates were fixed in glutaraldehyde and stained with crystal violet at day 10 or when colonies were visible to the naked eye. Colonies were photographed and counted using ImageJ software.

2.5. Migration and Invasion Assays

For the wound-healing assays, neuroblastoma cells were plated at a density of 3 $\times$ 10^6 cells/well in a 6-well plate. The next day, an artificial wound was created in the confluent cell monolayer. Six predefined fields per condition were photographed under contrast phase microscopy at the indicated time points, and the wound area was measured using Image J software. The migration rate was calculated by normalizing the wound area to time 0. For the transwell invasion assays, 2 $\times$ 10^5 cells were seeded in serum-free media in the upper chamber of 8.0 μm pore size transwells (Corning Life Sciences, Corning, NY, USA) previously coated with a barrier of rat tail collagen I (Corning). The lower chamber was filled with media supplemented with fetal bovine serum. After 16 h, remaining cells were removed from the upper chamber and the cells that migrated to the lower surface of the membrane were fixed with 4% paraformaldehyde, and stained with crystal violet. Invading cells were imaged by bright field microscopy, quantified by diluting crystals in acetic acid, and read at 590 nm.

2.6. Differentiation Assays

Neuroblastoma cells were plated at low density (1–1.2 $\times$ 10^5 cells) in collagen-coated 60 mm plates. One day later, cells were treated with 10 μM 13-*cis*-retinoic acid (Selleckchem, Munich, Germany). Cells were collected at day 5 post-treatment for Western blot analysis. For *RARβ* gene expression analysis, RNA was extracted from cell lysates using a miRNeasy Mini Kit (Qiagen, Germantown, MA, USA) and retrotranscribed with a high-capacity cDNA reverse transcription kit (Thermo Fisher Scientific). Real-time PCR was performed with PerfeCTa SYBR Green Fastmix (Quantabio, Beverly, MA, USA) using L27 as the internal standard. Primers are listed in Table S2. Relative quantification of gene expression was calculated using the 2^{-DDCt} method [17]. For neurite length analyses, 1$\times$ 10^4 cells per well were seeded in collagen-coated glass covers in 24-well plates and treated with retinoic acid for 5 days before fixation with 4% paraformaldehyde. Cells were stained with phalloidin-iFluor 594 (Abcam, Cambridge, UK), following manufacturer's instructions, and DAPI 10 μ/mL (Invitrogen). Slides were visualized with a FV1000 confocal microscope (Olympus, Shinjuku, Tokyo, Japan). Ten fields were acquired for each biological replicate and processed using ImageJ software. Actin prolongations longer than twice the length of the nucleus (~30 μm) were considered as neurites.

2.7. Vectors and Lentiviral Infection

pEV-*ZRF1*, pCAG-*ZRF1*, and pLKO with different sh*ZRF1* vectors were kindly provided by Luciano DiCroce. Lentiviruses were generated in HEK293T cells using previously described methods [18,19]. Silent mutations were introduced into the *ZRF1* overexpression vector using three sequential site-directed mutagenesis reactions in pCAG-*ZRF1*, using the QuikChange II XL Site-Directed Mutagenesis Kit (Agilent, Santa Clara, CA, USA) and checked by Sanger sequencing. Primers used for site-directed mutagenesis and sequencing

are listed in Table S2, and the shRNA target sequences are listed in Table S3. After mutagenesis, the *ZRF1* sequence was excised from the pCAG by XhoI digestion and ligated into the FG12 lentiviral overexpression vector.

2.8. ZRF1 Overexpression Experiments

Neuroblastoma cells plated at a density of 5×10^5 cells in 60 mm plates were transduced with viral supernatant. pEV-transduced cells were selected by separating green fluorescence protein (GFP)-positive cells by fluorescence-assisted cell sorting (FACSAria, BD Biosciences, San Jose, CA, USA) at the Flow Cytometry facility of VHIR.

2.9. ZRF1 Knockdown Experiments

For shRNA transduction, 2–8 $\times$ 10^5 cells were plated in 60 mm plates with viral supernatant containing either pLKO-non-silencing control (NSC) or shZRF #1, #2, or #3. After 16 h, the supernatant was replaced with fresh medium, and 24 h later, transduced cells were selected by puromycin resistance (1 μg/mL). Three days after transduction, the cells were detached and used for proliferation experiments. For siRNA knockdown, a set of four pre-designed ON-TARGETplus siRNAs against *ZRF1* were purchased from Dharmacon (Lafayette, CO, USA). The siRNA target sequences are listed in Table S3. Neuroblastoma cell lines at a concentration of 1.67×10^5 cells/mL were transfected with siRNA at 25 nM using Lipofectamine 2000 (Life Technologies) following the manufacturer's instructions. After incubation for 16 h, the medium was replaced.

3. Results

3.1. ZRF1 Is an Independent Prognostic Factor in Neuroblastoma

To determine whether *ZRF1* is involved in the biology of neuroblastoma, we analyzed publicly available mRNA expression datasets to search for correlations between *ZRF1* mRNA levels and different clinicopathological parameters of neuroblastoma patients. A receiver operating characteristic (ROC) curve analysis of a cohort of 498 patients was performed in order to assess a *ZRF1* cut-off value (Youden index) that maximized the capacity for overall survival prediction (Table S4). Using this cut-off, patients with higher *ZRF1* levels showed a reduction in overall survival when compared to patients with low *ZRF1* levels (Figure 1a). *ZRF1* was found to be upregulated in MYCN-amplified (MNA) patients, even when patients were split into early (1, 2, 4S) or advanced (3, 4) stages (Figure 1b). *ZRF1* levels were also found to be increased in advanced stages of the disease, and this upregulation was maintained even when MNA tumors were excluded (Figure 1c).

To verify whether the expression of *ZRF1* has prognostic value independent of MYCN amplification or disease stage (both factors intrinsically associated with poor survival), correlation analyses were performed excluding the MNA samples and in the different stages. The results showed that the association between *ZRF1* mRNA expression and poor survival remained in non-MNA and low stage tumors (Figure 1d). These findings were validated by contingency analyses (Table S5) and confirmed with two different and independent supplementary neuroblastoma mRNA expression datasets (Figure S1). Finally, univariate and multivariate regression analyses confirmed *ZRF1* to be independent prognostic factor of overall survival in neuroblastoma (Figure 1e,f).

Next, we analyzed the expression of *ZRF1* mRNA in patients with the most common segmental copy alterations associated with neuroblastoma prognosis, including 1p36 loss of heterozygosity (LOH), unbalanced 11q LOH, and unbalanced 17q gain [20,21]. *ZRF1* expression levels were found to be higher in patients with 1p36 loss and 17q gain (Figure 2a). A similar trend was also observed in patients with loss of 11q, although the difference was not statistically significant. Of note, the association between *ZRF1* expression and poor prognosis was maintained in tumors without these alterations (Figure 2b), further supporting the expression of *ZRF1* as an independent prognostic factor.

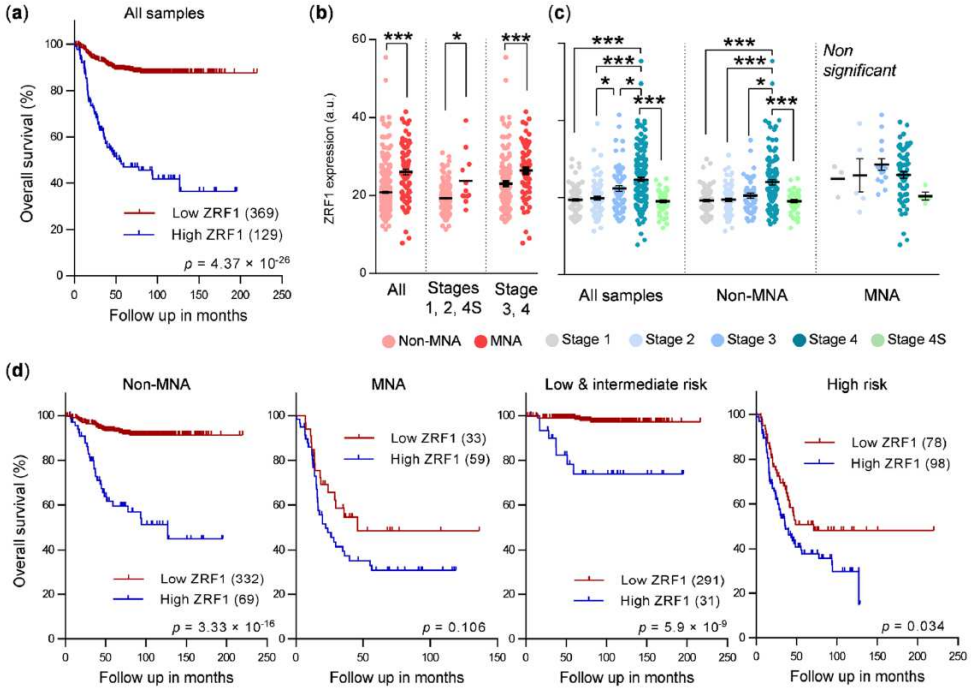

(e)

Univariate regression analysis

Factors	Overall survival	
	HR (95% CI)	*p* value
Sex (M vs F)	-	0.252
Age (≥18 months vs <18 months)	8.114 (4.980-13.221)	0.000
MYC (Amp vs no amp)	7.793 (5.262-11.542)	0.000
INSS Stage (4 vs others)	8.660 (5.441-13.783)	0.000
ZRF1 (High vs low)	6.387 (4.307-9.472)	0.000
Risk (High vs others)	21.423 (11.932-38.464)	0.000

(f)

Multivariate regression analysis

Factors	Overall survival	
Model 1	HR (95% CI)	*p* value
Age (≥18 months vs <18 months)	2.755 (1.587-4.781)	0.000
MYCN (Amp vs no amp)	2.994 (1.970-4.550)	0.000
INSS Stage (4 vs others)	3.176 (1.887-5.347)	0.000
ZRF1 (High vs others)	2.062 (1.328-3.204)	0.001
Model 2		
ZRF1 (High vs low)	1.985 (1.306-3.016)	0.001
Risk (High vs others)	15.522 (8.323-28.946)	0.000

Figure 1. *ZRF1* is an independent prognostic factor in neuroblastoma. (**a**) Kaplan–Meier survival plot of a cohort of 498 patients (GSE62564) split into high and low *ZRF1* mRNA expression, based on the Youden index. (**b**) *ZRF1* mRNA levels in MYCN-amplified tumors (MNA, dark red) vs non-MYCN amplified tumors (non-MNA, light red), according to the indicated disease stages. (**c**) *ZRF1* mRNA levels according to disease stage in the whole cohort (left) or considering patients with non-MNA (middle) or with MNA tumors (right). (**d**) Kaplan–Meier survival plots comparing samples with high and low *ZRF1* levels in the indicated groups of patients. (**e**) Cox univariate regression analysis of overall survival with different clinic-pathological features. (**f**) Cox multivariate regression analysis of overall survival results confirm *ZRF1* mRNA levels as an independent prognostic marker in neuroblastoma. * means $p < 0.05$; *** means $p < 0.001$. HR: hazard ratio.

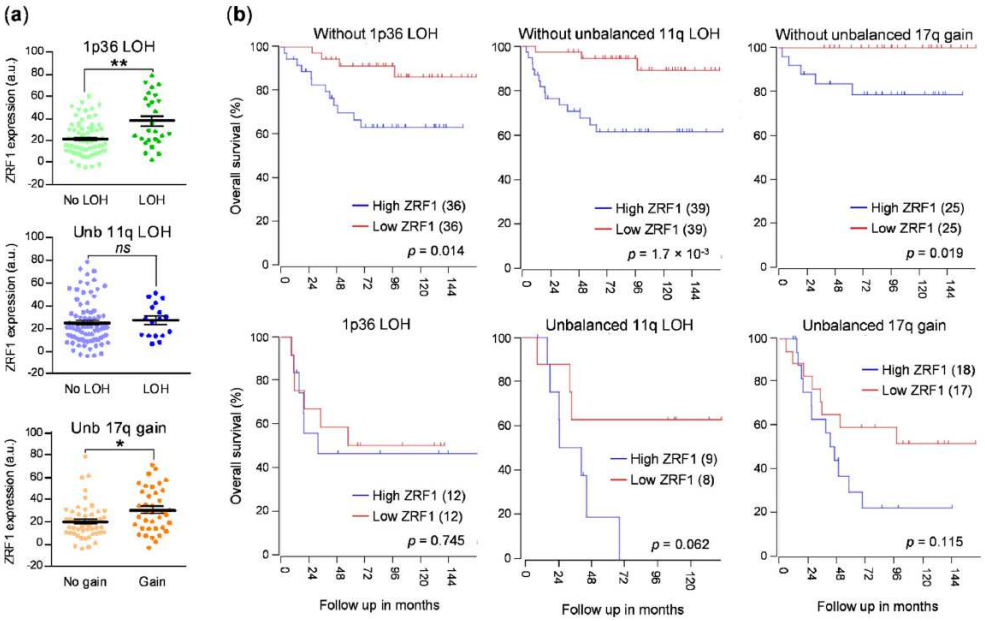

Figure 2. *ZRF1* levels correlate with low survival in the absence of genomic alterations associated with poor prognosis. (**a**) *ZRF1* mRNA levels in the presence or absence of the indicated segmental copy alterations (GSE3960, $n = 101$). (**b**) Kaplan–Meier survival plots comparing high and low *ZRF1* samples from the GSE3960 dataset, in the absence or presence of the different segmental copy alterations. *ns* means non-significant; * means $p < 0.05$; ** means $p < 0.01$.

Analysis of *ZRF1* protein expression by Western blot on 24 tumor frozen samples from a cohort of 22 neuroblastoma patients was performed to confirm the mRNA results (Figure S2). Two pairs of samples corresponded to the same patients at different stages of the disease: early tumor resection or biopsy, and resection of metastatic lesions, respectively (Table S6). In most of the samples, the intensity of the *ZRF1* band was low or barely detectable, using SK-N-BE(2) cell line lysates as positive control. However, it is interesting to point out that the cases with higher expression of *ZRF1* were those corresponding to relapsed or metastatic neuroblastoma, thus supporting the fact that high *ZRF1* levels are present in the most aggressive neuroblastomas. Nevertheless, these results are preliminary and should be validated in a larger cohort of matched neuroblastoma samples.

Since most tumors contain heterogeneous cell populations, including malignant cells, immune cells, fibroblasts, and vascular cells, we proceed to confirm by immunohistochemistry that the *ZRF1* signal was from tumor cells. Figure S3 shows a representative image of a neuroblastoma tumor where the stromal component of the tumor shows a weak *ZRF1* immunoreactivity while tumor cells are highly positive.

In summary, *ZRF1* mRNA levels are associated with poor prognosis in neuroblastoma and may be used as an independent prognostic marker in the absence of MYCN amplification and other poor prognosis-related chromosomal aberrations.

3.2. ZRF1 Is Not Sufficient to Enhance Neuroblastoma Aggressiveness

Given the role of *ZRF1* in the regulation of neuronal differentiation and the observed correlations in neuroblastoma samples, we studied the functional consequences of *ZRF1* overexpression in neuroblastoma cell lines. Protein expression analysis showed homogeneous levels of *ZRF1* among a panel of different neuroblastoma cell lines, regardless of

MYCN amplification status (Figure 3a). To explore whether increasing the levels of *ZRF1* enhanced neuroblastoma aggressiveness, we transduced the SK-N-BE(2) and SK-N-AS neuroblastoma cell lines with a *ZRF1* lentiviral overexpression vector (Figure 3b), and then analyzed the effects of *ZRF1* on different oncogenic properties. Overexpression of *ZRF1* did not enhance proliferation (Figure 3c) or ability to form colonies when cells were plated at a low density (Figure 3d). Drug sensitivity assays were performed against cisplatin, an alkylating agent, and topotecan, an inhibitor of topoisomerase-I, which are two of the neuroblastoma standard-of-care chemotherapies. However, overexpression of *ZRF1* did not produce an increased resistance of neuroblastoma cells after 72 h of treatment (Figure 3e).

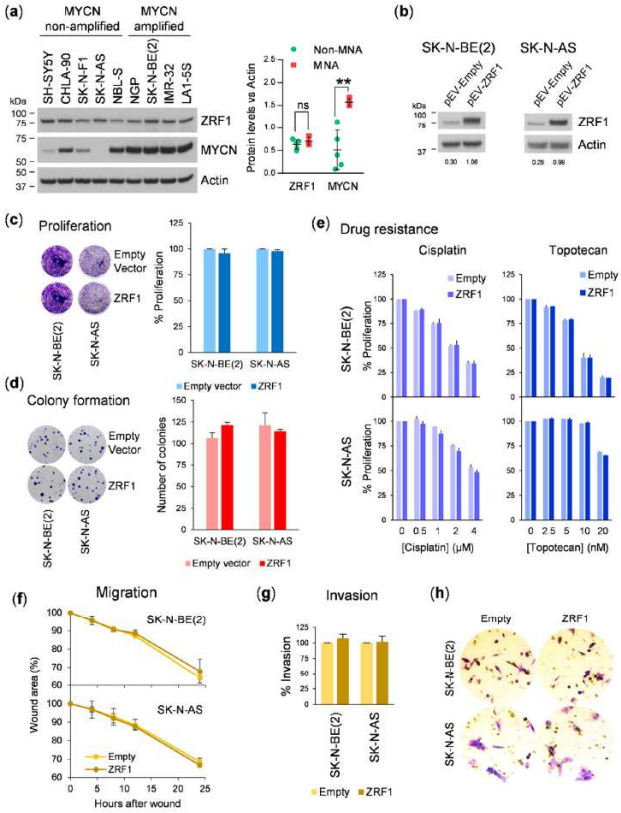

Figure 3. *ZRF1* overexpression does not enhance neuroblastoma cell line aggressiveness. (**a**) Left, protein expression analysis of *ZRF1* and MYCN by Western blot of a 9-neuroblastoma cell line panel. Right, densitometry quantification. (**b**) Western blot validation of *ZRF1* overexpression in SK-N-BE(2) and SK-N-AS cell lines at 96 h post-transduction. (**c**) Proliferation assay of neuroblastoma cell lines overexpressing *ZRF1* compared to empty-vector (pEV-empty)-transduced cells. (**d**) Colony formation assay of neuroblastoma cells overexpressing *ZRF1*. Graph represents the average of three independent experiments, $n = 3$ per condition. (**e**) Cisplatin and topotecan resistance assay of *ZRF1*-overexpressing cell lines. Cells were treated for 72 h at the indicated doses, and proliferation was assessed by crystal violet staining. (**f**) Wound-healing assay in neuroblastoma cells overexpressing *ZRF1*. Graphs represent percentage of the wound area at the indicated times, normalized to time = 0. (**g**) Invasion assay of *ZRF1* overexpressing cells through a collagen barrier for 16 h. Invasive cells were detected and quantified by crystal violet staining. (**h**) Representative microscopic pictures of crystal violet-stained invasive cells. *ns* means non-significant; ** means $p < 0.01$.

Owing to the lineage-conferring migratory capability of neuroblastoma cells, we next explored whether higher levels of *ZRF1* alters the migration or the invasion of cells in wound-healing and transwell assays, respectively. *ZRF1*-transduced cells closed the wound at the same pace as empty vector-infected cells (Figure 3f). Moreover, invasion through a collagen barrier was not affected by *ZRF1* overexpression in transwell assays (Figure 3g,h), thereby suggesting that *ZRF1* does not modulate the ability of neuroblastoma cells to migrate or invade.

13-*cis*-retinoic acid (hereafter referred to as RA) is a naturally occurring differentiating and therapeutic agent for the treatment of neuroblastoma minimal residual disease [6,22]. Because *ZRF1* has been previously demonstrated to be involved in maintaining neural progenitor stemness [8] and in altering retinoic acid induced differentiation [16], we analyzed the effect of modulating *ZRF1* in RA-differentiated neuroblastoma cells. After 5 days of RA treatment, *ZRF1* levels were found to be decreased 3–4 times in the RA-treated SH-SY5Y and SK-N-BE(2) neuroblastoma cell lines, as compared with vehicle-treated cells (Figure 4a). To evaluate the function of *ZRF1* in the process of RA-mediated differentiation, neuroblastoma cell lines overexpressing *ZRF1* were treated with the differentiating agent and the differentiation outcomes were analyzed. First, *ZRF1* overexpression did not rescue or attenuate the decrease in proliferation induced by RA-induced differentiation (Figure 4b); secondly, *ZRF1* overexpression did not alter the RA-induced upregulation of the RA receptor RAR-β(Figure 4c); finally, neither the percentage of cells with neurites (Figure 4d,e) nor the neurite length (Figure 4f) were modulated by overexpressing *ZRF1*.

These results indicate that sustained high levels of *ZRF1* are not enough to enhance oncogenic properties in neuroblastoma cells or impair RA-mediated neuroblastoma differentiation.

3.3. ZRF1 Knockdown Does Not Impair Neuroblastoma Proliferation and Reveals Inconsistencies between Different Gene Silencing Methodologies

As *ZRF1* expression was noted in all the neuroblastoma cell lines tested, loss of function experiments represented a good strategy to fully dissect any relevant function of *ZRF1* in neuroblastoma cells. Thus, we knocked down *ZRF1* using lentiviral vectors. Two different shRNAs targeting the *ZRF1* coding region were transduced in six different neuroblastoma cell lines and showed a marked reduction in *ZRF1* levels compared to non-silencing control (NSC)-transduced cells (Figures 5a and S4A). In all tested cell lines, shRNA-mediated depletion of *ZRF1* significantly reduced the proliferative capacity of neuroblastoma cells (Figures 5b and S4B).

Transcriptomic analyses of shRNA-mediated *ZRF1* depleted cells showed the involvement of several genes related to the cell cycle (Figure S4C,D). When we validated the expression of some of those genes (i.e., AURKB), discrepancies among the molecular effects of the three different shRNAs were observed. For example, while one of the shRNAs (shRNA #1) completely abolished the expression of AURKB, the other two (shRNA #2 and #3) did not (Figure 5c). Cell cycle analyses in *ZRF1*-depleted cells also showed different profiles. The shRNAs #1 and #2 against *ZRF1* showed an increase in the percentage of cells in the G1 phase, whereas shRNA #3 showed a trend towards G2/M arrest (Figure 5d). To discard potential shRNA off-target effects, we performed rescue experiments by overexpressing a *ZRF1* variant with silent mutations in the shRNA target sites (Figure S5). This new mutant *ZRF1* was completely insensitive to shRNAs #1 and #3, and partially sensitive to shRNA #2 (Figure 5e). When the phenotypic effects were analyzed, the ectopic expression of *ZRF1* did not rescue the reduction in proliferation caused by the transduction of the three different shRNAs (Figure 5f). Thus, we concluded that the phenotypic consequences induced by the different shRNAs were not attributable to *ZRF1* depletion.

To exclude the possibility that some of the *ZRF1* knockdown effects were masked by the shRNA off-targets, we repeated the experiments with small interfering RNA (siRNA). Up to four different siRNA sequences were transfected into neuroblastoma cells. All the sequences reduced the *ZRF1* level by more than 85% (Figure 6a). When the phenotypic consequences of siRNA-mediated *ZRF1* depletion were analyzed, no differences were found in cell proliferation (Figure 6b), wound healing (Figure 6c), invasion through col-

lagen (Figure 6d), or resistance to neuroblastoma therapies such as chemotherapeutics or RA (Figure 6e).

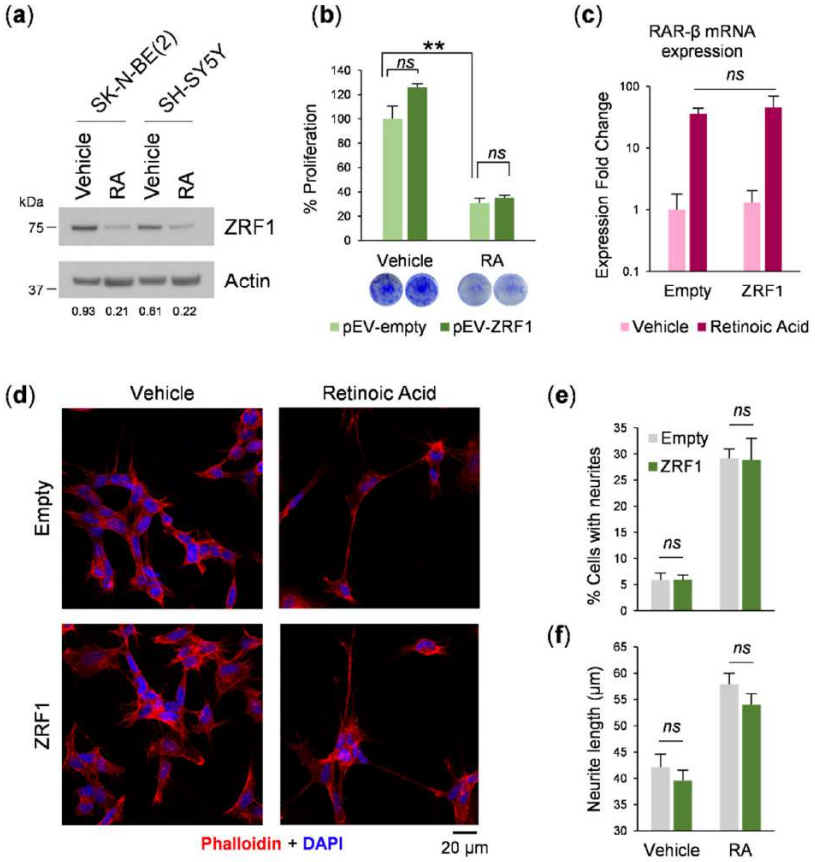

Figure 4. *ZRF1* overexpression does not attenuate retinoic acid-induced differentiation. (**a**) *ZRF1* levels after RA-induced differentiation measured by western blot. Actin-normalized densitometry quantification of *ZRF1* levels is shown beneath their respective Western blot panels (**b**) Cell proliferation assay of SK-N-BE(2) cells overexpressing *ZRF1* treated with RA and normalized versus empty vector-transduced cell treated with vehicle. (**c**) mRNA levels of the RA-induced differentiation reporter RAR-β, assessed by RT-qPCR in SK-N-BE(2) cells. (**d**) Confocal microscopy representative images of ZRF-overexpressing SK-N-BE(2) cells stained with phalloidin and DAPI. (**e**) Quantification of the number of cells with neurites (>30 µm prolongations) per field. (**f**) Average neurite length for each group. *ns* means non-significant; ** means $p < 0.01$.

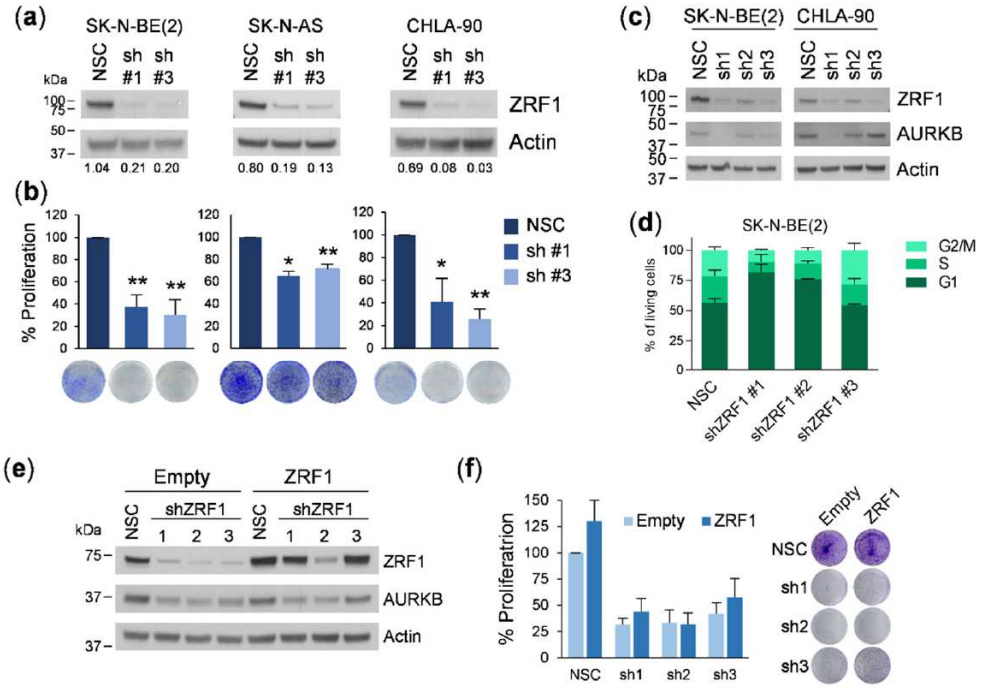

Figure 5. *ZRF1* shRNA silencing results in inconsistent and unspecific effects in neuroblastoma cells. (**a**) *ZRF1* expression levels in neuroblastoma cells transduced with two different shRNAs against *ZRF1*, and a non-silencing control (NSC) as negative control. (**b**) Cell proliferation in shZRF1-transduced neuroblastoma cell lines compared with those transduced with NSC, measured by crystal violet. (**c**) *ZRF1* and AURKB levels of sh*ZRF1* transduced neuroblastoma cell lines. (**d**) Cell cycle analysis of SK-N-BE(2) 72 h post-infection by FACS. (**e**) Western blot analysis of *ZRF1* and AURKB levels in SK-N-BE(2) cells overexpressing *ZRF1* insensitive to shZRF1, at 96h post-transduction. (**f**) Cell proliferation assay of SK-N-BE(2) cells overexpressing insensitive *ZRF1* transduced with 3 shRNAs against *ZRF1*. * means $p < 0.05$; ** means $p < 0.01$.

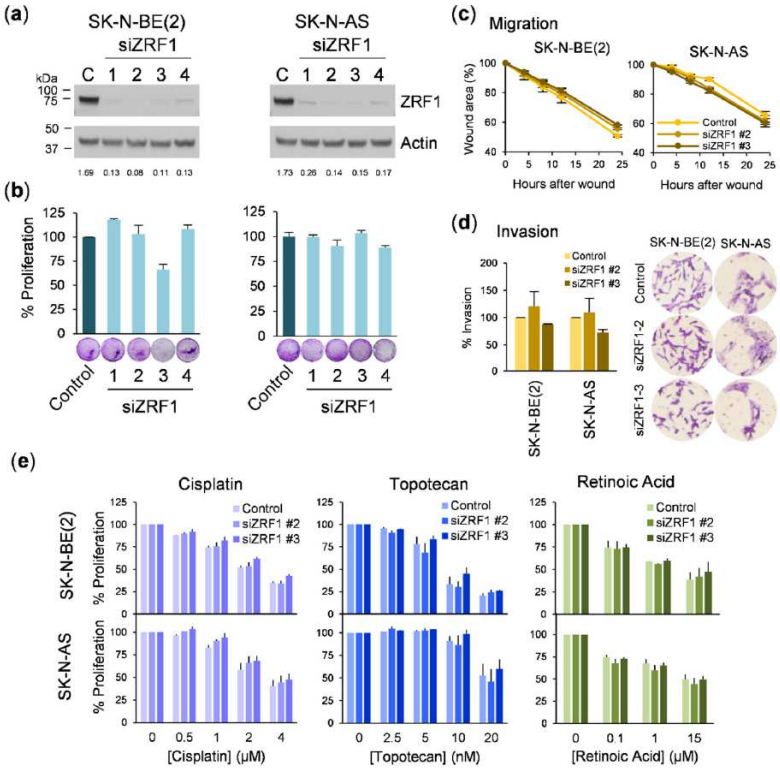

Figure 6. *ZRF1* is dispensable for neuroblastoma growth, migration, and drug resistance. (**a**) *ZRF1* levels in neuroblastoma cells transfected with siRNA control and 4 different si*ZRF1*. Actin-normalized densitometry quantification of *ZRF1* levels is shown beneath their respective *ZRF1* knockdown validation Western blot panels (**b**) Cell viability assay in neuroblastoma cells transfected comparing siControl vs si*ZRF1* at 96h post-transfection. (**c**) Wound-healing assay in si*ZRF1* transfected neuroblastoma cells at 72 h post-transfection. (**d**) Invasion assay through a collagen barrier of si*ZRF1* transfected cells at 72 h post-transfection. Left, crystal violet quantification of invaded cells. Right, representative images of the invasion assay. (**e**) Cisplatin (left), topotecan (middle), and retinoic acid (right) resistance assay of si*ZRF1*-transfected cell lines. Cells were treated after 72 h of transfection at the indicated doses for 72 h more and proliferation was assessed by crystal violet staining.

In summary, our results indicate that *ZRF1* has a prognostic value, but is not functionally relevant in neuroblastoma cells.

4. Discussion

Neuroblastoma is thought to originate from cells of the neural crest that are transformed during differentiation and migration toward tissues of the sympathoadrenergic lineage. The occurrence of a transformative event during tissue differentiation dictates the aggressiveness of the tumor. In general, patients with poor prognosis have histologically undifferentiated tumors, whereas those with better prognosis have tumors with histological evidence of cellular differentiation [23]. This differentiation program is tightly regulated by a complex set of signals, including external signaling, activation of specific transcriptional programs, and/or epigenetic events (reviewed in [24]). Experimental results in transgenic mouse models have identified activating ALK mutations and MYCN overexpression as

the main oncogenic drivers of neuroblastoma [25,26]. These molecular alterations often converge on mechanisms that block differentiation and confer sustained proliferation capabilities. In particular, genes associated with the maintenance of embryonic and adult stem cells, such as the components of PRC1 or PRC2, have been linked to the initiation and progression of neuroblastoma [27]. For example, BMI1, a core component of the PRC1 complex, has been shown to cooperate in MYCN-driven neuroblastomas by inhibiting cell death and differentiation [28–30]. Focusing on the role of PRC1 in neuronal differentiation, Aloia et al. identified *ZRF1* as a transcriptional regulator of neural fates in embryonic stem cells [9]. Furthermore, *ZRF1* expression has been associated with poor outcomes in other tumors, such as breast [14,31] or gastric cancer [15], thus suggesting an oncogenic role in cancer. Thus, we sought to determine whether *ZRF1* plays a functional role in aggressive neuroblastomas. Data mining of multiple neuroblastoma gene expression datasets confirmed that *ZRF1* mRNA expression was elevated in subsets of patients with the most common genetic alterations associated with poor outcomes, thereby supporting our initial hypothesis, although this correlation could not be confirmed at the protein level in neuroblastoma patient samples.

Nevertheless, our functional data do not support a relevant contribution of *ZRF1* in the oncogenesis of neuroblastoma. Ectopic expression of *ZRF1* did not offer proliferation, colony formation, or migratory or invasive advantages to neuroblastoma cells. In acute myeloid leukemia, *ZRF1* is a regulator of RA-induced differentiation [16], and because of the relevance of retinoids in neuroblastoma therapy [22], we investigated whether *ZRF1* interferes with the response of neuroblastoma cells to RA. When neuroblastoma cells were exposed to 13-*cis*-RA, a clear reduction in the *ZRF1* level was observed, concomitant with an expected reduction in cell proliferation and morphological changes such as neurite outgrowth. However, maintaining high *ZRF1* expression ectopically was not sufficient to reverse the RA effect. These results suggest that the downregulation of *ZRF1* is a consequence of the RA-induced differentiation process.

Although *ZRF1* is not sufficient to provide oncogenic advantages, it could still be necessary to maintain the undifferentiated and highly proliferative state of neuroblastoma cells. Previous reports demonstrated that depletion of *ZRF1* resulted in a reduction of cell proliferation and the induction of apoptosis in gastric [15] or breast cancer models [14]. Conversely, Kaymak et al. also showed that the reduction in cell proliferation mediated by *ZRF1* depletion was accompanied by an increase in the migration and invasion properties of breast cancer cells [31]. Our first set of experiments silencing *ZRF1* using two different shRNAs resulted in a marked reduction in cell proliferation in six neuroblastoma cell lines. However, these effects were not rescued by overexpressing the shRNA-insensitive form of *ZRF1*, thereby indicating that the depletion of *ZRF1* was not the causal factor for the reduction in cell proliferation. Consistent with this previous finding, siRNA-mediated depletion of *ZRF1* did not alter the proliferative, migratory, or invasive capacities or the sensitivity to RA in neuroblastoma cells, thus confirming that *ZRF1* is dispensable for the progression of this type of tumor. It is important to highlight that inconsistencies between different gene silencing methods could have misled the conclusion of this study. However, our use of independent silencing tools and rescue experiments with target protein ectopic expression leaves no room for doubt.

Imamura et al. demonstrated that while the effects of *ZRF1* on cell proliferation were p53-dependent, those related to migration and invasion were p53-independent [15]. In our work, we covered this aspect by using cell lines with non-functional (CHLA-90, SK-N-BE(2), and SK-N-AS) and functional p53 (SH-SY5Y and IMR-32), and we did not find any differential response in the gain-of-function or loss-of-function experiments.

The paradoxical discrepancy between the strong correlation between *ZRF1* expression and poor patient outcome, and its dispensable function in tumor cells could be due to one or more of the following reasons: (i) one key characteristic of cancer is uncontrolled transcription. Thus, many genes are likely to be differentially expressed incidentally, rather than reflecting a gene that is driving a biologically significant outcome [32]; (ii)

the *ZRF1*-PRC1 axis may regulate different sets of genes in a lineage-dependent manner; (iii) molecular alterations present in neuroblastoma (i.e., mutation burden, chromosomal copy number variations, etc.) deactivate the physiological regulation of *ZRF1*-PRC1 on cell proliferation/differentiation programs and become *ZRF1* independent; and (iv) the ambivalent molecular function of *ZRF1* in neuroblastoma cells may be inclined to a non-essential chaperone role. This hypothesis is supported by our subcellular fractionation analysis in different neuroblastoma cell lines, where *ZRF1* was found to be predominantly enriched in the cytosolic fraction (Figure S6).

In summary, our data suggest the potential use of *ZRF1* expression as an independent prognostic factor, particularly in cases without any other associated molecular prognostic factors. However, *ZRF1* does not seem to be a promising target candidate for differentiation therapy for neuroblastoma.

5. Conclusions

ZRF1 was found to be an independent prognostic factor of survival in neuroblastoma. However, this correlation cannot be explained by the molecular role of *ZRF1* by itself, and it could be the reflection of an underlying molecular mechanism promoting neuroblastoma aggressiveness. Nevertheless, our functional studies highlight the need of proper verification of shRNA-mediated knockdown experiments through consistent validation with different gene silencing technologies and rescue experiments.

Supplementary Materials: The following are available online at https://www.mdpi.com/article/10.3390/cancers13194845/s1, Figure S1: *ZRF1* is associated to poor prognosis in neuroblastoma. Figure S2: *ZRF1* protein levels Western blot analysis in patient tumor samples. Figure S3: *ZRF1* protein is detected by immunohistochemistry (IHC) in the tumor cells of a neuroblastoma formalin-fixed paraffin-embedded human sample. Figure S4: Functional and molecular consequences of shRNA-mediated depletion of *ZRF1* in neuroblastoma cells. Figure S5: Design of a triple shRNA insensitive *ZRF1* overexpression construct. Figure S6: Subcellular localization analysis of *ZRF1* by Western blot in a panel of neuroblastoma cell lines. Figure S7. Original Western Blot image of Figures 3a,b, 4a, 5a,c,e, 6a, S2a and S4. Table S1: Antibodies used for Western blot analyses. Table S2: Oligonucleotides used for silent *ZRF1* mutagenesis and RARB RT-qPCR. Table S3: *ZRF1* targeting sequences. Table S4: Cut-off value for *ZRF1* levels analysis, based on the ability for overall survival prediction (using GSE62564, $n = 498$). Table S5: *ZRF1* mRNA expression correlations with clinical variables in neuroblastoma using Fisher's test (GSE62564, $n = 498$). Table S6: Neuroblastoma tumor sample clinical data.

Author Contributions: Conceptualization, C.J. and M.F.S.; methodology, C.J., R.A., M.M., L.D.-J., J.C., A.M., G.G., L.J. and M.F.S.; bioinformatic analyses, C.J., A.S., L.D.-J., D.L.-N. and M.F.S.; validation, C.J. and M.F.S.; formal analysis, C.J., A.S., R.A. and M.F.S.; investigation C.J. and M.F.S.; data curation, C.J., A.S., L.D.-J., G.G., R.H. and M.F.S.; writing—original draft preparation, C.J. and M.F.S.; writing—review and editing, J.R., D.L.-N., J.S.d.T., L.M. and S.G.; supervision, M.F.S.; funding acquisition J.S.d.T., S.G. and M.F.S. All authors have read and agreed to the published version of the manuscript.

Funding: This work was funded by Instituto de Salud Carlos III (Grant no. CP16/00006, PI17/00564 and PI20/00530 to M.F Segura and MS17/00063 to D. Llobet-Navas); Asociación Española Contra el Cáncer (LABAE18009SEGU, LABAE19004LLOB); Generalitat de Catalunya AGAUR/European Social Fund (Grant no. 2017FI_B_00095 to C Jiménez); Asociación NEN; Joan Petit foundation; Asociación Pulseras Candela foundation; the #delhospitalalacatedral initiative led by Xavi Vallés; and the Rotary Clubs of Barcelona Eixample, Barcelona Diagonal, Santa Coloma de Gramanet, München-Blutenburg, Deutschland Gemeindienst, and others from Barcelona and its province.

Institutional Review Board Statement: Not applicable.

Informed Consent Statement: Tumor samples from Vall d'Hebron Hospital neuroblastoma patients are under the registered collection Ref. C.0002311 from *Instituto de Salud Carlos III*. All patients gave written informed consent.

Data Availability Statement: Publicly available datasets were analyzed in this study. These data can be found at http://r2.amc.nl under the accession numbers GSE45547, GSE3960, GSE62564.

Acknowledgments: We thank members of the Translational Research in Child and Adolescent Cancer laboratory for their support. We thank Professor Luciano Di Croce for sharing the *ZRF1* shRNA vectors, overexpression vectors and the anti-*ZRF1* antibody.

Conflicts of Interest: The authors declare no conflict of interest.

References

1. Maris, J.M. Recent Advances in Neuroblastoma. *N. Engl. J. Med.* **2010**, *362*, 2202–2211. [CrossRef] [PubMed]
2. Cheung, N.-L.V.; Dyer, M.A. Neuroblastoma: Developmental biology, cancer genomics and immunotherapy. *Nat. Rev. Cancer* **2013**, *13*, 397–411. [CrossRef] [PubMed]
3. Matthay, K.K.; Maris, J.M.; Schleiermacher, G.; Nakagawara, A.; Mackall, C.L.; Diller, L.; Weiss, W.A. Neuroblastoma. *Nat. Rev. Dis. Prim.* **2016**, *2*, 16078. [CrossRef] [PubMed]
4. Pudela, C.; Balyasny, S.; Applebaum, M.A. Nervous system: Embryonal tumors: Neuroblastoma. *Atlas Genet. Cytogenet. Oncol. Haematol.* **2020**, *24*, 284–290. [CrossRef] [PubMed]
5. Maris, J.M.; Hogarty, M.D.; Bagatell, R.; Cohn, S.L. Neuroblastoma. *Lancet* **2007**, *369*, 2106–2120. [CrossRef]
6. Reynolds, C.P. Detection and treatment of minimal residual disease in high-risk neuroblastoma. *Pediatr. Transplant.* **2004**, *8*, 56–66. [CrossRef]
7. Durinck, K.; Speleman, F. Epigenetic regulation of neuroblastoma development. *Cell Tissue Res.* **2018**, *372*, 309–324. [CrossRef] [PubMed]
8. Aloia, L.; Di Stefano, B.; Sessa, A.; Morey, L.; Santanach, A.; Gutierrez, A.; Cozzuto, L.; Benitah, S.A.; Graf, T.; Broccoli, V.; et al. *ZRF1* is required to establish and maintain neural progenitor identity. *Genes Dev.* **2014**, *28*, 182–197. [CrossRef]
9. Aloia, L.; Gutierrez, A.; Caballero, J.M.; Di Croce, L. Direct interaction between Id1 and *ZRF1* controls neural differentiation of embryonic stem cells. *EMBO Rep.* **2015**, *16*, 63–70. [CrossRef] [PubMed]
10. Matsumoto-Taniura, N.; Pirollet, F.; Monroe, R.; Gerace, L.; Westendorf, J.M. Identification of novel M phase phosphoproteins by expression cloning. *Mol. Biol. Cell* **1996**, *7*, 1455–1469. [CrossRef]
11. Hundley, H.A.; Walter, W.; Bairstow, S.; Craig, E.A. Human Mpp11 J protein: Ribosome-tethered molecular chaperons are ubiquitous. *Science* **2005**, *308*, 1032–1034. [CrossRef] [PubMed]
12. Otto, H.; Conz, C.; Maier, P.; Wölfle, T.; Suzuki, C.K.; Jenö, P.; Rücknagel, P.; Stahl, J.; Rospert, S. The chaperones MPP11 and Hsp70L1 form the mammalian ribosome-associated complex. *Proc. Natl. Acad. Sci. USA* **2005**, *102*, 10064–10069. [CrossRef]
13. Richly, H.; Rocha-Viegas, L.; Ribeiro, J.D.; Demajo, S.; Gundem, G.; Lopez-Bigas, N.; Nakagawa, T.; Rospert, S.; Ito, T.; Di Croce, L. Transcriptional activation of polycomb-repressed genes by *ZRF1*. *Nature* **2010**, *468*, 1124–1130. [CrossRef] [PubMed]
14. Rath, S.K.; Deb, M.; Sengupta, D.; Kari, V.; Kar, S.; Parbin, S.; Pradhan, N.; Patra, S.K. Silencing of *ZRF1* impedes survival of estrogen receptor positive MCF-7 cells and potentiates the effect of curcumin. *Tumor Biol.* **2016**, *37*, 12535–12546. [CrossRef] [PubMed]
15. Imamura, T.; Komatsu, S.; Ichikawa, D.; Miyamae, M.; Okajima, W.; Ohashi, T.; Kiuchi, J.; Nishibeppu, K.; Kosuga, T.; Konishi, H.; et al. Overexpression of *ZRF1* is related to tumor malignant potential and a poor outcome of gastric carcinoma. *Carcinogenesis* **2018**, *39*, 263–271. [CrossRef] [PubMed]
16. Demajo, S.; Uribesalgo, I.; Gutiérrez, A.; Ballaré, C.; Capdevila, S.; Roth, M.; Zuber, J.; Martín-Caballero, J.; Di Croce, L. *ZRF1* controls the retinoic acid pathway and regulates leukemogenic potential in acute myeloid leukemia. *Oncogene* **2014**, *33*, 5501–5510. [CrossRef] [PubMed]
17. Livak, K.J.; Schmittgen, T.D. Analysis of relative gene expression data using real-time quantitative PCR and the 2-ΔΔCT method. *Methods* **2001**, *25*, 402–408. [CrossRef]
18. Naldini, L.; Blömer, U.; Gallay, P.; Ory, D.; Mulligan, R.; Gage, F.H.; Verma, I.M.; Trono, D.; Naldini, L.; Blomer, U.; et al. In Vivo Gene Delivery and Stable Transduction of Nondividing Cells by a Lentiviral Vector. *Science* **1996**, *272*, 263–267. [CrossRef]
19. Zufferey, R.; Dull, T.; Mandel, R.J.; Bukovsky, A.; Quiroz, D.; Naldini, L.; Trono, D. Self-Inactivating Lentivirus Vector for Safe and Efficient In Vivo Gene Delivery. *J. Virol.* **1998**, *72*, 9873–9880. [CrossRef]
20. Caron, H. Allelic loss of chromosome 1 and additional chromosome 17 material are both unfavourable prognostic markers in neuroblastoma. *Med. Pediatr. Oncol.* **1995**, *24*, 215–221. [CrossRef]
21. Attiyeh, E.F.; London, W.B.; Mossé, Y.P.; Wang, Q.; Winter, C.; Khazi, D.; McGrady, P.W.; Seeger, R.C.; Look, A.T.; Shimada, H.; et al. Chromosome 1p and 11q Deletions and Outcome in Neuroblastoma. *N. Engl. J. Med.* **2005**, *353*, 2243–2253. [CrossRef]
22. Reynolds, C.P.; Lemons, R.S. Retinoid therapy of childhood cancer. *Hematol. Oncol. Clin. N. Am.* **2001**, *15*, 867–910. [CrossRef]
23. He, S.; Liu, Z.; Oh, D.Y.; Thiele, C.J. MYCN and the epigenome. *Front. Oncol.* **2013**, *3*, 1–10. [CrossRef] [PubMed]
24. Johnsen, J.I.; Dyberg, C.; Wickström, M. Neuroblastoma—A neural crest derived embryonal malignancy. *Front. Mol. Neurosci.* **2019**, *12*, 9. [CrossRef] [PubMed]
25. Weiss, W.A.; Aldape, K.; Mohapatra, G.; Feuerstein, B.G.; Bishop, J.M. Targeted expression of MYCN causes neuroblastoma in transgenic mice. *EMBO J.* **1997**, *16*, 2985–2995. [CrossRef] [PubMed]
26. Heukamp, L.C.; Thor, T.; Schramm, A.; De Preter, K.; Kumps, C.; De Wilde, B.; Odersky, A.; Peifer, M.; Lindner, S.; Spruessel, A.; et al. Targeted expression of mutated ALK induces neuroblastoma in transgenic mice. *Sci. Transl. Med.* **2012**, *4*, 141ra91. [CrossRef]
27. Kamijo, T. Role of stemness-related molecules in neuroblastoma. *Pediatr. Res.* **2012**, *71*, 511–515. [CrossRef]

28. Nowak, K.; Kerl, K.; Fehr, D.; Kramps, C.; Gessner, C.; Killmer, K.; Samans, B.; Berwanger, B.; Christiansen, H.; Lutz, W. BMI1 is a target gene of E2F-1 and is strongly expressed in primary neuroblastomas. *Nucleic Acids Res.* **2006**, *34*, 1745–1754. [CrossRef]
29. Cui, H.; Hu, B.; Li, T.; Ma, J.; Alam, G.; Gunning, W.T.; Ding, H.F. Bmi-1 is essential for the tumorigenicity of neuroblastoma cells. *Am. J. Pathol.* **2007**, *170*, 1370–1378. [CrossRef]
30. Ochiai, H.; Takenobu, H.; Nakagawa, A.; Yamaguchi, Y.; Kimura, M.; Ohira, M.; Okimoto, Y.; Fujimura, Y.; Koseki, H.; Kohno, Y.; et al. Bmi1 is a MYCN target gene that regulates tumorigenesis through repression of KIF1BB and TSLC1 in neuroblastoma. *Oncogene* **2010**, *29*, 2681–2690. [CrossRef]
31. Kaymak, A.; Sayols, S.; Papadopoulou, T.; Richly, H. Role for the transcriptional activator *ZRF1* in early metastatic events in breast cancer progression and endocrine resistance. *Oncotarget* **2018**, *9*, 28666–28690. [CrossRef] [PubMed]
32. Rodriguez-Esteban, R.; Jiang, X. Differential gene expression in disease: A comparison between high-throughput studies and the literature. *BMC Med. Genom.* **2017**, *10*, 59. [CrossRef] [PubMed]

The work presented in this thesis was funded by competitive grants from *Instituto de Salud Carlos III* (PI17/00564, PI20/00530) and *Generalitat de Catalunya* AGAUR/European Social Fund (2017FI_B_00095); as well as by the non-profit organizations NEN association and *Posa't la gorra*-Balaguer initiative.